Investigating the effect of maternal age on human follicle development



Charlotte Anna Walker
Jesus College

Nuffield Department of Women's and Reproductive Health
University of Oxford

Thesis submitted for the degree of
Doctor of Philosophy

Michaelmas 2018

“Ex ovo omnia”

from the egg, all

- William Harvey

Abstract

With increasing maternal age, the likelihood of pregnancy declines primarily due to a decrease in oocyte number and quality. Increasing the supply of high-quality eggs for use in assisted reproduction techniques is essential for those faced with indications that limit this supply, such as advanced maternal age. This thesis established a method of *in vitro* follicle development and identified pathways associated female reproductive aging with the overall aim of developing a treatment for age-related infertility in women. To ascertain when age-related changes manifest, culture of cryopreserved human ovarian cortical tissue was established to investigate and manipulate follicle development from the primordial stage. An analysis of ovarian cortical tissue from 12 patients aged 9-25 years revealed variation between patients both in follicle health of non-cultured tissue post-cryopreservation as well as follicle health and development after six days in culture. Furthermore, tissue fragments selected for culture using neutral red had healthier morphology than those that were not. Cortical strip culture was used to explore the effect of lysine specific demethylase 1 (GSK-LSD1) inhibition on follicle development in human ovarian tissue. In tissue cultured with 2 μM GSK-LSD1 for six days, follicles were more likely to be asymmetric primary or secondary stage follicles, and less likely to be classified as degenerating or atretic. These findings support epigenetic manipulation of follicle development as a potential strategy for *in vitro*-based therapeutic interventions. To maximise follicle health and development tissue was cultured with two different media composition, media volume, and dish permeability. Of six conditions tested, fragments of cortical tissue cultured in a low volume of αMEM medium had the greatest likelihood of developing heathy follicles. Finally, RNA-seq was used to identify changes in cumulus cell gene expression between reproductively young (<35 years) and older women (≥37 years). Identification of GO enrichment and upstream regulators were consistent with the emerging theory that advanced maternal age may be associated with a hypoxic follicle environment.

Acknowledgements

There are many people without whom this work would not have been possible. I would like to express my sincerest thanks to Dr Suzannah Williams and Professor Dagan Wells for their guidance and support.

Thank you to Ginny Mounce, Karen Turner and the team at Oxford Fertility, Sheila Lane and the OCTB staff, and to all the patients who donated their cells or tissue for this work. To Dhruti and Katharina for always being available to sound board the genetic aspects of my project and for being friendly faces at the IRS. To Helen Lockstone and Ben Wright for their patience in teaching me about bioinformatic processing and gene expression data analysis. To Thomas Tapmeier and Wei Zhang for their assistance with RT-PCR. Thank you to Karl Morton, Rebecca Dragovic, and Christian Becker for being examiners at various stages through my DPhil, for providing constructive criticism and useful discussion on the direction of the project.

Thank you to Sairah, Belinda, Briet, Xi, and Eleni for being the most wonderful lab friends I could ask for. To all my other incredible friends who have made my years in Oxford an unforgettable experience. Lien, James, Olivia, Olivia, Tatiana, Anna, Shiva, Laura, Jehan, Edyta, Caitlin, Janak, everyone in OUNC and at Jesus College.

Thank you to my family; Clare, Steve, Madeleine, Isabelle, Charlie and George – I love you and could not have done this without you.

Table of contents

Chapter 1 Introduction 1

1.1 Overview 1
1.2 Global trends in motherhood 2
1.3 The ovary and its structure 3
1.4 Oogenesis and folliculogenesis 4
1.5 Follicle development 4
1.5.1 Initial recruitment and activation 7
1.5.2 Preantral follicle growth 7
1.5.3 Antral follicle development 8
1.5.4 Ovulation and corpus luteum formation 10
1.6 Atresia 11
1.7 Meiosis, nuclear and cytoplasmic maturation 12
1.8 Factors involved in follicle development 14
1.8.1 Hormonal regulation 14
1.8.2 Oocyte-secreted factors: GDF-9 and BMP-15 18
1.8.3 Other signalling factors 19
1.9 The epigenome 19
1.9.1 Epigenetic modifications as drug targets 21
1.10 The aging follicle 22
1.10.1 Insights from assisted reproductive techniques 22
1.10.2 Oocyte changes 24
1.10.3 Cumulus changes 26
1.10.4 Existing treatments for maternal age in assisted reproductive techniques 27
1.11 Growth and development of human follicles *in vitro* 30
1.11.1 Culture from the primordial stage 30
1.11.2 Culture from the preantral stage 34
1.12 Use of cryopreserved human ovarian tissue for research 36
1.12.1 Source of tissue 36
1.12.2 Advantages and rationale for using cryopreserved tissue 37
1.13 Rationale and research questions 40

Chapter 2 Materials and methods 41

2.1 Human ovarian tissue samples 41
2.1.1 Patients and ethical approval 41
2.1.2 Sourcing tissue from the Oxford Cell and Tissue Biobank 42
2.1.3 Inclusion and exclusion criteria for studies using cryopreserved cortical tissue 42
2.1.4 Information on patient characteristics 42

2.2 Collection and cryopreservation of ovarian tissue 43
2.3 Thawing of cortical strips 44
2.4 Human cortical strip culture 45
2.4.1 Preparation of cortical strip tissue for culture 45
2.4.2 Set up and culture of tissue 47
2.4.3 Tissue fixation before or following culture 47
2.5 Visualisation of follicles with Neutral Red 47
2.6 Histological processing 48
2.6.1 Dehydration 48
2.6.2 Embedding 49
2.6.3 Sectioning 49
2.6.4 Haematoxylin-eosin staining 50
2.7 Assessment of follicle health and development 50
2.7.1 Classification of developmental stage 50
2.7.2 Classification of follicle health 52
2.8 Calculation of follicle density 54
2.9 Imaging 54
Chapter 3 Establishing a culture method for cryopreserved human ovarian cortical tissue 55
3.1 Introduction 55
3.1.3 Aims and hypotheses 57
3.2 Note to the reader 57
3.3 Materials and methods 57
3.3.1 Human cortical strip culture 57
3.3.2 Processing and histology 58
3.3.3 Validation of sampling interval for density 58
3.3.4 Statistical analysis 60
3.4 Results 60
3.4.1 Sampling interval for density calculation 60
3.4.2 Patient characteristics 61
3.4.3 Number of growing follicles in non-cultured cryopreserved tissue varies between patients 64
3.4.4 Follicle health varies between patients in non-cultured cryopreserved tissue 66
3.4.5 Follicle health, but not development is greater in non-cultured tissue selected by neutral red staining 67
3.4.6 Cultured cryopreserved tissue has a dominant population of growing follicles in all patients 68
3.4.7 Neutral red selected tissue has superior follicle health post-culture 69
3.4.8 Follicles grown in culture have asymmetric granulosa cell distribution 71
3.5 Discussion 72

Chapter 4 Investigating the effect of LSD1 inhibition on human follicle development 81

4.1 Introduction 81

4.1.2 Aims and hypotheses 83

4.2 Materials and methods 84

4.2.1 Preliminary experiment with tissue from a single patient 84
4.2.2 Dose response experiment with multiple patients 84
4.2.3 Processing and histology 85

4.3 Results 86

4.3.1 Preliminary experiment with tissue from a single patient 86
4.3.2 Dose response experiment with multiple patients 89

4.4 Discussion 99

Chapter 5 Exploring methods to visualise follicles in human ovarian cortex 105

5.1 Introduction 105

5.1.1 Aims and hypotheses 107

5.2 Materials and methods 107

5.2.1 Processing of cortical tissue for incubation with Neutral Red 107
5.2.2 Staining of fixed tissue to identify follicles 108

5.3 Results 109

5.3.1 Identification of follicles in unstained tissue 109
5.3.2 NR staining can be observed in tissue after 1 hour 110
5.3.3 Dewaxing and rehydration of fixed cortical tissue 113
5.3.4 Partial or complete haematoxylin staining 114

5.4 Discussion 116

Chapter 6 Analysing methods of human cortical strip culture 119

6.1 Introduction 119

6.1.2 Aims and hypotheses 121

6.2 Materials and methods 121

6.2.1 Patient information 121
6.2.2 Human cortical strip culture 122
6.2.3 Processing and histology 124
6.2.4 Statistical analysis 124

6.3 Results 125

6.3.1 Patient characteristics 125
6.3.2 Experimental conditions and number of follicles analysed 126
6.3.3 Distribution of follicles across health parameters 128
6.3.4 Effect of culture condition of follicle health 129
6.3.5 Effect of culture condition on follicle development 131

6.4 Discussion 140

Chapter 7 Identifying differential gene expression with maternal age in cumulus cells using RNA-seq 148

7.1 Introduction 148

7.1.1 Aims and hypotheses 149

7.2 Materials and methods 149

7.2.1 Ethical approval 149
7.2.2 Inclusion and exclusion criteria 150
7.2.3 Information on patient characteristics 150
7.2.4 Cumulus cell collection for sequencing 150
7.2.5 RNA-sequencing 151
7.2.6 RNA-seq data analysis 154
7.2.7 Validation of RNA-seq with real time-polymerase chain reaction 156

7.3 Results 158

7.3.1 Older patients have higher basal FSH and a lower peak level of oestradiol 158
7.3.2 Mapping metrics 159
7.3.3 Data exploration and normalisation 160
7.3.4 Cumulus cell samples cluster based on age and show significant differences in gene expression 164
7.3.5 Genes encoding enzymes and transcription regulators are differentially expressed with age 166
7.3.6 Gene ontology analysis reveals enrichment of biological process terms 167
7.3.7 Age-associated differentially expressed genes are associated with several putative upstream regulators 170
7.3.8 RT-PCR data agrees with RNA-seq gene expression 174
7.3.9 Variation in differentially expressed genes between studies highlights heterogeneity of maternal age effects 175

7.4 Discussion 177

Chapter 8 Discussion 185

8.1 Novel findings from this thesis 186
8.2 Future treatments for age-related infertility 189
8.3 Barriers to progress 192
8.4 Final remarks 194

References 195

Appendix I. *Variation in follicle health and development in non-cultured tissue prior to LSD1 treatment* 213

Appendix II. *Medium composition of McCoy's 5A and αMEM* 214

Appendix III. *Identifying the optimal method for RNA extraction* 216

Appendix IV. *RNA-seq differentially expressed gene list* 223

Appendix V. *Gene ontology analysis* 229

Appendix VI. *Top 600 differentially expressed genes* 232

List of abbreviations

αMEM	Alpha Minimal Essential Medium
17β HSD	17β-Hydroxysteroid Dehydrogenase
2D	Two-Dimensional
3D	Three-Dimensional
AH	αMEM High Volume
Akt	Protein Kinase B
AL	αMEM Low Volume
AMH	Anti-Müllerian Hormone
AMHKO	Anti-Müllerian Hormone Knock Out
AP	αMEM Permeable
AR	Androgen Receptor
ART	Assisted Reproductive Techniques
ASE	Allele-Specific Gene Expression
Bcl-2	B-Cell Lymphoma 2
BCV	Biological Coefficient of Variation
BMI	Body Mass Index
BMP15	Bone Morphogenetic Protein 15
BMP4	Bone Morphogenetic Protein 4
BMP6	Bone Morphogenetic Protein 6
BMP7	Bone Morphogenetic Protein 7
BMPR2	Bone Morphogenetic Protein Receptor Type 2
CACNA1	Calcium Voltage-Gated Channel Subunit Alpha 1
cAMP	Cyclic Adenosine Monophosphate
CC	Cumulus Cell
CCN2	Connective Tissue Growth Factor
cDNA	Complementary DNA
ChIP	Chromatin Immunoprecipitation
CI	Confidence Interval
COC	Cumulus Oocyte Complex
CpG	5'—C—Phosphate—G—3'
CPM	Counts Per Million
CYP11A1	Cytochrome P450 Family 11 Subfamily A Member 1
CYP19	Aromatase
DGE	Differential Gene Expression

DHEA	Dehydroepiandrosterone
DMSO	Dimethyl Sulfoxide
DNA	Deoxyribonucleic Acid
EBSS	Earle's Balanced Salt Solution
ECM	Extracellular Matrix
EGF	Epidermal Growth Factor
ERα	Oestrogen Receptor α
ERs	Oestrogen Receptors
ERβ	Oestrogen Receptor β
FAD	Flavin Adenine Dinucleotide
FDR	False Discovery Rate
FGF	Basic Fibroblast Growth Factor
FOXO1	Forkhead Box Protein O1
FSH	Follicle-Stimulating Hormone
FSHR	Follicle Stimulating Hormone Receptor
GDF-9	Growth Differentiation Factor 9
GLM	Generalized Linear Model
GnRH	Gonadotrophin-Releasing Hormone
GO	Gene Ontology
GSK-LSD1	GlaxoSmithKline - Lysine Specific Demethylase 1
GV	Germinal Vesicle
H1	Histone 1
H2A	Histone 2A
H2B	Histone 2B
H3	Histone 3
H3K4	Lysine 4 Of Histone 3
H3K9	Lysine 9 Of Histone 3
H4	Histone 4
HAS	Hyaluronan Synthase
HIF-1A	Hypoxia-Inducible Factor 1-Alpha
hMG	Human Menopausal Gonadotrophin
HPG	Hypothalamic–Pituitary–Gonadal
ICM	Inner Cell Mass
ICSI	Intracytoplasmic Sperm Injection
IGFBP	Insulin-Like Growth Factor Binding Protein
IGF	Insulin-Like Growth Factor

IPA	Ingenuity Pathway Analysis
ITS	Insulin, Transferrin and Selenium
IVF	*In Vitro* Fertilisation
IVM	*In Vitro* Maturation
KGF	Keratinocyte Growth Factor
KIT	Stem Cell Factor
KITL	Kit Ligand
LH	Luteinising Hormone
LHR	Luteinising Hormone Receptor
LncRNA	Long Non-Coding RNA
LSD1	Lysine-Specific Demethylase 1
MAO-A	Monoamine Oxidase A
MAO-B	Monoamine Oxidase B
MCM	Minichromosome Maintenance Protein
MDS	Multidimensional Scaling
MH	McCoy's 5A High Volume
MI	Meiosis I
MII	Meiosis II
ML	McCoy's 5A Low Volume
MMPs	Matrix Metalloproteinases
MP	McCoy's 5A Permeable
MRD	Minimal Residual Disease
mtDNA	Mitochondrial DNA
mTORC1	Mechanistic Target of Rapamycin Complex
NAD+	Nicotinamide Adenine Dinucleotide Oxidized
NADH	Nicotinamide Adenine Dinucleotide Reduced
NGS	Next Generation Sequencing
NHS	National Health System
NR	Neutral Red
NR2F2	Nuclear Receptor Subfamily 2 Group F Member 2
NRES	National Research Ethics Service
OCTB	Oxford Cell and Tissue Biobank
OR	Odds Ratio
PA	Preantral
PADIs	Peptidyl Arginine Deiminases
PCNA	Proliferating Cell Nuclear Antigen

PET	Per Embryo Transfer
PGC-1α	Peroxisome Proliferator-Activated Receptor Gamma Coactivator 1 alpha
PGC	Primordial Germ Cell
PGR	Progesterone Receptor
PGT	Preimplantation Genetic Testing
PI3K	Phosphatiddylinositol 3 Kinase
PPARGC1	Peroxisome Proliferator-Activated Receptor Gamma Coactivator 1 alpha
PR-A	Progesterone Receptor-A
PR-B	Progesterone Receptor-B
PTC	Per Treatment Cycle
PTEN	Phosphatase and Tensin Homolog
PTX3	Pentraxin 3
QC	Quality Control
RIN	RNA Integrity Number
RNA	Ribonucleic Acid
RT	Reverse Transcription
RT-PCR	Real Time-Polymerase Chain Reaction
RYR2	Ryanodine Receptor 2
SOP	Standard Operating Procedure
TE	Trophectoderm
TGF-β	Transforming Growth Factor Beta
TIMPs	Tissue Inhibitors of Metalloproteinases
UK	United Kingdom
URA	Upstream Regulator Analysis
US	United States
VEGF	Vascular Endothelial Growth Factor
WGCNA	Weighted Gene Co-Expression Network Analysis
WHG	Wellcome Centre For Human Genetics
YAP	Yes-Associated Protein

Chapter 1

Introduction

1.1 Overview

Age is the most significant determinant of natural conception and the past decade has seen a steady increase in the average age of first-time parents (1). A substantial shift in the age at which women have fertility treatment reflects the trend in childbearing age in the general population. The impact of age on success with assisted reproductive techniques (ART) is discussed later in Section 1.9. Approximately two-thirds of patients receiving *in vitro* fertilization (IVF) treatment in the United States (US) and the United Kingdom (UK) are over 35 (2, 3). Current assisted reproductive technologies are unable to circumvent the age-related decline in female fertility without the use of donor oocytes. The primary reason for poorer pregnancy outcomes in older women is due to a decrease in oocyte number and quality – two factors that cannot yet be controlled or changed. Therefore, a central challenge for the field is understanding how aging impacts egg quality in order to determine a means to increase the number of available high-quality eggs for all women undergoing IVF, and especially for those with advanced chronological age.

1.2 Global trends in motherhood

The percentage of live births to mothers over the age of 35 years in the UK rose from 8.7% in 1990 to 19.3% in 2004, and the average age of first time mothers exceeded 30.0 years in 2013 (1). Similar trends have been observed in the US with the average maternal age increasing by over two-and-a-half years in the past two-and-a-half decades (4, 5). The frequency of first births to women over the age of 35 years in the United States rose from 1 in 100 women in 1970 to approximately 1 in 12 in 2006 (4, 6). In 2016, the average age of European women at the birth of their first child was 29.0 years; Ireland, Greece, Luxembourg, Spain, Switzerland, and Italy all had an average age at first child above 30 years (7).

The Royal College of Obstetricians and Gynaecologists in the United Kingdom declared that "later maternal age is an emerging public health issue" bringing with it new challenges (8). Despite this, there is a wide misconception of fertility enduring irrespective of age. A 2011 study surveyed 3345 childless women in Canada between the ages of 20 and 50 years. The statement 'For women over 30, overall health and fitness level is a better indicator of fertility than age' was incorrectly marked as 'True' by 72.9% of respondents. Of the same cohort 90.9% incorrectly believed: 'Prior to menopause, assisted reproductive technologies (such as IVF) can help most women to have a baby using their own eggs' when, as discussed in the following sections, this is age dependent (9). A recent study of Australian university students aged 18-30, mirrored these responses with over 75% of participants underestimating the impact of female age on fertility (10). This highlights a need for better education of the public with respect to fertility, and the market for a treatment that mitigates the effects of age on fertility.

1.3 The ovary and its structure

In women as in other female mammals, the two ovaries house female gametes, oocytes, and are functionally homologous to the testes in the male. Ovaries are small almond-shaped structures housed in the pelvis, each with a weight of around 2-4 grams. The outermost layer of the ovary is a simple squamous mesothelium called the ovarian surface epithelium, or germinal epithelium (11). Lying underneath the epithelial layer is the tunica albuginea, a dense layer of connective tissue which overlays the ovarian cortex.

Cortical tissue is comprised of fibroblasts and fibres of collagen and elastin, and is characterised by its dense, rigid structure. The cortex is the site of primordial follicles, those at the earliest stage of development, and the rigid physical environment structure is essential for the early stages of preantral follicle development (see Section 1.5.2). The importance of this physical environment is evidenced by the successful development of primordial follicles *in vitro* when encapsulated in a rigid biomaterial, compared to the otherwise poor survival of isolated follicles at this stage (discussed further in Section 1.11) (12). Follicle distribution in the cortex of human ovaries is extremely heterogeneous. The density of primordial follicles between different pieces of cortex from the same ovary can vary by greater than two orders of magnitude (13). In young girls the cortex is heavily populated by follicles which, with age, are largely replaced by collagen fibres due to ovulation and follicle atresia (14). The inner most fraction of the ovary is the ovarian medulla containing blood and lymphatic vessels (see Figure 1.1, page 5) (11). Follicles at more advanced stages of development are primarily found in the less dense medullary region (15).

An oocyte and its surrounding follicular cells constitute a follicle, the functional unit of the ovary. The pool of follicles is established before birth and declines across a female's

reproductive life. There is a steady decline in follicle number across childhood and adulthood and culminates with the onset of menopause when approximately 1000 follicles remain (16, 17). In recent years the purported existence of oocyte stem cells has challenged the dogma that the ovarian reserve is finite (18, 19). While there is some evidence that a limited population of oogonial stem cells may exist in adult ovaries it remains unclear what contribution, if any, the small number of putative oocyte stem cells has on the reproductive life span of individuals (20, 21).

1.4 Oogenesis and folliculogenesis

Primordial germ cells become oogonia when they arrive in the gonadal ridge from the yolk sac endoderm around the 7th week of gestation (22). They proliferate by mitosis before differentiating into primary oocytes. Some oogonia begin transformation into primary oocytes and enter the first stages of meiosis at around 11–12 weeks of gestation (23). Human foetal ovaries contain millions of germ cells, with a peak in numbers at around 20 weeks gestation (24). Germ cells may degenerate before ovarian follicles are formed, regulating the number of primordial follicles present in the ovaries. Primordial follicle formation, when oocytes become enclosed in a single layer of flattened pre-granulosa cells, begins around mid-gestation and continues until just after birth (25). Oocytes that are not enclosed in pre-granulosa cells undergo atresia, most likely via apoptosis (26). Germ cell numbers decrease leading up to birth, and with 300,000 to 400,000 remaining it is believed to be less than 20% of the maximal number reached in gestation (24, 27).

1.5 Follicle development

Guidance for the developmental staging of ovarian follicles was first proposed for the mouse (28) and subsequently adapted to the human (Figure 1.1) (29).

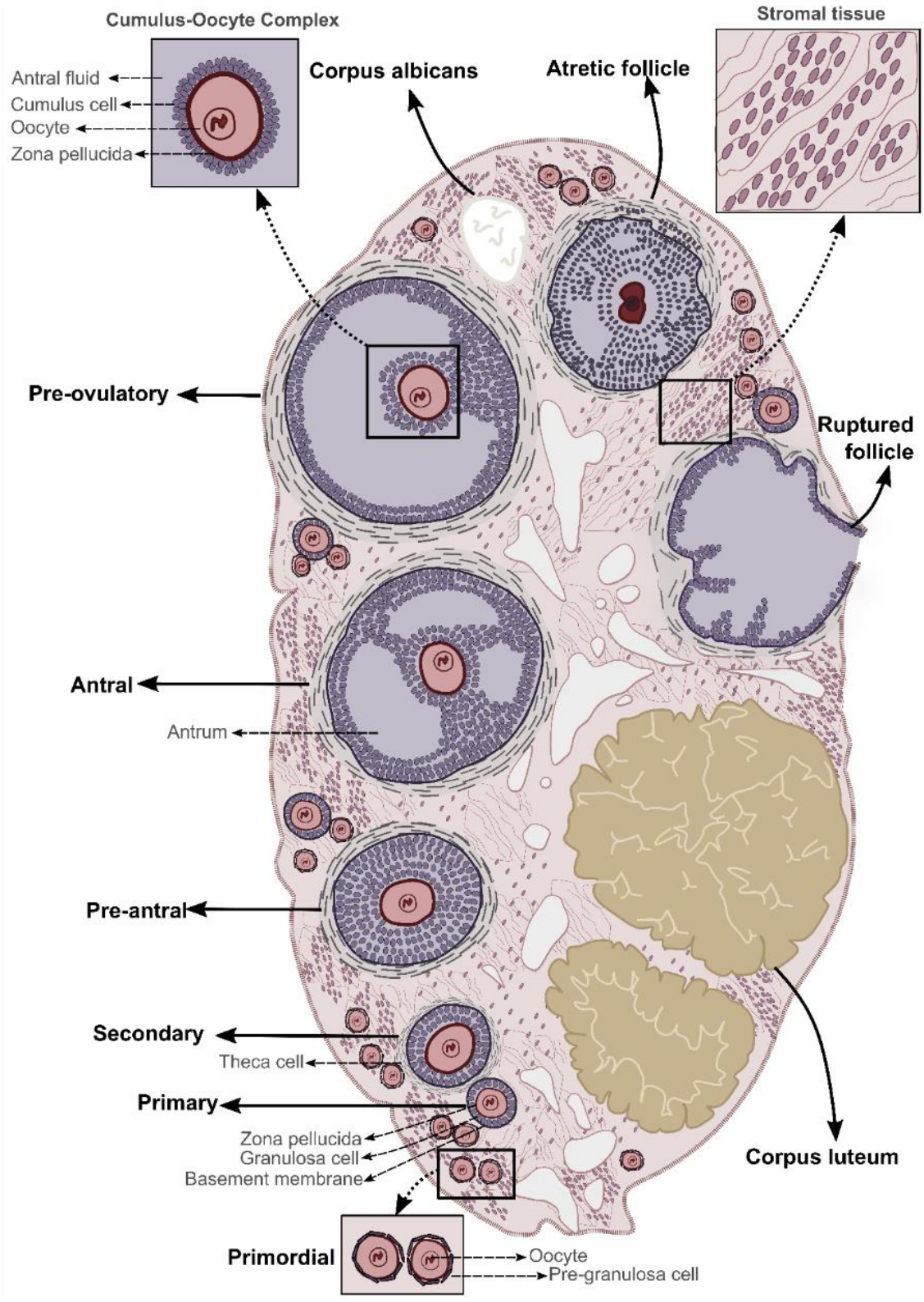


Figure 1.1 Follicle development in the human ovary

Follicles start at the primordial stage, progressing through the primary, secondary, pre-antral, antral, and preovulatory stages before ovulation. Across this period pre-granulosa cells become cuboidal and proliferate, oocytes develop a glycoprotein layer (zona pellucida), basement membrane, and theca cell layer. After rupture the remaining follicular cells form a corpus luteum, which regresses to a corpus albicans. Follicles may undergo atresia at any stage between the primordial and pre-ovulatory stage.

Follicle development is characterised by massive growth of both the oocyte and its associated follicle (Table 1.1).

Table 1.1 Changing oocyte and follicle diameter in human follicles across follicle development *in vivo* from the primordial to the pre-ovulatory stage (30, 31)

Follicle stage	Primordial	Primary	Secondary to preantral	Early antral to antral	Pre-ovulatory
Follicle diameter (mm)	0.026-0.040	0.040-0.070	0.114-0.302	0.2-10	17-20
Oocyte diameter (μm)	36	40-73	73-120	~120	~120

Follicle development is initiated at the primordial follicle stage, followed by follicle growth, selection of a dominant follicle, ovulation and luteinisation. *In vivo* follicle development occurs over a protracted period, the estimated duration of various stages is detailed in Figure 1.2.

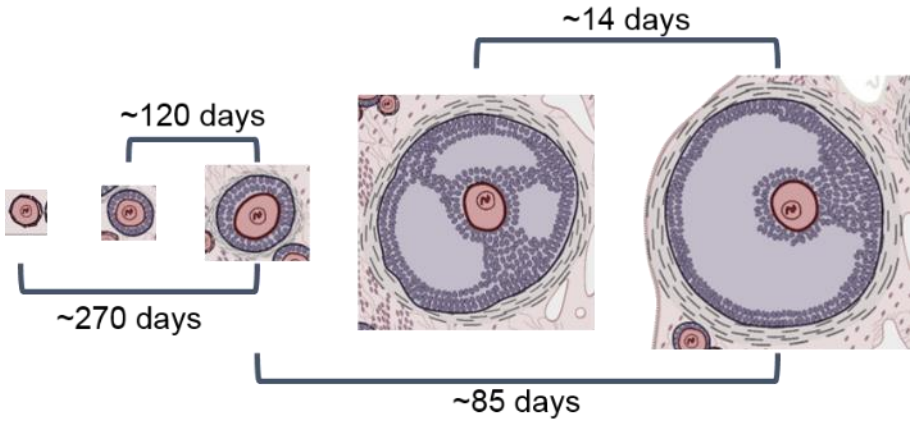


Figure 1.2 Estimated timeline of follicle development in humans

The timeframe over which follicle development occurs is considerable and is believed to be around 270 days from the primordial to the secondary stage (31). It is estimated that more than 120 days are required for follicles to develop from the primary to the secondary stage (32), and longer still for primordial follicles to activate and reach the primary follicle stage (29). More than 85 days are needed for follicles to develop from the late secondary through to the preovulatory stage (32). Progression from the antral to preovulatory stage is comparatively quick, occurring across the 14-day follicular phase of the menstrual cycle.

1.5.1 Initial recruitment and activation

Recruitment starts with the follicles at the innermost part of the ovarian cortex. Primordial follicles can remain arrested in a meiotically quiescent state in the ovarian cortex for many years before recruitment for follicle development, by contrast some are activated immediately after formation. This recruitment is believed to be a continuous process that commences after follicle formation. As described previously, oocytes that do not become enclosed by granulosa cells are believed to degenerate (33).

Initiation of follicle growth includes oocyte growth (Table 1.1) as well as transformation of the single layer of flattened, squamous cells into cuboidal granulosa cells which proliferate by mitosis (Figure 1.1) (34, 35). Primordial follicle recruitment occurs independently of gonadotrophins and is instead believed to be regulated by local ovarian factors, discussed in Section 1.8.3. The intermediary stage where follicles are surrounded by a combination of flattened and cuboidal granulosa cells are classed as transitional follicles (Figure 1.1) (34). Follicle with a single layer of cuboidal granulosa cells are referred to as primary follicles. At this stage a glycoprotein layer forms between the oocyte and granulosa cells in the perivitelline space, called the zona pellucida, as well as a basement membrane enclosing the follicle outside the granulosa cell layer (Figure 1.1) (36). Cytoplasmic processes from the granulosa cells transverse the zona pellucida to maintain intercellular contact via gap junctions (37, 38). It has recently been revealed that in mice these structures are specialised filopodia which are locally remodelled in response to oocyte-derived signals (38).

1.5.2 Preantral follicle growth

From the primary stage the oocyte continues to grow (see above Table 1.1) and the granulosa cells proliferate to form multiple granulosa cell layers (36). Secondary follicles are oocytes surrounded by two complete layers of granulosa cells. Further oocyte growth coupled with granulosa cell proliferation leads to the formation of a preantral follicle (39).

It is around the secondary follicle stage that theca cells begin to emerge and form a layer around the granulosa-oocyte structure outside the basement membrane (see Section 1.5.2.1) (40). Preantral follicle growth is gonadotrophin responsive but independent and regulated by crosstalk between the oocyte and granulosa cells.

1.5.2.1 Theca cell development

Theca cells are vital components of the follicle providing both structural support and necessary substrates for oestradiol production by the granulosa cells as they are the site of androgen production in the ovary (41). Fibroblast-like precursor cells from within the stroma near the basal lamina become aligned parallel to one another, forming the theca cell layer (42-44). Theca cells are first observed when follicles have two or more layers of granulosa cells which coincides with the period when theca cells become responsive to luteinising hormone (LH) (40). However, putative theca cell precursors do not express LH receptors and are not LH responsive indicating that theca cell differentiation is gonadotrophin independent (40). It is presumed that since theca cells are only associated with growing follicles, they are recruited in response to signals or factors produced by the follicle. Little is known about the factors underlying theca cell recruitment and it is unclear whether the cells surrounding the follicle differentiate into the theca layer or whether they are recruited from the stroma to form the theca layers.

1.5.3 Antral follicle development

As the follicular cells continue to proliferate, granulosa cells secrete a viscous fluid that creates small fluid-filled spaces which finally coalesce to form a single central cavity known as the antrum (29, 45). This fluid filled space is the hallmark of an antral follicle which also consists of a fully-grown oocyte, several layers of granulosa cells, and well differentiated thecal layers. Antral fluid contains a wide range of molecules such as steroid hormones,

electrolytes and enzymes and plays an important role in mediating signals between the different cell types of the follicle (46).

Once a follicle transitions through the pre-antral stage its development switches from being gonadotrophin responsive to gonadotrophin-dependent. Although follicle stimulating hormone (FSH) receptors are expressed in follicles prior to gonadotrophin-dependence, FSH does not play an essential role in follicle growth until the antral stage (47, 48). It is at this stage that FSH and LH receptors are further up-regulated, and gonadotrophins are required for further follicle growth (48).

Antrum formation is also the catalyst for the granulosa cells to differentiate into two subpopulations; the inner cells that surround the oocyte are termed cumulus cells which continue to proliferate and respond to FSH. The outer mural granulosa cells stop dividing and those in the dominant follicle continue to express P450 aromatase and LH receptors (49, 50). Cumulus cells express many of the same genes as granulosa cells, reflecting their shared origin, with some distinct aspects related to cellular functions such as cell communication, extracellular matrix, steroid receptor activity and inflammatory responses (51). Mural granulosa cells have higher expression of CYP11A1, whilst androgen receptor expression is higher in cumulus cells (51, 52). There is variation in the gap junction proteins expressed with gap junction alpha-1 protein (GJA1) and GJA5 more highly expressed in cumulus compared to granulosa cells (51, 52). Cumulus cells have a high expression of plasma membrane calcium-transporting ATPases, RYR2, and CACNA1 which play a critical role in intracellular calcium regulation and homeostasis (51, 53, 54). By contrast, fibrinogen is selectively expressed in mural granulosa cells supporting its postulated role in the clotting process following tissue rupture at ovulation (55, 56).

Cumulus cells provide the physical support and microenvironment required for oocyte maturation during the later stages of follicular growth (57). Cumulus cells supply nutrients and relay endocrine signals through an extensive network of inter-cellular connections (37), and in turn, the oocyte responds and regulates its surrounding microenvironment by secreting factors that influence cumulus cells function (58-60). This bi-directional communication between the oocyte and its surrounding layers of cumulus cells is essential for oocyte competence. Studies in rodent models highlight the mutual dependency of the oocyte and cumulus cells; cumulus expansion is inhibited in the absence of an oocyte, similarly oocytes with intact cumulus cells are required to yield viable offspring at rates comparable to *in vivo* derived oocytes (57, 59). Furthermore, there is evidence that the transcriptome of human oocytes matured *in vitro* with mature cumulus cells from the same patient more closely mirrors those of *in vivo* derived oocytes (61).

1.5.4 Ovulation and corpus luteum formation

Ovulation is a highly specialised process that culminates in the release of a mature oocyte capable of fertilisation, from a pre-ovulatory (or Graafian) follicle. It involves the coordination of many different cell types within the follicle; mural granulosa, cumulus, and theca cells, as well as stromal cells and those of the ovarian surface epithelium (62).

The preovulatory follicle ruptures in response to the surge of luteinising hormone (LH), releasing the oocyte and surrounding cumulus cells into the Fallopian tube. The LH surge initiates the process of ovulation by reactivating oocyte meiosis, generating tissue restructuring and inducing the expansion of the cumulus-oocyte complex which is closely associated with the breakdown of gap junction communication (63, 64). Cumulus cells lack LH receptors and are unresponsive to LH, instead the effects of LH are mediated through EGF-like growth factors produced by the mural granulosa cells (65). EGF-like growth factors induce the production of cumulus matrix proteins, such as pentraxin 3 (PTX3) and

hyaluronan synthase 2 (HAS2) by the cumulus cells, which cause cumulus oocyte complex expansion. Cumulus expansion is initiated under the control of several endocrine and oocyte-derived factors including growth and differentiation factor 9 (GDF9) and bone morphogenetic protein 15 (BMP15) (66-68). Cumulus expansion is essential for oocyte maturation and ovulation, for effective transportation of the oocyte through the Fallopian tubes and for successful fertilization (69, 70).

The LH surge also induces breakdown of the basal lamina, and granulosa and theca cell luteinisation, resulting in the formation of a corpus luteum in the residual follicular space. This highly vascularised endocrine gland produces progesterone at high rates to support any subsequent pregnancy. In the absence of a pregnancy, the corpus luteum undergoes luteolysis, a functional and structural regression of the gland, whereby progesterone production ceases and the cells within the corpus luteum undergo various forms of cell death (71).

1.6 Atresia

Atresia is the most common fate of follicles as more than 99.9% of the ovarian follicles present at birth never reach ovulation (29). Follicles undergo atresia during oogenesis (Section 1.4) and at various stages of development. During follicle development, rates of atresia increase, and subsequently most follicles observed are at the early stages of development. The highest incidence of atresia occurs at the antral follicle stage, with preantral and preovulatory follicles rarely undergoing atresia (72).

Antral follicle attrition is believed to be primarily due to granulosa cell apoptosis. Apoptosis, also known as programmed cell death, is thought to be caused by the reduction in anti-apoptotic factors (e.g. oestrogen, gonadotrophins) or the increase of pro-apoptotic

factors (e.g. androgens), death ligand-receptor systems and members of the B-cell lymphoma 2 protein family (Bcl-2) (73). It is characterised by a series of morphological changes, including condensing of nuclear material (pyknosis) and fragmentation (karyorrhexis), as well as plasma membrane blebbing (74). Compared to our understanding of survival at later stages of follicle development, relatively little is known about the regulation of survival of preantral follicles in humans (75). Studies in rat and bovine models suggest two patterns of atresia in follicles; one in which the oocyte degenerates while granulosa cells remain intact, observed primarily in preantral follicles, and another in which the granulosa cells show signs of extensive degeneration while the oocyte remains initially unaffected, observed primarily in antral follicles (76, 77). A recent study by Meng and colleagues suggests that activation of different cell death pathways is the root of this difference, with preantral follicle atresia being mediated mainly by autophagy rather than apoptosis (78). Autophagy, generally considered a protective response, is used primarily for cellular adaptation to limited nutrient resources. Damaged proteins and organelles are broken down and recycled by the cell for reuse (74).

1.7 Meiosis, nuclear and cytoplasmic maturation

During foetal development, germ cells enter meiosis and progress through leptotene (chromosome condensation), zygotene (beginning of synapsis) and pachytene (complete synapsis and recombination), before arresting at the diplotene stage of Prophase I. Oocytes remain in this state of meiotic arrest throughout follicular development and the completion of the first division can thus occur years later just before ovulation. As such, for some oocytes this state will be maintained from mid-gestation to the onset of menopause.

Prior to the first meiotic cell division, the oocyte nucleus is known as the germinal vesicle (GV) and the oocyte itself as a GV oocyte. The GV breaks down when the oocyte enters

metaphase I of meiosis I (MI). Throughout follicular development, the oocyte slowly gains the competency for nuclear and cytoplasmic maturation, but it is only following the LH surge of ovulation that meiosis is resumed in the oocyte. A meiotic spindle assembles which aligns the chromosomes in metaphase of MI. Completion of MI involves the separation of homologous chromosomes from one another (Figure 1.3). One set of homologous chromosomes is extruded in the first polar body and the other remains in the oocyte. The oocyte then enters the second meiotic division and arrests again at metaphase II (MII). The second division is only completed once the egg is fertilised. During anaphase II the cleavage of centromeric cohesion allows separation of the sister chromatids which segregate into the egg and second polar body (Figure 1.3). This entire process is referred to as nuclear maturation.

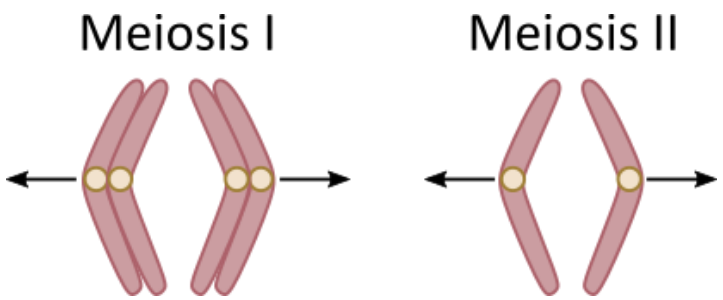


Figure 1.3 Meiosis in human oocytes

A normal meiosis I (MI) division results in the segregation of homologous chromosomes. A normal meiosis II (MII) division involves the segregation of sister chromatids. Arrows indicate direction of movement.

Ovarian stimulation protocols generate predominantly mature MII oocytes, those that have successfully completed MI and have arrested in MII, ready for fertilisation (79, 80). However, germinal vesicle stage oocytes are frequently obtained and are only evident once stripped of cumulus cells. When stripped and cultured in appropriate medium these oocytes show a high incidence of resumption and completion of nuclear maturation.

Unlike nuclear maturation which can be followed under a light microscope, cytoplasmic maturation cannot be observed in the same way. Cytoplasmic maturation involves the accumulation of mRNA, proteins, substrates, and nutrients, all of which are required for the oocyte to be developmentally competent (81, 82). In particular, large amounts of RNA are stored in the cytoplasm and there is a dramatic increase in the number of mitochondria (83). Organelles are formed and reorganised, and lipids, granules, and proteins required for the formation of new membranes are stored (84).

1.8 Factors involved in follicle development

1.8.1 Hormonal regulation

The Hypothalamic-Pituitary-Gonadal (HPG) axis is the feedback loop that exists between the hypothalamus, anterior pituitary, and gonads, and is primarily involved in the regulation of fertility. The pulsatile release of gonadotrophin-releasing hormone (GnRH) from the hypothalamus stimulates the anterior pituitary to secrete LH and FSH into the circulation (85-87). Circulating levels of FSH and LH are regulated via positive and negative feedback mechanisms by other hormones such as oestrogen, progesterone, activins, inhibins and Anti-Müllerian hormone (AMH), discussed below.

1.8.1.1 Gonadotrophins

The gonadotrophins FSH and LH share a common α subunit, but differing β subunits, the latter of which confers receptor specificity (88). Oestrogen regulates FSH and LH release, via regulation of the frequency of GnRH pulsatile release by the hypothalamus. Low oestrogen levels feedback to lower the frequency of GnRH release, which promotes the production of FSH by the pituitary. Conversely, high oestrogen levels increase the pulse frequency of GnRH release, which promotes LH release and suppresses FSH release by the pituitary gland (89, 90). Progesterone also regulates LH release via regulation of GnRH

pulse frequency, in the presence of oestrogen (91). FSH is modulated by several members of the transforming growth factor beta (TGF-β) superfamily (92); inhibin A and B inhibit production and release (93), activin A, AB and B promote production and release (94), BMP4 inhibits production and the effects of activin, and BMP6, BMP7 and BMP15 promote production (95).

The receptors for FSH and LH are found on granulosa and theca cells, respectively. The two-cell, two-gonadotrophin theory describes the role of and cooperation between theca and granulosa cells in oestrogen production (Figure 1.4). In theca cells, under the influence of LH, cholesterol is converted to pregnenolone and metabolised through a series of substrates ending in androgen production. The two-cell dynamic comes into play when the androgens synthesised by the theca cells are transported to granulosa cells where they are converted to estrone and 17b-oestradiol by P450 aromatase (96).

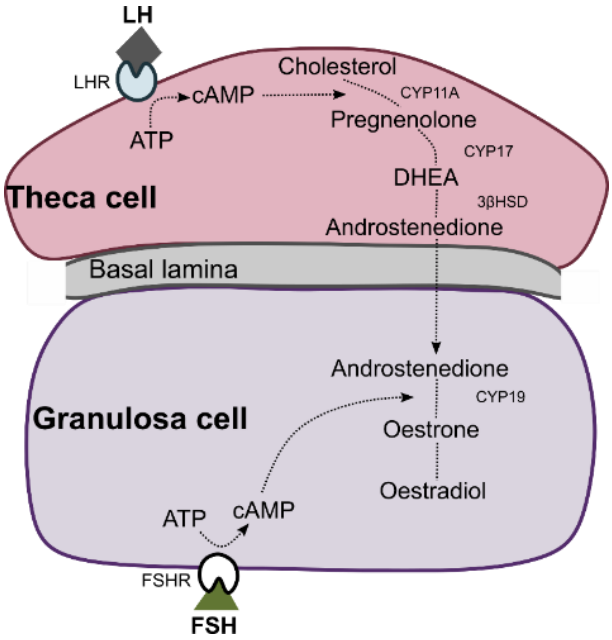


Figure 1.4 Two-cell, two-gonadotrophin model for follicular steroid production

Luteinising hormone (LH) binds to LH receptors (LHR), which stimulates the adenylyl cyclase pathway (cAMP pathway), leading to the production of androstenedione from cholesterol, via the sequential production of pregnenolone and dehydroepiandrosterone (DHEA). Androstenedione diffuses through the basal lamina, into the granulosa cells. Here, upon follicle stimulating hormone (FSH) binding to the FSH receptor (FSHR), activation of the cAMP pathway stimulates production of aromatase (CYP19), which aromatises androstenedione into oestrone. Oestrone can then be converted into oestradiol by 17β-Hydroxysteroid dehydrogenase (17βHSD).

1.8.1.2 Oestrogen

Oestrogen is produced by follicles from around the secondary stage and oestradiol, the principal oestrogen, is highest in pre-ovulatory follicles (97). Pre-ovulatory follicles have the largest number of granulosa cells present and can aromatise androgens readily (98). Oestrogen also has mitogenic effects on granulosa cells (99), and acts through a positive feedback mechanism to promote follicle responsiveness to FSH and LH action, stimulating further oestrogen production (100, 101). Oestrogens act via oestrogen receptors (ERs), which have two main forms; ERα and ERβ (102). The ERβ form is the predominant form within the ovary (103, 104). The critical role both ERs have in fertility is evidenced by ERα and ERβ-specific knockout mice. ERα knockout mice are infertile due to follicle development arrest at the antral stage (105). ERβ knockout mice are subfertile due to abnormal ovulation (105, 106). The different roles performed by ERα and ERβ is further demonstrated by the used of selective agonists; ERα inhibits ovulation, likely through the HPG axis, while ERβ promotes follicle growth, decreases atresia and increases the number of oocytes ovulated (107).

1.8.1.3 Progesterone

As described earlier, progesterone is secreted by the corpus luteum that is formed following ovulation. Progesterone acts through the progesterone receptor and plays a key role in ovulation, implantation and the maintenance of pregnancy (108). The two isoforms of the progesterone receptor; PR-A and PR-B, arise from a single gene (109, 110), but have functionally different roles (111, 112). The balance of the two isoforms determines cellular responsiveness to progesterone, and i*n vitro* data suggests that PR-A is a dominant repressor of PR-B action (113, 114). It's major role in ovulation appears to be predominantly mediated through PR-A, as selective knockouts of PR-A cause infertility in mice due to anovulation (115). Histological analyses of PR-A knockout ovaries reveal

several mature anovulatory follicles (115), by contrast ovulation is not affected in PR-B knockout mice (116).

1.8.1.4 Androgens

Androgens, in particular androstenedione and testosterone, are produced in theca cells in response to stimulation by LH and are central to the production of oestradiol in the granulosa cells (Figure 1.4). Androgens play a critical role in regulating follicle development by enhancing granulosa apoptosis (99) and inhibiting FSH-stimulated LH receptor expression in granulosa cells (117), which is required for ovulation. Androgens act via the androgen receptor (AR) and have been shown to have both stimulatory and inhibitory effects on follicle development. Androgens can stimulate an increase in follicle diameter and granulosa cell proliferation in mice preantral follicles (118). Mice treated with a single injection of dihydrotestosterone, a non-aromatisable androgen, become subfertile (119). Furthermore, AR knockout mice, are subfertile, with abnormal follicle development and fewer corpus lutea (120).

1.8.1.5 Anti-Müllerian Hormone

In addition to its role in sex differentiation, AMH has also been hypothesised to play a role in inhibiting primordial follicle activation (121). AMH is first detected in the granulosa cells of primary follicles (122, 123), and reaches its highest expression levels in preantral and small antral follicles (123). The role of AMH in the ovary was revealed by studies using AMH-knockout (AMHKO) mice; in the absence of AMH, the mice have accelerated depletion of the primordial follicle pool due to increased recruitment of primordial follicles, indicating that AMH inhibits follicle activation (124). *In vitro* culture with AMH inhibits primordial follicle activation in cultured of human and mouse ovary tissue (125, 126).

1.8.2 Oocyte-secreted factors: GDF-9 and BMP-15

The oocyte plays an essential role in its own fate; however the regulatory capacity of oocyte-specific factors has only been discussed in the last two decades (127). Several oocyte-specific growth factors that play key roles in the regulation of the development of the follicles have been identified, including growth differentiation factor 9 (GDF-9), BMP-15 and BMP-6. GDF-9 and BMP-15 are essential for fertility and are expressed by oocytes from the primary stage in mice and humans right through to ovulation (128-130). Both factors significantly improve oocyte developmental competence, and act directly on the granulosa cells to effect granulosa cell proliferation and differentiation (131), cumulus expansion (132), steroidogenesis, and apoptosis (60).

GDF-9 and BMP-15 are part of the TGF-β superfamily. TGF-β ligands bind as homodimers or heterodimers to their respective transmembrane-bound serine/threonine kinase type I receptor (activin receptor-like kinase, ALK) or type II receptor, forming an oligomeric complex. The phosphorylated type I receptor phosphorylates receptor-regulated SMADs, which subsequently associate with the co-SMAD (SMAD4). The activated heterodimeric SMAD complex translocates from to the nucleus, where it regulates gene transcription. GDF-9 activates SMAD2/3 signal transducers via its type II receptor and the recruitment and phosphorylation of ALK5 (133), whereas BMP-15 activates SMAD 1/5/8 via the BMP type 2 receptor and ALK6 (134). GDF-9 knockout mice have impaired follicle progression past the primary stage (128), additionally it has been demonstrated *in vivo* that treatment of human ovarian tissue with GDF-9 promotes primary follicle progression (135). GDF-9 and BMP-15 have a high degree of amino acid homology, similar protein structure. Mouse knockout studies suggest synergistic roles for GDF-9 and BMP-15 in oocyte survival and folliculogenesis (136).

1.8.3 Other signalling factors

The oocyte is the key organiser of follicle assembly and development and it acts in concert with numerous other factors. Vascular endothelial growth factor (VEGF), other BMPs, leukaemia inhibitory factor, basic fibroblast growth factor (FGF), keratinocyte growth factor (KGF), and others are reviewed in (137-140). Pathways including the phosphatidylinositol 3 kinase (PI3K) and the mechanistic target of rapamycin complex 1 (mTORC1) pathways, have been shown to be important for primordial follicle activation (35, 141-143). KIT ligand (KITL) produced by primordial pre-granulosa and granulosa cells acts through KIT signalling as one of the major upstream mechanisms that activates the PI3K signalling pathway (144, 145). Insulin-like growth factors (IGFs) and several small-molecular weight insulin-like growth factor binding proteins (IGFBPs) are modulators of follicle development and signalling may be important in primordial follicle activation (146).

1.9 The epigenome

Additional levels of regulation exist above the level of the genome to mediate cell fate and behaviour, termed "epigenetics". Epigenetic mechanisms include post-transcriptional modifications and cause heritable changes to gene expression programs without modifying the nucleotide sequence (147). Chromosomes in our genome hold genetic information, while the epigenome is responsible for the functional use and stability of that information - linking the genotype with the phenotype (148). A differentiated cumulus cell shares the same DNA sequence as those in the granulosa cell pool it arose from, however the behaviour and function of this cell is now quite different largely due to changes in the "epigenome" or chromatin organisation of the cell.

Eukaryotic DNA is bound to small, positively charged histone proteins that package the DNA in the cell nucleus (149) (Figure 1.5). There are five types of histone proteins that

serve varying roles. Two molecules of each H2A, H2B, H3, and H4 form the octameric histone core around which 147 base pairs of DNA are wound to form a nucleosome, the functional repeating units of chromatin (150). The fifth histone, H1, wraps a further 20 base pairs and links nucleosomes by binding to linker DNA (151). The tightly wound structure results in a transcriptionally inactive, condensed chromatin state termed "heterochromatin" contrasted by the transcriptionally active, open arrangement of "euchromatin".

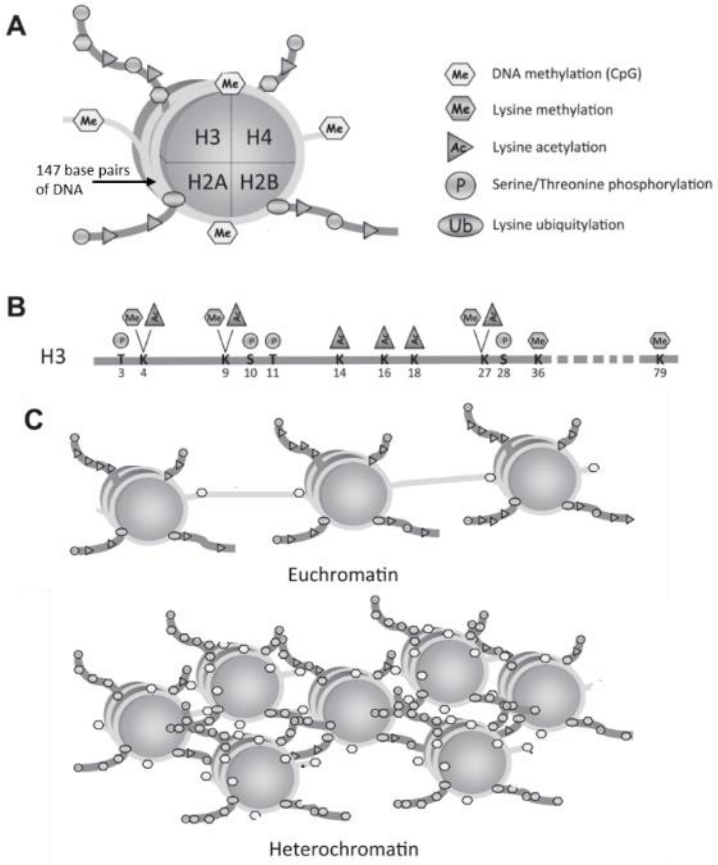


Figure 1.5 Organisation of DNA in a eukaryotic cell.

A) Diagram of a nucleosome; DNA packaging is aided by small, positively charged histone proteins that strongly bind negatively charged DNA. DNA is wound approximately 1.7 times around a single nucleosome, comprised of a hetero-octamer of histones H2A, 2B, H3 and H4. Histone tails protruding from the nucleosome core are shown with a variety of posttranslational modifications. B) Tail of histone 3 is shown with the corresponding posttranslational modifications at specific residues. C) Euchromatin is characterised by hyperacetylation of histones and hypomethylation of histones and DNA. In contrast, heterochromatin shows hypoacetylation of histones and hypermethylation of histones and DNA. (Adapted from 152).

DNA methylation, chromatin remodelling and histone modifications are the primary mechanisms that alter chromatin structure and result in differential accessibility to transcription factors in mammalian cells (153). Modification of DNA via methylation occurs primarily at CpG dinucleotides in the genome by covalent modifications of the fifth carbon in the cytosine base (147). Furthermore, unstructured amino terminal regions of the histone proteins extend beyond the nucleosome core and provide sites for post-translational modification (153). These modifications include histone acetylation and methylation.

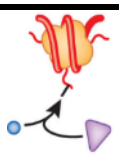
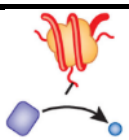
The "epigenetic" signature or "histone code" (154) is often found to be reversible and dynamically regulated, and is modulated and interpreted by so-called 'readers', 'writers', and 'erasers' (155). Enzymes that introduce post-translational histone modifications are termed 'writers' while those enzymes that remove such modifications are the 'erasers'. 'Readers' are effector proteins that are recruited to and recognize specific epigenetic marks and modifications eventually leading to changes in gene transcription (155). Some of these post-translational modifications of histone are summarised in Table 1.2.

1.9.1 Epigenetic modifications as drug targets

Over the past decade there has been a growing body of literature seeking to unpick the progressive changes to epigenetic information that accompany aging. Amongst these changes are a loss of DNA methylation (156, 157), and an imbalance of activating and repressive histone modifications (158, 159). Epigenetics represents the reversible mechanisms that occur without any alteration of the underlying DNA sequence, and 'druggable' targets that may be used to counter human aging and disease. From a clinical perspective, epigenetic modifications and enzymes have the potential to form the basis of new therapeutics as well as biomarkers. Drugs that inhibit histone deacetylases and DNA methyltransferases are approved by the FDA and have entered clinical practice in oncology,

while others are currently in development and clinical trials, comprising e.g. methyltransferases or bromodomain inhibitors (160). In addition to their clinical value, small molecular inhibitors are excellent chemical tools for studying epigenetics biology and were employed in this thesis to investigate the role of histone methylation in human follicle development.

Table 1.2 The concept of chromatin modification. Modified from Tarakhovsky (161).

				
Modification	**Role**	**Writers**	**Readers**	**Erasers**
Histone acetylation	*Transcriptional activation, associated with euchromatin (162)*	Histone acetyl-transferases	Tandem bromodomains, tandem PHD fingers	Histone deacetylases
Histone methylation (lysine)	*Largely transcriptional repression. Also, activation, DNA repair, stress response,* ***aging*** *(163)*	Histone methyl-transferases	MBT domains, chromodomains, tudor domains, PHD finger domains	Histone demethylases **e.g. lysine-specific demethylase 1 (LSD1)**
Histone methylation (arginine)	*Transcriptional regulation (164)*	Protein arginine methyl-transferases (PRMTs)	Tudor domains	Histone demethylases, peptidyl arginine deiminases (PADIs)
Histone phosphoryl-ation	*DNA damage, DNA repair, transcription, chromatin compaction (mitosis) and relaxation (165)*	Kinases (e.g. protein kinase C)	Chromoshadow domains (phosphor-Tyrosine), 14-3-3 proteins (phosphor-Serine), BCT proteins	Protein tyrosine phosphatases, protein serine/ threonine phosphatases
Histone ubiquitination	*Transcriptional activation, crosstalk with other chromatin modifications (166)*	Ubiquitin E2 conjugases, ubiquitin E3 ligases	Unknown	Ubiquitin-specific proteases
DNA methylation	*Genomic stability (167)*	DNA methyl-transferases	Methyl-CpG binding domains	Active and passive DNA demethylation

1.10 The aging follicle

1.10.1 Insights from assisted reproductive techniques

Assisted reproductive techniques (ART) are believed by many to be a means of overcoming the age-related decline in fertility (see Section 1.2). Indeed, *in vitro* fertilisation (IVF)

revolutionised fertility treatment. Overall IVF success rates have improved dramatically in the 40 years since the birth of Louise Brown, the world's first IVF child, in 1978. In 2016, 25% of fresh treatment cycles and 20% of fresh embryo transfers in the UK resulted in a live birth, compared to 9% per embryo transfer in 1980, however the live birth rate following IVF is highly dependent on maternal age at the time of egg collection as shown in Figure 1.6 (3, 168).

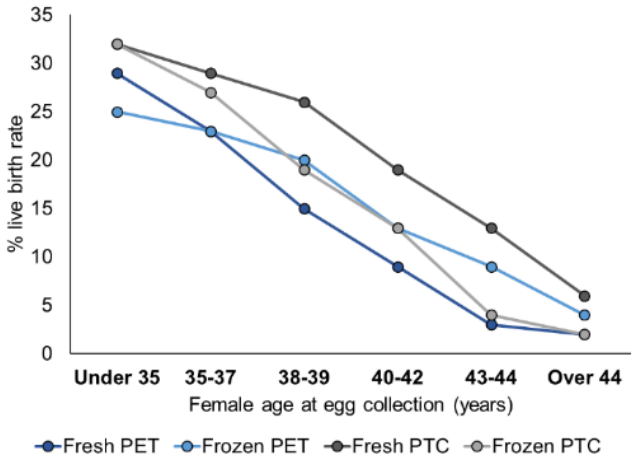


Figure 1.6 Percentage of *in vitro* fertilisation treatment cycles or embryo transfers resulting in a live birth from women using their own eggs in 2016

For women using their own eggs and their partners sperm, the percentage of live births per embryo transfer (PET) and the percentage of live births per treatment cycle (PTC) for fresh or frozen cycles decreases with increasing age at the time of egg collection. Data from (3).

It is well accepted that success of generating one or more embryos of sufficient quality for transfer back to the patient, is positively correlated with the number of eggs retrieved (169). Critically, of those eggs collected through stimulation, at least one needs to be of sufficient quality to give rise to a successful pregnancy. As the primordial follicle pool declines with age there is a concomitant decrease in the growing follicle cohort (72). Antral follicle count, as detected by ultrasound, declines with age with a rate of decline of 4.8% before age 37 and 11.8% thereafter (170, 171). This manifests in a smaller pool of follicles available to develop in response to exogenous gonadotrophins and a lower mean number

of oocytes retrieved (172-174). Interestingly, a recent retrospective study suggests that reduced oocyte yield is independent of reduced oocyte quality (175). In patients over 38 years old with either precycle evidence of diminished ovarian reserve or poor response to stimulation, there was no associated change in blastulation rate, aneuploidy or euploid live birth rate (175). Suggesting that, for a given maternal age, size of the ovarian reserve or response to stimulation is independent of oocyte quality.

1.10.2 Oocyte changes

Analysis of single and pooled MII oocytes reveals distinct differences in the transcriptome of oocytes from older or younger women (176, 177). Several genes involved in cell cycle control and checkpoint regulation (spindle and cytoskeletal organisation) were found to be down-regulated in older human oocytes, genes related to DNA repair, and metabolism were also differentially regulated with age (176, 177). MII oocytes that have been matured *in vitro* from young and older women also exhibit divergent transcriptomes, possibly suggesting a molecular basis for the reduced developmental potential observed in oocytes from older women (178).

1.10.2.1 Aneuploidy

In 1991, Navot and colleagues showed that live birth rate depended on the age of the donor rather than the recipient, demonstrating for the first time that oocyte quality, rather than uterine or endometrial insufficiency was responsible for the age-related decline in female fertility (179). An analysis of human embryos suggests that the majority of meiotic errors are of maternal origin (180). Rates of aneuploidy in embryos and oocytes increases dramatically with biological age, and in contrast to meiotic errors, post-zygotic errors do not appear to be related to maternal age (181-183).

Aneuploidy is only subtly related to oocyte morphology making it near impossible to identify without genetic approaches. As such, with increasing maternal age even morphologically high-quality embryos are more likely to be aneuploid and have little reproductive potential. Aneuploidy rates are somewhat stable until age 34 when the rate of aneuploidy increases steeply with increasing maternal age. It is estimated that the percentage of aneuploid embryos increases from 30% to 40% between the ages of 34 and 37 years, and to over 60% at age 40 (184). Complexity of aneuploid errors also increases with age. Among aneuploid samples over two-thirds of errors involved a single chromosome in women between 26-30 years, and steadily decreased to 32% in women over 43 years (183, 184).

1.10.2.2 Mitochondrial content

Mitochondria are maternally inherited organelles that use oxidative phosphorylation to supply ATP to the cell. Mammalian cells contain several thousands of mitochondria, the overall mitochondrial content is determined by the cells volume and energy needs. Mitochondrial DNA (mtDNA) is a circular, double-stranded DNA molecule that encodes 13 essential genes of oxidative phosphorylation (185).

Mitochondrial DNA content has been intimately linked to human reproductive success. A low mitochondrial copy number has been associated with fertilisation failure suggesting that mitochondrial content is critical for oocyte developmental competence (186, 187). Mitochondrial DNA content has been shown to be higher in blastocysts from reproductively older women (age 38-42 years) irrespective of ploidy (188). Blastocysts capable of implantation have a significantly lower mtDNA compared to those incapable of initiating a clinical pregnancy (188). However, others have failed to observed age-related differences (189), and it has been suggested that a correction factor that accounts for genomic variation due to embryo gender and ploidy is necessary to accurately determine mtDNA levels in

blastocysts (190). When this correction factor is considered no difference in the mtDNA content of aneuploid or euploid, or reproductively young or old patients was distinguished (190).

1.10.3 Cumulus changes

Cumulus cells are routinely removed from oocytes and discarded during IVF or intracytoplasmic sperm injection (ICSI) workflows. Since they are relatively easy to access and due to their intimate relationship with the oocyte across development, cumulus cells are an attractive candidate to non-invasively provide information about the quality of oocytes. Indeed, several authors have used single gene (191-194), or global gene expression profiling (195-197), to find differences in gene expression between cumulus cells connected to oocytes that did, or did not, go on to yield a live birth.

A summary of the literature on human cumulus cell gene expression with respect to maternal age is detailed in Table 1.3. Early targeted gene expression studies identified disparate candidate genes suggesting female age may have a broad impact on gene expression and affect multiple pathways. The first high-throughput gene expression study of cumulus cells was performed by Al-Edani, Assou (198) in 2014, however the authors did not specify whether oocyte maturity was considered in the collection of cumulus cells. As cumulus cell gene expression is differentially regulated by oocyte maturity their findings may not be reflective of the changes observed in MII COCs alone (199, 200). A later study in 2016 used next generation sequencing to profile mRNA expression in cumulus cells from individual MII oocytes from individual patients. An over-representation of genes involved in hypoxia inducible factor 1 alpha (HIF-1A) was present in older women, and an upregulation of genes involved in angiogenesis is suggested to be a buffering response to the deleterious impact of age-associated hypoxia. Both studies observed an increased

NR2F2 expression with age, a nuclear receptor with a critical role in the development of a number of tissues and organs, including limbs, heart and blood vessels (198, 201).

A significant portion of the human genome consists of non-coding RNAs, long non-coding RNAs (lncRNA) can play critical regulatory roles in many biological processes and have been postulated to play a role in ovarian aging. Indeed, analysis of RNA-seq data identified decreased expression of lncRNAs associated with angiogenesis, lipid transport, cell cycle regulation and transcriptional control in cumulus cells from older women (202).

Taken together, the literature strongly indicates an effect of maternal age on oocyte and cumulus cell gene expression. The relative scarcity of literature limits the wider application of the findings, as it remains to be determined what overall pattern of gene expression changes are observed in mature oocytes with increased maternal age. In this thesis I used next generating sequencing (NGS) to evaluate cumulus cells pooled from MII oocytes from individual patients to profile the pathways differentially regulated with age.

1.10.4 Existing treatments for maternal age in assisted reproductive techniques

Currently the only assisted reproductive technique (ART) interventions available to address maternal age are the use of oocyte donors or preimplantation genetic testing. Preimplantation genetic testing (PGT) can be used in ART to identify genetically normal embryos for transfer. It involves taking a biopsy of cells of an embryo, usually at the blastocyst stage, which is then screened for genetic abnormalities. Systematic reviews of the literature did not find sufficient evidence to support the efficacy of PGT (203, 204), with a subsequent publication by one group concluding that PGT is inappropriate clinically and should be restricted to research studies (205). Recently, the transfer of euploid embryos has been demonstrated to reduce the time to pregnancy and miscarriage rate however has not been shown to affect cumulative delivery rates (206). The most critical rate-limiting

factor of conventional assisted reproductive technologies, is the limited number of good-quality mature oocytes that can be recovered from a single female. Ultimately, PGT is only a selection tool for existing embryos as it cannot improve the quantity or quality of oocytes or embryos.

Table 1.3 Summary of studies on analyses of human cumulus cells

Samples used	Age (years)		Analysis method	Regulation with age		Refs
	Young (n)	Old (n)		Up	Down	
Pooled samples of CC	≤28 (3)	≥38 (3)	Microarray	Cell cycle (CUL1, CYR61, MT1E, **CKB**, **CDK4**) Apoptosis (IER3, CUL1, FOSB, **CDK4**) Metabolism (PRDX2, RPS28, **CKB**, P4HB) Other (SERPINA3, LOC91663, EIF5A, TUBB5, RPS28, HSD3B1, PPIF, TGFB1, CYP19A1, IFITM3, MGC4368, NME1, PCBP1, SEC61B, COX8, MDH2, STIP1, DKFZP586A0522, UCHL1)	Cell cycle (ADD3)	(207)
Pooled CC, MII oocytes, individual patients	20-33 (32) *	40-45 (32)**	Proteomic analysis, RT-PCR	Oxidative phosphorylation (ATP5I, NDUFA1) Metabolism (ACAT2, HSD17B4, FASN, SCD, ACSL3, CPT2)	Oxidative phosphorylation (ATP6V1A, COX10) Post-transcriptional mod (SFPQ, SNRPF)	(208)
Pooled samples of CC	<30; 31-34 (ns, 16 total)	>37 (ns, 16 total)	Microarray	1,874 differentially regulated genes Steroidogenesis/fatty acid metabolism (HSD17B1, HSD17B6, NSDHL, SRA1, CYP19A1, PPARA) Glucose metabolism/transporters (ALG13, GLT8D3, SLC2A3, SLC2A1, SLC2A13, SLC2A8) Angiogenesis (**ANGPTL4**, **LEPR**, **TGFBR3**, VEGFC, FGF2, NR2F2) Cumulus-oocyte dialog (INHA, CD200, IL6ST) Genome integrity (MSRB3, UCHL5IP, POLH, OBFC2B, CHAF1A)	1,874 differentially regulated genes TGF-β signaling (AMH, TGFB1, INHA, ACVR2B)	(198)
Individual CC, MII oocytes, individual patients	<35 (8)	>40 (7)	RNA-seq	37 genes upregulated Hypoxia–response pathway (NR4A3, **PTHLH**, **NOS2**, TFRC, PDE4D, **CRIM1**, RORA, NEDD9) Vasculature development (**CRIM1**, CTGF, NR2F2)	8 genes downregulated ECM turnover (**ADAMTS14**)	(201)
Pooled CC, MII oocytes, individual patients	<35 (9 data) (5 RT-PCR)	>40 (9 data) (5 RT-PCR)	Analysis of existing RNA-seq data for lncRNAs RT-PCR	n/a	147 lncRNAs downregulated Cumulus-oocyte dialog (**IL10RB-AS1**, **APOA1-AS**, IGF2BP2-AS1, **LINC00548**, **PSMB8-AS1**, LAMTOR5-AS1	(202)

*Abbreviations: **CC** cumulus cells, * fertile, ** infertile, **ns** not specified, underline subject to validation, **bold underline** confirmed with validation*

1.11 Growth and development of human follicles *in vitro*

To develop a treatment for reproductive aging, we must first elucidate the differences in follicle development and/or oocyte quality that arise with age and when they manifest. The rationale for developing a method of supporting follicle development *in vitro* is that it can be used to as a research tool to understand the impact of age throughout follicle development, and to provide an alternative starting point for ART. The optimal starting point of an *in vitro* growth system is at the primordial follicle stage. For the majority of a female's reproductive life span, primordial follicles housed within the ovarian cortex are the dominant population in the ovary. Follicles can exist in this dormant state for decades before initiating development, therefore to understand the changes in follicle development associated with age they are a critical population to investigate. This is also a logical starting point for clinical applications of *in vitro* growth. For patients who have undergone ovarian tissue cryopreservation for fertility preservation this is the only starting material available and the cryoprotection and cryopreservation of the tissue adds another consideration for optimising protocols. To extend existing assisted reproductive techniques, an increasingly plausible strategy may be to access dormant primordial follicles within cortical tissue as a possible source of extra gametes that can be obtained without stimulation, with the obvious caveat that laparoscopic surgery is required.

1.11.1 Culture from the primordial stage

In mice, the first live birth from an oocyte grown entirely *in vitro* was reported by Eppig and O'Brien Eppig and O'Brien (209) in 1996. Follicles were developed within whole ovary culture for 8 days, enzymatically isolated, and cultured for a further 14 days as oocyte-granulosa complexes. Oocytes were matured, fertilised, and transferred to pseudo-pregnant females. In contrast, the greater size, and protracted *in vivo* development of oocytes from humans and large mammals has proved challenging when adapting culture

systems initially designed for rodent models. Over two decades after this proof of concept study in 2018, McLaughlin and colleagues reported the success of a four-step method to generate mature MII human oocyte from primordial follicles, discussed further in Section 1.11.2.2 (210). This protocol was an extension of the group's earlier work from 2008, describing a two-step culture method that facilitated the development of antral follicles from human cortical tissue in serum-free medium (211). Isolated primordial follicles do not survive well in culture due to a lack of rigidity and development is better supported when grown *in situ* within the cortex (212, 213). Studies on enzymatically isolated primordial and primary follicles demonstrated growth within the first 24 hour of culture, but no further growth was observed and there was poor survival across the culture period (214, 215).

Existing systems for cortical strip culture differ based on medium composition and volume, duration of culture, and use of extra-cellular matrix (ECM), and are summarised in Table 1.4. In earlier studies, basal media were commonly supplemented with serum due to the beneficial effect on follicle growth, but complex and batch-variable composition has moved the field toward serum-free media. Serum contains albumin, amino acids, proteins, hormones, growth factors, precursors for steroid biosynthesis and ECM components which are mimicked in serum-free media by the addition of insulin, transferrin and selenium (ITS), and a source of albumin to support follicle development *in vitro* (216, 217). Gonadotrophins FSH and LH are commonly included in culture medium for early stage follicle development despite gonadotrophic stimulation not being essential until the early antral stage. FSH is a commonly used medium supplement for the culture of follicles from several species as it promotes survival and antrum formation, as well as reducing atresia in follicles from the primordial to the secondary stage (217-222). Whether there is a role for LH in *in vitro* culture has not been addressed in humans. In sheep the addition of LH to FSH-containing medium did not impact antrum formation however evidence in non-human

primates suggests it may have an effect on steroidogenic activity of pre-antral follicles (221, 223).

Extracellular matrices provide structural support to the tissue but must also remain permeable to culture medium and factors produced by the tissue. ECMs are most often used with human tissue cultured over long periods when it becomes more difficult to prevent tissue attachment and loss of tissue integrity, and has been shown to improve survival of human follicles in long term culture (233). Matrigel is the ECM most commonly used in ovarian culture and is derived from Engelbreth-Holm-Swarm mouse sarcoma cells. Although it has been widely used to support early stages of human follicle development, the exposure of human cortical tissue to unknown levels of growth factors may not be conducive with later stages of follicle and oocyte development. Alternative, non-animal derived ECMs have not been widely reported for human cortical strip culture. One group published results demonstrating superior follicle health and development with alginate compared to Matrigel and followed on to find a PEG-fibrinogen scaffold superior to alginate, however these results are yet to be repeated (227, 228).

Table 1.4 Culture systems for the *in vitro* growth of human preantral follicles in cortical tissue

Tissue culture system	Medium	Follicle stage		Culture duration	Comments	References
		Start of culture	*End of culture*			
Floating, low volume, serum free medium	McCoy's 5A	P_0	S, PA	6-8 days	Tissue pieces mechanically stretched before culture. Follicles isolated were developed to MII oocytes.	(142, 210, 211)
Floating, high volume, gas-permeable plate	αMEM	P_0	S	6-9 days	Gas-permeable plate with high medium volume gave superior follicle development to conventional plate with high or low volume. No increased development between 6 and 9 days.	(224)
ECM-coated inserts, serum-free	DMEM	P_0	S	7 days	Chemo- or radio-therapy exposure prior to cryopreservation is detrimental to follicle health in culture but MRD is not.	(225, 226)
PEG-fibrinogen, serum-free	αMEM	P_0	Growing	6 or 12 days	Increased developing and decreased atretic follicles in PEG-fibrinogen scaffold-compared to alginate.	(227)
Alginate scaffold, serum free	αMEM	P_0	Growing	Up to 14 days	Increased developing and decreased atretic follicles in alginate scaffold-compared to Matrigel.	(228)
ECM-coated inserts, serum-free	αMEM	P_0	Data not shown	Up to 14 days	Compared strip to small piece culture, greater viability in small pieces.	(229-232)
ECM-coated inserts ± serum	αMEM, Waymouth's, EBSS	P_0	S	Up to 15 days	ITS and FSH resulted in lower atresia compared to serum.	(217)
ECM-coated inserts, serum-based	αMEM, EBSS	P_0	PA	Up to 28 days	Tissue cultured on ECM had superior viability.	(233)

*Abbreviations: **P_0** primordial, **P_1** primary, **S** secondary, **PA** preantral, **EBSS** Earles Balanced Salt Solution, **ECM** extra-cellular matrix, **MRD** minimal residual disease*

1.11.2 Culture from the preantral stage

1.11.2.1 Methods of isolation

Culture of ovarian cortex can facilitate the development of human follicles from the primordial to the secondary follicle stage, at which point the rigid cortical environment becomes limiting to follicle development and follicles must be excised to facilitate progress to the antral stage. Follicles can be isolated mechanically or enzymatically. Roy and Treacy Roy and Treacy (222) were the first to successfully isolate and culture preantral follicles from human ovaries, some of which reached antral stage, and they emphasized the toughness of the human ovarian cortex. A prolonged period of enzymatic digestion yielded high numbers of multilaminar preantral follicles with no discernible theca cell layer. Collagenase has been used in numerous studies to isolate follicles that were competent to grow and develop in culture, both in animal models and in humans (209, 213, 219, 221, 234). Success of isolation and culture of preantral human follicles has been limited in several subsequent studies. Abir and colleagues mechanically isolated and grew individual human preantral and early antral follicles from whole ovaries for over four weeks in culture; however, oestradiol production decreased after 3 weeks, and sectioning revealed that few follicles contained oocytes (220).

Enzymatic approaches have the advantage of being less labour intensive and resulting in higher yields however follicles commonly suffer loss of the basement membrane and surrounding theca cells. In mice, sheep, and pigs, the presence of a differentiated and intact theca cell layer is a prerequisite for survival and antral development (219, 235, 236). Liberase has been suggested as an alternative over collagenase as it may improve the viability of isolated follicles, though sacrificing follicle yield as a result (237). Collagenase is derived from bacteria and not applicable for clinical situations whereas liberase has the advantage of being a purified mammalian-tissue free blend which could be used in a clinical workflow (238).

Mechanical isolation can avoid destruction of follicle structure by using a combination of needles, scissors, forceps, or scalpels. In humans where the ovarian stroma is tougher and more collagenous than that of rodents, mechanical isolation is technically challenging, more time intensive, and the yield of follicles isolated mechanically is lower compared to enzymatic approaches (213, 239). Telfer and associates were able to obtain late preantral and early antral follicles by mechanically isolating follicles from cultured cortical strips which were cultured for a further four days in the presence of activin (211).

1.11.2.2 Isolated follicle culture systems

Culture systems for isolated follicles are generally classified as two dimensional (2D) or three dimension (3D). In typical two-dimensional (2D) culture the follicle structure is not well maintained as part of the follicle surface makes contact with the culture plate causing the granulosa and theca cells to attach and the follicle to flatten (215, 240). Three-dimensional cultures using V-bottomed dishes or encapsulation by hydrogels to maintain the follicles spherical architecture has been employed successfully to culture human preantral follicles (210, 211, 240-242). Use of hydrophobic membranes and hanging droplet culture, often used in other species are not commonly used in human follicle culture (219, 243).

Meiotically competent human MII oocytes were first successfully cultured from multilaminar secondary follicles encapsulated in 0.5% alginate gel for 10-15 days to promote antrum formation followed by culture in low-attachment plates for a further 30-40 days and *in vitro* maturation (240). Initial studies from this group found that despite secondary follicles progressing to the antral stage, terminal diameters after 30 days in culture were smaller than *in vivo* antral follicles (242). Transferring follicles to low attachment plates after antrum formation was designed to mimic the transition from the

rigid collagen-dense cortex to the dense medulla region during development, and significantly increased terminal follicle diameters compared to un-released follicles (240). An alternative system published by McLaughlin, Albertini (210) successfully developed human MII oocytes from follicles grown from the primordial stage *in vitro.* Mechanically isolated multilaminar follicles were cultured in V-bottom culture plates and cultured for eight days, compared to the longer 10-15 day culture of gel-encapsulated follicles. Cumulus-oocyte complexes were released from antral follicles and cultured on a nucleopore membrane for a further four days before being subject to IVM. Surprisingly, the overall success as determined by number of MII oocytes generated was similar between follicle derived *in vivo* derived versus *in vitro*, 4/65 (6%) and 9/87 (10%) respectively (210, 240). The *in vitro* derived follicles gave rise to MII oocytes with abnormally large polar bodies which was not observed in the *in vivo* derived MII oocytes, the methodological differences between the studies make it difficult to attribute the abnormalities to initial *in vitro* development and optimisation at all stages needs to follow these proof of concept studies.

1.12 Use of cryopreserved human ovarian tissue for research

1.12.1 Source of tissue

Tissue for cortical strip culture can be fresh or cryopreserved. Fresh tissue is most commonly obtained through biopsy during an associated gynaecological procedure. This thesis used ovarian tissue cryopreserved for fertility preservation from the Oxford Cell and Tissue Biobank (OCTB). The OCTB has been operating since 2013 and has stored ovarian tissue from over 200 patients in the five years since its inception. The cryopreservation protocol used is that established at the Hadassah Hebrew University Hospital (244), which is based on the protocol published by Gosden (245). It utilises a specialised combination of ethylene glycol and sucrose which is not commercially available and has been demonstrated to yield high rates of oocyte and follicle survival (246). Routine histological

assessment of the tissue is performed on tissue fixed before cryopreservation. Live births following auto-transplantation of tissue cryopreserved using this system have been reported by the Israeli group however the cryoprotective agent used was dimethyl sulfoxide and sucrose (247, 248). Functionality of OCTB-cryopreserved tissue has been demonstrated in xenotransplantation studies where 75% of follicles in grafted tissue were classified as growing compared to 40% of follicles in non-grafted tissue (249). No patients have had re-transplantation of tissue cryopreserved by OCTB and as a result, information about the quality of tissue banked at the OCTB is yet to be fully elucidated.

1.12.2 Advantages and rationale for using cryopreserved tissue

Most studies using *in vitro* growth systems have utilised fresh ovarian tissue obtained from women undergoing gynaecological surgeries. Cryopreservation of ovarian cortical tissue is becoming a widely used method of fertility preservation for women and girls undergoing gonadotoxic treatments (250). Cryopreserved tissue is an exceptionally valuable source of tissue for research. The scarcity of human ovarian tissue is a significant barrier in developing *in vitro* growth systems, optimising and determining the effect of cryopreservation, and understanding basic follicle development in human ovaries (251). The rational for targeting cortical tissue is described in Section 1.11.

Using cryopreserved tissue obtained from a bank allows experiments to be planned, using a cohort of patients who have given consent. Experiments can be better controlled due to flexibility of when tissue is obtained, and as all tissue is collected, processed and cryopreserved according to a standard operating procedure (SOP) the tissue pieces are more uniform in size and condition than is possible with fresh biopsy material. Multiple experimental repeats can use tissue from the same patient without repeated surgeries, giving scope to look at variation within individual patients or to control for biological variation. Importantly for this work, using cryopreserved material from the OCTB allows

us access to tissue from younger patients. Studies using tissue from women undergoing gynaecological surgeries or caesarean sections commonly include women of advanced reproductive age, into their early 40s (135, 142, 211, 213, 233). Understanding how follicle development progresses in non-aged tissue *in vitro* is imperative before progressing on to older patients. Ovarian cortical tissue has been proposed as an additional source of gametes as a precursor to ART (discussed in Section 1.8) that is likely to utilise frozen tissue.

At the time of writing Table 1.5 contains a list of all studies that cultured slow-frozen cryopreserved human ovarian tissue. Studies where cryopreserved tissue was used alongside fresh tissue and not analysed separately, and studies culturing from the preantral stage are not included. The expected development of follicles *in vitro* from human tissue that has been cryopreserved is not well understood due to this very small body of literature. Less information is available about the behaviour of follicles in human tissue in culture that has been cryopreserved for fertility preservation. A large, well-controlled study demonstrated that prior chemotherapy or radiation treatment is detrimental to follicle development and survival in culture (225), and subsequently only patients who had tissue cryopreserved prior to treatment were used in this thesis.

Table 1.5 Parameters assessed in studies using slow-frozen cryopreserved human cortical tissue in culture

Reference	Patients (n)	Follicles (n)	Follicle health (% atretic)		Follicle development		Culture system
			Non-cultured	Cultured	Non-cultured	Cultured	
Hovatta, Silye (233)	4	113	3%	60%	NR	NR	Earle's medium + ECM
Huang, Mo (230)	26	NR	15% (P_0 only)	NR	NR	51% P_0, 49% growing	αMEM medium + Millicell inserts
Garor, Abir (231)	12*	4489 across 40 end points	NR	NR	96% P_0, 4% growing	55% P_0, 45% growing	αMEM medium + Millicell inserts + ECM
Kedem, Hourvitz (228)	12*	2084	0%	13% / 36%	78% P_0, 22% growing	36% P_0, 51% growing / 46% P_0, 18% growing	αMEM medium + alginate scaffold / Matrigel
Isachenko, Mallmann (252)	9*	NR	NR	15%	NR	NR	AIM-V + suspension culture / CAM-culture
Lerer-Serfaty, Samara (227)	15*	1229	4%	19% / 1%	74% P_0, 22% growing	51% P_0, 30% growing / 33% P_0, 68% growing	αMEM medium + alginate scaffold / PEG-fibrinogen hydrogel
Sanfilippo, Canis (253)	13	345	1.2%	62.2%	68.5% P_0, 19.3% P_1, 12.2% S	53.6% P_0, 17.9% P_1, 28.6% S	αMEM medium + low-attachment coated plate
Xiao, Wang (232)	6	132	NR	39.4% (P_0 only)	NR	NR	αMEM medium + Matrigel
Azarbaijani, Sheikhi (225)	34*	17,212 non-cul, 41,231 cul	8%	53%	Reported as densities	Reported as densities	DMEM medium + Matrigel
Asadi-Azarbaijani, Sheikhi (226)	14*	4694 non-cul, 18,264 cul	32-50% atretic	53-81% atretic	Reported as densities	Reported as densities	DMEM medium + Matrigel

*Abbreviations: *patients had cancer diagnoses,* ***P_0*** *primordial,* ***P_1*** *primary,* ***S*** *secondary,* ***NR*** *not reported,* ***non-cul*** *non-cultured,* ***cul*** *cultured*

1.13 Rationale and research questions

Increasing the supply of high-quality eggs for use in assisted reproduction techniques is a desirable goal for all patients, and essential for those faced with indications that limit this supply such as advanced maternal age. For this to be achieved, target pathways must be identified and a timeframe for intervention must be determined. This thesis sought to address the overall aim of developing a treatment for patients of advancing reproductive age by answering five main questions;

1. How does follicle health and development from the primordial to early antral stage differ between reproductively young patients *in vitro*? (Chapter 3)
2. How does altered histone methylation impact early follicle health and development *in vitro*? (Chapter 4)
3. Can methods can be incorporated into *in vitro* culture to visualise follicles in human ovarian tissue? (Chapter 5)
4. How does culture medium, medium volume, and gas permeability of culture dishes, impact follicle growth and development *in vitro*? (Chapter 6)
5. What genes or pathways can be identified by RNA-sequencing of human cumulus cells as being altered by advancing maternal age? (Chapter 7)

Chapter 2

General materials and methods

2.1 Human ovarian tissue samples

2.1.1 Patients and ethical approval

Donated ovarian cortical tissue was used in several investigations included in this thesis. Informed consent was obtained from all patients prior to collection of ovarian tissue and Oxford University Hospitals, NHS Foundation Trust pre-approved the study (Ethics Reference Number: 14/SC/0041, R&D Reference: 8825). At the time of consent for the procurement and storage of tissue, patients were given the option of donating material to research. Donated material could be limited to remnant material which would otherwise be discarded for example medulla tissue or medium, or where over 50 cortical strips were collected and cryopreserved, a maximum of 10 strips could be allocated to research provided no fewer than 50 strips remained in storage.

2.1.2 Sourcing tissue from the Oxford Cell and Tissue Biobank

Tissue was obtained from the Oxford Cell and Tissue Biobank (OCTB) located at the John Radcliffe Hospital, Oxford, UK. The ovarian tissue service is available to children and young women who, due to treatment, are at a high risk of premature infertility and for whom standard hormone stimulation and egg collection and storage is not appropriate.

2.1.3 Inclusion and exclusion criteria for studies using cryopreserved cortical tissue

The inclusion criteria were patients who had tissue stored for fertility preservation at the OCTB and had consented to the use cortical strips for research where more than 50 cryopreserved strips remained in storage. Age of patients included in the three studies varied and is detailed in the relevant chapters. Patients were not selected if they had undergone chemotherapy or radiation treatment prior to tissue collection, or if no information about prior treatment was available.

2.1.4 Information on patient characteristics

Non-identifying information was collected about patients whose tissue was used in this thesis to assist in drawing conclusions.

2.1.4.1 Diagnosis and prior treatment

The disease or disorder prompting fertility preservation was obtained from the OCTB.

2.1.4.2 Pubertal status and menstrual cycle

Patients were classified as having gone through puberty if on the referral form 'yes' was selected in response to the prompt 'post-pubertal?'. Patients where 'no' was selected were considered 'not post-pubertal' rather than pre-pubertal. Information on whether the

patient had regular periods [yes/no] and was on the oral contraceptive pill [yes/no] was also obtained from the referral form.

2.1.4.3 Evidence of malignancy

A routine histopathology report is carried out by the Cellular Pathology Department at the John Radcliffe Hospital on all ovarian tissue stored by the OCTB. A fragment of fresh tissue from each patient is used for the report and includes a statement about whether evidence of malignancy was observed.

2.1.4.4 Time from surgery to cryopreservation

The time of surgery was taken as the time recorded by the surgeon as the time the surgery was completed. The time of cryopreservation was the time the controlled rate freezing programme was started as recorded by the programme. The time from surgery to cryopreservation was calculated as the difference between these two times.

2.2 Collection and cryopreservation of ovarian tissue

All tissue was collected by laparoscopic oophorectomy or resection of the ovarian cortex at the John Radcliffe Hospital Oxford, and cryopreservation performed by the OCTB. The protocols used by the OCTB for medium preparation, tissue processing, cryoprotection, and cryopreservation of ovarian tissue are those used in the well-established programme at Hadassah Hebrew University Hospital and have been reported to be successful for ovarian tissue cryopreservation (244, 245).

Following surgical removal, the excised ovary or ovarian tissue was transported immediately to the tissue processing centre in chilled Leibovitz's L-15 medium (Sigma Aldrich, Dorset, UK). Dissection of the ovarian tissue was performed as soon as possible

after procurement. Dissection was performed by OCTB technicians under aseptic conditions. The ovary was bivalved using a scalpel, and great effort was taken to remove the medulla to leave a thin layer of ovarian cortex. The ovary was cut into smaller pieces as required to achieve a suitable depth of 1-2 mm and then cut into pieces or fragments of approximately 1 x 2 x 5 mm in size.

The specialised cryoprotective medium used is prepared by the OCTB (1.5 M ethylene glycol (Merck Chemicals Ltd, Hull Yorkshire, UK), 0.1 M sucrose (Sigma Aldrich), 10% v/v serum substitute supplement (Irvine Scientific, Newtown Wicklow, Ireland) in L-15 medium). Up to 6 cortical strips were placed into a single cryovial (2 ml, internal thread; Nunc, Rochester, New York, USA) containing 1 ml of cryoprotectant medium and incubated for 1 hour at 4°C before being frozen using the Sy-Lab Ice Cube controlled rate freezer (Sy-Lab, Neupurkersdorf, Austria). Cryovials were loaded into the pre-cooled 0°C controlled rate freezer and set to cool at -2°C/min until the chamber reached -9°C, after which each tube was manually seeded to enable controlled ice crystal formation. After seeding, the cryovials were cooled to -40°C at a rate of -0.3°C/min, and finally to -140°C at -10°C/min. Following cryopreservation, the vials were stored in vapour phase liquid nitrogen (-196°C).

2.3 Thawing of cortical strips

Prior to removing the cryovials from liquid nitrogen storage, 10 ml of each thawing medium per cryovial (Solution 1, Solution 2, and Solution 3; constituents from Sigma Aldrich, with the exception of L-15 medium from Gibco (Loughborough, UK)) were made and sterile filtered into 15 ml Falcon tubes (see Table 2.1)

Table 2.1 Thawing medium constituents.

	Solution 1	Solution 2	Solution 3
Ethylene glycol	1 M	0.5 M	0 M
Sucrose in sterile H_2O	1 M	1 M	1 M
Human Serum Albumin	3 mg/ml	3 mg/ml	3 mg/ml
With Leibovitz's L-15 medium	✓	✓	✓

The composition of thawing medium (Solutions 1, 2, and 3) and the protocol used to thaw is the same as that used by the OCTB with the exception that human serum albumin (HSA) is used in the place of serum substitute supplement used by the OCTB. HSA been demonstrated to yield comparable rates of follicle survival to those observed using a human serum substitute (254). The 3 mg/ml concentration of HSA used was based on that used for transporting fresh tissue prior to culture (211) and in the dissection medium described below (Section 2.4).

Cryovials containing cryopreserved tissue were obtained from the OCTB and transported to the laboratory in a liquid nitrogen filled table top dewar (Dilvac; Day Impex, Colchester, Essex, UK). Cryovials were removed from liquid nitrogen, held at room temperature for approximately 1 min then immersed in a 30°C water bath for 3 min. After thawing, the cortical strips were transferred to the Falcon tube containing Solution 1 under sterile conditions and inverted by hand for 5 min. This was repeated for Solution 2 and Solution 3.

2.4 Human cortical strip culture

2.4.1 Preparation of cortical strip tissue for culture

Representative images of cortical strips at the various stages of processing are shown in Figure 2.1. Following the final wash step in Solution 3, the cortical strips were transferred to a Petri dish containing dissection medium (3 mg/ml HSA, 100 U/ml penicillin and 100 µg/ml streptomycin (Invitrogen, Dorset, UK), 2 mM L-glutamine (Sigma Aldrich) and 2 mM

sodium pyruvate (Sigma Aldrich) in L-15 medium and briefly washed. A single cortical strip was placed on sheets of filter paper on the stage of a McIlwain Tissue Chopper (The Mickle Laboratory Engineering Co. Ltd., Surrey, UK), a Pasteur pipette was used to ensure the strip remained covered in a layer of dissection medium at all times. The tissue chopper was used to cut at 0.25 mm intervals along the longest length of the strip endeavouring to keep slices very thin. The cut fragments were transferred immediately back to a new Petri dish containing dissection medium. Under a dissecting microscope any pieces of filter paper were removed, and the tissue fragments were further cut by hand using No. 24 scalpels (Swann-Morton Ltd.) into approximately 0.5 x 0.5 mm pieces.

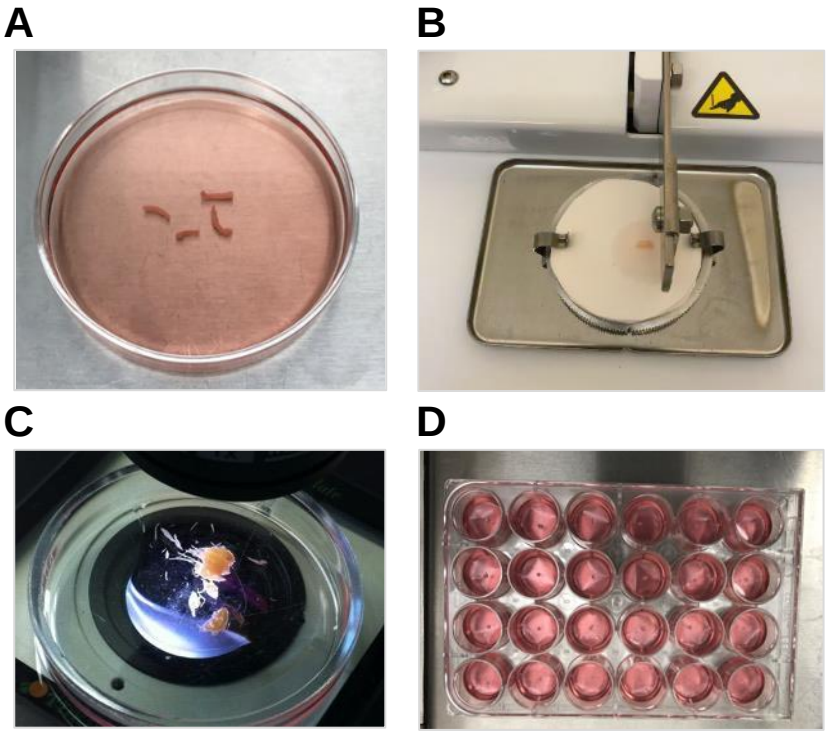


Figure 2.1 Preparation of cryopreserved human cortical strips for culture

A) Four frozen-thawed cortical strips prior to processing. B) A single cortical strip on the McIlwain Tissue Chopper. C) Fragments post-tissue chopper and before manual cutting. D) Tissue fragments cut to approximately 0.5 x 0.5 x 0.25 mm in a 24-well plate.

2.4.2 Set up and culture of tissue

Tissue pieces of uniform size were distributed randomly and evenly between wells of a 24-well plate with excess remnant tissue discarded. Tissue fragments were cultured on Whatman® Nuclepore™ Track-Etched polycarbonate membranes (13 mm diameter, 8 μm pore size; Sigma Aldrich) floating on 1 ml of culture medium in a 24-well culture plate; culture medium contained McCoy's 5A (Gibco) supplemented with 1 mg/ml HSA, 100 U/ml penicillin and 100 μg/ml streptomycin, 2 mM L-glutamine, 10 μg/ml insulin, 5.5 μg/ml transferrin, 5 ng/ml selenium (ITS; Sigma Aldrich), 50 μg/ml ascorbic acid (Fisher Scientific, Dorset, UK) and 1.25 IU/L recombinant human FSH (GONAL-f, Merck Serono, Darmstadt, Germany). Tissue was cultured for 6 days at 37°C under 5% CO_2 in air, with half the medium being replaced with fresh medium every other day.

2.4.3 Tissue fixation before or following culture

A portion of non-cultured tissue was fixed overnight in Bouin's solution (Sigma Aldrich) as a non-cultured control. Following 6 days of culture, the remaining tissue pieces were fixed overnight in Bouin's solution and all fixed tissue was stored in 70% ethanol at 4°C until histological processing.

2.5 Visualisation of follicles with Neutral Red

Neutral Red (NR) was used to identify which fragments of tissue contained viable follicles. Optimisation of the use of NR with *in vitro* culture is described in Chapter 6. NR is a weak cationic supravital dye that is soluble in water, it diffuses through the plasma membrane and concentrates in the lysosomes of viable cells (255), allowing the user to visualise viable cells by their deep red colour (256). NR is therefore especially concentrated in follicles making it possible to distinguish follicles in larger pieces of tissue (257). NR is non-toxic and has been used to identify and assess the viability of human follicles (257).

After processing cortical tissue with the tissue chopper (see Section 2.4.1), tissue fragments were incubated in NR (25 μg/ml in dissection medium; for medium composition see Section 2.4.1) at room temperature for 1 hour while the tissue was manually cut as in the standard culture protocol (Section 2.4.1). Tissue pieces were washed briefly in fresh dissection medium and observed using standard dark-field microscopy for the presence of red colouration. Fragments where red-stained follicles were observed were selected before those with no staining and randomly assigned to the culture group (to fill a 24-well plate), or non-cultured control group, and remnant tissue discarded as described above.

2.6 Histological processing

2.6.1 Dehydration

The protocol for tissue processing prior to embedding is detailed in Table 2.2. For ethanol washes, a 96-well plate containing 200 μl reagent per well was used with a single tissue fragment in each well. Tissues were moved through increasing concentrations of ethanol (70% to 100% ethanol) using a wide bore P200 or P1000 tip (Starlab, Milton Keynes, UK) to minimise tissue damage while handling. Due to the small size of the tissue fragments, they were lightly stained with 10% eosin (Eosin Y solution, alcoholic, Sigma Aldrich) in 70% ethanol for 15 min to aid visibility. As xylene rapidly dissolves plastics, tissue fragments were moved to glass embryo dishes each containing 1 ml xylene for the three xylene washes.

Table 2.2 Dehydration protocol for embedding

Reagent	Time
70% Ethanol with 10% eosin	15 min
80% Ethanol	15 min
95% Ethanol	15 min
100% Ethanol	15 min
100% Ethanol	15 min
100% Ethanol	15 min
Xylene	20 min
Xylene	20 min
Xylene	20 min

2.6.2 Embedding

After saturation with xylene, tissue fragments were carefully transferred to plastic moulds containing melted paraffin wax (Histoplast; Fisher Scientific, Loughborough, UK). Up to 4 tissue fragments were transferred to each mould and incubated in the wax at 62°C for 3 hours. Labelled cassettes were placed on top of the moulds after incubation to secure the wax embedded tissue, and the moulds left to cool overnight. To aid removal of the paraffin block and cassette from the mould, moulds were place in the fridge for a minimum of 1 hour.

2.6.3 Sectioning

Excess wax was trimmed from around the paraffin blocks. Blocks were sectioned using a microtome (Leica, Nussloch, Germany) at 5 µm. Wax sections were floated in a water bath at ~40°C and serially mounted on positively charged glass slides (Superfrost® Plus, VWR International, Leuven, Belgium) using electrostatic adhesion. Slides were left to dry for a minimum of 2 hours before being placed in an oven at 62°C for 1 hour to bind the tissue to the slide. Baked slides were stored in slide boxes at room temperature.

2.6.4 Haematoxylin-eosin staining

Details for the haematoxylin-eosin staining are presented in Table 2.3. The haematoxylin staining used is regressive. Slides were dewaxed with three xylene washes before being rehydrated in decreasing concentrations of ethanol (100% to 50%) and water. Nuclear staining was performed by immersing slides in haematoxylin (Shandon Gill 2 haematoxylin; Fisher Scientific) for 2 min before washing with tap water. To remove excess staining from the tissue, slides were exposed to acid alcohol (1% HCl in 70% ethanol) for 5 sec and washed with tap water. Sections were washed through 80% ethanol before eosin was used for cytoplasmic staining. Slides were dehydrated in increasing concentrations of ethanol and washed twice through xylene. Slides were coverslipped using DPX (Sigma Aldrich) and left flat to dry overnight.

Table 2.3 Haematoxylin and eosin staining protocol

Step	Reagent	Time
Dewaxing	Xylene	1 x 8 min, 2 x 4 min
Rehydration	100% ethanol	2 x 3 min
	90% ethanol	1 x 2 min
	70% ethanol	1 x 2 min
	50% ethanol	1 x 3 min
	Tap water	1 x 3 min
Staining	Haematoxylin	1 x 2 min
	Running water	1 x 5 min
	Acid alcohol	1 x 5 sec
	Running water	1 x 5 min
	80% ethanol	1 x 1 min
	Eosin	1 x 2 sec
Dehydration	95% ethanol	1 x 30 sec
	100% ethanol	1 x 45 sec, 1 x 1 min, 1 x 2 min
	Xylene	2 x 8 min

2.7 Assessment of follicle health and development

2.7.1 Classification of developmental stage

Developmental staging was based on that reported by Gougeon (29) and is detailed in Figure 2.2. Non-growing follicles were those at the primordial stage; transitional, primary, and secondary follicles were classed as growing follicles.

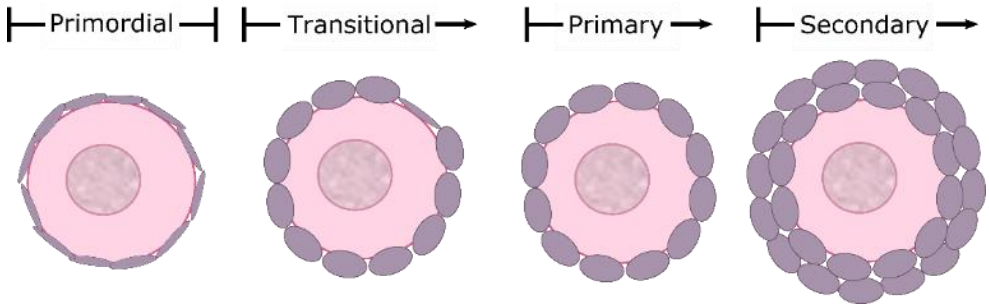


Figure 2.2. Classification follicle developmental stage in cryopreserved human ovarian tissue.

Follicles were staged as primordial with a single layer of flattened pre-granulosa cells, transitional with a single layer with at least one cuboidal granulosa cell, primary with a complete single layer of cuboidal granulosa cells, or secondary with two or more complete layers of cuboidal granulosa cells.

2.7.1.1 Classification of asymmetric follicles

Where follicles had a single complete layer of cuboidal cells, the number of any additional partial layers of granulosa cells was recorded. Follicles with a single complete layer and one partial layer were recorded as such but considered to be developing normally. Those follicles with a single layer of cuboidal granulosa cells and two or more partial layers of granulosa cells were classed as asymmetric (Figure 2.3).

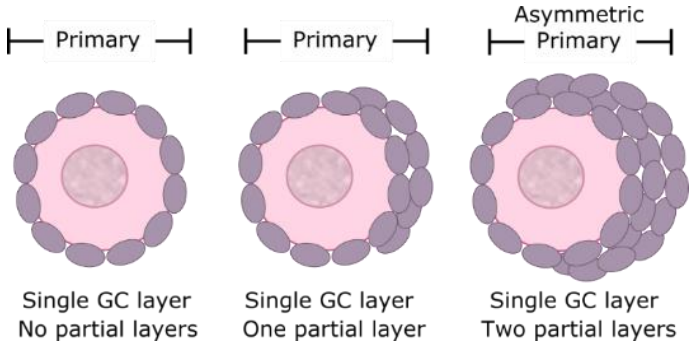


Figure 2.3. Classification of asymmetry in primary follicles from cryopreserved human ovarian tissue.

Primary follicles which had partial granulosa cell (GC) layers were recorded. Primary follicles with a single complete GC layer and one partial GC layer were classed as normal. Primary follicles with a single complete GC layer and two or more partial GC layers were classed as asymmetric.

2.7.2 Classification of follicle health

The classification system used for follicle health is detailed in Figure 2.4. Based on the existing literature (29), and the ease of assessing health factors in a non-biased and histological stain-independent manner, granulosa cell and oocyte pyknosis, and shrinkage of ooplasm were selected as markers for follicle health. Healthy follicles were defined as having a non-pyknotic oocyte with normal ooplasm and non-pyknotic granulosa cells. Degenerating follicles had at least one of a pyknotic oocyte, pyknotic granulosa cells, or shrunken ooplasm or a combination of one pyknotic cell type (oocyte or granulosa cell) and shrunken ooplasm. Follicles were classified as atretic if they had both an oocyte with a pyknotic nucleus and pyknotic granulosa cells, irrespective of whether the ooplasm was shrunken or not.

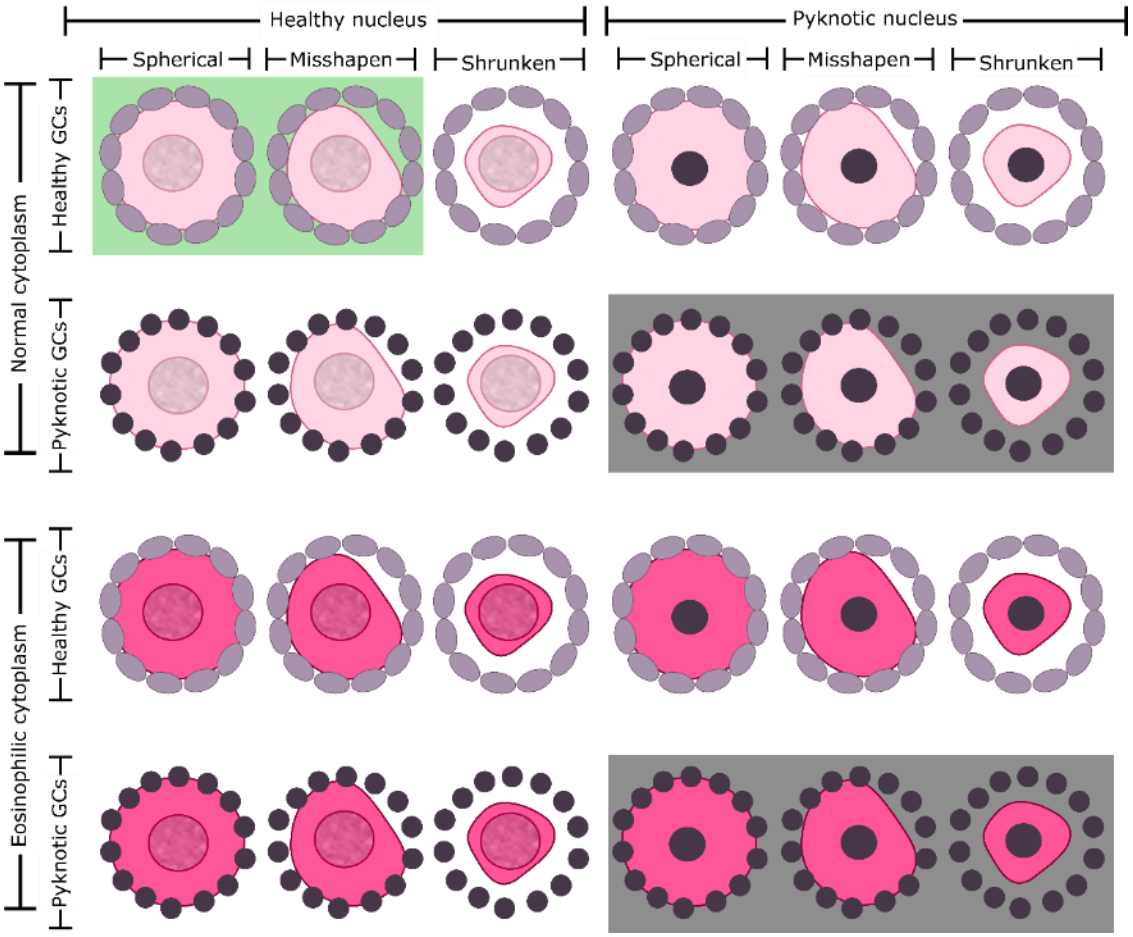


Figure 2.4 Classification of follicle health in cryopreserved human ovarian tissue based on morphology with haematoxylin-eosin staining.

Morphological characteristics related to follicle health assessed were pyknosis of the oocyte and granulosa cells (GC), shrinkage of the ooplasm, and eosinophilia of the ooplasm. Healthy follicles are backed by the green box, atretic follicles by the dark grey boxes, and those follicles with a white background show some sign of degeneration and are classified as degenerating.

2.8 Calculation of follicle density

The area of every 12th tissue section was measured using ImageJ 1.46r (National Institutes of Health, Bethesda, MD, USA). For each sample the tissue volume, V, was calculated using the equation:

$$V = \bar{A} \cdot N_s \cdot t$$

where $\bar{A}$ denotes the average area of every 12th section measured (in mm^2), N_s denotes the total number of sections in the sample, and t denotes the section thickness (0.005 mm). Every tissue section was analysed and only follicles with a visible nucleolus or a clearly defined nuclear membrane were counted and staged, to avoid double-counting. Follicle density was determined by dividing the total number of follicles counted in a tissue sample by the tissue volume.

2.9 Imaging

Stained tissue sections were visualised at 100X or 400X magnification using a Leica DM2500 microscope (Leica Microsystems, Germany). Images were captured using a QImaging Micropublisher 5.0 RTV camera with the QCapture Pro 7 software (QImaging, Canada). Light intensity and exposure were adjusted as appropriate within each imaging session.

Chapter 3

Establishing a culture method for cryopreserved human ovarian cortical tissue

3.1 Introduction

To understand the effects of aging, with a potential long-term view to 'treating' reproductive age, it is first critical to ascertain at what stage of follicle development intervention is required. This necessitates the development of a technique that allows all stages of follicle development to be explored and/or manipulated. This Chapter is focused on supporting the development of follicles from the primordial stage.

3.1.1 Current understandings of cortical strip culture

Primordial follicles represent the earliest stage of follicle development and are located in the ovarian cortex. Isolated primordial follicles do not grow successfully in culture therefore follicle culture is not practical for observing the early stages of follicle development (see Chapter 1.11.1) (213, 214). Culturing ovarian cortical tissue in the form of small pieces is

considered to be optimal and capable of supporting follicle development from the primordial to the secondary stage over a period of one to two weeks (210, 211, 233). In humans, an *in vitro* system capable of generating metaphase II oocytes from fresh cortical tissue has recently been described using a three-step culture method prior to *in vitro* maturation (210).

3.1.2 Culture of cryopreserved cortical tissue

Ovarian tissue cryopreservation is indicated for patients who risk significant damage to their ovarian reserve due to chemotherapy, radiotherapy or other predictable causes of premature ovarian insufficiency. The value of this tissue for fertility preservation is evident but given the challenges in obtaining human tissue for research, it also represents a valuable source of tissue for research into follicle development.

Auto-transplantation of cryopreserved tissue has yielded promising results with over 130 live births reported, though is still considered an experimental procedure (258, 259). In some cancer patients however, auto transplantation carries a risk for retransmission of malignant cells and in these cases the only safe alternative is reimplantation of *in vitro* fertilised oocytes obtained from cryopreserved tissue matured *in vitro* (260).

Culture systems aiming to support the initiation of follicle growth and early development have predominantly used fresh tissue from healthy women undergoing gynaecological operations. To date, there is no data regarding the variation in health and development of follicles *in vitro* from tissue cryopreserved for fertility preservation in patients undergoing gonadotoxic treatments, despite its high importance for the feasibility of developing such techniques for alternative methods of fertility restoration, or for use of this tissue in research.

3.1.3 Aims and hypotheses

The aims and hypotheses of this chapter were to determine:

(i) How the health and developmental stage of follicles differs between patients who have cryopreserved cortical tissue for fertility preservation;

   a. *Follicle health and developmental stage in cryopreserved tissue does not vary significantly between patients.*

(ii) Whether the developmental capacity of follicles *in vitro* from cryopreserved tissue varies between patients;

   a. *The developmental capacity of follicles* in vitro *is not significantly different between patients.*

(iii) Whether using neutral red, a vital dye, to identify tissue with viable follicles could improve the percentage of healthy follicles following six days of culture.

   a. *Follicles in tissue positively stained with neutral red will not have more healthy follicles after six days in culture*

3.2 Note to the reader

The culture experiments presented in Chapter 3 were performed concurrently with the work presented in Chapters 4 and 5. As a result, NR was not used in Chapter 4 and the optimisation of NR is presented later in this thesis in Chapter 5.

3.3 Materials and methods

3.3.1 Human cortical strip culture

Tissue from 12 patients aged 9-25 years were obtained as detailed in Chapter 2, Sections 2.1 to 2.3. All patients had a diagnosis of malignancy or blood disorder and were undergoing ovarian tissue cryopreservation for fertility preservation.

Human cortical strip culture was set up and performed as described in Chapter 2, Section 2.5. Briefly, after thawing, tissue was cut into fragments approximately 0.5 x 0.5 mm in size and cultured in on a polycarbonate membrane in a 24-well plate with a McCoy's 5A-based medium for six days. Tissue was fixed in Bouin's solution before culture (as a non-cultured control) or after six days of culture. Tissue from three patients (E, I, L) were incubated with Neutral Red (NR) after processing as described in Chapter 2, Section 2.9.

3.3.2 Processing and histology

Tissue was processed and embedded in paraffin wax before being sectioned at 5 μm and stained with haematoxylin-eosin (Chapter 2, Section 2.6). Follicle development and health was assessed based on morphology (Chapter 2, Section 2.7) and follicle density for each patient was calculated (Chapter 2, Section 2.8).

3.3.3 Validation of sampling interval for density

Tissue fragments for culture experiments are embedded and sectioned at 5 μm intervals. The volume, and subsequently number of sections yielded from each tissue fragment varies, as does the shape of each fragment.

Fragment volume can be calculated using the following calculation:

$$V = \sum (A_1 \cdots A_n) \times d$$

Where $A_1 \ldots A_n$ is the sum of all section areas of the tissue fragment (mm^2) and d is the thickness of the section (mm).

Serial sections from a single fragment of haematoxylin-eosin stained tissue (Chapter 2, Section 2.6) were imaged as described in Section 2.11. The area of each section was measured using ImageJ software (1.48v) (261).

A power calculation was performed to determine whether volume could accurately be estimated by measuring the area of every 6th or 12th sections, rather than the area of every section of tissue assessed.

$$n = \frac{((\sigma_A^2 + \sigma_B^2) \div k)(z_{1-\frac{\alpha}{2}} + z_{1-\beta})^2}{\Delta^2}$$

where:

n is the minimum sample size per condition required to detect a significant difference, σ_A^2 and σ_B^2 are the variances of area numbers from fragment sections where all or every 6th/12th were measured, k is the ratio of allocated samples in the two conditions.

$$\kappa = {}^{n_A}/_{n_B}$$

Where every 6th section is measured

$$\kappa = {}^{1}/_{6}$$

Where every 12th section is measured

$$\kappa = {}^{1}/_{12}$$

$z_{1-\frac{\alpha}{2}}$ is the z score of $1 - \frac{\alpha}{2}$, where α is the probability of making Type I errors (false positives). For a 95% confidence interval, α is 0.05. $z_{1-\beta}$ is the z score of the power, where β is the probability of making Type II errors (false negatives). For 80% power, β is 0.2. Δ is $|\mu_1 - \mu_2|$, the absolute value of the difference between the mean fragment areas when measured from all, every 6th, or every 12th section.

Rearrangement of the formula to calculate the sample size required for 80% power and 95% confidence is therefore:

$$n = \frac{((\sigma_A^2 + \sigma_B^2) \div \frac{1}{n_B} \times 7.84}{\Delta^2}$$

3.3.4 Statistical analysis

All statistical analyses were performed using R statistical software, version 3.5.0 (R foundation for Statistical Computing, Vienna, Austria). Statistical analysis was performed using Fisher's Exact Test unless stated otherwise. Analyses where it was appropriate to adjust for patient variation used the lme4 package in R (262). Data are presented as mean or as odds ratio with 95% confidence intervals where available, and statistical significance was defined as $P<0.05$.

All logistic regressions were offset for tissue volume and included patient as a random effect. Logistic regressions were performed to determine the effect of puberty, and time from surgery to cryopreservation on follicle health. To assess the impact of NR tissue selection on follicle health, follicles were given a binary classification as healthy (no evidence of pyknosis in any cell compartments, Chapter 2 Section 2.9.2) or not healthy. For assessment of asymmetry, follicles were given a binary classification of asymmetric (two or more partial layers of granulosa cells, Chapter 2 Section 2.9.11) or not asymmetric.

3.4 Results

3.4.1 Sampling interval for density calculation

A power calculation was performed to determine whether average tissue area, and subsequently tissue volume, could accurately be estimated by measuring tissue area at intervals of 6 or 12 sections rather than in serial sections. The true average tissue area was

0.0342 mm^2 and very similar values were obtained by measuring every 6th or 12th area, 0.0357 and 0.0354 mm^2 respectively (Figure 3.1). The sample size required to find a significant difference between these values was 12427 at a sampling interval of 6, and 39591 for a sampling interval of 12, suggesting both intervals give an accurate representation of the mean. As a result, the density calculations were based on the measurement of every 12th tissue area in a given fragment.

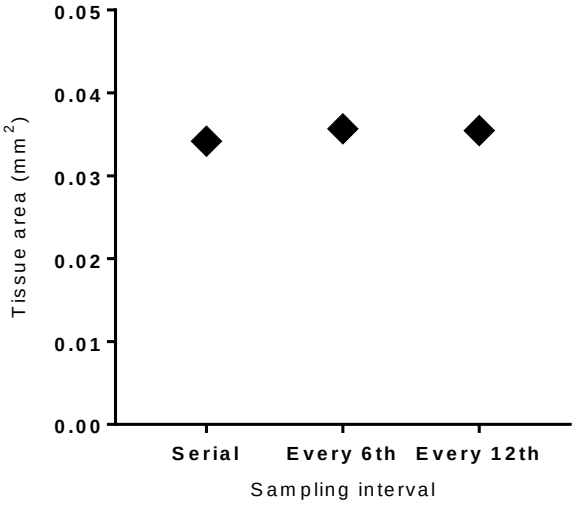


Figure 3.1 Mean tissue area of a single fragment of tissue as a function of sampling interval.

3.4.2 Patient characteristics

The characteristics of the 12 patients whose tissue was used in this chapter are detailed in Table 3.1. Two patients were undergoing ovarian tissue cryopreservation due to a blood disorder, two due to blood cancer, and the remaining eight due to solid cancers. Nine of the twelve patients were confirmed as having gone through puberty, the remaining three patients had not. Of the nine post-pubertal patients, information about menstrual cycle was available for three who were reported as having regular cycles (Table 3.1). Two patients where information on menstrual cycle was unavailable were on the oral contraceptive pill. The mean age of patients who had gone through puberty was significantly higher than for

those who had not (20.56 ± 1.04 years and 12.00 ± 2.08 years, respectively; $p<0.01$). No evidence of malignancy was reported in the histopathology reports from any of the patients.

There was no difference in the time from tissue procurement to cryopreservation between the pre- and post-pubertal groups. The mean time from completion of surgery to start of cryopreservation was 4 h 13 min ± 19 min (Table 3.1).

Table 3.1 Characteristics of patients diagnosed with malignant disease or blood disorder and underwent ovarian tissue cryopreservation for fertility preservation

Patient	Age (years)	Post-pubertal	Regular periods	Diagnosis	Prior treatment	Time from surgery to cryopreservation
A	9	No	N/A	Medulloblastoma	None	3 h 16 min
B	11	No	N/A	Sickle cell	None	4 h 19 min
C	16	No	N/A	Osteosarcoma	None	5 h 20 min
D	16	Yes	Unknown	Ewing's sarcoma	None	5 h 10 min
E	17	Yes	Yes	Ewing's sarcoma	None	2 h 05 min
F	18	Yes	Unknown	Sickle cell	None	3 h 57 min
G	19	Yes	Unknown	Low grade serous papillary peritoneal carcinoma	None	6 h 15 min
H	22	Yes	Unknown [a]	Burkitt lymphoma stage 1A	None	4 h 18 min
I	22	Yes	Unknown	Atypical teratoid rhabdoid tumour (Grade IV)	None	5 h 00 min
J	23	Yes	Yes	Breast cancer, grade 3, oestrogen positive, non-metastatic	None	3 h 05 min
K	23	Yes	Unknown [a]	Hodgkin's lymphoma	None	4 h 20 min
L	25	Yes	Yes	Cervical cancer	None	3 h 32 min

[a] *Patient on the oral contraceptive pill*

The follicular density of the tissue from the 12 patients used in this study is shown in Figure 3.2 and the number of follicles counted per patient in non-cultured and cultured tissue is detailed in Table 3.2. The density of follicles in cortical tissue varied from 18.10 to 448.43 follicles/mm^3 between the patient samples, and all patients tissue contained follicles.

Despite the small sample of tissue and the known heterogeneity of follicle distribution in the ovary, there was a significant inverse correlation between follicular density and age (r= -0.62, $p<0.05$).

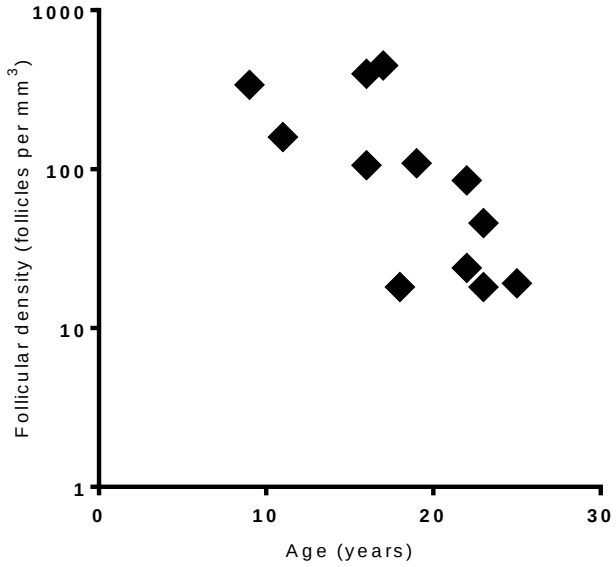


Figure 3.2 The density of follicles in relation to age in cryopreserved ovarian cortical tissue from 12 patients diagnosed with a malignant disease or blood disorder.

There was a significant inverse correlation between follicular density and age (r= -0.62, $p<0.05$). Y axis = Log 10.

Table 3.2 Number of follicles observed in cultured and non-cultured cryopreserved human ovarian tissue

Patient	Non-cultured	Cultured	Total	Selected using neutral red
A	99	27	126	-
B	63 [b]	85	148	-
C	168 [b]	67 [b]	235	-
D	70	58	128	-
E	1224	489 [b]	1713	Yes
F	0	14	14	-
G	67 [b]	68	135	-
H	13	14 [b]	27	-
I	874	90	964	Yes
J	133 [b]	15 [b]	148	-
K	3 [b]	12	15	-
L	139	33 [b]	172	Yes

[b] *Secondary follicles observed*

3.4.3 Number of growing follicles in non-cultured cryopreserved tissue varies between patients

Follicles were observed in non-cultured tissue from 11 of the 12 patient samples. Non-growing follicles were those classed as primordial (Figure 3.3A), growing follicles were those classified as transitional, primary, or secondary (Figure 3.3B-D).

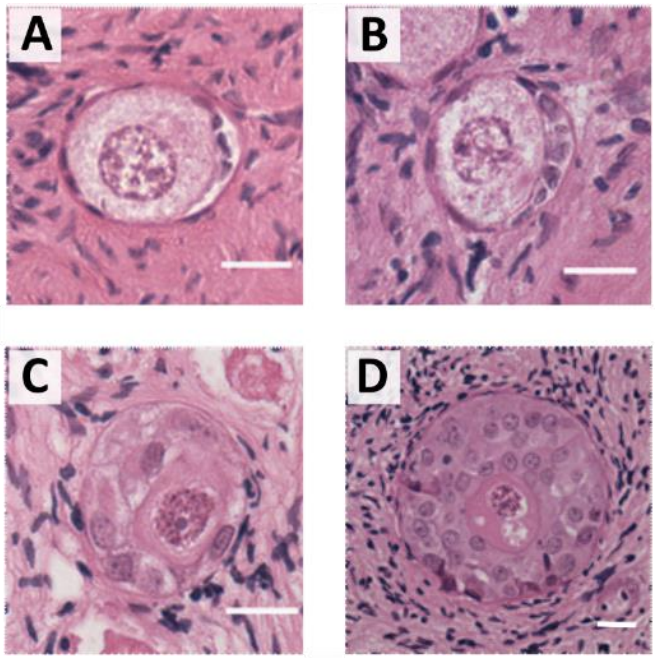


Figure 3.3 Developmental staging of human follicles from cryopreserved ovarian tissue from patients diagnosed with malignant disease or blood disorder.

Representative images of follicles in cryopreserved-thawed ovarian tissue. Tissue was fixed in Bouin's, embedded and stained with haematoxylin and eosin. Follicles were staged as (A) primordial with a single layer of flattened pre-granulosa cells, (B) transitional with a single layer of at least one cuboidal granulosa cell, (C) primary with a complete layer of cuboidal granulosa cells, or (D) secondary with two or more complete layers of cuboidal granulosa cells. Scale bar: 20 μm.

The number of growing compared to non-growing follicles in non-cultured tissue varied significantly based on patient ($p=0.0005$) (Figure 3.4A). Non-growing follicles were the dominant population in non-cultured tissue for five patient samples (patients A, B, E, H, and I), an equal percentage of growing and non-growing were seen in two patient samples (patients C, D), and the percentage of growing follicles dominated in four patient samples (patients G, J, K, and L). Interesting, only growing follicles were observed in non-cultured

tissue from patient K however as only three follicles were seen in this tissue (Table 3.2) it may be due to the small sample size.

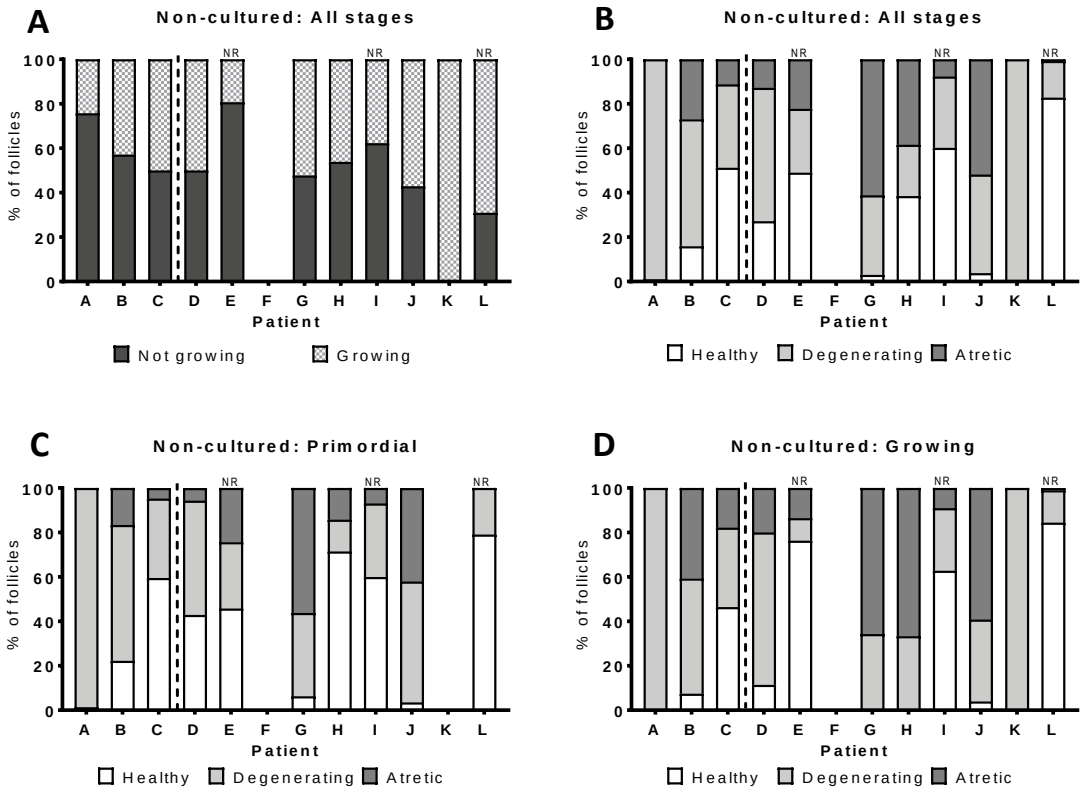


Figure 3.4 Variation between patients in the percentage of growing and healthy follicles in non-cultured cryopreserved human ovarian tissue from patients diagnosed with malignant disease or blood disorder.

Patients listed by ascending age. Dashed line indicates the patients who were not post-pubertal (patients A-C) and those who were post-pubertal (patients D-L). A) Significant variation in the number of growing follicles was seen in tissue from all patients (p=0.0005, Fishers Exact Test); no follicles were observed in non-cultured tissue from patient F. B) The number of healthy, degenerating, and atretic varied significantly between patients p=0.0005, Fishers Exact Test). C-D) The percentage of healthy primordial follicles was greater than that of the growing follicle population in non-cultured tissue, except for those follicles stained with neutral red (NR; patients F, I, and J) which showed a similar percentage of healthy follicles in the primordial and growing follicle populations. NR: tissue was incubated with neutral red and fragments with positive staining were preferentially selected for culture.

3.4.4 Follicle health varies between patients in non-cultured cryopreserved tissue

Follicles were graded as being healthy, degenerating or atretic (Figure 3.5) (see Section 2.7.2). There was significant variation between patient samples in the percentage of healthy follicles in non-cultured tissue (Figure 3.4B) ($p=0.0005$). In three patient samples, tissue fragments were preferentially selected for culture based on visualisation of follicles using the vital dye NR. Tissues from these samples (patients E, I, and J) showed a similar percentage of healthy follicles in the primordial and growing follicle populations. This was in contrast to the 9 patient samples in which NR was not used as in 5 of these, the percentage of healthy follicles was greater in the primordial population compared to the growing population (Figure 3.4C-D). The probability of a follicle being healthy in non-cultured tissue did not differ between pre- and post-pubertal patients and was unaffected by the time from surgery to cryopreservation.

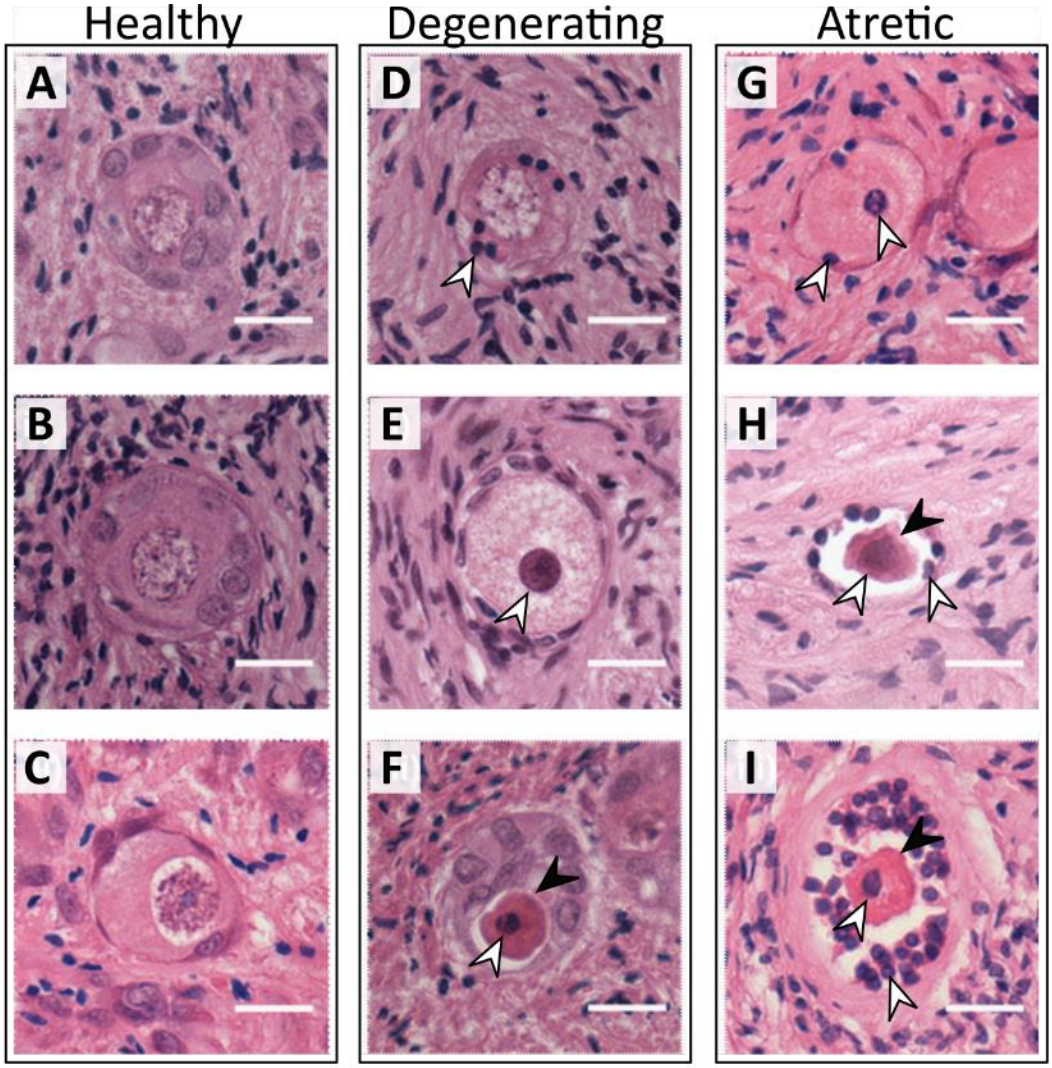


Figure 3.5 Classification of follicle health in human follicles from cryopreserved ovarian tissue from patients diagnosed with malignant disease or blood disorder.

Follicle health was assessed based on the presence or absence of pyknotic granulosa cells, a pyknotic oocyte and a shrunken ooplasm. A-C) Healthy follicles had healthy granulosa cells, a non-pyknotic and non-shrunken oocyte. Degenerating follicles had either D) pyknotic granulosa cells (white arrowhead) or E) a pyknotic oocyte (white arrowhead) with normal ooplasm, or F) a pyknotic oocyte (white arrowhead) with a shrunken ooplasm (black arrowhead) and normal granulosa cells. Atretic follicles had both pyknotic granulosa cells and a pyknotic oocyte (white arrowheads), without shrunken ooplasm (G), or with shrunken ooplasm (black arrowheads, H-I). Scale bar: 20 μm.

3.4.5 Follicle health, but not development is greater in non-cultured tissue selected by neutral red staining

An example of a follicle with NR staining can be seen in Figure 3.6. In non-cultured tissue where NR was used to select tissue fragments as described above, the odds of a follicle being healthy was over 11 times that for follicles from tissue where NR was not used (Figure 3.6B)

(OR=11.4, 95% CI (1.7- 77.4) p=0.0125). There was a smaller percentage of growing follicles in tissue selected using NR though this was not significant (Figure 3.6B).

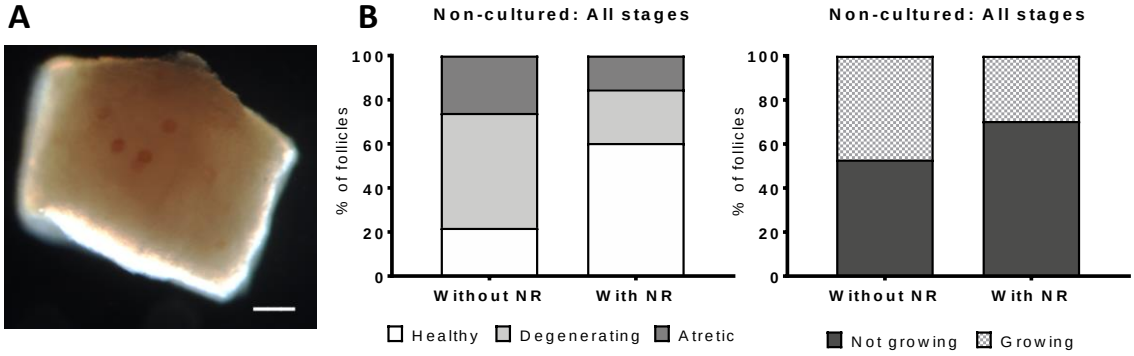


Figure 3.6 Use of neutral red facilitates selection of tissue fragments containing viable follicles in cryopreserved ovarian tissue from patients diagnosed with malignant disease or blood disorder.

A) A cortical tissue fragment containing follicles with NR staining. Scale bar: 100 μm. B) Thawed cryopreserved tissue fragments incubated in neutral red (NR) (n=3 patients) and selected based on presence of staining contained significantly more healthy follicles compared to tissue where NR was not used (n=9 patients) (p=0.0125, OR=11.4, 95% CI (1.7 – 77.4), logistic regression adjusted for tissue volume with patient as a random effect). There was no difference in the number of growing follicles in non-cultured tissue selected by NR staining compared to tissue where NR was not used.

3.4.6 Cultured cryopreserved tissue has a dominant population of growing follicles in all patients

Overall, culture resulted in a significant change in the non-growing and growing follicle populations, with the odds of a growing follicle in cultured tissue being 52 times that of non-cultured tissue (OR=52.44, 95% CI (37.05- 76.41), p<2.2e-16). The health and development of follicles in tissue from each patient are detailed in Figure 3.7. The percentage of growing follicles in cultured tissue did not vary significantly between patient samples with 83-100% of follicles growing following culture, i.e. at the transitional, primary, or secondary stage (Figure 3.7A). The percentage of growing follicles in tissue after six days of culture was not different between fragments that had been selected based on NR staining and those that had not been selected based on NR (Figure 3.7F). The composition of the growing follicle population is shown in Figure 3.7B and there was a significant difference in the number of

transitional, primary, and secondary follicles between patient samples. Primary follicles were the dominant growing follicles in all patient samples except for patient K, and in patient B where 50% of follicle were growing. The number of secondary follicles observed after six days of culture was low compared to transitional and primary follicles and represented at most 9% of the total follicles in cultured tissue (Figure 3.7B; Patient C).

3.4.7 Neutral red selected tissue has superior follicle health post-culture

Despite significant activation and development of follicles in cultured tissue, overall follicle survival in cultured tissue was low. Following six days of culture, all follicles from tissue not selected using NR showed some sign of degeneration (Figure 3.7E), however, this is not surprising as 78% of follicles in this cohort showed some sign of degeneration in non-cultured cryopreserved tissue (Figure 3.6). In tissue selected by NR staining, 18% (n=612; 3 patients) of follicles were healthy after six days of culture (Figure 3.7E). Sixty percent of follicles were healthy in non-cultured tissue selected using NR (Figure 3.6), this meant that follicles in these tissues were over 13 times more likely to be healthy in non-cultured compared to cultured tissue (OR= 13.67, 95% CI (10.04-18.91), $p<2.2e-16$). The odds of a follicle from NR selected tissue being healthy after six days in culture were over 100 times that of a follicle from tissue where NR was not used to select fragments for culture (Figure 3.7E) (OR=108.9, 95% CI (12.3-962.8), $p=2.46e-05$).

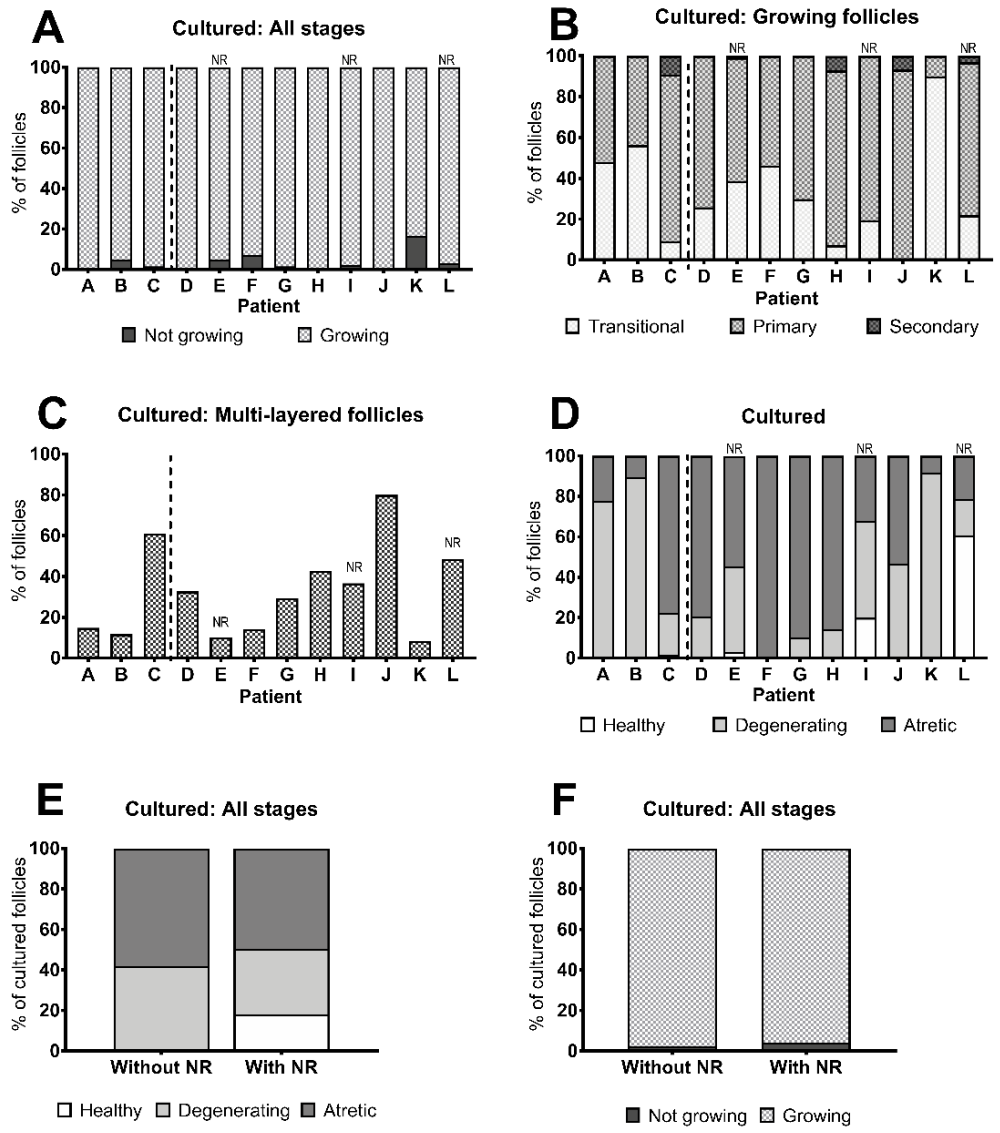


Figure 3.7 Variation between patients in percentage of growing, and healthy follicles and the effect of tissue selection using neutral red in cultured cryopreserved ovarian tissue from patients diagnosed with malignant disease or blood disorder.

A) There was no variation in the number of growing follicles in cultured cryopreserved ovarian cortical tissue from patients A – L (p=0.289, Fishers Exact Test). B) Within the growing population of follicles in cultured tissue, the relative number of transitional, primary, and secondary follicles varied between patients (p=0.0005, Fishers Exact Test). Primary follicles were the dominant stage in the growing population for all patients except patient K, and patient B (50% growing). C) The percentage of multi-layered follicles, multi-laminar follicles with more than one layer of granulosa cells D) The number of healthy (no morphological evidence of degeneration), degenerating (presence of either a pyknotic oocyte, pyknotic granulosa cells, or shrunken ooplasm), and atretic (presence of both pyknotic oocyte and pyknotic granulosa cells) varied significantly between patients p=0.0005, Fishers Exact Test). E-F) Tissue selection using neutral red had a significant impact on the proportion of healthy follicles present but did not impact the number of growing follicles (p=2.46e-05, OR=108.9, 95% CI (12.3-962.8), logistic regression adjusted for tissue volume with patient as a random effect; p>0.05, Fishers Exact Test). NR: neutral red staining used to select tissue.

3.4.8 Follicles grown in culture have asymmetric granulosa cell distribution

In cultured tissue, primary follicles were 3.2 times more likely to have at least one additional partial granulosa cell layer compared to non-cultured primary follicles (OR=3.17, 95% CI (1.83-5.80), p=5.772e-06) (Figure 3.8A). Asymmetric follicles, primary follicles with two or more partial layers of granulosa cells and only one complete layer of granulosa cells, were observed in eight of the cultured patient samples (Figure 3.8C-D). By contrast in non-cultured tissue, only two asymmetric primary follicles were observed, each in fragments of tissue from different patients (Figure 3.8A). When adjusted for tissue volume and patient, the odds of a primary follicle being asymmetric in cultured tissue was 1117 times that of non-cultured tissue (OR=1117.3, 95% CI (250.2-4990.7), p<2e-16).

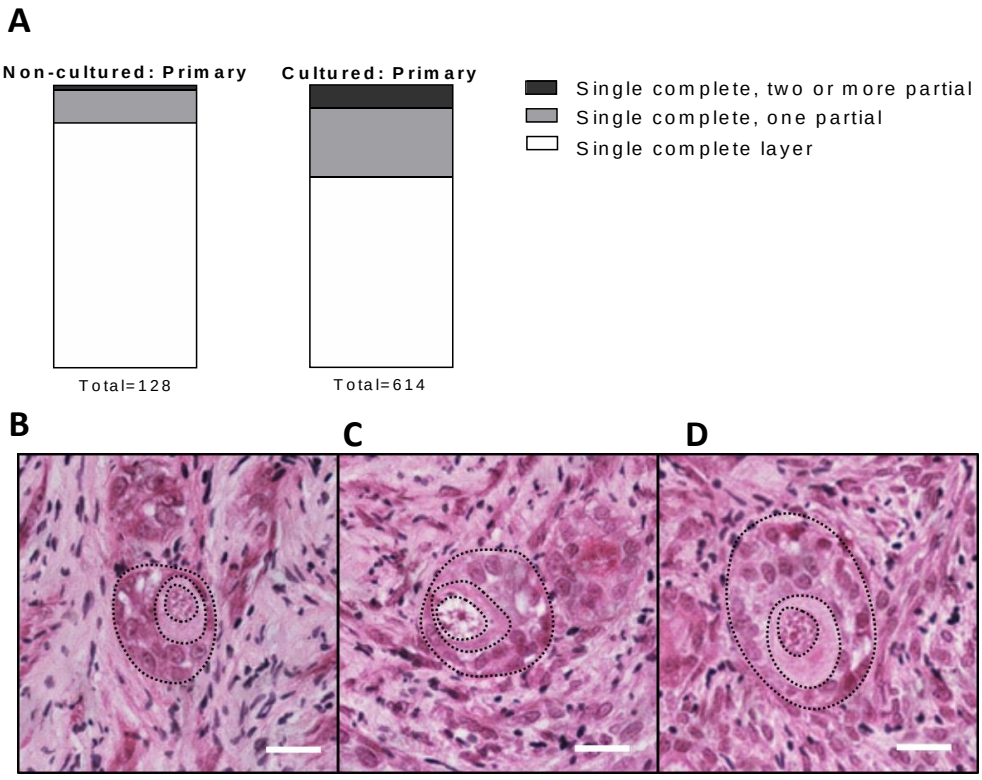


Figure 3.8 Asymmetric primary follicles were more common in cultured cryopreserved tissue.

Asymmetric primary follicles with variable numbers of partial granulosa cell layers were observed in non-cultured and cultured tissue. (A) The likelihood of primary follicles being asymmetric (those with a single complete layer of granulosa cells and two or more partial layers) increased with culture (OR=1117.3, 95% CI [250.2-4990.7], p<2e-16, logistic regression adjusted for tissue volume and patient). (B) Follicle with a single complete granulosa cell layer and one partial layer. (C) Follicle with a single complete granulosa cell layer and two partial layers. (D) Follicle with a single complete granulosa cell layer and three partial layers. Scale bar: 20 μm.

3.5 Discussion

Presented here is the first human cortical strip culture method established in our department. It is also the first patient-specific evaluation of health and development of follicles in cortical tissue cryopreserved for fertility preservation before and following *in vitro* culture. Furthermore, this Chapter describes a new protocol for human cortical strip culture utilising NR to identify fragments with viable follicles for culture. The results highlight wide variation between patients in the health and developmental stage of follicles in cryopreserved ovarian cortical tissue, and how the use of NR can make a significant difference to outcome following culture.

3.5.1 Sources of variation in follicle health

3.5.1.1 Cryopreservation

Early studies looking at the viability of ovarian cortical tissue cryopreserved in humans focused primarily on follicle development following xenotransplantation to demonstrate function, without accompanying histological assessment (263). Variation and lack of clarity in morphological criteria for atresia between studies, as well as differing methods of cryoprotection, has made it challenging to define a baseline for cryopreservation-induced follicle degeneration. Here I describe the morphological criteria assessed as well as representative images of each variation of follicle health we observed. There is evidence that primordial follicles are resistant to cryoinjury with no change in morphology from fresh tissue with very few cells in fresh or frozen tissue exhibiting any sign of atresia (264). Variation in follicle health post-thaw may be tied to follicle health in fresh tissue as despite finding no difference between fresh and frozen-thawed follicles, 27% of follicles in fresh tissue showed multiple signs of atresia; eosinophilia of the ooplasm, contraction and clumping of the chromatin material, and wrinkling of the nuclear membrane (265). In stark contrast to the results detailed in (265) where over 70% of follicles were viable after

cryopreservation, other groups have reported that only half of follicles are completely viable following cryopreservation (254, 266, 267).

Short-term culture post-thaw has been used to ascertain a more accurate assessment of follicle viability. In cryopreserved bovine tissue an improvement in morphological parameters were observed after four hours of culture suggesting a capacity for recovery of some damage from cryoprotection. By contrast, Hreinsson et al. Hreinsson, Zhang (254) found the likelihood of a follicle being atretic in cryopreserved human tissue post-thaw increased from 1-in-5 to 1-in-3 after four hours of culture. It raises the question of whether there is latent damage induced by the cryopreservation procedure which is not evident based on morphology or viability assay when tissue is assessed immediately post-thaw. To ensure non-cultured and culture tissue fragments were comparable, non-cultured tissues in this study were out of cryoprotection for approximately an hour before fixation - the time taken to process tissue for culture. As a result, non-cultured fragments are likely more similar to short-term cultured tissue. Indeed the levels of atresia observed in non-cultured tissue selected with NR in this study are in line with approximately two-thirds reported by Hreinsson et al. Hreinsson, Zhang (254).

3.5.1.2 Alternative methods of assessing follicle health

In this study I saw a large variation in the percentage of healthy follicles between 12 patients from 0-83% whereas Maltaris, Kaya (268) assessed follicle health post-cryopreservation in 10 patients with a cancer diagnosis by LIVE/DEAD assay and reported variation in the percentage of healthy follicles of 39-55%. The wider range observed here could be due to numerous factors; greater variation in patient diagnoses, patient age, cryoprotection protocol, or assessment of health as Maltaris et al. state the LIVE/DEAD assay likely overestimates the survival rate (268).

Use of viability or assays that differentiate between live and dead cells provide a useful additional measure of follicle health in conjunction with morphological assessment. We considered using them in this work but ultimately chose not to because of the aims of the study and the quantity of tissue required. Tissue fixed and stained has the advantage of being able to confer information about the number of follicles at various stages of development, their health, and surrounding tissue architecture in addition to the density of follicles in a given piece of tissue. Viability stains require the digestion of tissue precluding it from being used to assess follicle development *in situ* or evaluate follicle density (234, 254). After the digestion process follicles may remain fully or partially enclosed in granulosa cells thus limiting the conclusions that can be made about overall follicle health. Morphological analysis was judged to permit a more holistic assessment of follicles given the availability of tissue for research.

3.5.1.3 Patient diagnoses

Ten patients had a cancer diagnosis. A systematic review and meta-analysis evaluating the available data on response to ovarian stimulation in women with malignancy found an increased incidence of poor ovarian performance compared to healthy age-matched IVF patients, with a lower mean number of oocytes retrieved and a reduced number of mature oocytes retrieved (269). This would suggest that ovarian function in cancer patients is altered in some way. Based on our results and those of Azarbaijani, Sheikhi (225) and Asadi-Azarbaijani, Sheikhi (226), more limited secondary follicle development is observed compared to healthy cryopreserved tissue (253), although publications on this are limited (discussed in Section 1.12.2).

The variation in the degree of follicle atresia observed in non-cultured tissue was also observed after six days in culture. In five patient samples (patients C, D, F, G, and H) >80% of follicles were atretic (oocyte and granulosa cells pyknotic) after six days of culture. These

patients did not have fewer healthy follicles before culture, and while tissue from patients G and H had a higher percentage of atretic follicles than other patients before culture, patients C and D did not. There was no common diagnosis between these patients and I found that follicle health was not dependent on pubertal status or time from surgery to cryopreservation.

The impact of patient characteristics on follicle health must be discussed with the caveat that there was no information available on the reproductive health of the patients. Of the twelve patients' tissue used in this work, nine were post-pubertal and it is unknown whether any of these patients had a reproductive disorder that would affect any of the parameters assessed. Similarly, there was no information on body weight, day of cycle, or regularity of cycles.

3.5.1.4 Optimising survival with Neutral Red

Irrespective of the source of variation in follicle health from cryopreserved tissue, identifying viable follicles for further development is essential. I found the use of NR effective and easy to implement within the culture workflow. Viable follicles could be identified in thin cortical fragments by their red staining after one hour. A significantly greater number of follicles in non-cultured tissue had a healthy morphology when tissue was selected by NR-staining (60% compared to 22%, respectively). These findings support those from Kristensen et al. Kristensen, Rasmussen (270) who demonstrated specificity of NR for viable follicles in medulla tissue from patients undergoing fertility preservation before gonadotoxic treatment. Additionally, the results presented here demonstrate the value of such a technique in selecting tissue for culture with the aim of optimising the proportion of healthy follicles.

Follicle health declines over the course of culture, and there is evidence to suggest that this decline is more marked in cryopreserved tissue (233). I assessed whether tissue selection using NR-staining would lead to better follicle development after culture. When NR was not used, nearly all follicles showed some sign of degeneration after six days of culture which was unsurprising given that only 22% were healthy in the non-cultured tissue. By contrast from 60% healthy follicles present in NR-selected non-cultured tissue, 18% of follicles retained a healthy morphology. These results of NR-selected tissue are consistent with the 2.5-to-3 fold decrease in the proportion of healthy follicles reported by other groups culturing cryopreserved tissue over a similar timeframe, despite differences in culture systems (225, 226, 233, 253).

3.5.2 Follicle development in cultured tissue

Six days in culture resulted in a significant increase in the number of developing follicles, with most follicles at the primary stage. Within the growing population, there was variation in the size and morphology of the transitional, primary, and secondary populations between patients.

3.5.2.1 Current understanding of follicle development in cultured cryopreserved tissue

The existing literature on cultured slow-frozen human cortical tissue was discussed in Section 1.12.2. The focus of the studies varied from comparison of culture condition (227, 228, 231, 233, 252), freezing method (230, 232, 253), or the impact of disease on ovarian function (225, 226). The aim of the studies therefore was *not* to assess the development of cryopreserved tissue and this is reflected in the sparsity of information regarding follicle health and development. As a result, our understanding of the expected development of follicles in cryopreserved tissue in culture is limited. Follicle development is most commonly grouped into 'primordial' or 'growing', encompassing both primary and secondary follicles. While this provides a useful measure of the number of follicles activating

and starting to develop in culture, where advanced follicle development is the desired endpoint it provides no clarity. It is possible that the authors observed modest secondary follicle development and grouped follicles in these stages to reflect this.

3.5.2.2 Perturbation to normal follicle development in culture tissue

Interestingly, a significant proportion of primary follicles in cultured tissue were asymmetric, with two or more partial granulosa cell layers in addition to a single complete layer. It is unclear whether the asymmetry is a result of the physical culture environment or whether it is a result of accelerated growth due to culture conditions or an as yet unknown factor. The two-dimensional membrane on which the tissue is placed may encourage proliferating granulosa cells to move away from the oocyte (271), no 'direction' to the asymmetry was observed so it is not immediately evident if this is the case. It is important to ascertain the impact of asymmetry on subsequent follicle growth and developmental competence of the enclosed oocytes as current multi-step *in vitro* protocols involve the excision of secondary follicles based on size following cortical strip culture (210, 211). However, based on size asymmetric follicles would be indistinguishable from non-asymmetric follicles when using a dissecting, brightfield microscope. Signalling between the oocyte and its surrounding granulosa cells is essential for the development of a maturation, healthy oocyte as well as for granulosa cell proliferation (37, 272, 273).

Future work could assess whether physical culture environment or culture medium is contributing to this phenomenon and look to quantify whether there is altered granulosa cell proliferation. Proliferating cell nuclear antigen (PCNA), Ki67, and minichromosome maintenance protein 2 (MCM2) have all been used to assess granulosa cell proliferation in human tissue (274-276).

3.5.3 Rationale for culture system

There is no consensus of a gold standard culture medium and system for cryopreserved human cortical tissue (see Section 1.12.2, Table 1.4). To date, the most successful method, namely that which has afforded the development of human oocytes to the most advanced stage, is that used by Telfer and colleagues (210, 211). Their work has used predominately fresh tissue, biopsied from women undergoing gynaecological surgeries. I chose to use medium supplemented as they describe (see Section 2.4) and this is, to the best of my knowledge, the first evaluation of the follicle development in cryopreserved tissue cultured in this medium. The method of tissue preparation used in this study differed from their published work, where they use larger fragments of tissue mechanically stretched with small gauge needles, I used an automated tissue chopper. The chopper had two advantages; firstly, human cortex is extremely fibrous and difficult to stretch with needles, the tissue chopper removes an element of user bias which may improve reproducibility between groups, secondly it is less labour intensive and thus more conducive to clinical implementation. Thinner fragments of tissue allowed us to avoid issues with necrosis observed by other groups who had attempted the method (N Spears 2017, Personal Communication, 30 January). By using the same culture medium used by Telfer and colleagues, I aimed to create a basis for evaluating the performance of cryopreserved tissue in culture compared to fresh tissue.

3.5.4 Heterogeneity of follicle distribution

Despite sampling a small volume of tissue per patient, an inverse correlation between age and follicle density was observed, confirming and extending that reported by Schmidt et al. Schmidt, Byskov (13) with a sample of tissue from 21 women. The heterogeneity in follicle distribution within the human cortex is well described (13, 264, 277), and has been cited as a strong reason that multiple pieces of ovarian cortex should be replaced upon re-implantation. It is possible that this heterogeneity extends to the response of follicles within

a single ovary to the effects of cryopreservation, culture, or transplantation and the variation between patients reported in this study lends support to this idea. The patients used in this study had their tissue cryopreserved in the hope that in the future following treatment, the tissue could either be transplanted to restore their fertility or that intervening research would enable us to develop eggs *in vitro*. With less than 5% of stored tissue used per patient in this study compared with over one third routinely used for transplantation, the potential for optimised *in vitro* culture systems to improve the utilisation of cryopreserved tissue is clear (278).

3.5.5 Relevance of these results to research and treatment development

3.5.5.1 As a research tool

The findings in this chapter suggest cryopreserved cortical tissue is a useful source of tissue for the investigation of follicle development. It appears that cryopreserved tissue behaves differently in culture than fresh tissue based on published literature and the findings reported here. As the publications looking specifically at cryopreserved tissue in culture are few and of variable quality, more investigation in this area is warranted. The culture system used in this study can adequately support follicle development to the primary stage, and alterations to the culture system may be required to permit development to a more advanced stage of development. The variation between patient tissue also enforces the need for appropriate statistical tests to be employed when analysing the data. This issue has been discussed by Webber, Stubbs (279), yet such methods remain underutilised in the field (142, 217, 280).

3.5.5.2 As an alternative method of fertility restoration

As the first study to look at the variation between fragments of tissue from different patients it draws attention to variation at a patient level not previously described. It highlights the need for a comparison between fresh and frozen-thawed tissue in culture, on an individual

basis to ascertain what parameters of processing or patient-related factors are driving variation so that protocols for cryopreservation and culture can be optimised to address these.

3.5.6 Conclusion

In summary this chapter describes the human cortical strip culture technique established for the first time in our department. It has revealed that variation between patients in the health and development of follicles may necessitate a more individual approach to downstream treatment options. The findings demonstrated for the first time that there is variation between patients both in the health of non-cultured tissue post-cryopreservation as well as the health and development after six days in culture. The culture system described was effective in initiating follicle activation and growth in this tissue, but optimisation is required to improve the survival of follicles across the culture period. Given the heterogeneity of tissue and clear variation in follicle health post-thaw in these patients, including a non-toxic viability marker as described here is a critical step in improving the efficiency and effectiveness of *in vitro* follicle development as a research tool for investigating follicle development as well as an alternative method of fertility restoration. Having established a means of investigating the earliest stages of follicle development the next step is to use this system to manipulate follicle development.

Chapter 4

Investigating the effect of LSD1 inhibition on human follicle development

4.1 Introduction

Conceptually, epigenetic events may be responsible for the differential follicular gene expression patterns observed with age, and subsequently are an appropriate target for intervention. Small molecules provide a means of targeting specific epigenetic machinery without genetic modifications. The molecule used in this thesis to study follicle epigenetics, targets Lysine-specific demethylase 1A (LSD1, KDM1A). LSD1 is a flavin adenine dinucleotide (FAD)-dependent amine oxidase, which can act on mono- and dimethylated histone 3 lysine 4 and lysine 9 (H3K4me1, H3K4me2 and/or H3K9me1, H3K9me2). Demethylation of methylated H3K4 removes the chromatin mark for transcriptional activation, whereas demethylation of methylated H3K9 removes the signal for epigenetic transcriptional repression thus allowing LSD1 to function both as a transcriptional co-repressor or co-activator (281-283). LSD1 is critical for normal development and its global

knockdown results in developmental arrest during murine embryogenesis at or before embryonic day 5.5 (284).

The LSD1 ortholog is critical for male and female fertility in *Drosophila* and *Caenorhabditis elegans*. In flies its absence results in a complete loss of oocytes in females and immotile sperm in males (285), in nematodes a loss of LSD1 ortholog causes defective oogenesis and spermatogenesis which increases the incidence of sterility across generations (286). LSD1's role in mammalian ovarian biology was unknown until recently, when a knockout study in mice showed that it was critical for normal oocyte meiotic progression (287). The oocyte-specific deletion resulted in precocious resumption of meiosis, in addition to spindle and chromosome abnormalities, the effects were shown to be mediated through the altered regulation of H3K4me2.

LSD1 epigenetically regulates cellular energy balance. Adipocytes treated with an LSD1-inhibitor showed increased mitochondrial activity and increased mitochondrial mass (288). In particular, Peroxisome Proliferator-Activated Receptor Gamma Coactivator 1 Alpha (PPARGC1), a key gene in mitochondrial biogenesis identified in Chapter 7, is upregulated in response to LSD1 inhibition making it an interesting target to explore in human ovarian tissue (288, 289).

4.1.1 GSK-LSD1, a chemical probe for LSD1

GSK-LSD1 is an irreversible, mechanism-based inhibitor of LSD1 developed by GlaxoSmithKline and made available as part of the Structural Genomic Consortium (SGC) epigenetics initiative. GSK-LSD1 inhibits LSD1 with an IC50 of 16 nM (the concentration of an inhibitor where the response (or binding) is reduced by half) and is > 1000 fold more selective over other closely related FAD utilizing enzymes (i.e. LSD2, MAO-A, MAO-B) (290).

GSK-LSD1 induces gene expression changes in cancer cell lines (average EC50 < 5 nM; the concentration of a drug that gives half-maximal response) (290).

4.1.2 Aims and hypotheses

The aims and hypotheses of this chapter were to determine:

(i) Whether human ovarian tissue cultured in the presence of GSK-LSD1 and/or DMSO is viable after six days of culture;

   a. *Follicles in ovarian cortical tissue cultured with DMSO for six days will be viable;*

   b. *Follicles in ovarian cortical tissue cultured with GSK-LSD1 and DMSO for six days will be viable.*

(ii) Whether the health or development of follicles in human ovarian tissue treated with DMSO for six days differed to that of non-treated human ovarian tissue cultured for six days;

   a. *Follicle health and development in tissue treated with DMSO for six days will not differ to tissue cultured without DMSO.*

(iii) Whether the health or development of follicles in human ovarian tissue treated with GSK-LSD1 for six days differed to that of DMSO-treated human ovarian tissue cultured for six days;

   a. *Follicle health and development in tissue treated with GSK-LSD1 for six days will not differ to tissue cultured with DMSO for six days.*

4.2 Materials and methods

4.2.1 Preliminary experiment with tissue from a single patient

Tissue was selected from a single patient (aged 19 years) based on the inclusion and exclusion criteria detailed in Section 2.2. GSK-LSD1 was reconstituted in DMSO and stored at -20 °C until use. Ovarian tissue fragments were processed and cultured as described in Section 2.6, with GSK-LSD1 in 100% DMSO, 50 nM, 100 nM, 250 nM, or 500 nM, Sigma-Aldrich, UK). As GSK-LSD1 was reconstituted in DMSO, a DMSO only control was included in addition to a non-treated control and a non-cultured control. To minimise the amount of tissue used, 500 nM DMSO (the maximal quantity included with 500 nM GSK-LSD1) was used in all conditions, irrespective of GSK-LSD1 concentration (Table 4.1). Tissue was also fixed in Bouin's without culture as described in Section 2.6.

Table 4.1 Preliminary GSK-LSD1 dose response conditions for human ovarian tissue culture

Condition	Cultured	Type	Concentration GSK-LSD1	Concentration DMSO	Base medium
Non-cultured	No	Control	-	-	McCoy's 5A (see Section 2.6.2)
Non-treated	Yes	Control	-	-	McCoy's 5A (see Section 2.6.2)
DMSO	Yes	Control	-	500 nM	McCoy's 5A (see Section 2.6.2)
50 nM GSK-LSD1	Yes	Treatment	50 nM	500 nM	McCoy's 5A (see Section 2.6.2)
100 nM GSK-LSD1	Yes	Treatment	100 nM	500 nM	McCoy's 5A (see Section 2.6.2)
250 nM GSK-LSD1	Yes	Treatment	250 nM	500 nM	McCoy's 5A (see Section 2.6.2)
500 nM GSK-LSD1	Yes	Treatment	500 nM	500 nM	McCoy's 5A (see Section 2.6.2)

4.2.2 Dose response experiment with multiple patients

Four patients aged 17 – 25 years were selected based on the inclusion and exclusion criteria detailed in Section 2.2. Ovarian tissue fragments were processed and cultured as described

in Section 4.2.1 however a wider concentration range of GSK-LSD1 was used (125 nM, 250 nM, 500 nM, 1 μM, or 2 μM) (Table 4.2). As the maximal concentration of GSK-LSD1 increased to 2 μM, the DMSO concentration of all conditions was increased to 2 μM, including the DMSO only control. Experimental repeats; repeat-01, repeat-02, repeat-03, and repeat-04 each used tissue from a single patient.

Table 4.2 Extended GSK-LSD1 dose response conditions for human ovarian tissue culture

Condition	Cultured	Type	Concentration GSK-LSD1	Concentration DMSO	Base medium
Non-cultured	No	Control	-	-	McCoy's 5A (see Section 2.6.2)
Cultured	Yes	Control	-	-	McCoy's 5A (see Section 2.6.2)
DMSO	Yes	Control	-	2 μM	McCoy's 5A (see Section 2.6.2)
125 nM GSK-LSD1	Yes	Treatment	125 nM	2 μM	McCoy's 5A (see Section 2.6.2)
250 nM GSK-LSD1	Yes	Treatment	250 nM	2 μM	McCoy's 5A (see Section 2.6.2)
500 nM GSK-LSD1	Yes	Treatment	500 nM	2 μM	McCoy's 5A (see Section 2.6.2)
1 μM GSK-LSD1	Yes	Treatment	1 μM	2 μM	McCoy's 5A (see Section 2.6.2)
2 μM GSK-LSD1	Yes	Treatment	2 μM	2 μM	McCoy's 5A (see Section 2.6.2)

4.2.3 Processing and histology

Tissue was processed and embedded in paraffin wax before being sectioned at 5 μm and stained with haematoxylin-eosin (Section 2.6). Follicle development and health was assessed based on morphology (Section 2.7). Follicle density for each tissue piece was calculated (Section 2.8).

4.2.4 Statistical analysis

All statistical analyses were performed using R statistical software, version 3.5.0 (R foundation for Statistical Computing, Vienna, Austria). A generalised linear mixed model following a negative binomial distribution (glmmPQL; 291) was performed to determine the effect of culture condition on follicle development, offset for tissue volume and treating patient as a random effect. For assessment of asymmetry, follicles were given a binary classification of asymmetric (two or more partial layers of granulosa cells, Chapter 2 Section 2.9.11) or not asymmetric. For assessment of advanced follicle development, follicles were given a binary classification of advanced (asymmetric primary and secondary follicles), or not advanced. An ordinal regression (clmm2) was performed to determine whether follicle health was affected by treatment condition, again adjusting for tissue volume and patient. Data are presented as mean (±SEM), as odds, or as odds ratio with 95% confidence intervals, unless otherwise stated, and statistical significance was defined as $P < 0.05$.

4.3 Results

4.3.1 Preliminary experiment with tissue from a single patient

The first aim of this Chapter was to see whether ovarian tissue cultured in the presence of GSK-LSD1 and/or DMSO was viable, and this was assessed using tissue from a single patient.

4.3.1.1 Trend towards more secondary follicles with increasing dose of GSK-LSD1

The dominant stages of follicle development in non-cultured control tissue were primordial (n=32 follicles, 47.8%) and transitional (n=25 follicles, 37.3%) (Figure 4.1 A). There were a modest number of more developed follicles with nine primary follicles (13.4%) and one secondary follicle observed (1.5%) (Figure 4.1 A). In the cultured non-treated control tissue, the population shifted to a predominantly primary follicle population (n=47, 69.1%), which

was also observed in the DMSO-treated cultured tissue (n=43, 71.7%), demonstrating that follicles in cortical tissue cultured with DMSO were capable of growth (Figure 4.1 A).

No secondary follicles were observed in the cultured control and two secondary follicles (3.3%) were observed in the DMSO control, however in a single patient no conclusions can be drawn as to whether this difference is significant (Figure 4.1 A).

A population of mainly primary follicles was observed in all GSK-LSD1 treatment conditions as seen in the D6 and DMSO controls (Figure 4.1 A), similarly demonstrating that follicles in cortical tissue cultured with GSK-LSD1 were capable of growth. For secondary follicles, in the 250 nM and 500 nM concentrations of GSK-LSD1 a greater percentage were observed compared to the cultured and DMSO controls (Figure 4.1 A). Four (6.2%) and seven (9.1%) secondary follicles were observed in the 250 nM and 500 nM GSK-LSD1 treatment groups, respectively.

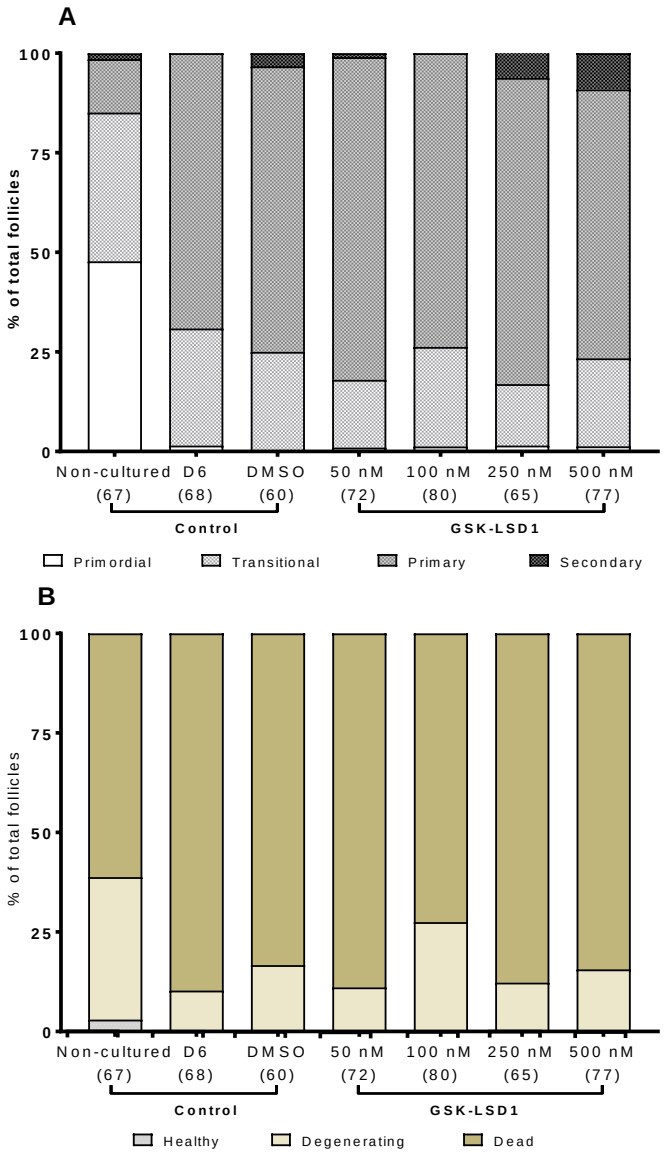


Figure 4.1 Follicle health and development in preliminary GSK-LSD1 dose-response experiment.

Ovarian tissue fragments analysed without culture or following six-day culture (D6) in the presence or absence of DMSO, or varying concentrations of GSK-LSD1. A; Follicle development is more advanced after culture in all conditions. B; Total follicle health is poor in both non-cultured tissue (healthy n=2, 3%) or cultured (D6) tissue. Follicle number per condition in parentheses.

4.3.1.2 Follicle health

A very low number of healthy follicles were observed in non-cultured tissue (n=2, 3%) therefore it was not possible to conclude whether any of the culture conditions measurably impacted follicle health (Figure 4.1 B). Two-thirds of all follicles observed in non-cultured tissue were atretic (n=41, 61.2%), with a further 35.8% (n=24) showing signs of

degeneration. As in the D6 and DMSO controls, there were no healthy follicles observed in any of GSK-LSD1 treatment groups (Figure 4.1 B).

4.3.2 Dose response experiment with multiple patients

4.3.2.1 Variation in follicle density between patient and treatment condition

Having demonstrated that follicles in tissue cultured with GSK-LSD1 and/or DMSO are capable of development, tissue from multiple patients across a greater range of doses was used to explore the effect of LSD1 inhibition on follicle health and development.

Four extended dose response repeats were performed. Each experimental repeat used tissue from a single patient. In repeat-04 no follicles were observed in the non-cultured control tissue, and those in the Day 6 non-treated group were all classed as atretic. As it could not be ascertained whether the follicles did not survive culture or were atretic before culture, this repeat was excluded from subsequent analysis.

Follicle density varied within fragments of tissue from a single patient, and mean follicle density varied significantly between all patients (Figure 4.2A). Tissue from the patient used in repeat-03 had a significantly higher density than that from the patients used in repeat-01 and repeat-02. The tissue from the patient used in repeat-01 was lower than both repeat-02 and -03. Despite variation between patients, there was no difference in the follicle density based on treatment condition; before or after culture, or between any of the culture conditions (Figure 4.2B).

Patient variation in the health and development of follicles was observed in tissue from different patients, as described in the previous chapter. Since this was not the focus of this chapter see Supplementary Figure 1(Appendix I).

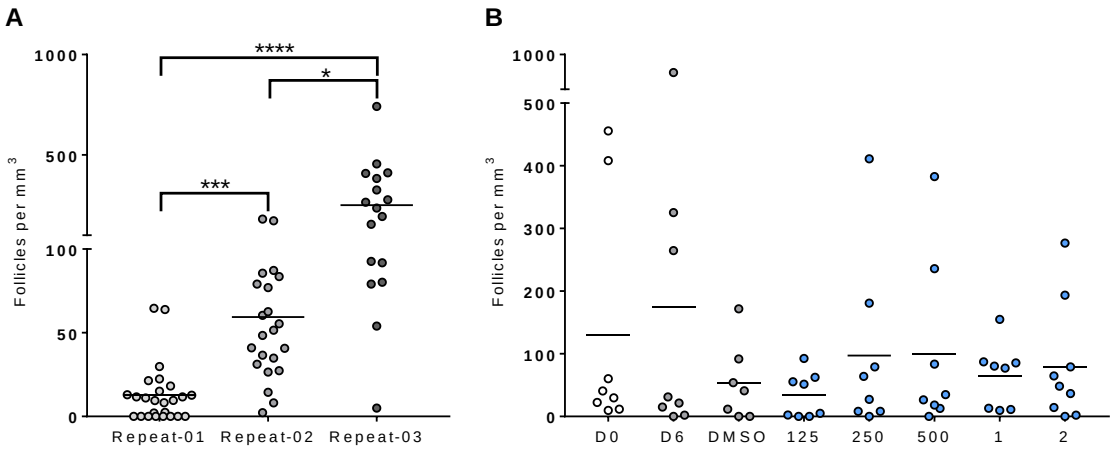


Figure 4.2 Variation in follicle density in tissue pieces from human ovarian cortical tissue from 3 patients.

Data presented as median and range, each point is the follicle density of a block of tissue. A) Variation in follicle density by patient. Tissue from the patient used in repeat repeat-03 had a significantly higher density than that from the patients used in repeat-01 and -02. B) Follicle density did not differ significantly between treatment conditions.

4.3.2.2 DMSO treatment affects follicle health but not development compared to non-treated, cultured control

The effect of DMSO on follicle health and development for each experimental repeat is detailed in Figure 4.3. Greater variation was observed between experimental repeat than culture conditions in both follicle development and health (Figure 4.3A and B, respectively). Three follicles were observed in the DMSO condition in repeat-01 compared to 37 follicles in the control cultured condition and 49 follicles and 101 follicles in the repeat-02 and -03, respectively. The lack of follicles observed in repeat-01 at the transitional or secondary stage is likely due to low follicle number.

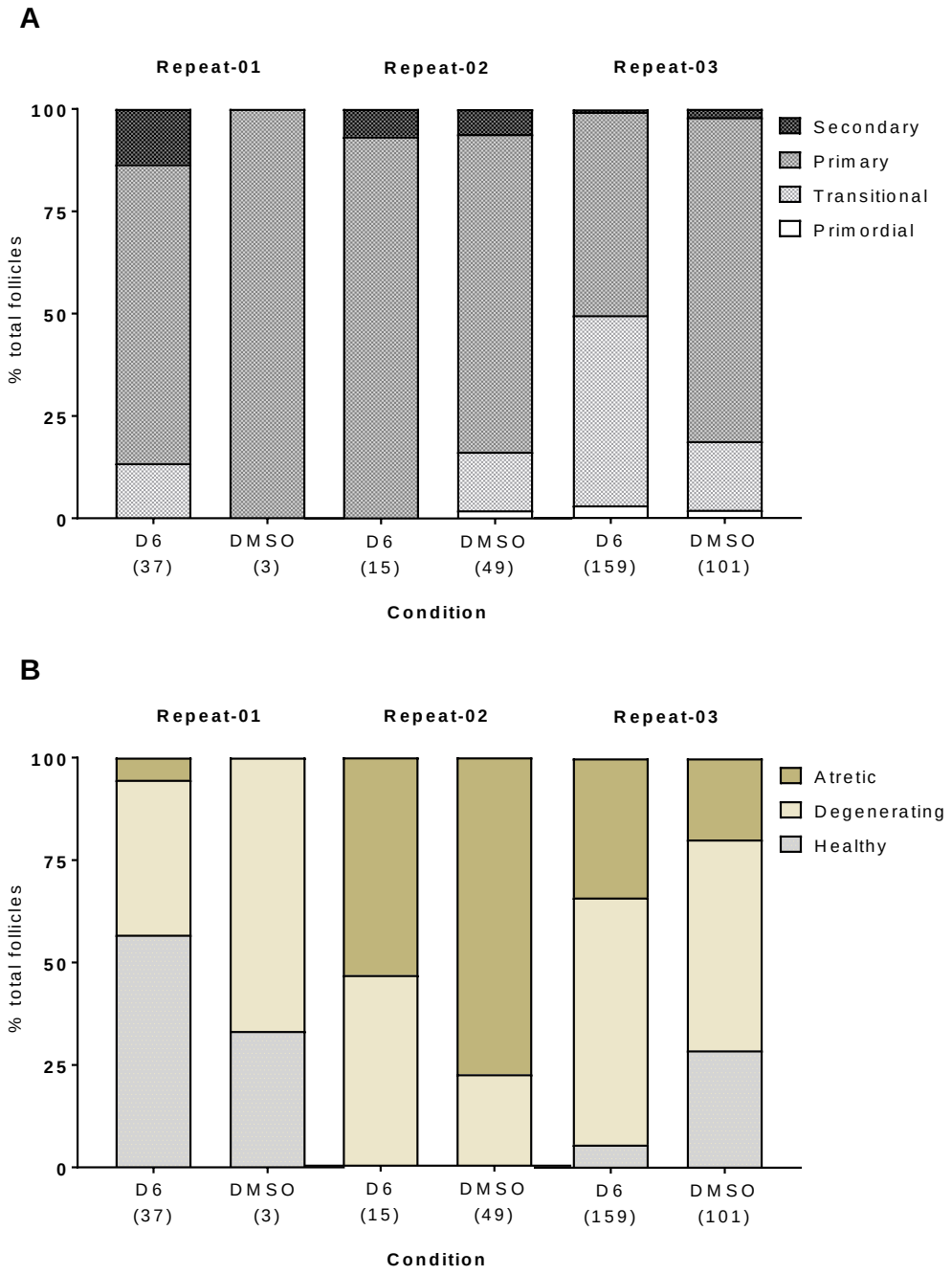


Figure 4.3 Follicle development and health in human cortical tissue cultured for 6 days in the presence or absence of DMSO

Data is presented as percentage of total follicles with total follicle number listed in brackets. A) The percentage of follicles at various stages of development showed little variation between culture condition. Primary follicles were the dominant population in all repeats in both DMSO and non-treated Day 6 controls. B) The percentage of follicles that were healthy, degenerating, or atretic after culture varied more dramatically between experimental repeat than culture condition. Ovarian tissue from 3 patients was fixed and stained with haematoxylin and eosin.

When both patient and tissue volume were adjusted for, there was no difference in the mean number of follicles per mm^3 at the primordial, transitional, primary, or secondary stage in cultured tissue treated with DMSO compared to tissue cultured without DMSO (Figure 4.4).

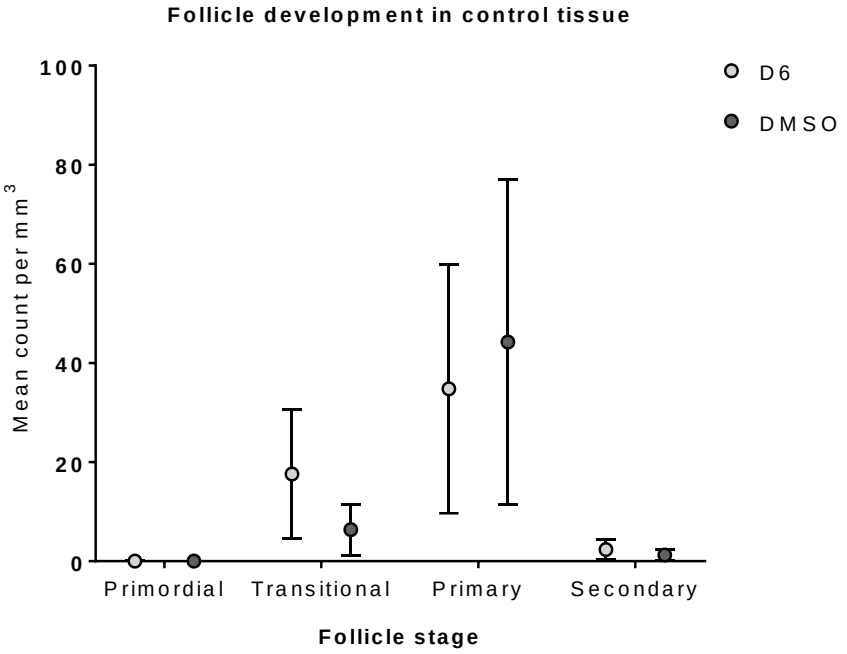


Figure 4.4 Mean follicle count per developmental stage in human ovarian cortical tissue cultured for 6 days with, or without DMSO

Mean follicle counts ± SEM of primordial, transitional, primary, and secondary follicles in non-treated cultured tissue (D6), or tissue cultured in medium supplemented with 2 μM DMSO for 6 days (DMSO). Generalised linear model adjusted for tissue volume with patient as a random effect. Ovarian tissue from 3 patients was fixed and stained with haematoxylin and eosin.

Interestingly, for tissue cultured in DMSO rather than D6 medium, the odds of "healthy" follicles versus "degenerating" or "atretic" follicles combined are 4.43 times greater, given that all other variables in the model are held constant (Table 4.3). Because of the effect of DMSO on follicle health, DMSO-treated tissue was used instead of non-treated D6 control as the control for ascertaining the effect of GSK-LSD1 on follicle development.

Table 4.3 Follicle health in DMSO-treated sections compared to cultured, non-treated control. Ordinal regression of follicle health with the levels: healthy, degenerating, atretic. Data presented as odds ratio and standard error.

	Dependent variable:
Condition:	Health
DMSO	0.226** (0.254)
Observations	364 follicles
Note:	**p<0.01

4.3.2.3 GSK-LSD1 does not affect the number of primordial, transitional, primary or secondary follicles

When both patient and tissue volume were adjusted for, there was no difference in the mean number of follicles per mm^3 at the primordial, transitional, primary, or secondary stage in cultured tissue treated with 125 nM – 2 μM GSK-LSD1 to tissue cultured with DMSO (Figure 4.5). In all conditions primary follicles were the most abundant developmental stage and primordial follicles were scarce. There was some variation in the mean number of early developmental stage follicles per mm^3 between the conditions with a noticeable difference between the 125 nM and 250 nM GSK-LSD1conditions.

There appeared to be a trend towards an increased number of secondary follicles per mm^3 with an increased concentration of GSK-LSD1 as shown in Figure 4.5, however a linear regression fit to secondary follicles per mm^3 found the slope did not differ significantly from zero (r^2=0.60, p=0.12).

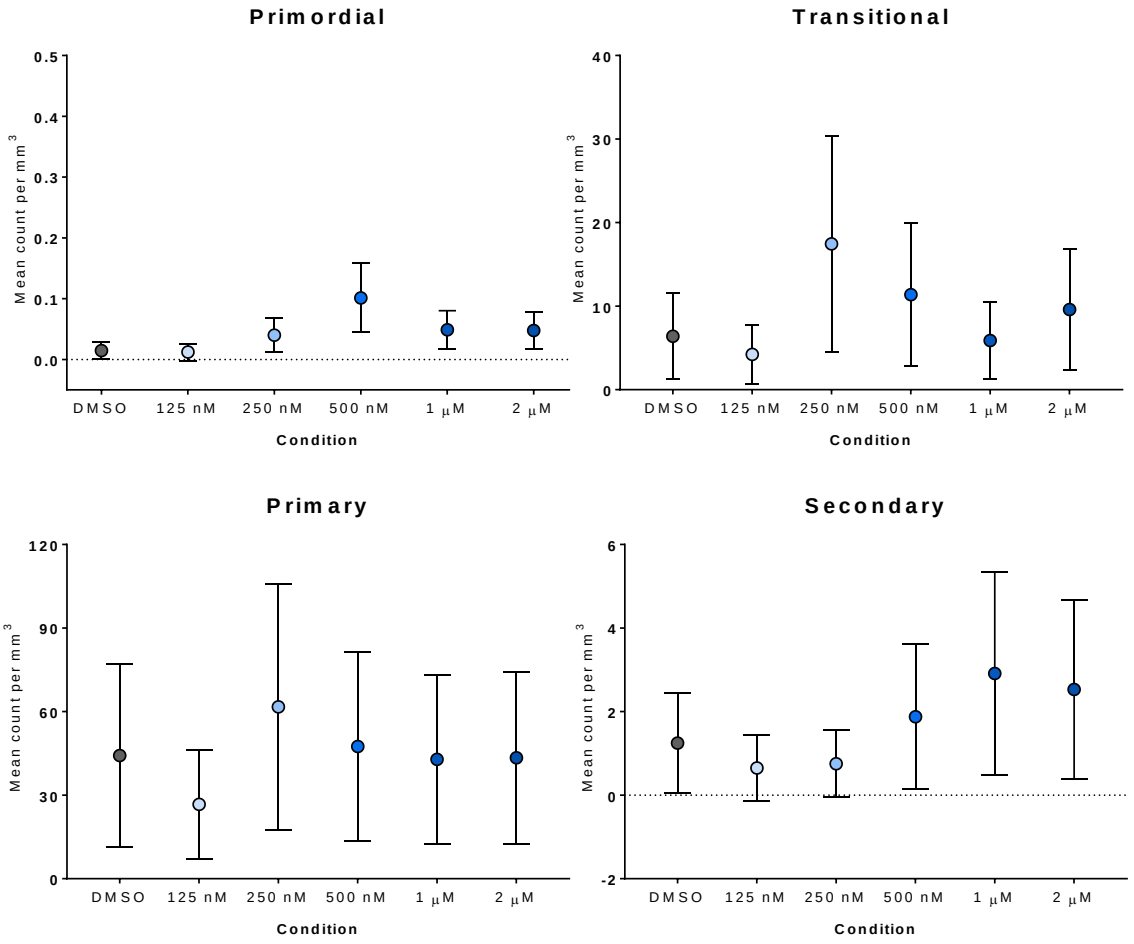


Figure 4.5 Mean follicle count per developmental stage in human ovarian cortical tissue cultured for 6 days with varying concentrations of GSK-LSD1, or with DMSO

Ovarian tissue fragments from 3 patients were cultured with 125 nM – 2 μM GSK-LSD1 reconstituted in DMSO, or in 2 μM DMSO for 6 days. Tissue was fixed and stained with haematoxylin and eosin to enable to the quantification of follicles at various stages of development by histology. Mean follicle counts ± SEM of primordial, transitional, primary, and secondary follicles are reported. Generalised linear model adjusted for tissue volume with patient as a random effect. Ovarian tissue was fixed and stained with haematoxylin and eosin.

4.3.2.4 2 μM GSK-LSD1 treatment of cortical tissue increases the likelihood of advanced stage follicles

As discussed in the previous chapter, follicles can have multiple granulosa cell layers. Multi-layer follicles include three types of follicles; primary follicles with a single partial granulosa cell layer, primary follicles with two or more partial granulosa cell layers (asymmetric primaries), and secondary follicles. A logistic regression found no difference in the likelihood of a follicle being multi-layered when cultured with GSK-LSD1 at any

concentration compared to DMSO alone (Table 4.4). However, within the multi-layered follicle cohort, at 2 μM GSK-LSD1 there was a trend towards a greater likelihood that follicles were more advanced in their development, i.e. staged as either asymmetric primary or secondary follicles, OR=1.99 p=0.072 (Figure 4.6).

Table 4.4 Odds ratio of multi-layered follicles in GSK-LSD1-treated tissue compared to DMSO-treated tissue. Logistic regression of follicle developmental stage with the levels: multi-layer, single-layer. Data presented as odds ratio and 95% confidence interval. Follicle stage assessed by histology.

		Dependent variable:
Condition:		Multi-layer compared to single-layer
	125 nM GSK-LSD1	0.802 (0.44 – 1.41)
	250 nM GSK-LSD1	0.79 (0.52 – 1.21)
	500 nM GSK-LSD1	0.87 (0.56 – 1.37)
	1 μM GSK-LSD1	0.958 (0.60 – 1.54)
	2 μM GSK-LSD1	1.33 (0.87 – 2.05)
	Observations	1289
Note:		*p<0.05; **p<0.01

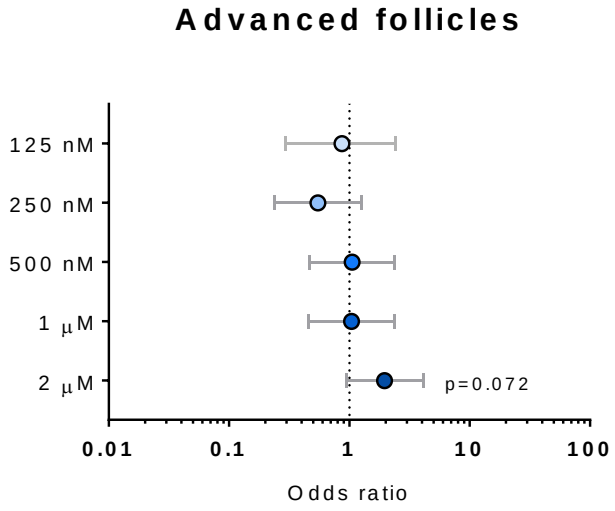


Figure 4.6 Odds ratio of advanced follicles within the multi-layer cohort from GSK-LSD1-treated tissue compared to DMSO-treated tissue.

Ovarian tissue fragments from 3 patients were cultured with 125 nM – 2 μM GSK-LSD1 reconstituted in DMSO, or in 2 μM DMSO for 6 days. Logistic regression of follicle developmental stage within the multi-layered cohort (n=380) with the levels: advanced, other. Advanced follicles are those staged as asymmetric primary or secondary. Data presented as odds ratio and 95% confidence interval. Grey bars indicate p>0.05.

4.3.2.5 2 μM GSK-LSD1 does not affect overall follicle health

Follicle health was assessed using an ordinal regression comparing follicle health in tissue cultured in various concentrations of GSK-LSD1 to the DMSO control. In all concentrations except for 2 μM GSK-LSD1, the odds of follicles being classified as "degenerating" or "atretic" was around 2-4 times greater for tissue cultured with GSK-LSD1 compared to DMSO, given that all other variables in the model are held constant (Table 4.5).

Table 4.5 Follicle health in GSK-LSD1-treated tissue compared to DMSO-treated control. Ordinal regression of follicle health with the levels: healthy, degenerating, atretic. Data presented as odds ratio and standard error.

		Dependent variable:
Condition:		Health
	125 nM GSK-LSD1	3.662** (0.265)
	250 nM GSK-LSD1	1.965** (0.180)
	500 nM GSK-LSD1	4.584** (0.201)
	1 μM GSK-LSD1	2.060** (0.218)
	2 μM GSK-LSD1	0.742 (0.189)
	Observations	1289
Note:		**p<0.01

4.3.2.6 Follicles at advanced stages of development are less likely to be degenerating or dead

To ascertain whether the variation in follicle health was due to differences in the number of follicles at different stages of development, an ordinal regression was performed for follicle health based on developmental stage. Indeed, follicles were more likely to be classed as "degenerating" or "atretic" when at an earlier follicle stage than the asymmetric primary follicles (Table 4.6). The largest difference was observed in asymmetric primaries compared to primordial follicles, which were 100 times more likely to be classed as "degenerating" or "atretic". Odds of follicles being classed as "degenerating" or "atretic" were 7.7 and 2.7 times higher for transitional and primary follicles, respectively. Secondary follicles were no more likely than asymmetric follicles to be "degenerating" or "atretic" indicating that in tissue cultured with DMSO and/or GSK-LSD1 with DMSO, follicles at more advanced stages of

development have superior morphological health compared to those at the early primary or below.

Table 4.6 Follicle health in follicles of different developmental stages compared to asymmetric primary follicles. Ordinal regression of follicle health with the levels: healthy, degenerating, atretic. Data presented as odds ratio and standard error.

		Dependent variable:
Stage:		Health
	Primordial	0.010** (0.753)
	Transitional	0.129** (0.244)
	Primary (*zero or one additional partial layers*)	0.368** (0.203)
	Secondary	0.652 (0.370)
	Observations	1289
Note:		**p<0.01

Representative images of asymmetric primary follicles from tissue cultured in 2 μM GSK-LSD1 are shown in Figure 4.7. Images A – E show follicles with healthy granulosa cell morphology, the follicle in image F also has some pyknotic granulosa cells which comprise less than half of the granulosa cell population. Images C, D, and E were from one patient with tissue with a high follicle density where clusters of follicles can be seen.

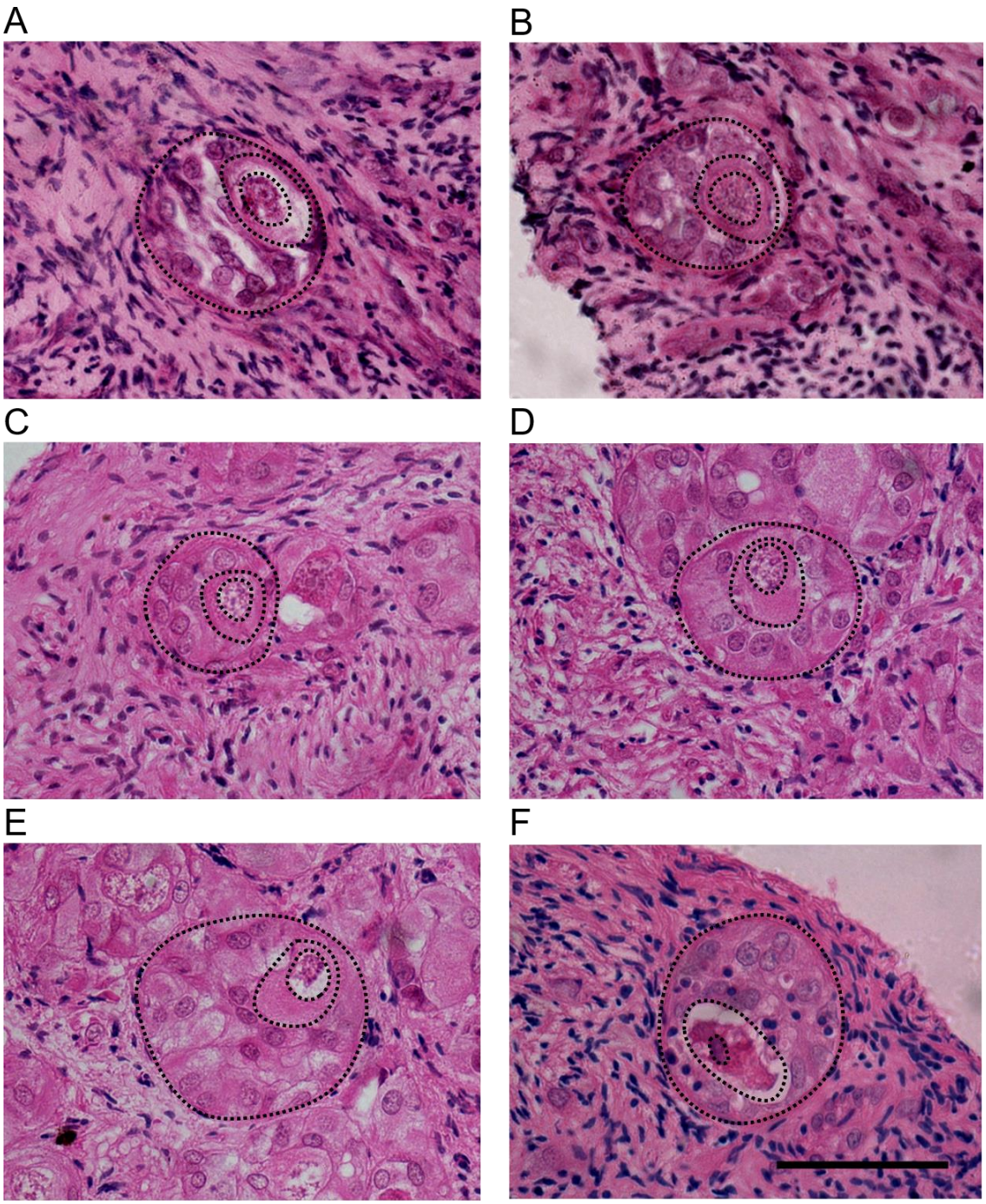


Figure 4.7 Representative images of asymmetric primary follicles from human ovarian tissue cultured in 2 μM GSK-LSD1.

Ovarian tissue fragments from 3 patients were cultured with 2 μM GSK-LSD1 reconstituted in DMSO for 6 days and stained with haematoxylin and eosin to enable morphological assessment of developmental stage. Asymmetric primary follicles A-F have a single complete layer of cuboidal granulosa cells and two or more partial layers of granulosa cells. Scale bar: 100 μm.

4.4 Discussion

In this Chapter I explored the effect of LSD1 inhibition on follicle development from the primordial stage in human ovarian tissue. Across the range of doses investigated only the highest dose, 2 μM, altered follicle health or development. At this dose follicles were more likely to be at an advanced developmental stage, asymmetric primary or secondary follicles, and were less likely to be classified as degenerating or atretic.

4.4.1 DMSO alters follicle health not development

Before the effect of GSK-LSD1 treatment on follicle health and development is discussed it is necessary to address the potential effect of DMSO, the control condition, on these parameters. As the inhibitor was dissolved in DMSO it was necessary to include DMSO alone as a control condition. To minimise the quantity of patient tissue used, each GSK-LSD1 dose was controlled to include 2 μM total DMSO, or 0.2% (vol/vol), to limit the required DMSO control conditions to one. While exposure to DMSO was consistent in all medium formulations it may mask the effect of GSK-LSD1 at lower doses and subsequently future experiments should seek to delineate the dose-matched effect of DMSO on development in this setting.

A recent study by Hao, Tuck (292) looking at the effect of aryl hydrocarbon receptor modulators in human ovarian cortical strip culture also dissolved the compounds used in DMSO, including a 0.1% DMSO control. The authors did not comment on the potential effect of DMSO, nor was there a comparison to a non-treated control condition. Morphologic analysis of follicle health by the authors revealed approximately one-third of follicles retained a healthy morphology following culture for seven days in DMSO which is in line with that observed for two out of three patients used in this study. This similarity is

interesting given Hao, Tuck Hao, Tuck (292) used fresh tissue which, as discussed in Chapter 3, appears to have superior survival in culture to cryopreserved tissue.

4.4.2 The role of LSD1 across follicle development

Histones can be methylated on lysine (K) or arginine (R) residues, among the most-studied sites of lysine methylation are that of H3 histone proteins (293). The roles of histone 3-lysine 4 (H3K4) and histone 3-lysine 9 (H3K9) methylation across mammalian follicle development are only starting to be elucidated. The most robust evidence comes from a study by Kim et al., who looked at the effect of an oocyte-specific deletion of LSD1 on the fertility of female mice (287). The *Zp3*-driven deletion of LSD1 resulted in knockout of LSD1 in growing oocytes, those at the primary stage or above, but not in primordial follicles. In the LSD1-KO mice, substantially elevated levels of H3K4me2 were observed in follicles of all developmental stage (from primary and above) by immunohistochemistry compared to minimal differential regulation of H3K4me1, H3K9me1, and H3K9me2. At one month of age there was no observable morphological difference between the control and LSD1-KO females. However, oocyte development was accelerated in the LSD1-KO females as evidenced by the presence of ovaries that were larger and had many advanced stage follicles than control mice at two months of age. At six months the follicle pool in the LSD1-KO females was largely depleted in contrast to the controls, with many fully-grown oocytes observed in the control females at this time point.

In agreement with that reported by Kim et al., culture of human ovarian tissue in the presence of a LSD1 inhibitor for 6 days increased the propensity for advanced follicle development. In the initial dose response experiment there was a trend towards increasing secondary follicle development, however while there was an increased likelihood of asymmetric primary or secondary follicles in LSD1-treated tissue, there was no change in the likelihood of secondary follicle development alone. The modest alteration in follicle

development in response to LSD1 inhibition can most likely be attributed to 1) dose of GSK-LSD1, 2) duration of treatment, 3) species variation or 4) the spatiotemporal effect of treatment.

Interestingly, follicles at this advanced stage were associated with a healthier morphology than those from control-treated tissue. Oocytes from LSD1-KO females undergo germinal vesicle breakdown at a significantly faster rate but fail to progress through MI as shown through superovulation studies (287). Our study only observed follicles across 6 days of culture, with follicles reaching the secondary or preantral stage. The next steps would be to isolate and continue to culture follicles in the presence of GSK-LSD1 to see whether the observed block in meiotic progression, and subsequent apoptosis, is also observed following *in vitro* maturation.

4.4.3 Possible sites of action of LSD1 within the follicle

The methylation pattern of H3K4 and H3K9, and the expression of LSD1 in the human ovary has not been reported. In mice, pigs, and cow oocytes robust LSD1 expression is found (294-296). In pigs, H3K4 methylation appears to be spatially and developmentally regulated. All oocytes from primary to large antral stage follicles show positive staining for H3K4me1, H3K4me2 and H3K4me3, with intensity increasing as development progresses (296). Granulosa cells of primary, secondary, and early antral follicles are negative for H3K4 methylation, suggesting that in the current experiment, the effect of LSD1 inhibition are likely mediated through the effect of GSK-LSD1 on the oocyte.

Interestingly, granulosa cells from large antral follicles show an upregulation in H3K4 methylation, specifically in the cumulus cells and the granulosa cells in the inner two cell layers of the follicular wall which then dramatically reduces immediately prior to ovulation (296). Given the major effect of oocyte-specific LSD1 inhibition on meiotic resumption, a

process that critically involves cumulus cells, it raises the question of whether the effects of LSD1 inhibition would be magnified if both the oocyte and follicular cells were targeted.

4.4.4 Time-specificity of action

Kim et al. used a transgenic mouse line with a knockout of LSD1 in growing oocytes. Inhibition of LSD1 in primordial follicles, the dominant population in cortical tissue, may have a different or opposing effect to that in growing follicles which would explain the results observed in this study. There is evidence in cell lines that the timing of LSD1 inhibition during development dictates its effect on differentiation. In pre-adipocytes, treatment with an LSD1-inhibtor (such as GSK-LSD1) initiated two days before differentiation induction significantly reduced adipogenesis however this effect was lost when treatment was started on day 3 after differentiation induction. This suggests that an inhibition of LSD1 acts on factors involved in initiating rather than maintaining adipogenic differentiation. Culturing cortical tissue for two-three days or treating tissue with a PTEN-inhibitor to force follicle activation before administering GSK-LSD1 would provide a starting point for a more direct comparison of LSD1 inhibition in growing follicles between mice and humans. Assessing the effect of LSD1 inhibition on a primordial follicle population alone is more challenging due to the many follicle stages present in the cortex. Human foetal ovarian tissue at 24 weeks gestation is reported to contain only primordial follicles and would be one option for investigating the effect of LSD1 inhibition on primordial follicles (297).

4.4.5 Challenges with follicle visualisation and identification

In contrast to the oocyte-specific deletion investigated in the study by Kim et al., the compound used in this study may affect any of the ovarian tissue. Western blots and/or immunohistochemistry would typically be used to quantify any change to H3K4 or H3K9 methylation states. The low follicle density in ovarian tissue means that a western blot

would largely give information about the differential regulation of histone methylation in stromal tissue which was not the focus of this study. When considering immunohistochemistry, the extreme heterogeneity in follicle distribution within and between patients creates issues in identifying slides of tissue containing follicles, as can be seen Figure 4.2, many cultured tissue fragments do not contain follicles. Furthermore, identifying a sufficient number of follicles to provide interpretable results is a secondary challenge. Developing methods to circumvent these limitations were identified as being critical to progressing our research in this area and are subsequently the focus of the next chapter.

4.4.6 Questions raised and future studies

Our understanding of the role of H3K4 and H3K9 methylation in normal human follicle development remains incomplete. Some key questions raised by this work around the effect of higher doses of GSK-LSD1 and its effects at later stages of development are primary avenues for future work. To understand the mechanism by which LSD1 is potentially having an effect in human follicle development, more advanced epigenetic techniques are required. Chromatin Immunoprecipitation (ChIP) represents the gold standard for analysing protein based epigenetic marks by providing very specific information on proteins associated with a particular genomic region, such as a promoter (298). The immunoprecipitation step targets one modification or transcription factor dictated by the chosen antibody but can be coupled to PCR for known genes or next generation sequencing to explore the overall role of that modification. Use of ChiP-seq for small numbers of cells is still in its infancy and histone profiling also requires high-quality monoclonal antibodies of which few are commercially available (299).

4.4.7 Conclusion

The present study lends credence to the concept that epigenetic manipulation of follicle development is a potentially applicable strategy for *in vitro*-based therapeutic interventions, however greater insights into the role of histone modifications in normal human follicle development are required for progress in this area.

Chapter 5

Exploring methods to visualise oocytes in human ovarian cortex

5.1 Introduction

A limitation of working with human ovarian cortical tissue is the difficulty in assessing the follicular cohort before or after culture. Follicle distribution through the human ovarian cortex is exceptionally heterogeneous and can vary up to two orders of magnitude from within the same ovary (13). The inability to determine whether the starting material contains follicles has significant ramifications for our ability to use human cortical tissue to study the regulation of follicle development or optimise techniques for clinical use.

The greatest success in developing follicles from the primordial stage *in vitro* has been found when follicles are left *in situ* within cortical tissue (Section 1.11.1). We and others have found that often multiple non-cultured or cultured tissue fragments will be processed for histology only to find that some fragments are devoid of follicles (Section 3.4.3, Section 4.3.2.1) (213, 242). Where the endpoint of interest is an aspect of follicle development, low

follicle numbers limit the conclusions drawn, and increasing the amount of tissue used to compensate for low follicle numbers significantly increases the costs and analysis time. Being able to identify fragments of tissue that contain follicles at the beginning of an experiment would be highly advantageous.

The vital dye Neutral Red (NR) has been used in cytotoxicity studies as a marker of cell viability (256, 300). It has been demonstrated to effectively label viable follicles within ovine cortical tissue and has subsequently been used to determine follicular density of fresh human cortical tissue or medulla by incubating the tissue for 4 hours before visualisation (257, 270). As NR did not affect tissue and follicle survival in culture in an ovine model, it has strong promise for identifying follicles in human tissue before culture (257). It remains to be investigated whether this dye can be incorporated into the workflow of human cortical strip culture without the use of a 4-hour incubation to allow visualisation of follicles in fresh tissue before culture.

For histological analysis of embedded tissue, every section of a non-cultured or cultured tissue fragment is analysed for the presence of follicles (211, 224), but for immunohistochemical applications this is not practical. As follicles can be dispersed or present in clusters followed by areas of cortex without follicles, regular sampling of serial sections from small cultured tissue fragments may not capture a sufficient number of follicles for subsequent analysis (13, 301).

The ability to efficiently employ immunohistochemical techniques to investigate molecular markers during follicle development would greatly expand the strength of cortical strip culture as a research tool, and for this reason this chapter aimed to assess the ability of two straightforward methods of identifying frozen-thawed or fixed and embedded tissue that contained follicles.

5.1.1 Aims and hypotheses

The aims and hypotheses of this chapter were to determine:

(i) Whether an incubation with NR for 1 hour was sufficient to visualise follicles in tissue fragments before culture;

   a. *Incubating ovarian cortical tissue fragments with NR for 1 hour will not be sufficient to visualise follicle in tissue fragments before culture.*

(ii) Whether dewaxing or partial haematoxylin staining could allow the stroma and follicles to be discriminated in fixed, embedded, and sectioned tissue, prior to histological analysis;

   a. *Neither dewaxing, nor partial haematoxylin staining of fixed, embedded and sectioned tissue will allow sufficient discrimination of stroma and follicles.*

5.2 Materials and methods

5.2.1 Processing of cortical tissue for incubation with Neutral Red

Cortical tissue from a whole ovary donated by a 43-year-old woman undergoing elective oophorectomy was used for this study. The ovary was bivalved and the medulla removed before being cut into strips 1 mm x 2 mm x 5 mm (Section 2.2). A single strip was processed as detailed in Section 2.4.1.

5.2.1.1 Incubation of un-fixed tissue with Neutral Red

Tissue fragments were transferred from the tissue chopper into a Petri dish containing NR diluted to a final concentration of 25 μg/ml in dissection medium and tissue was cut manually into pieces an appropriate size for culture as described in Section 2.4.1. Tissue fragments were left in NR at room temperature and staining assessed at 1 hour from the time the tissue was first in contact with NR. A room temperature incubation was used for

the first hour to assess whether NR could be included in the dissection medium while the tissue was manually cut by hand as part of the existing protocol.

After visualising tissue pieces after 1 hour, dissection medium was replaced with 25 μg/ml NR in culture medium (composition: Section 2.4.2) and incubated at 37°C with 5% CO_2 in air for a further 3 hours with staining visualised at the 2-hour and 4-hour time points.

5.2.1.2 Visualisation of NR staining

After 1, 2, and 4 hours of incubation tissue pieces were washed in fresh dissection medium without NR to wash away dye crystals and improve discrimination of red staining. Pieces were observed using standard dark-field microscopy at 1X, 2X, or 5X magnification for the presence of red colouration. Tissue fragments were rotated in the dish using forceps to assess all sides for the presence of staining as in thicker pieces it is not possible to see through the tissue. Pieces with red-stained structures were imaged at all time points.

5.2.2 Staining of fixed tissue to identify follicles

Three fragments of cultured tissue, one each from Patients B, D, and J from Section 3.4.2, and three pieces of tissue that had not been cultured, one each from Patients B, D, and J, were fixed in 10% formalin for 4 hours at 4°C. After fixation tissue was stored in 70% ethanol; processed, embedded, and sectioned as described in Section 2.6. The middle slide from each tissue piece, six slides in total, were used to assess with follicles could be assessed in fixed tissue.

5.2.2.1 Dewaxing, rehydration, and haematoxylin staining

A variation of the protocol described in Section 2.6.4 was used here (Table 5.1). All slides were dewaxed in xylene and rehydrated through a decreasing ethanol gradient. Once in tap water slides were placed in haematoxylin, left for 5 sec and returned to tap water. Slides

were placed back in haematoxylin for a further 15 secs (20 sec total) then returned to tap water, placed in haematoxylin for 40 sec (1 min total) then returned to tap water, placed in haematoxylin for 1 min (2 min total) and returned to tap water, and finally placed in acid alcohol for 5 sec before being washed in tap water for a final time. Slides were imaged under the 10X objective of a standard bright field microscope at each time point (as Section 2.9. Tissue sections were imaged while wet, so the tissue did not dry out.

Table 5.1 Intervals of haematoxylin staining and imaging of human cortical tissue

Solution	Time	Total staining time
Haematoxylin	5 sec	5 sec
Tap water	>5 sec	-
Image		
Haematoxylin	15 sec	20 sec
Tap water	>5 sec	-
Image		
Haematoxylin	40 sec	1 min
Tap water	>5 sec	-
Image		
Haematoxylin	1 min	2 min
Tap water	>5 sec	-
Image		
Acid alcohol	5 sec	-
Tap water	>5 sec	-
Image		

5.3 Results

5.3.1 Identification of follicles in unstained tissue

In unstained tissue pieces follicles could not easily be identified by darkfield microscopy (Figure 5.1). In thinner fragments the light penetrated the tissue piece and revealed some areas which were spherical and more translucent but could not be easily recognised as follicles. In thicker fragments there was very little light through the body of the tissue, severely limiting the ability to identify potential follicles.

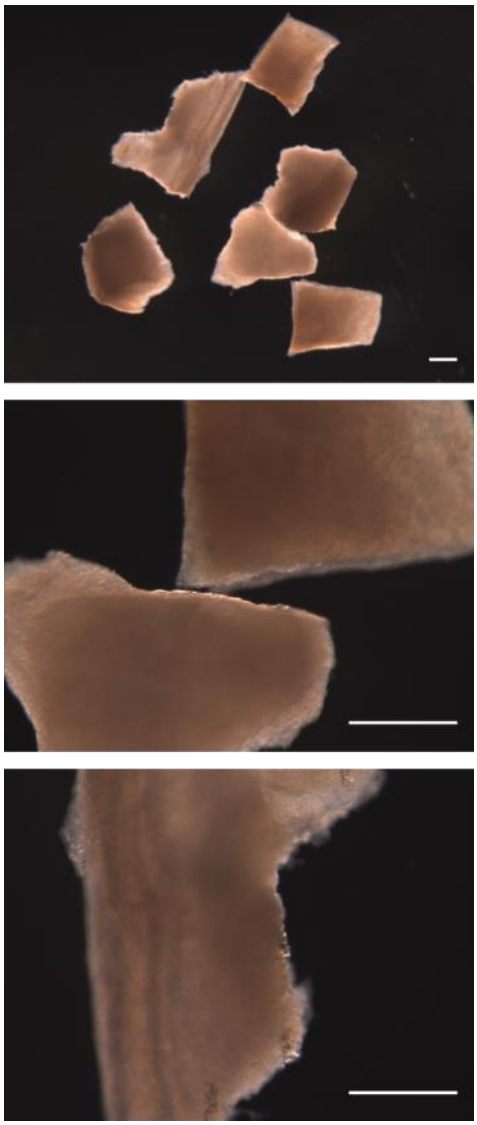


Figure 5.1 Darkfield images of unstained human cortical tissue

Tissue fragments processed to size for *in vitro* culture were imaged before incubation with neutral red. Scale bar: 150 μm.

5.3.2 NR staining can be observed in tissue after 1 hour

After incubating tissue pieces in NR for 1-hour, red follicle structures could be clearly observed (Figure 5.2). These follicles were identified by their red circular appearance. Inspection at higher magnification found the staining appeared as a ring around the oocyte.

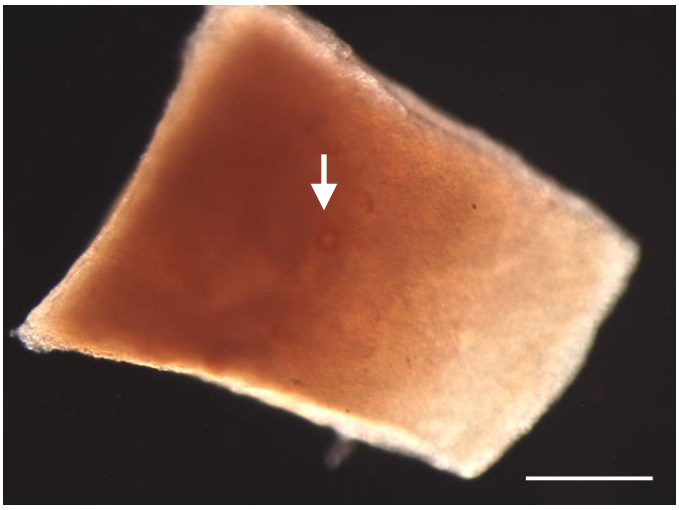


Figure 5.2 Darkfield images of human cortical tissue a NR-stained follicle: 1hour

Tissue fragments processed to size for *in vitro* culture were imaged after a 1-hour incubation with neutral red. Scale bar: 150 µm. Arrow indicates follicle.

A greater number of red-stained follicles were observed after 2 hours, and a greater number still were seen after incubating the tissue with NR for 4 hours (Figure 5.3). The pattern of staining observed after 1 hour was consistent with that observed in the longer incubations. Follicles closer to the tissue surface were the first to show positive staining, with those deeper in the tissue becoming visible with red staining at the 2 and 4-hour time points. Some dye crystals became apparent on the tissue at the end of the 4-hour incubation, these were very small, darkly staining red dots observed on the surface of the tissue (indicated by arrows in Figure 5.3). The red staining observed was specific to follicle-like structures and absent from the stromal tissue. Some tissue fragments did not show any red staining across the incubation period, and no background staining was observed at any of the time points assessed (Figure 5.4).

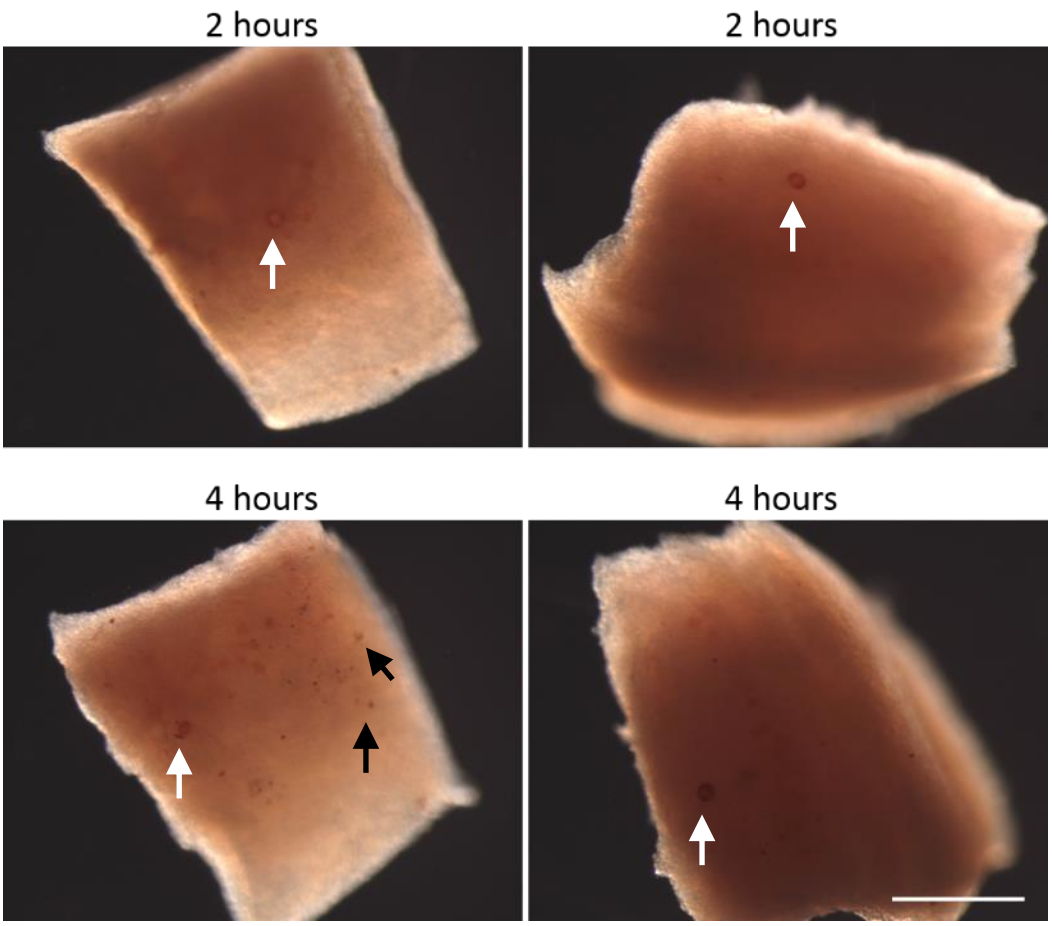


Figure 5.3 Darkfield images of human cortical tissue with NR-stained follicles: 2-4 hours

Tissue fragments processed to size for *in vitro* culture were imaged after 2 hours and 4 hours incubation with neutral red. Scale bar: 150 µm. White arrows indicate follicles, black arrows indicate dye crystals.

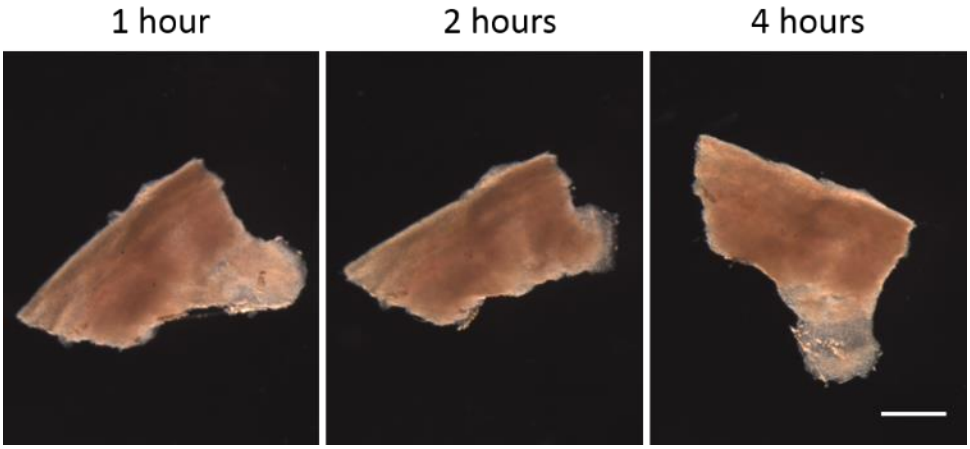


Figure 5.4 Darkfield images of human cortical tissue without NR-stained follicles

Tissue fragments processed to size for *in vitro* culture were imaged after a 1-, 2-, and 4-hour incubation with neutral red that did not have positive staining. Scale bar: 150 µm.

5.3.3 Dewaxing and rehydration of fixed cortical tissue

Dewaxing and rehydrating were ineffective as a method to improve the discrimination of stroma and follicles in tissue. Images of tissue after dewaxing and rehydration can be found in Figure 5.5. In some sections the tissue architecture could be visualised more clearly but overall there was no consistency in the ability to discern the presence of follicles after dewaxing and rehydrating the tissue.

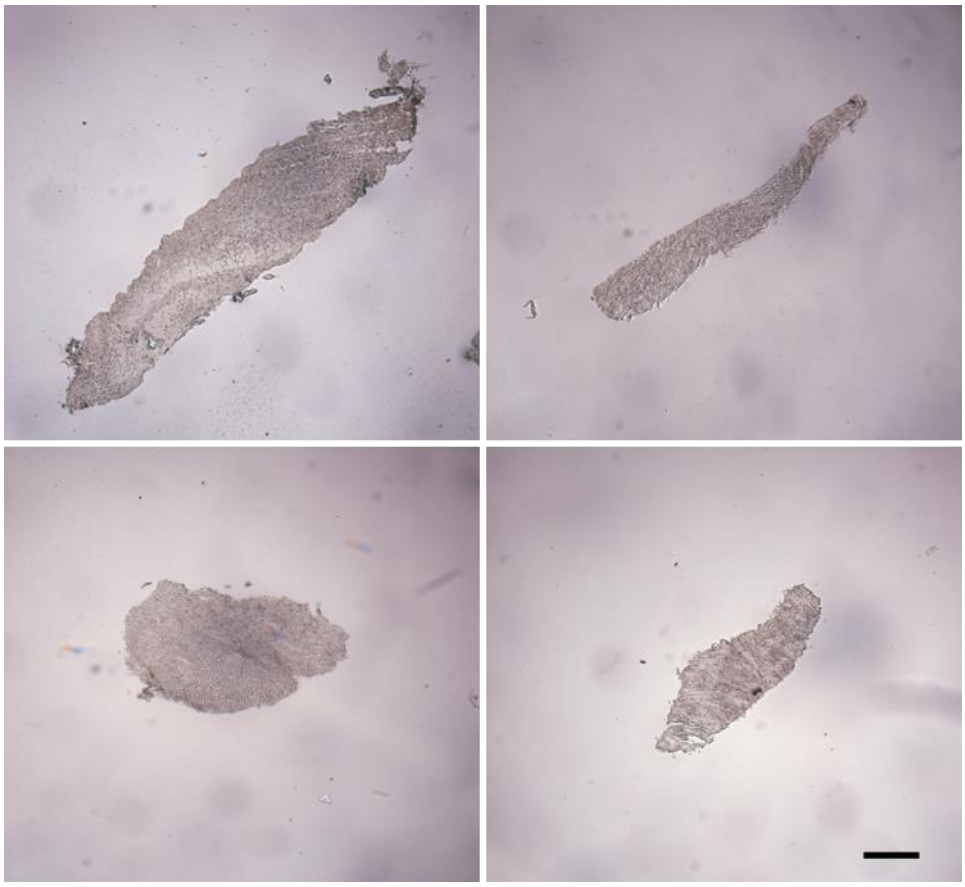


Figure 5.5 Dewaxed and rehydrated human cortical tissue

Human cortical strips cut to size appropriate for *in vitro* culture were fixed in 10% formalin, paraffin-embedded and serially sectioned at 5 µm. Sections were dewaxed and rehydrated. Scale bar: 150 µm. Note: higher magnification not possible due to water droplet on sections.

5.3.4 Partial or complete haematoxylin staining

Dewaxing, rehydrating, and partially staining with haematoxylin were also ineffective as a method to improve the discrimination of stroma and follicles in tissue. Representative images of the gradual haematoxylin stain are shown in Figure 5.6. A slight improvement in the resolution of the tissue was observed following a 5 sec incubation in haematoxylin. The purple stain left by the haematoxylin, though light in colour, was specific to the cell nuclei with minimal background. However, as the staining period increased the increase in background staining was greater than the increase in nuclear stain. Tissue where the stroma was very dense was particularly affected by the increased background with increased staining time. The de-stain with acid alcohol following the 2 min stain with haematoxylin removed the excess staining to minimally improve the contrast between true nuclear staining and background.

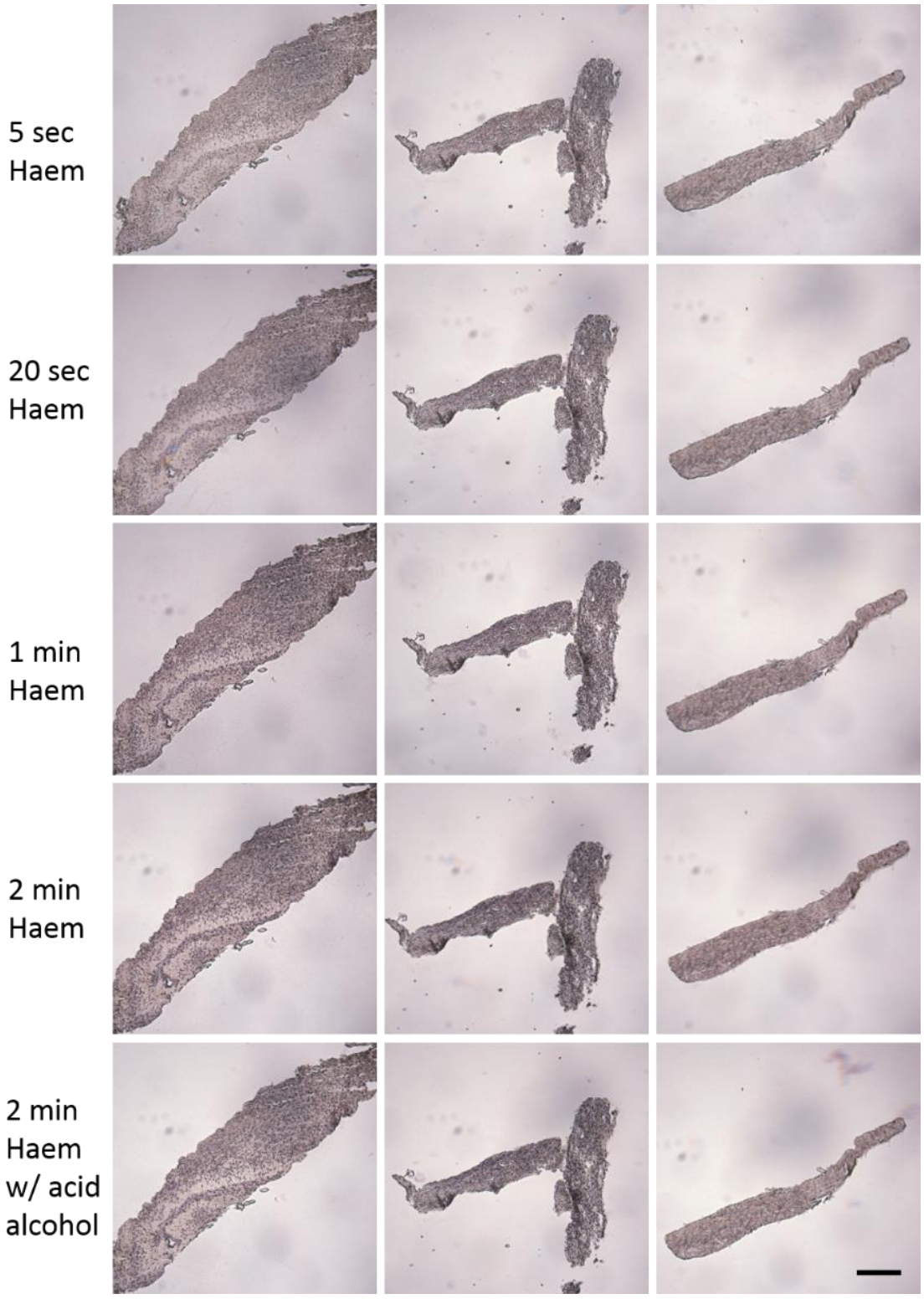


Figure 5.6 Representative images of dewaxed and rehydrated human cortical tissue with increasing duration of haematoxylin stain.

Human cortical strips cut to size appropriate for *in vitro* culture were fixed in 10% formalin, paraffin-embedded and serially sectioned at 5 µm. Sections were dewaxed and rehydrated and stained with haematoxylin (Haem) for between 5 sec and 2 min. w/: with. Scale bar: 150 µm.

5.4 Discussion

5.4.1 Use of neutral red for fresh tissue

Neutral red is a non-toxic vital stain that can be visualised under standard light microscopy. It can be reconstituted in a physiological medium and has been used to accurately identify viable human oocytes. Reported protocols call for 4-6-hour incubation with the dye (257, 270). In setting up culture strip culture, minimising the processing time is crucial. This experiment found that follicles in small fragments of tissue approximately 0.25 x 0.5 x 0.5 mm in size could be observed after a 1-hour incubation in NR. Follicles at the surface were the first to become visible with the longer incubation periods allowing a greater number of follicles deeper within tissue fragments to be seen. The overall number of follicles observed in this tissue was low which is unsurprising given the patient was 43 years old and follicle density is known to decrease with age (13).

Quantification and localisation of follicles within unstained fresh or frozen-thawed tissue fragments is feasible with stereomicroscopy, however it is laborious and unreliable due to the dense and fibrous nature of ovarian cortex (213, 302). NR was demonstrated here to be a quick and effective method of visualising follicles in tissue fragments.

5.4.2 Alternative vital dyes for fresh tissue

Protocols are well established to visualise and quantify viable follicles *in situ* however these are limited in their use both practically as they may affect further development of the tissue. Calcein AM and rhodamine 123 are fluorescent probes used to visualise follicles in human cortical tissue (302, 303). Both require exposure to short wavelength light to excite fluorophores which may damage cells (304, 305), and require a confocal microscope. By contrast NR can be visualised by stereomicroscopy offering greater time efficiency. Calcein and Rhodamine 123 have the advantage of providing a more direct indication of cell health

by the visualisation of active esterases and healthy mitochondria, respectively. Both Calcein and Rhodamine 123 are cell-permanent dyes which in this context is not an advantage as NR was being used as a marker only to visualise follicles in tissue before culture.

5.4.3 Visualisation of follicles in fixed tissue

Dewaxing, rehydrating, and staining fixed tissue with haematoxylin was ineffective as a method to improve the identification of tissue. While some increase in resolution could be achieved with a brief incubation 5 sec haematoxylin stain, it was not sufficient to allow the presence or absence of follicles in a section of tissue to be identified with any certainty. It is possible that larger follicles could be more easily identified but this does not address the need to also identify primordial and earlier stage follicles in non-cultured tissue. The fixed tissue used in this study had not been stained with NR, though other tissue pieces analysed for histology had shown the presence of follicles (Section 3.4.3). It could not be determined whether the fixed tissue used did in fact contain follicles as the slides were not mounted and coverslipped for histological analysis described in Chapter 2. This is a clear limitation of the experiment; however, the aim was to identify whether this method could reliably allow us to identify whether a tissue section contained follicles by dewaxing and/or dewaxing and lightly staining the tissue such that it could be used for downstream immunohistochemistry. Based on the results it can be concluded that this method is ineffective for this purpose.

5.4.4 Alternative methods of identifying follicles in fixed tissue

NR could be used to stain cultured tissue for the presence of follicles in tissue before fixation, however as only viable follicles would take up the dye, this would limit downstream analysis to primarily viable follicles unless used in conjunction with a dead cell stain such as Trypan Blue. As neither Trypan Blue or NR bind to anything within the cellular compartment their

stability in fixation and embedding can be poor, limiting their ability to identify follicles in tissue sections.

Live/dead stains that are stable after fixation have been developed for flow cytometry. For example, the LIVE/DEAD™ Fixable Near-IR stain is an amine reactive dye that binds covalently to intracellular and extracellular amines allowing the staining pattern to be preserved after fixation in formaldehyde (306). Future work could look to optimise a stain of this kind for cortical tissue, to enable to the user to visualise live and dead oocyte without the use of immunohistochemical approaches.

5.4.5 Conclusion

The results of this chapter show that a short incubation with NR can be used to identify pieces of tissue that contain follicles without altering the standard workflow in setting up cortical strip culture. Using NR to identify and utilise tissue pieces that contain follicles will decrease the likelihood that any given tissue section would not contain a follicle, thereby increasing the efficiency of both culture and analysis. In Chapter 3 this method was used to demonstrate that tissue fragments selected due to positive NR staining contained more follicles with a healthy morphology than tissue fragments that had not been selected using NR. As some experiments in this thesis were performed concurrently, NR was not used in Chapter 4.

Chapter 6

Analysing methods of human cortical strip culture

6.1 Introduction

The results from Chapter 3 revealed that follicles in cryopreserved human ovarian tissue can develop in culture and that tissue from different patients differed in the health and developmental stage of follicles present in both non-cultured and cultured tissue. Culture resulted in the development of asymmetric follicles, largely absent in non-cultured tissue. In addition, the results indicated that follicles from cryopreserved tissue did not develop to the secondary stage at the frequency described in some of published literature using fresh tissue. However, it couldn't be determined whether the development observed here was a result of the physical culture system, the culture medium used, or an otherwise unknown factor.

6.1.1 Optimisation of *in vitro* growth systems

Because of the limited amount of human tissue available for clinical use and research, as well as declining follicle numbers in specimens obtained from older versus younger patients, optimizing the yield of good-quality follicles is essential.

The need for a method of *in vitro* culture that adequately supports and sustains follicle development is critical not only to maximise success rates but to ensure the health of resulting offspring. The importance of culture condition is well illustrated by the seminal work of Eppig and colleagues. Eppig and O'Brien were the first to develop a culture system capable of supporting the growth and maturation of oocytes from the primordial to MII stage in mice (209). Despite low success rates (0.5% of embryos transferred) a single live pup, Egbert, was born. Perhaps commensurate with the relative success of the culture protocol, Egbert suffered from several health problems including obesity and neurological abnormalities in adulthood (307). While the authors emphasize that culture conditions cannot be assumed to be causative as only one mouse was produced, subsequent changes to the culture conditions both increased live birth rate and pups had no known health problems (308).

The cortical strip culture system developed by Telfer and colleagues has led to the most advanced follicle development in humans, from primordial to MII oocytes. This system has three key components; 1) it uses a McCoy's 5A-based medium which has primarily been used with fresh tissue, 2) tissue is cultured without a membrane or other physical support in a low volume of medium, and 3) the tissue, approximately 1 x 0.5 x 0.5 mm in size, is mechanically stretched with needles prior to culture. By contrast, alpha-MEM (αMEM) medium is the most commonly used medium for cryopreserved human cortical strip culture (227, 228, 230-232, 253). However, there is no consensus in the optimal method of culture for cryopreserved tissue (discussed in Section 1.12.2). The culture system described in

Chapter 3 employs a membrane and a high volume of medium to provide adequate grow factors and hormones while minimising the oxygen diffusion distance between the tissue and the medium. Pertinent to this chapter, a recent paper reported superior follicle development and health with cortical tissue culture in gas-permeable plates due to increased oxygen availability (224), further alternative culture systems are discussed more extensively in Chapter 1.

6.1.2 Aims and hypotheses

The aims and hypotheses of this chapter was to:

(i) Investigate the effect of culture medium, medium volume, and dish permeability on the health and development of follicles from cryopreserved cortical tissue to identify the condition(s) that best facilitate the development of healthy preantral follicles.

   a. *There will be no difference in the health or development of follicles as a result of the cortical strip culture environment.*

6.2 Materials and methods

B. Bjarkadottir and I jointly performed the culture, processing, and histology detailed in this Chapter.

6.2.1 Patient information

Ovarian tissue obtained as described in Section 2.1, from three post-pubertal patients aged 17 to 25 years were used in this study.

6.2.2 Human cortical strip culture

Cortical strips were thawed as described in Section 2.3, and prepared for culture as detailed in Section 2.4.1. Tissue from all patients was stained with neutral red (NR) as described in Section 2.5 to identify fragments of tissue that contained follicles. Fragments where red-stained follicles were observed were allocated before fragments with no staining to the non-culture and culture groups. Due to the short incubation period with NR, we could not conclude that tissue fragments without NR staining were devoid of viable follicles. Therefore, where there was not a sufficient amount of tissue available with NR staining after 1 hr, fragments without staining were also included in equal amounts to both groups and remnant tissue was discarded as described above. Allocation of tissue between the groups was performed without a microscope to blind the researcher to the degree of staining and detail of the tissue pieces.

Six culture conditions were used in this experiment detailed in Figure 6.1 and Table 6.1. Two different culture medium (McCoy's 5A medium and αMEM medium, see Appendix II) were tested, each with three different plate conditions: 1 ml of medium and a polycarbonate membrane (13 mm diameter, 8 µm pore size) in a conventional 24-well culture plate, 300 µl of medium in a conventional 24-well plate, and 1 ml of medium in a gas-permeable Lumox® 24-well plate (Sarstedt, Nümbrecht, Germany). The McCoy's 5A and αMEM-based culture medium were each supplemented as described in Section 2.4.2, with HSA, penicillin and streptomycin, L-glutamine, insulin, transferrin, selenium, ascorbic acid and recombinant human FSH.

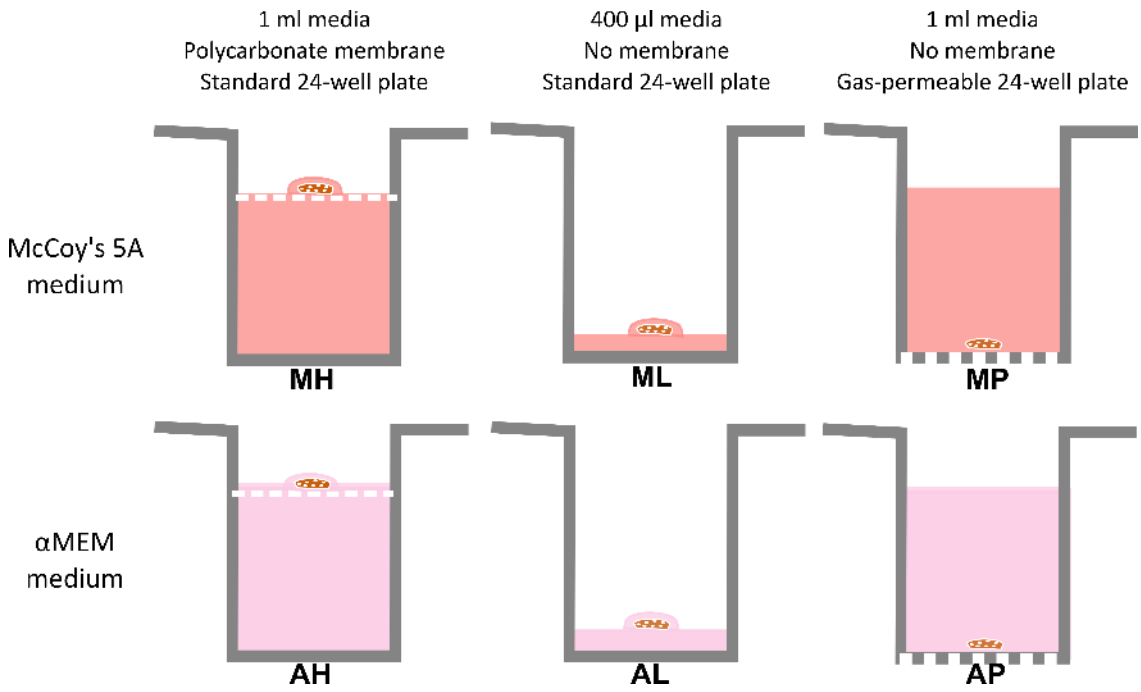


Figure 6.1 Experimental design to investigate the effect of culture condition on health and development of follicles in cryopreserved human ovarian cortical tissue.

Table 6.1 Experimental conditions and abbreviations used to investigate the effect of culture condition on health and development of follicles in cryopreserved human ovarian cortical tissue.

Abbreviation		Medium	Volume	24-well plate	Membrane
MH*	McCoy's High	McCoy's 5A	1 ml	Conventional	Yes
AH	αMEM High	αMEM	1 ml	Conventional	Yes
ML	McCoy's Low	McCoy's 5A	0.3 ml	Conventional	No
AL	αMEM Low	αMEM	0.3 ml	Conventional	No
MP	McCoy's Permeable	McCoy's 5A	1 ml	Gas-permeable	No
AP	αMEM Permeable	αMEM	1 ml	Gas-permeable	No

** as used in Chapter 3*

Tissue was fixed in Bouin's solution before culture, as a non-cultured control, or after six days of culture as described in Section 2.4.3.

6.2.3 Processing and histology

Tissue was processed and embedded in paraffin wax before being sectioned at 5 μm and stained with haematoxylin-eosin (Section 2.6). Follicle development and health was assessed based on morphology (Section 2.7). Follicle density for each tissue piece was calculated (Section 2.8).

6.2.4 Statistical analysis

All statistical analyses were performed using R statistical software, version 3.5.0 (R foundation for Statistical Computing, Vienna, Austria). A generalised linear mixed model following a negative binomial distribution (glmmPQL; 291) was performed to determine the effect of culture condition on follicle development, offset for tissue volume and treating patient as a random effect. Due to the small number of secondary follicles observed, no statistical analysis was performed on this cohort. An ordinal regression was performed to determine whether follicle health was affected by treatment condition, again adjusting for tissue volume and patient. For assessment of asymmetry, follicles were given a binary classification of asymmetric (two or more partial layers of granulosa cells, Chapter 2 Section 2.9.11) or not asymmetric. For assessment of advanced follicle development, follicles were given a binary classification of multi-layer (primary follicles with a single cuboidal granulosa cell layer and any number of partial granulosa cell layers, and secondary follicles), or not. Data are presented as mean (±SEM), as odds, or as odds ratio with 95% confidence intervals, unless otherwise stated, and statistical significance was defined as $P < 0.05$.

6.3 Results

6.3.1 Patient characteristics

Information about menstrual cycles were available for two of the three patients (1 and 2) confirming normal cyclicity. The mean time from completion of surgery to start of cryopreservation was 3 h 32 min ± 51 min (data not shown). Histopathology reports found no evidence of malignancy in tissue from any of the patients.

Follicle density in cortical tissue sections varied as a function of age with the highest density, 244.5 follicles per mm^3, seen in the 17-year-old patient, followed by 92.5 and 17.2 follicles per mm^3 in the 22 and 25-year-old patients, respectively (Figure 6.2, Figure 6.3). There was also variation within tissue pieces from the same patient (Figure 6.2). Primordial follicles were the dominant population in non-cultured tissue from patients 2 and 3 (80.7% and 62.2%, respectively). In patient 1 30.9% were primordial and 54.7% were transitional in non-cultured tissue. No secondary follicles were seen in non-cultured tissue in any of the patients (data not shown).

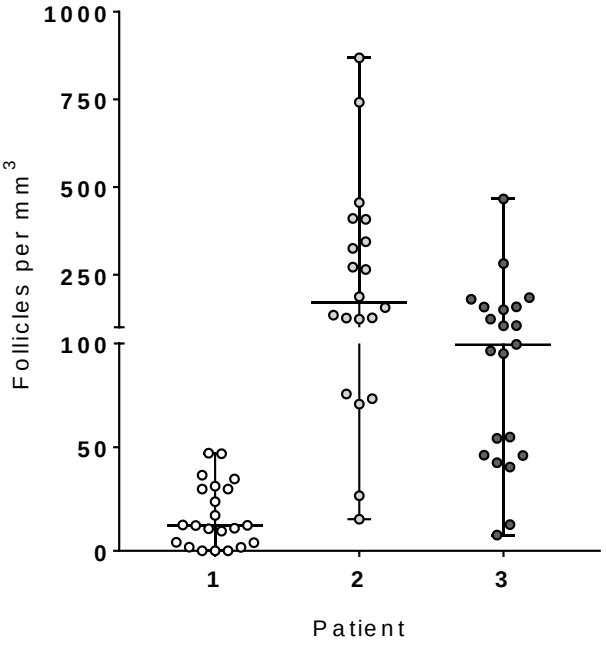


Figure 6.2 Follicle density in tissue pieces analysed using histology from human ovarian cortical tissue from 3 patients. Data presented as median and range.

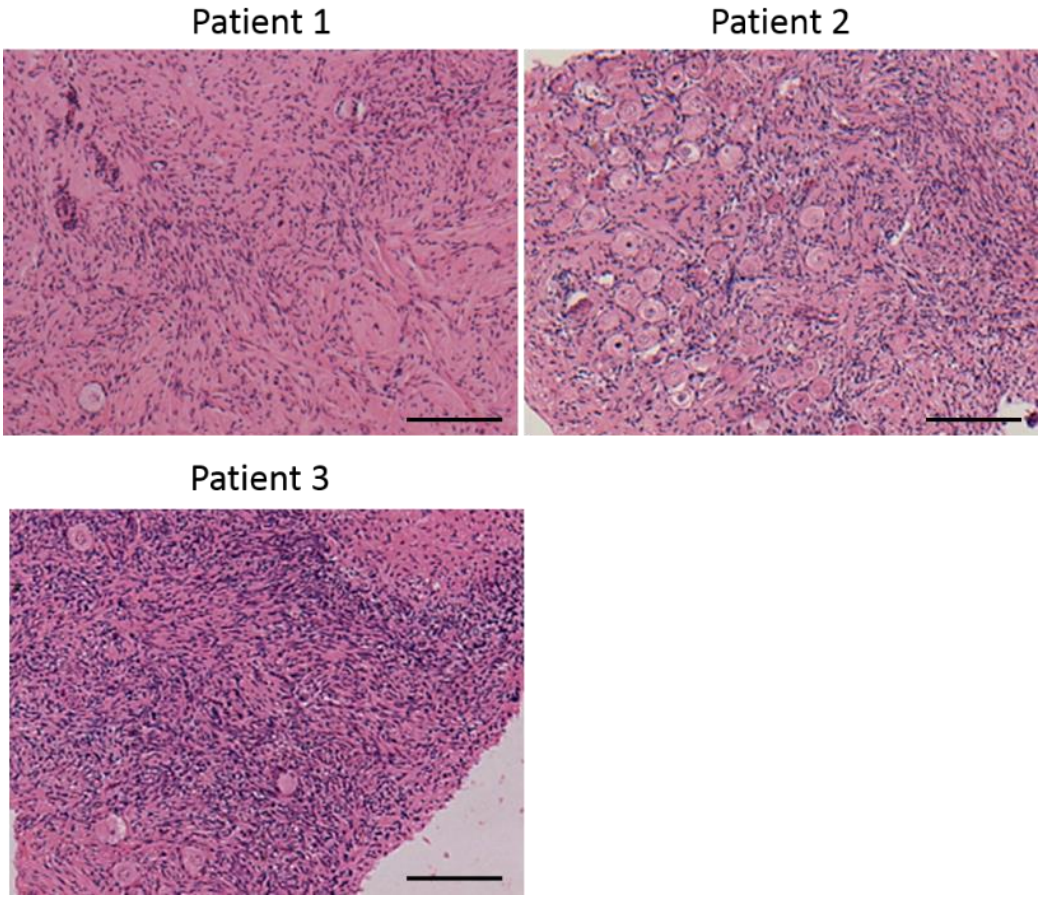


Figure 6.3 Representative images of non-cultured human ovarian cortical tissue sections from 3 patients. Scale bar: 500 µm.

6.3.2 Experimental conditions and number of follicles analysed

A total of 5836 follicles were analysed in this experiment. The experimental conditions and the abbreviation used for each is listed in Table 6.1. The number of follicles analysed from each of the three patients in non-cultured tissue and in the six culture conditions is detailed in Table 6.2. The number of follicles within sub-group analyses is detailed in Figure 6.4.

Table 6.2 Number of follicles counted in each experimental condition per patient (n=3).

Patient	Number of follicles							
	Day 0	**MH**	**AH**	**ML**	**AL**	**MP**	**AP**	**Total**
1	139	33	37	9	25	12	48	303
2	1224	489	59	163	551	304	409	3199
3	874	90	268	266	234	277	286	2295
Total	2237	612	364	438	810	593	743	5797

Day 0 *non-cultured tissue,* ***MH*** *McCoy's 5A high volume on a membrane;* ***AH*** *αMEM high volume on a membrane;* ***ML*** *McCoy's 5A low volume;* ***AL*** *αMEM low volume;* ***MP*** *McCoy's high volume in a permeable bottom plate;* ***AP****, αMEM high volume in a permeable bottom plate*

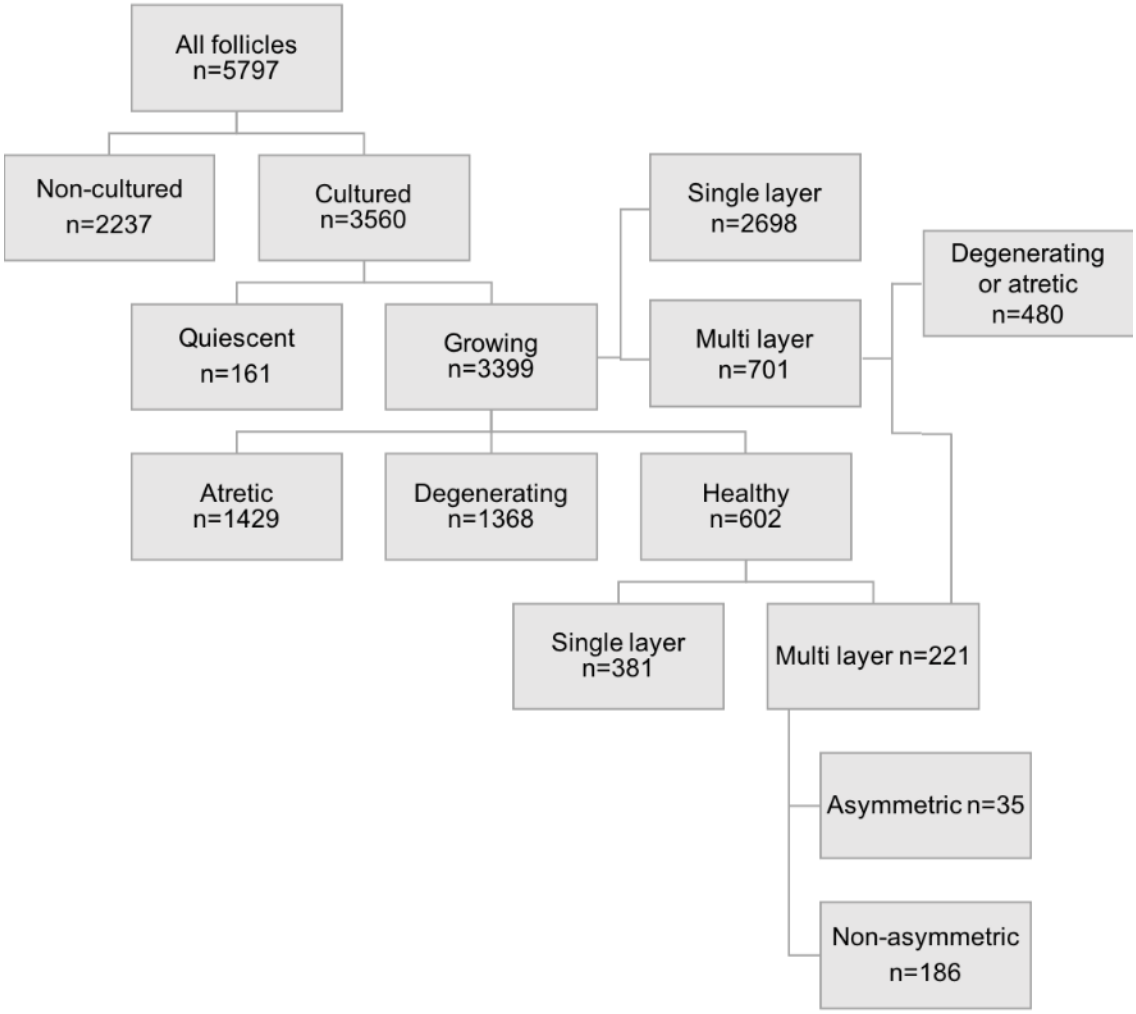


Figure 6.4 Hierarchy of sub-groups used for analyses. n=follicle number

6.3.3 Distribution of follicles across health parameters

Follicles were graded as being healthy, degenerating or atretic based on the presence or absence of pyknotic granulosa cells, a pyknotic oocyte and a shrunken ooplasm (see Section 2.7 and Section 3.4). Follicles of all developmental stages and health parameters were observed in all three patients, irrespective of tissue treatment, with great variation in follicle numbers between patients. Non-cultured tissue contained a majority of healthy primordial follicles, whereas after six days of culture (irrespective of culture condition) the follicle population consisted mostly of degenerating or atretic primary follicles (Figure 6.5).

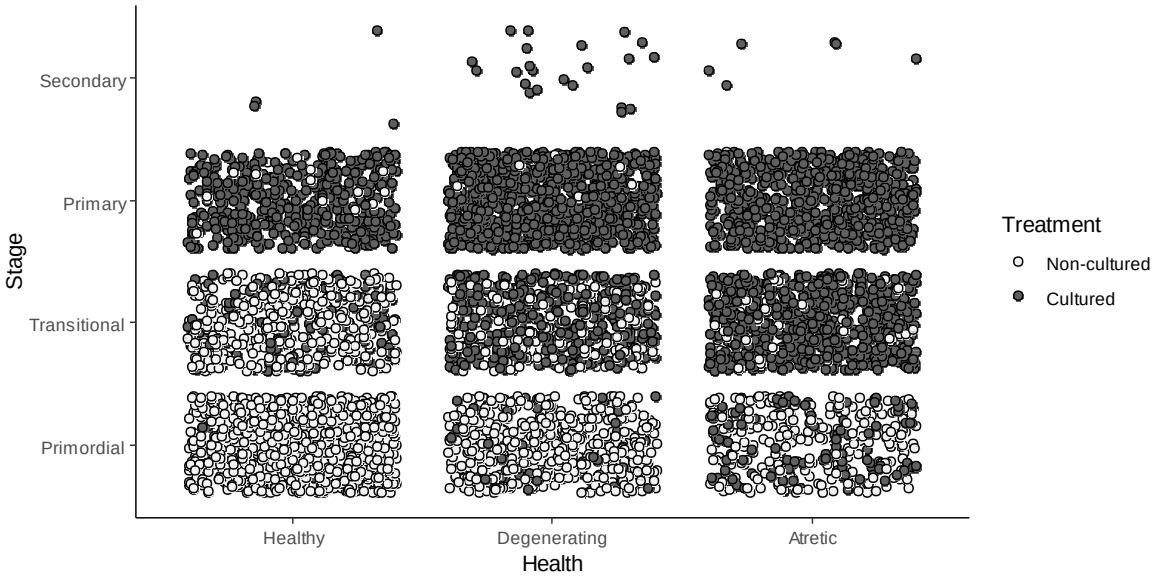


Figure 6.5 Distribution of non-cultured and cultured follicles based on health parameters and developmental stage.

Follicles (non-cultured and cultured for 6 days under six culture conditions) at each developmental stage were classified as healthy, degenerating or atretic based on morphological characteristics. Most follicles in non-cultured tissue were at the primordial stage and healthy. Most follicles in cultured tissue were primary and degenerating or atretic.

6.3.4 Effect of culture condition of follicle health

McCoy's 5A high volume (MH) is the standard culture system established in Chapter 3. Compared to the established culture system MH, tissue cultured in low volume conditions (McCoy's 5A low volume, ML or αMEM low volume, AL) or permeable dish conditions (McCoy's 5A permeable, MP or αMEM permeable, AP) had greater odds of multi-layered follicles classified as "healthy" follicles versus "degenerating" or "atretic" (Figure 6.6). The most marked difference in multi-layered follicle health was seen in the low volume conditions. In AL compared to MH, tissue cultured in AL had 5 times greater odds of multi-layered follicles being classified as "healthy" follicles versus "degenerating" or "atretic" (0.20; 95% CI 0.13 to 0.32; P=6.16E-28). Tissue cultured in ML had 2.6 times greater odds of multi-layered follicles being classified as "healthy" follicles versus "degenerating" or "atretic" (0.38; 95% CI 0.23 to 0.64; P=4.32E-08).

AL was the only culture condition to have greater odds of "healthy" follicles versus "degenerating" or "atretic" in primordial, transitional, primary, and multi-layered follicle stages (Figure 6.6). As the low volume conditions had the greatest change in the odds of healthy multi-layered follicles, AL was set as the baseline level of comparison in the ordinal regression to ascertain whether medium affected follicle health within the low volume condition. Compared to AL, multi-layered follicles from tissue cultured in ML had 1.9 times greater odds of being classified as "degenerating" or "atretic" then "healthy" (1.92; 95% CI 1.24 to 2.97; P=3.38E-03), showing that AL yielded superior follicle health compared to the other conditions tested.

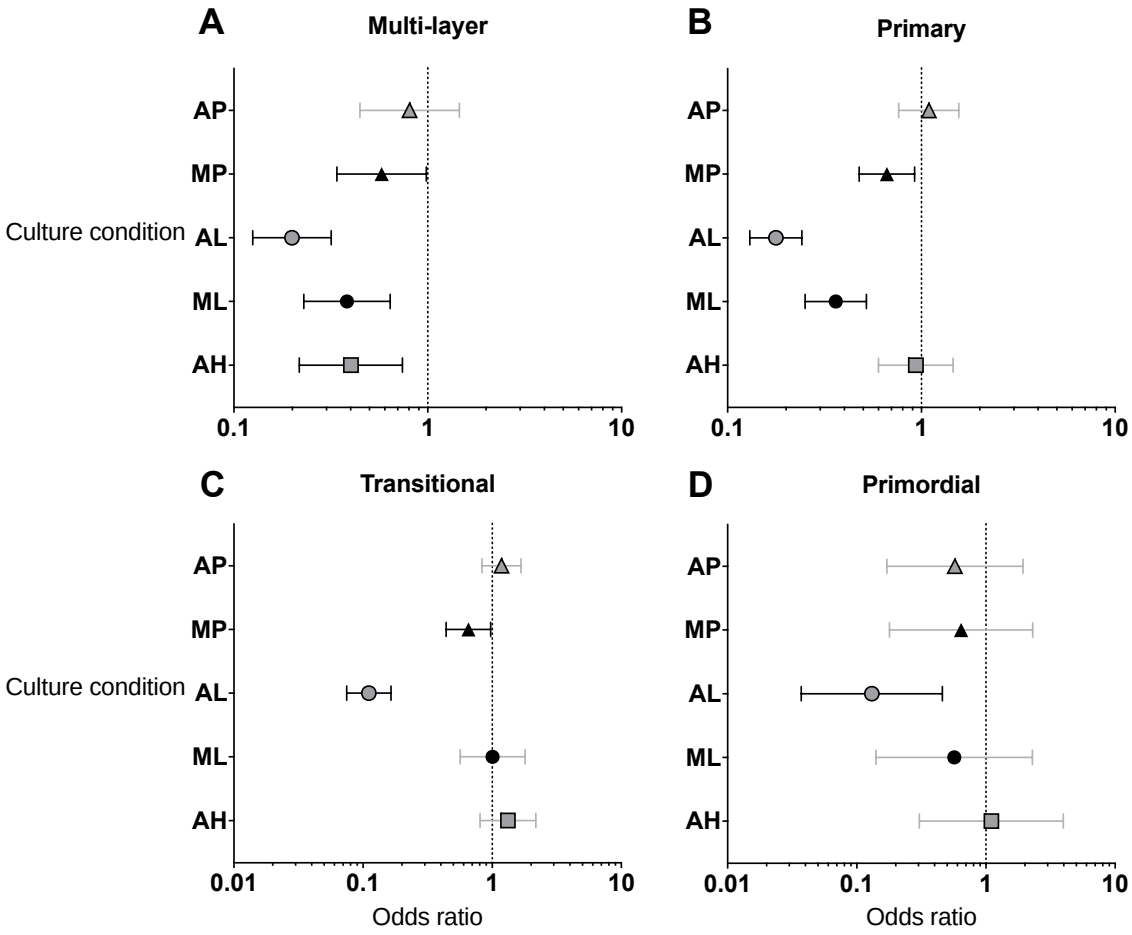


Figure 6.6 Effect of culture condition on follicle health in cultured tissue

Ordinal regression of follicle health with the levels: healthy, degenerating and atretic, adjusting for tissue volume and patient (n=3). Data presented as odds ratio and 95% confidence intervals for each condition compared to MH of A) multi-layered follicles, B) primary follicles, C) transitional follicles, D) primordial follicles. MH, McCoy's 5A high volume on a membrane; AH, αMEM high volume on a membrane; ML, McCoy's 5A low volume; AL, αMEM low volume; MP, McCoy's 5A high volume in a permeable bottom plate; AP, αMEM high volume in a permeable bottom plate. Grey error bars p=ns, black error bars p<0.05.

6.3.5 Effect of culture condition on follicle development

Change in distribution of follicle stage with culture

In non-cultured tissue both mean primordial and transitional follicle counts were significantly greater than the primary follicle counts (Figure 6.7; p<0.0001). An inverse relationship was observed in MH where a greater number of transitional and primary follicles were observed compared to primordial follicles (transitional and primary; p<0.01

and p<0.0001 respectively; Figure 6.7). Mean secondary follicle counts were not calculated due to low numbers.

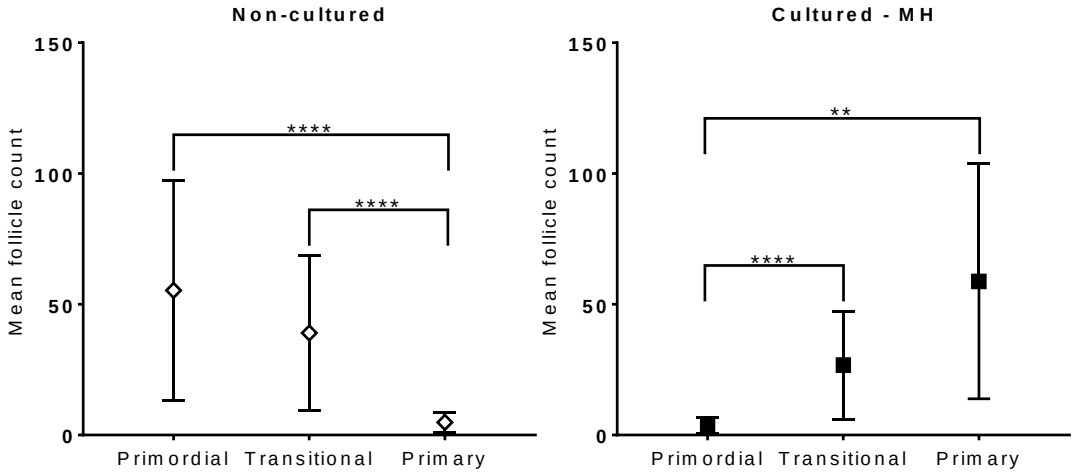


Figure 6.7 Mean follicle count per developmental stage in human ovarian cortical tissue not cultured or cultured in MH

Mean follicle counts ± SEM of primordial, transitional, and primary follicles in non-cultured tissue, or tissue culture on a polycarbonate membrane floating on 1 ml of McCoy's 5A medium (MH).

Follicle quiescence after culture

Follicles were classed as quiescent if staged as primordial based on morphology, whereas all other follicle stages were considered activated (transitional, primary, secondary). Compared to MH there was no difference in the likelihood of follicles becoming activated after 6 days of culture in ML, MP, and AP conditions (Figure 6.8). Interestingly, follicles cultured in AH were 2.9 times more likely to be quiescent after culture compared to those cultured in MH (2.86; 95% CI 1.58 to 5.20; P=0.001) (Figure 6.8). Follicles cultured in AL were over 2 times more likely to be activated after culture compared to those culture in MH (0.44; 95% CI 0.24 to 0.78; P=0.005) (Figure 6.8).

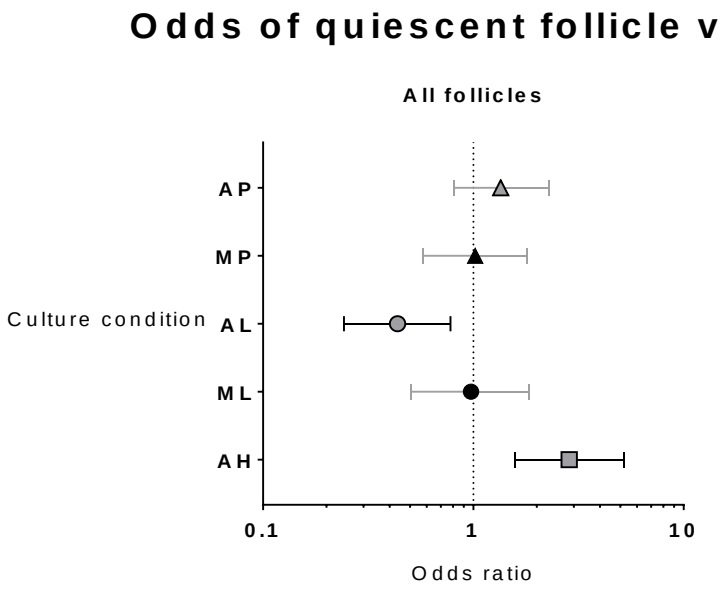


Figure 6.8 Effect of culture condition on follicle activation

Odd ratios with 95% confidence intervals for each condition compared to MH. Odds of follicles in a quiescent state (those staged as primordial based on morphology) within the total population. Odds ratios were modelled by a logistic regression model with MH set as the baseline, adjusting for tissue volume and patient (n=3). MH, McCoy's 5A high volume on a membrane; AH, αMEM high volume on a membrane; ML, McCoy's 5A low volume; AL, αMEM low volume; MP, McCoy's 5A high volume in a permeable bottom plate; AP, αMEM high volume in a permeable bottom plate. Grey error bars p=ns, black error bars $p<0.05$.

Mean follicle counts across developmental stages

The mean number of follicles at a given developmental stage, irrespective of health was largely unaffected by culture condition. Mean primordial and primary follicle counts were no different from MH in any of the cultured tissue conditions. A lower number of transitional follicles were observed in ML compared to MH ($P<0.01$; Figure 6.9B).

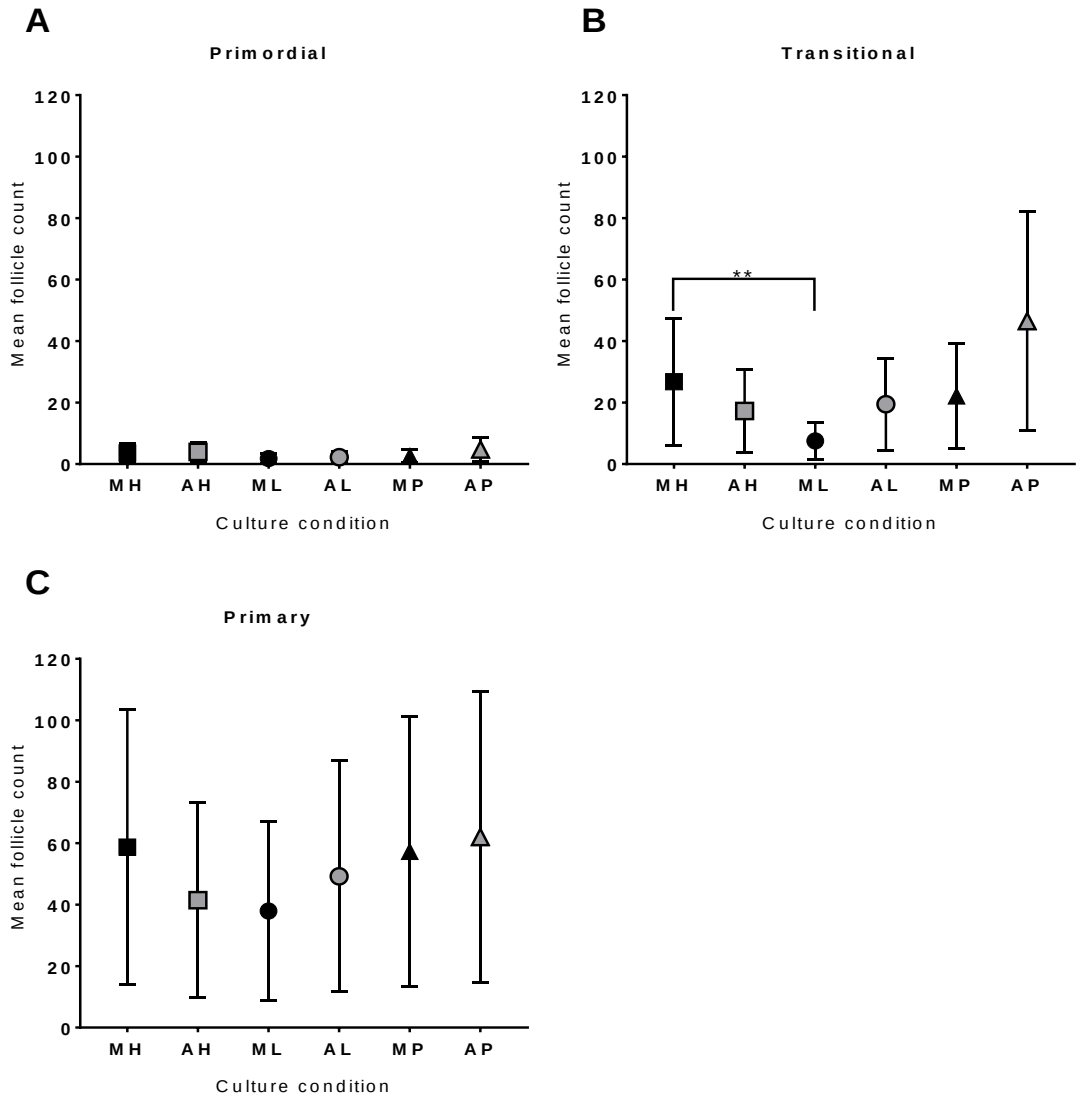


Figure 6.9 Mean follicle count per developmental stage in human ovarian cortical tissue cultured under different conditions

Mean follicle counts ± SEM of A) primordial follicles, B) transitional follicles, and C) primary follicles. Mean follicles counts were not calculated for secondary follicles due to low numbers. MH, McCoy's 5A medium high volume on a membrane; AH, αMEM high volume on a membrane; ML, McCoy's 5A low volume; AL, αMEM low volume; MP, McCoy's 5A high volume in a permeable bottom plate; AP, αMEM high volume in a permeable bottom plate. Significance compared to MH, ** $p<0.01$.

Multi-layer follicle development

Follicles must reach a multi-layered stage to be suitable for follicle isolation and further culture. Having reported above that there is some difference in the likelihood of follicles initiating development in culture we then looked at the development of the growing population. Follicles were classed as multi-layered if they had more than a single layer of

cuboidal granulosa cells; this included primary follicles with partial granulosa cell layers and secondary follicles.

When all growing follicles were considered, those cultured in AH were 1.6 times less likely to be multi-layered compared to those cultured in MH (0.63; 95% CI 0.43 to 0.92; P=0.005), however this difference disappeared when only non-atretic, or healthy growing follicles were considered (Figure 6.10). Follicles cultured in AP were significantly less likely to be multi-layered compared to those cultured in MH irrespective of follicle health (0.33; 95% CI 0.14 to 0.75; P=0.008) (Figure 6.10).

Looking at the entire cohort of growing follicles both low volume conditions had greater odds of having multi-layer follicles compared to MH (ML, 1.63; 95% CI 1.18 to 2.25; P=0.003, AL, 1.41; 95% CI 1.07 to 1.86; P=0.02) (Figure 6.10). However, within the non-atretic growing follicles only ML maintained this increase (1.53; 95% CI 1.05 to 2.24; P=0.02), and there was no difference in the odds of multi-layered follicles in healthy growing follicles between any of the conditions and MH (Figure 6.10).

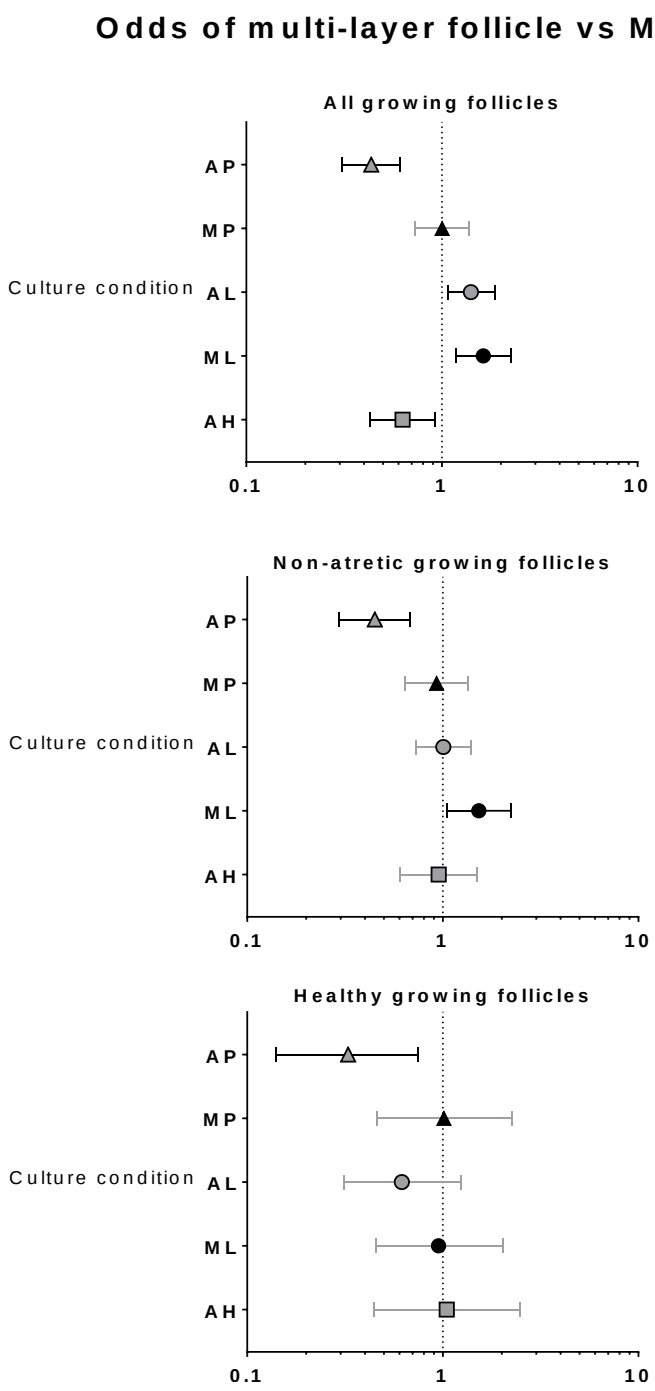


Figure 6.10 Likelihood of multi-layer follicles under different culture conditions

Odd ratios with 95% confidence intervals for each condition compared to MH. Odds of multi-layer follicles (those staged as primary with a single complete layer of granulosa cells and any number of partial layers, and those staged as secondary based on morphology) within the growing follicle population (all growing), the growing population that were not classed as atretic (non-atretic growing follicles), and the growing population with a healthy morphology (healthy growing follicles). Odds ratios were modelled by a logistic regression model with MH set as the baseline, adjusting for tissue volume and patient (n=3). MH, McCoy's 5A high volume on a membrane; AH, αMEM high volume on a membrane; ML, McCoy's 5A low volume; AL, αMEM low volume; MP, McCoy's 5A high volume in a permeable bottom plate; AP, αMEM high volume in a permeable bottom plate. Grey error bars p=ns, black error bars p<0.05.

Asymmetric follicle development

In Chapter 3 I found that asymmetric follicles were more prevalent in cultured tissue and would likely be indistinguishable from secondary follicles when isolating follicles for culture. In this experiment, asymmetric follicles comprised 15.8% (35/221) of the healthy, multi-layered follicles in cultured tissue. I wanted to see whether asymmetry was more likely based on culture condition. With the exception of AP, there was no difference in the likelihood of follicles being multi-layer after culture in MH than in the other culture conditions. Within all multi-layer follicles those cultured in AL and AP were less likely to be asymmetric compared to those cultured in MH (AL, 0.45; 95% CI 0.24 to 0.89; P=0.019, AP, 0.39; 95% CI 0.16 to 0.91; P=0.036) (Figure 6.11). However, within healthy multi-layer follicles there was no difference in the likelihood follicles would be asymmetric based on culture condition (Figure 6.11).

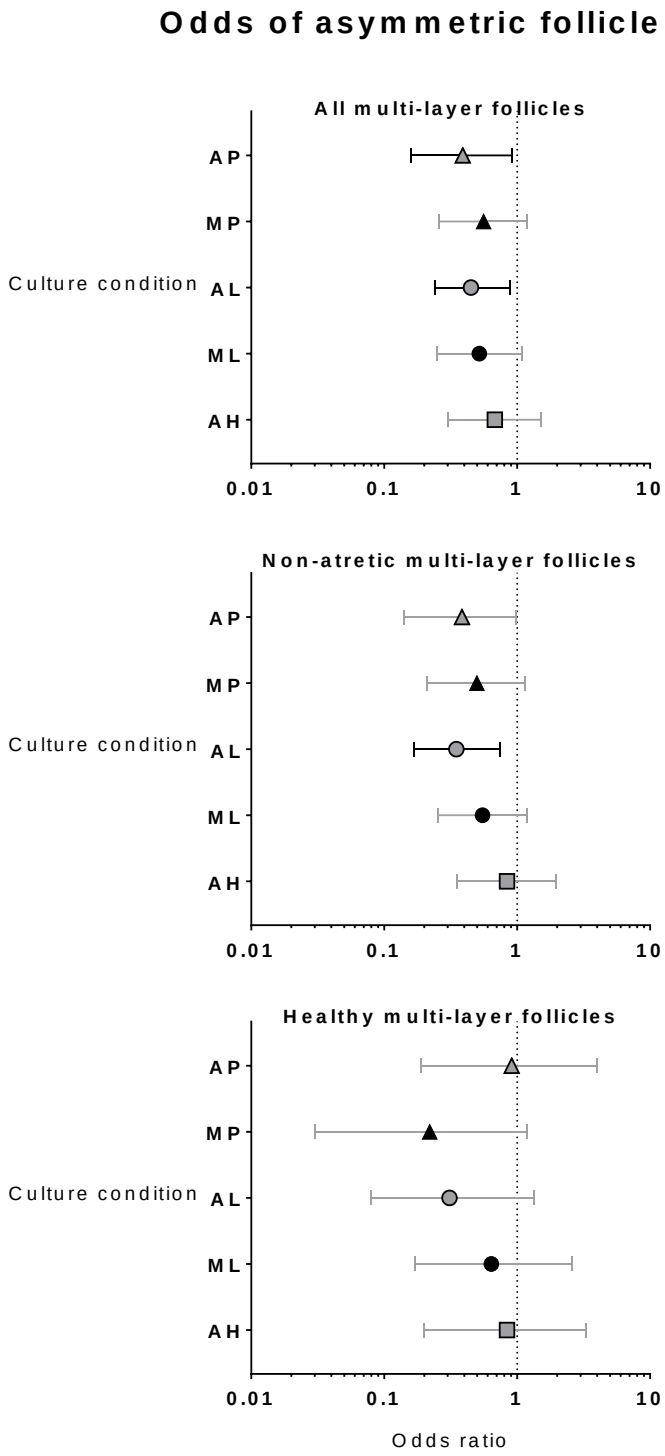


Figure 6.11 Likelihood of asymmetric follicles under different culture conditions

Odd ratios with 95% confidence intervals for each condition compared to MH. Odds of asymmetric follicles (primary follicles with two or more partial granulosa cell layers) within the growing follicle population (all growing), the growing population that were not classed as atretic (non-atretic growing follicles), and the growing population with a healthy morphology (healthy growing follicles). Odds ratios were modelled by a logistic regression model with MH set as the baseline, adjusting for tissue volume and patient (n=3). MH, McCoy's 5A high volume on a membrane; AH, αMEM high volume on a membrane; ML, McCoy's 5A low volume; AL, αMEM low volume; MP, McCoy's 5A high volume in a permeable bottom plate; AP, αMEM high volume in a permeable bottom plate. Grey error bars p=ns, black error bars $p<0.05$.

Secondary follicle development

Secondary follicles were observed in all cultured tissue conditions (Table 6.3). The proportion of total follicles at the secondary stage ranged from 0.4% - 2.3%, with ML resulting in the highest proportion of secondary follicles. No statistical analyses were performed as the number of secondary follicles was too low for this test. Most secondary follicles observed were degenerating irrespective of culture condition (Figure 6.12). A total of four healthy secondary follicles were observed, one in MH, two in AL, and one in MP. Three out of the four observed secondary follicles were from a single patient (patient 3). Interestingly, ML yielded the highest number of atretic secondary follicles.

Table 6.3 Secondary follicle development in cultured tissue. N=follicles analysed

	Culture condition					
Patient	**MH**	**AH**	**ML**	**AL**	**MP**	**AP**
1	3.0% (1)	0% (0)	22% (2)	0% (0)	0% (0)	0% (0)
2	0.8% (4)	1.7% (1)	2% (3)	0.4% (2)	0.7% (2)	0.2% (1)
3	0% (0)	0.7% (2)	2% (5)	2.1% (5)	0.7% (2)	0.7% (2)
Total	0.8% (5)	0.5% (3)	2.3% (10)	0.9% (7)	0.7% (4)	0.4% (3)

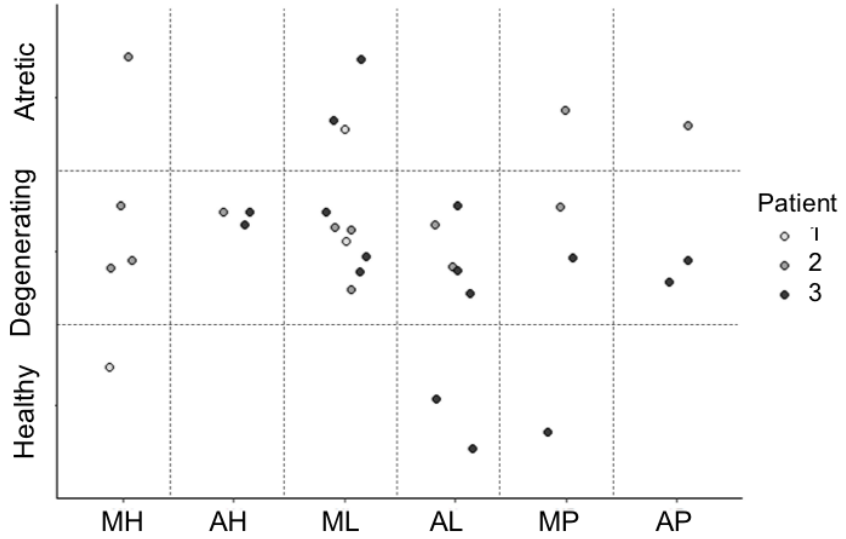


Figure 6.12 Health of secondary follicles in cultured ovarian tissue.

Secondary follicles were classed as healthy, degenerating or atretic based on morphological characteristics. Most secondary follicles were atretic, and only four healthy secondary follicles were observed. MH, McCoy's 5A high volume on a membrane; AH, αMEM high volume on a membrane; ML, McCoy's 5A low volume; AL, αMEM low volume; MP, McCoy's 5A high volume in a permeable bottom plate; AP, αMEM high volume in a permeable bottom plate.

6.4 Discussion

It was evident from Chapter 3 that to investigate the stages of follicle development beyond the primary stage, the culture system would need to be optimised. In this Chapter two different medium under three different physical conditions were evaluated to see whether follicle health or development was affected.

6.4.1 Medium volume and follicle survival

Both low volume conditions, AL and ML, had the lowest odds of atretic follicles after culture. Furthermore, follicles cultured in AL were 5 times less likely to be atretic compared to those from tissue cultured in MH. Compared to AL and ML, the other four culture conditions had over twice the amount of medium for tissue of the same size. Greater concentration of paracrine signals in the tissue cultured in low volumes of medium may explain the decreased atresia in the low volume conditions. In mouse follicle culture, co-culture of groups of five or ten primary follicles had a positive effect on the growth and survival of follicles culminating in the formation of meiotically competent oocytes (309). The most significant benefit was observed when the largest number of follicles was grown together, which the authors suggest is due to the exposure of follicles to paracrine factors secreted by the other follicles in the co-culture (309). Analysis of the spatial relationships between follicles of different stages in the mouse and human ovary has provided evidence that follicles surrounded by growing follicles are more likely to be growing themselves (310, 311). This might suggest that initial activation in culture is tied to survival as follicles cultured in AL were significantly less likely to be quiescent following culture compared to MH.

A recent paper that used a gas-permeable plate for cortical strip culture reported conflicting results to that observed in this study. Talevi, Sudhakaran (224) reported superior

morphological health of bovine follicles cultured in a high volume of medium in a gas-permeable plate compared to those cultured in a high or low volume of medium in a conventional plate. The group used larger 0.5 x 0.5 x 1 mm pieces which were cultured in groups of five pieces per dish. Higher medium volume that still allows adequate oxygenation of the medium and tissue may be important when multiple tissue pieces are cultured together to ensure appropriate exposure to growth factors and nutrients. The medium used in the Talevi study was αMEM supplemented as described in this study (Section 6.2.2) however without the addition of FSH which was added in this study. Research has demonstrated a key role for FSH in follicle survival as well as development *in vitro* in human and bovine studies (217, 312). FSH promotes follicle survival in rodents by enhancing the expression of oxidative stress response genes and promoting glutathione production by follicles, which suppresses reactive oxygen species production, subsequently reducing the level of apoptosis occurring due to oxidative damage (313, 314). It is possible that the absence of FSH makes follicles less resilient to sub-optimal oxygen levels and therefore may explain some of the discrepancy between the results of the Talevi study with those obtained in this Chapter.

6.4.2 Culture condition and follicle development

Within the cohort of growing follicles with a healthy morphology after culture, the odds of follicles being multi-layered was no different between the six culture conditions. ML had higher odds of multi-layered follicles in the total growing and total non-atretic growing cohort but not within the healthy growing follicles. ML also had the highest percentage of secondaries of all culture conditions, but all showed some sign of degeneration. This would suggest that the culture environment of ML is promoting follicles to reach more advanced stages of development but in a way that is detrimental, or rather not supportive to, their survival across the culture period.

Glucose is an energy source provided in both, αMEM and McCoy's 5A, at 5.3 mM and 16.7 mM, respectively. The medium composition of αMEM and McCoy's 5A is detailed in Appendix II. In addition to glucose, αMEM medium also contains 1 mM sodium pyruvate. Previous research has shown that follicles utilise both glucose and pyruvate; glucose metabolism is favoured by the somatic cells of the follicle, whereas oocytes are incapable of metabolising glucose efficiently for ATP production, instead utilising pyruvate as their main energy source. Under normal conditions the oocyte is supplied with pyruvate by its supporting somatic cells however experimental evidence has also shown that pyruvate is taken up from the culture medium during *in vitro* follicle culture (315). Tissue sitting at the bottom of a well as in the low volume conditions may be subject to an increased diffusion distance compared to tissue on a membrane on top of the medium, or tissue on the bottom of a gas-permeable dish. Therefore, it is more likely that tissue in the low volume condition is exposed to lower oxygen concentrations. Under anaerobic conditions NAD+ is replenished through the conversion of pyruvate to lactate with simultaneous conversion of NADH to NAD+. It has been demonstrated that the addition of FSH to mouse follicle culture causes a significant increase in lactate production (316). Furthermore, when oocyte cellular volume is accounted for, pyruvate consumption by the oocyte is highest at the primary stage of follicular development (315).

In ML, the high glucose McCoy's 5A medium may be supporting granulosa cell proliferation – leading to the higher likelihood of multi-layered follicles in this culture condition – however, the lower oxygen driving increased conversion of pyruvate to lactate may be detrimental to the oocyte leading to the overall poor survival of multi-layered follicles in ML across culture. This is supported when the degenerating follicles are evaluated further. In ML, of those follicles which were classed as degenerating, 91.3% of these had pyknotic or shrunken oocytes with healthy granulosa cells, with only 8.7% having healthy oocytes and unhealthy granulosa cells. Therefore, although it is not essential to add pyruvate to the

culture medium as it can be provided by the somatic cells, and/or glucose can be used as an alternative energy source, the lack of pyruvate supplementation as seen with McCoy's 5A compared to αMEM medium, may be detrimental to preantral follicle survival. Future work could investigate the effect of sodium pyruvate supplementation to the current composition of McCoy's 5A medium to explore this further.

6.4.3 Asymmetric follicle development

Follicles with asymmetric granulosa cell proliferation were identified in Chapter 4 as being significantly more likely to occur in culture. In this study 15.8% of healthy, multi-layered follicles were asymmetric and interestingly, were equally likely to be present in all culture conditions. Within the total cultured follicle cohort, asymmetric follicles were less likely to develop in tissue cultured in AP and AL compared to MH however within each physical culture condition there was no difference in the likelihood of asymmetry, nor was there a difference in odds of asymmetry within the healthy multi-layered follicle cohort. This would suggest that the different physical conditions used in this study do not reduce the likelihood of asymmetry, nor is it due to the base composition of the culture medium used.

The asymmetry may simply be explained by the culture-induced activation of multiple primordial follicles that inherently lack the capacity to develop normally, and under *in vivo* conditions would have continued to remain dormant, indeed almost two-thirds of the asymmetric follicles showed some sign of degeneration at the end of culture. Asymmetric granulosa cell distribution may in part be explain by the supra-physiological FSH supplementation. It is well described to stimulate granulosa cell proliferation in preantral follicles (317-319).

6.4.4 Tissue preparation

In this Chapter I evaluated a modified version of the cortical strip culture method reported by Telfer and colleagues, using the same well size, medium, and volume of medium but with a different method of tissue preparation. Telfer and colleagues use larger fragments of tissue cut into a wedge shape. The point of the wedge includes a small amount of medullary tissue with the base of the wedge formed of cortical tissue. This tissue is then teased apart with needles or stretched with the blunt side of a scalpel and any large follicles removed before culture (142, 211). It is proposed that the shape and volume of the cortical fragments is linked to the level of follicle activation observed *in vitro*, and that the small inclusion of medulla tissue affects development (211, 319, 320).

In this study we processed the tissue with a tissue chopper to yield very thin fragments. In our study the 37.6% primordial, 46.2% primary, and 16.2% secondary follicles (classified as described by Telfer and colleagues) was in line with that published by their group; 54% primordial, 30% primary, and 16% secondary follicles albeit with a higher percentage of primary follicles (142). The classification used by McLaughlin, Kinnell (142) defines secondary follicles as "multilaminar follicles with more than a single layer of cuboidal granulosa cells". Follicle activation appear to be comparable between the two systems based on the percentage of follicles remaining at the primordial stage as classified by Telfer and colleagues (which includes those classified as transitional in our study, see Chapter 2). This suggests that rapid chopping of cortical tissue with a tissue chopper as described here may cause sufficient disruption to the tissue to stimulate follicle activation.

The Hippo signalling pathway first received attention with respect to follicle activation when it was reported to be the mechanism underlying the success of ovarian drilling and wedge resection as a treatment for infertility due to aberrant follicle growth such as polycystic ovarian syndrome (321). Telfer et al. postulate the mechanical disruption caused

by stretching the tissue activates the HIPPO pathway giving superior follicle activation (322).

A recent study elegantly demonstrated the interaction between Hippo and PI3K/Akt/mTOR signalling during early follicle development (143). Using cryopreserved human tissue, they suggest that Hippo disturbance occurs during tissue preparation and cryopreservation, which may explain the slightly higher percentage of activated follicles in this study compared to that published by McLaughlin, Kinnell (142), (143). They propose a model for Hippo signalling in follicle activation whereby ovarian fragmentation disrupts Hippo signalling within the granulosa cells causing activation of Yes-associated protein (YAP) and its translocation to the nucleus where it promotes the transcription of connective tissue growth factor (CCN2/CTGF) and Baculoviral IAP repeat-containing protein 1 (BIRC1) which are involved in granulosa cell proliferation. BMP-15 and GDF-9 from the oocyte coupled with activated YAP activate Mothers against decapentaplegic homolog (SMAD)2/3 to form the YAP-SMAD2/3/4 complex which promotes the transcription of growth factors (143). While the role of Hippo signalling in reproduction is yet to be fully elucidated, it would be of interest to compare expression of key genes in the Hippo pathway such as YAP and CCN2 between cortical tissue that had been stretched versus processed with a tissue chopper.

6.4.5 Stromal health

A limitation of the current study was that it did not evaluate stromal health before or after culture. The importance of stromal tissue health is gaining recognition, particularly with respect to the effects of cryoprotection and cryopreservation (323, 324). Stromal cells have an important role in the recruitment and development of follicles, providing a scaffold without which oocyte-somatic cell interactions would be compromised (92). This is particularly true for follicles in the early stages of development *in vitro*, whose development requires a cortical structure. There is concern that current cryopreservation protocols are

optimised to maximise follicle survival at the expense of stromal tissue, this may have serious implications for the subsequent survival and revascularisation of the tissue, more pertinent to this work is the impact this may have on the tissues ability to function in culture (325, 326). Similarly, in our study the primary endpoints were related to follicle rather than stromal health. Stromal density and staining for apoptosis markers such as TUNEL have been used as indicators of stromal health but it would also be useful to identify a wider variety of markers to assess stroma health during culture (327).

In hindsight, collecting the spent medium on days two, four, and six of culture to assay the production of steroid hormones and growth factors to provide additional parameters of follicle health and survival would have been interesting. Assaying metabolites in spent medium may provide insight into what is being depleted or is accumulating in different culture conditions to further our understanding of the specific requirements of ovarian tissue in culture. Evaluating non-invasive markers of tissue and follicle health across the culture period to provide a more continuous assessment of tissue function would allow us to better tailor culture medium to the specific requirements of the tissue.

6.4.6 Summary and implication of findings

Of the six culture conditions, tissue cultured in a low volume of αMEM medium had the highest odds of producing healthy follicles, and the lowest odds of atretic follicles. McCoy's low volume also yielded follicles with greater morphological health to a lesser degree. While tissue cultured in a low volume of McCoy's 5A medium had a higher likelihood of multi-layer follicles there was no difference when the healthy growing follicles were assessed, suggesting this condition does not adequately support the increased development. Based on the results reported here, pieces of cryopreserved human cortical tissue should be cultured individually in a low volume of αMEM medium to give the greatest likelihood of

developing heathy follicles. Further work is required to ascertain whether co-culture of tissue fragments, or culture of high follicle density fragments is more beneficial.

Chapter 7

Analysing cumulus cell gene expression using RNA-seq

7.1 Introduction

Oocyte quality is a critical determinant of the capacity to achieve a pregnancy (179), and it is well established that the quality of the oocyte deteriorates with aging (see Section 0). A key step in developing a treatment for female reproductive aging is identifying the pathways affected by age. Substantial advances in next-generation sequencing technologies have revolutionized our understanding of the human genome architecture. However, our knowledge of the broad changes to RNA expression in the aging human cumulus-oocyte-complex is still limited.

Our current understanding of the change in the cumulus cell transcriptome with age has been discussed in Section 1.10.3. To briefly summarise, at the time of writing there had been a single study published using RNA-seq to assess the cumulus cell transcriptome from reproductively young (mean age 29 years) and older women (mean age 43 years). Molinari

and colleagues biopsied approximately one-third of a single cumulus-oocyte complex from each patient, and only cumulus cells from MII oocytes were used (201). They suggest based on their findings that hypoxia in the follicular environment is one of the main contributors of age-related oocyte senescence (201). Live birth rates after assisted reproductive techniques in women 40 years or older are significantly lower than those of women younger than 35 years (3) and the work by Molinari suggests some genetic basis for this. However, female reproductive success declines from 35 years (3) and the transcriptomic changes of cumulus cells from women in that earlier period of decline are yet to be explored.

7.1.1 Aims and hypotheses

The aims and hypotheses of this chapter were to determine:

(i) Whether gene expression differs between pooled cumulus cells from MII oocytes obtained from young patients (<35 years) and older patients (≥37 years).

a. *Significant differences in gene expression will be detectable between pooled cumulus cells from MII oocytes from reproductively young and older women using RNA-seq.*

7.2 Materials and methods

7.2.1 Ethical approval

The use of human cumulus cells was approved by Health Research Authority NRES Committee South West - Exeter (REC reference: 11/SW/0334). Informed consent was obtained from all patients prior to egg collection at Oxford Fertility.

7.2.2 Inclusion and exclusion criteria

Patients undergoing IVF with ICSI treatment were eligible for the study. Patients were excluded if undergoing treatment for polycystic ovarian syndrome, endometriosis, premature ovarian insufficiency or unexplained infertility. For sequencing and RT-PCR, only samples containing MII oocytes were included and stripping dishes containing visible blood clots were excluded.

7.2.3 Information on patient characteristics

Information on patient date of birth, time stripping completed, and maturity of eggs stripped was written on the top of each stripping dish by the embryologist who performed the stripping. The total number of oocytes collected was calculated by summing the number of eggs stripped in each dish. Indication for treatment was provided by either the research nurse or embryology team. Information on brand of culture medium used was provided by the embryology team. Body mass index (BMI), cycle outcome, basal FSH, and oestradiol (E2) peak were provided by the research nurse for all patients whose cumulus cells underwent RNA-seq. Anti-Mullerian hormone (AMH) level was not measured in all patients but where available was also provided by the research nurse for those patients whose cumulus cells underwent RNA-seq.

7.2.4 Cumulus cell collection for sequencing

Cumulus cells were separated from the oocyte with strippers after brief exposure to hyaluronidase (80 IU/ml, Sydney IVF Hyaluronidase, Cook Medical, Hertfordshire, UK) at 37°C. Up to nine oocytes were stripped in a single dish and the maturity of all oocytes recorded. Immediately after stripping, dishes were transferred to a single cell room. Under a dissecting microscope, 40 – 80 µl of medium containing stripped cumulus cells from each stripping dish was transferred to a DNase and RNase-free tube and stored at −80°C until RNA extraction. The contents of each stripping dish were transferred to a single tube

resulting in more than one sample per patient in cases if multiple stripping dishes were used. Samples collected for real-time polymerase chain reaction (RT-PCR) validation, were centrifuged (Technico Mini, Fisher Scientific, UK) at 2000 x g for 1 min and the supernatant removed before the cells were stored at −80°C until RNA extraction.

7.2.5 RNA-sequencing

7.2.5.1 Patient demographics and baseline characteristics

Nineteen samples from 13 patients were processed for sequencing. Ten single samples from 10 patients were analysed for this thesis. On confirmation of patient characteristics one patient from the older age group was excluded due to mislabelling of oocyte maturity on the stripping dishes. Samples from nine patients were allocated to one of two cohorts based on maternal age; 'young' age <35 years (n=5), and 'older' aged ≥37 years (n=4) (Table 7.1).

Table 7.1 Demographics and baseline characteristics of patients whose samples used for sequencing

Variable	Unit	Young (n=5)	Older (n=4)	P value
Age	Years	31.13 ± 1.41	37.92 ± 0.325	<0.01
BMI		23.6 ± 1.44	22.5 ± 1.29	ns
AMH	pmol/L	16.9 ± 4.63 (n=3)	11.65 ± 2.55 (n=2)	ns
Basal FSH	mIU/ml	6.04 ± 0.48 (n=5)	8.08 ± 0.71 (n=4)	<0.05
E2 peak	pmol/L	12284 ± 2843	3962 ± 1221	<0.05
Oocytes collected	number	21.8 ± 4.59	8.75 ± 2.29	0.0518
Stimulation protocol		Long (n=4) Short (n=1)	Long (n=3) Short (n=1)	
Culture medium supplier		Cook (n=2) Sage (n=3)	Cook (n=2) Sage (n=2)	

Long *GnRH agonist protocol,* ***short*** *GnRH antagonist protocol. Data presented as mean ± standard error of the mean.*

7.2.5.2 RNA extraction for sequencing

As the samples were frozen as cell suspensions, a standard kit protocol could not be used. An assessment of different methods for extracting RNA from cells in suspension is detailed in Appendix III. Based on an evaluation of the yield and quality of RNA obtained through

three different protocols tested, a TRIzol/chloroform (Sigma) extraction followed by clean-up with the RNeasy Micro Kit (Qiagen, Manchester, UK) was found to give adequate yield and high-quality RNA.

Frozen samples were thawed by the addition of 1 ml TRIzol reagent and vortexed to homogenise. Homogenate was incubated for 5 min at room temperature, chloroform (200 µl per 1 ml TRIzol) was added and shaken vigorously for 20 sec before being incubated at room temperature for a further 3 min. Samples were centrifuged at 12,000 x g for 15 min at 4°C. Centrifugation separated the mixture into a lower red phenol-chloroform, a white interphase, and a colourless upper aqueous phase. Up to 700 µl of the aqueous phase containing the RNA was transferred to a new RNase free tube. One volume of 70% ethanol was added to the aqueous phase and mixed well by pipetting. Samples were transferred to a RNeasy MinElute spin column and processed as per the manufacturer's instructions including on column DNase digestion. RNA was eluted in 15 µl RNase-free water; 3 µl was transferred into a separate RNase-free tube to be used for quality control (QC) and along with the tube containing the remaining 12 µl of RNA, was stored at -80°C until QC.

7.2.5.3 Measurement of RNA quantity

RNA concentration was measured using a Qubit 2.0 fluorometer with the Qubit® RNA HS Assay Kit according to the manufacturer's instructions. Briefly, 10 µl standards or 1 µl RNA were mixed with Qubit® Working Solution and incubated for 2 min. Concentration values were calculated by the fluorometer built-in software.

7.2.5.4 Assessment of RNA integrity

RNA integrity was assessed using the High Sensitivity RNA ScreenTape System on the TapeStation 2200 according to the manufacturer's instructions. Briefly, the High Sensitivity RNA ScreenTape device and loading tips were loaded into the 2200 TapeStation instrument.

Samples were prepared by mixing 1 µl High Sensitivity RNA Sample Buffer with 2 µl RNA sample and loaded into the TapeStation instrument. The RIN value is determined by the TapeStation software.

Where possible only samples with a RIN score of 8.0 or higher were included for sequencing. A candidate list of samples for sequencing including RIN scores and RNA concentrations was sent to the Wellcome Centre for Human Genetics (WHG) where the library preparation and sequencing was to be completed, and all were deemed suitable for sequencing by the Project Manager.

7.2.5.5 Normalisation of RNA concentration

Samples were thawed on ice and normalised to an RNA concentration of 5 ng/µl in 15 µl of RNase-free water, concentration permitting. Any remaining RNA was returned to -80°C. Normalised samples were stored at -80°C until sequencing.

7.2.5.6 Library preparation

Library preparation and sequencing was performed by technicians at the WHG. Material was quantified using RiboGreen (Invitrogen) on the FLUOstar OPTIMA plate reader (BMG Labtech) and the size profile and integrity analysed on the 2200 or 4200 TapeStation (Agilent, RNA ScreenTape). Input material was normalised to 50 ng prior to library preparation. mRNA was isolated using the NEBNext Poly(A) mRNA Magnetic Isolation Module (E7490L). Library preparation was completed using NEBNext Ultra II Directional RNA Library Prep Kit for Illumina (E7760L) following manufacturer's instructions. Libraries were amplified using in-house unique dual indexing primers (based on (328)). Individual libraries were normalised using Qubit, and the size profile was analysed on the 2200 or 4200 TapeStation. Individual libraries were normalised and pooled together accordingly. The pooled library was diluted to ~10 nM for storage. The 10 nM library was

denatured and further diluted prior to loading on the sequencer. Paired end sequencing was performed using a HiSeq4000 75bp platform (Illumina, HiSeq 3000/4000 PE Cluster Kit and 150 cycle SBS Kit).

7.2.6 RNA-seq data analysis

7.2.6.1 Bioinformatic processing

Nineteen samples from 12 patients were multiplexed together across two lanes of sequencing and the depth achieved per sample was about 32 million reads. Bioinformatic processing was performed by the Bioinformatics and Statistical Genetics core group at the WHG. Relevant options are included in parentheses after the version number. Reads were aligned to the human reference genome (GRCh37.p13 including ERCC spike-ins Feature GTF: accession NCBI: GCA_000001405.14) using HISAT2 (Version 2.0.4; (–dta)) (329). Duplicate reads were removed using the Picard 'MarkDuplicates' tool (Version 1.9.2; (AS=true VALIDATION_STRINGENCY=LENIENT REMOVE_DUPLICATES=true)) (330), and sorted with samtools (Version 1.4; sort (-n)). Reads mapping uniquely to Ensembl-annotated genes were summarised using featureCounts (Version 1.5.0; (-p -F GTF)) (331).

7.2.6.2 Differential gene expression analysis

Of the 19 samples sent for sequencing, nine of these were used in this thesis and analysed for differential gene expression (DGE). The raw gene count matrix was imported into the R/BioConductor environment (332) for further processing and analysis with the edgeR package (333). EdgeR performs differential abundance analysis using a pairwise design based on negative binomial model which accounts for biological variability as well as correcting for batch effect (333). Genes with <0.5 CPM in less than four samples were excluded from the analysis. Normalization of the sequenced libraries in edgeR using the trimmed mean of M value (TMM) method was performed to remove effects due to differences in library size. DGE analysis was performed after fitting the generalized linear

model (GLM) approach to the normalized counts. The resulting P-values were corrected for multiple testing using the Benjamini–Hochberg false discovery rate (FDR) approach. Genes with a corrected P-value <0.05 were considered differentially expressed.

7.2.6.3 Gene ontology analysis

To gain insights into the biological implications of the DGE analysis, gene ontology (GO) over representation analysis was performed on the list of differentially expressed genes using ConsensusPathDb (334) Appendix IV. GO terms with a gene count of more than 3 and a hypergeometric p-value less than 0.05 as identified using ConsensusPathDb gene ontology level 4 categories were clustered for redundancy and visualised using REVIGO (335). Over-representation P-values are corrected for multiple testing using the false discovery rate method and are reported as q-values. Clusters of redundant terms were constructed using the Homo sapiens GO term database, using a similarity of 0.5, with SimRel as semantic similarity measure.

7.2.6.4 Identification of upstream regulators and causal networks

To predict upstream transcriptional regulators, the top 600 differentially-expressed genes were imported into Ingenuity Pathway Analysis (IPA, Qiagen) (Appendix V). Upstream Regulator Analysis was used to identify likely upstream regulators that are connected to dataset genes through a set of direct or indirect relationships using Fishers exact t-test and an algorithm which computes the consistency of these interactions. Overlapping P values were used to measure statistically significant overlap. Significance was generally attributed to a P value less than 0.01. The goal of Upstream Regulator Analysis is to identify molecules upstream of the genes in the dataset that potentially explain the observed expression changes between older and younger cumulus cells.

7.2.7 Validation of RNA-seq with real time-polymerase chain reaction

A selection of genes displaying a statistically significant difference of expression between older and younger cohort were validated with real time-polymerase chain reaction (RT-PCR).

7.2.7.1 Patient demographics and baseline characteristics

Thirteen cumulus cell samples from thirteen patients were used for RT-PCR validation of RNA-seq results. Six young and seven older patients were recruited as described in 7.2.2, and samples collected as described in Section 7.2.4. Cohort demographics are detailed in Table 7.2.

Table 7.2 Demographics and baseline characteristics of patients whose samples used for RT-PCR

Variable	Unit	Young (n=6)	Older (n=7)	P value
Age	Years	31.78 ± 1.20	39.75 ± 0.95	<0.01
Oocytes collected	number	15.00 ± 3.98	13.00 ± 2.53	ns
Culture medium		Sage (n=6)	Sage (n=7)	

Data presented as mean ± standard error of the mean.

7.2.7.2 RNA extraction and reverse transcription

Total RNA was isolated using RNeasy Micro Kit as per the manufacturer's instructions and quantified using Qubit as previously described (section 7.2.5.3). Complementary DNA (cDNA) was synthesized from 199 ng of RNA by reverse transcription in a total volume of 20µl using random hexamers and anchored oligo (dT) primers and 1µl of reverse transcriptase (SensiFAST cDNA Synthesis Kit, Bioline, London, UK). A no RT control was included, including 1µl of RNase/DNase free H_2O in place of reverse transcriptase. The reaction was performed as per the manufacturer's protocol; for 10 min at 25°C, for 15 min

at 42°C, for 15 min at 48°C, and for 5 min at 85°C. cDNA was stored at 4°C for up to 48 hours before use.

7.2.7.3 Real-time PCR

Real-time PCR was performed using Taqman Gene Expression Assays (Table 7.3 from Thermo Fisher Scientific, Rochford, UK). A reaction volume of 20 µl was comprised of 10 µl Taqman Fast Advanced Master Mix (Thermo Fisher Scientific, Rochford, UK), 9 µl cDNA, 1 µM Taqman gene expression assay. A no template control was included with 9 µl RNase/DNase free H_2O in place of cDNA. Samples were run in triplicate on the Rotor Gene 6000 (Corbett Research, Qiagen). RT-PCR was performed as per the manufacturer's recommendations; initial heat denaturation at 50°C for 2 min then at 95°C for 10 min, followed by 35 cycles of 95°C for 15 sec and 60°C for 1 min.

Table 7.3 Taqman gene expression arrays used for RNA-seq validation

Gene	Assay ID	Gene type	Assay design	Target species	Amplicon length	Reporter dye
PPARGC1A	Hs00173304_m1	Target	Probe spans exons	Human	83	FAM-MGB
CRIM1	Hs01070663_m1	Target	Probe spans exons	Human	70	FAM-MGB
GAS1	Hs00266715_s1	Target	Both primers and probe map within a single exon	Human	94	FAM-MGB
SSTR1	Hs00265617_s1	Target	Both primers and probe map within a single exon	Human	85	FAM-MGB
CTH	Hs00542284_m1	Target	Probe spans exons	Human	110	FAM-MGB
GAPDH	Hs02758991_g1	House-keeping	Probe spans exons	Human	93	FAM-MGB

The threshold for Ct values was set at 0.5. Relative quantitation was calculated by the 2-ΔΔCt method relative to human housekeeping gene GAPDH (Table 7.3). Ct values were normalized to the average of the housekeeping gene GAPDH to give the ΔCt. The ΔΔCt was

calculated by finding the difference between the ΔCt of the older and the ΔCt of the young groups. This value was transformed to the relative fold-change using the equation 2-ΔΔCt. The significance of the mean relative gene expression level differences was calculated using two-sample t-distribution test. All data analysis was performed using GraphPad Prism. Data is expressed as the mean ± standard deviation.

7.3 Results

7.3.1 Older patients have higher basal FSH and a lower peak level of oestradiol

Patients' demographics, baseline characteristics and cycle outcomes of the patients whose samples underwent RNA-sequencing are outlined in Table 7.1 and Table 7.4, respectively. As expected, mean age of the patients' in the older group was significantly higher than that of the young group (37.92 ± 0.325 and 31.13 ± 1.41, respectively; $p<0.01$). In the older group the E2 peak was significantly lower and basal FSH was higher, furthermore there was a trend towards a decrease in oocyte yield in the older cohort ($p=0.0518$). Of the three patients who had an embryo transfer in each group, none successfully achieved a pregnancy.

Table 7.4 Cycle outcome of patients whose cumulus cells underwent RNA-seq

Outcome		**Young (n=5)**	**Older (n=4)**
Non-clinical pregnancy (no foetal heart)		1	0
Negative pregnancy test		2	3
No embryo transfer	Embryo storage	1	1
	Eggs donated	1	0

7.3.2 Mapping metrics

There was an average of 29.2±0.69 million sequenced reads across the nine samples and there was no significant difference in the number of reads between the young and older age groups; 29.63±1.16 and 29.77±0.67 million reads, respectively (Figure 7.1). The percentage of genes mapping to the reference genome was similarly consistent between both age groups (Figure 7.2).

After the raw data was put through the primary bioinformatic processing to align and map the reads, filter low quality reads, and remove duplicates or ambiguously mapping reads there was an average of 20.92±0.32 million reads for differential gene expression (DGE). There was no difference between the two age groups with an average of 20.75±0.45 in the young group and 21.14±0.50 in the older group. The filtered data set showed 17474 expressed genes across all samples.

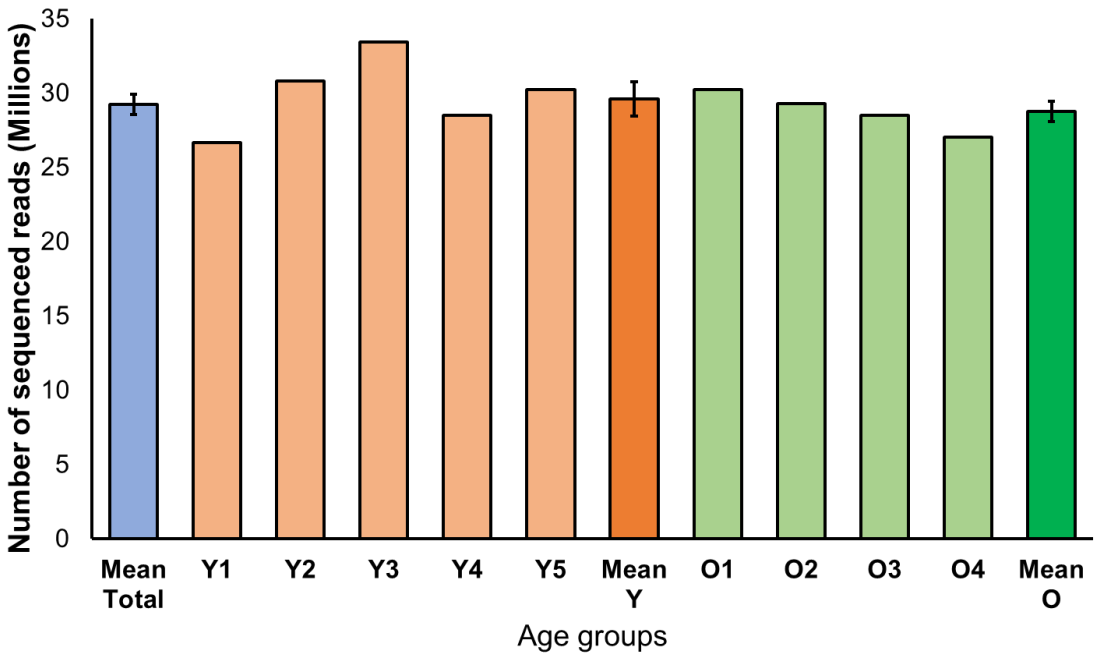


Figure 7.1 Number of sequenced reads in total and across young and older age groups

The number of sequenced reads (in millions) obtained from RNA-sequencing of human cumulus cell samples from young (Mean Y, Y1-Y5; >35 years, n=5), and older (Mean O, O1-O4; ≥37 years, n=4) women undergoing IVF with ICSI. Paired end sequencing was performed using a HiSeq4000 75bp platform. Data is presented as raw data or mean ± standard error of the mean where specified.

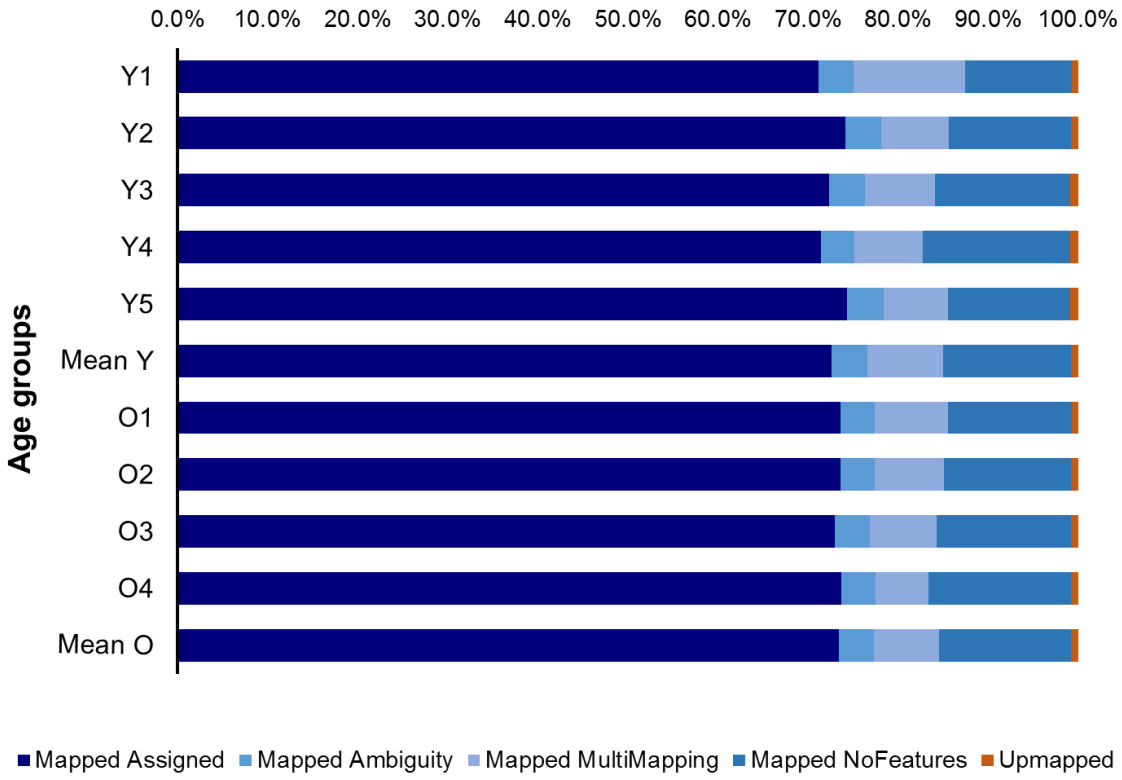


Figure 7.2 Mapping metrics across young and older age groups

The percentage of mapped and unmapped reads obtained from RNA-sequencing of human cumulus cell samples from young (Mean Y, Y1-Y5; >35 years, n=5), and older (Mean O, O1-O4; ≥37 years, n=4) women undergoing IVF with ICSI. Paired end sequencing was performed using a HiSeq4000 75bp platform. Reads were aligned to the human reference genome (GRCh37.p13 including ERCC spike-ins Feature GTF: accession NCBI: GCA_000001405.14) using HISAT2 2.0.4.

7.3.3 Data exploration and normalisation

Multidimensional scaling (MDS) plots are a means of visualizing the level of similarity of individual points in a dataset. Figure 7.3 is an MDS plot based on age group which demonstrates clear separation between the young and old age groups.

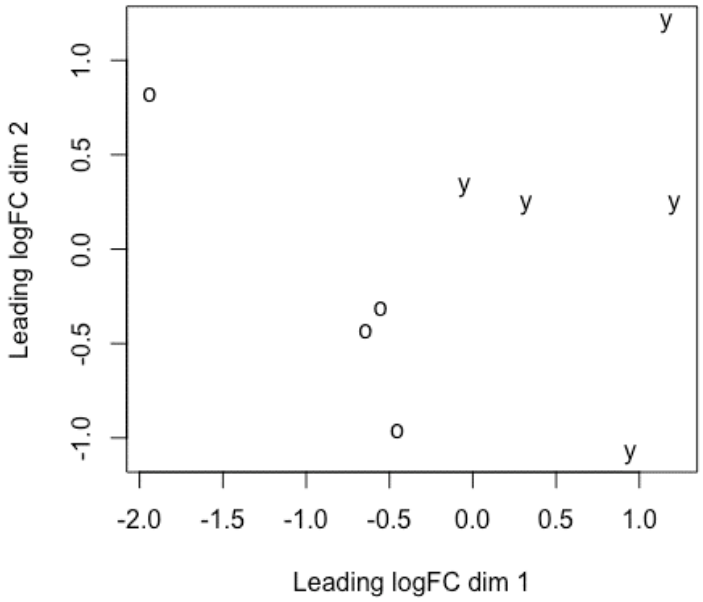


Figure 7.3 Multi-dimensional scaling (MDS) plot of age on gene expression

MDS analysis of age group as a factor contributing to differences in gene expression between cumulus cells from young (y) and older (o) women undergoing IVF with ICSI. Two-dimensional representation of the MDS results. Leading logFC dim 1: first MDS component (X axis); leading logFC dim 2: second MDS component (Y axis).

Data was collected on all parameters other than patient age that could impact gene expression. For the data exploration, MDS plots were generated to visualise the impact of these various factors detailed in Figure 7.4; this included the number of oocytes in a stripping dish (Figure 7.4A), RNA isolation batch (Figure 7.4B), and stimulation protocol (Figure 7.4C). Based on the MDS plots there was no clustering based on stimulation protocol or the number of oocytes in a stripping dish. There was some modest clustering between the two RNA isolation batches which was subsequently adjusted for in the DGE analysis.

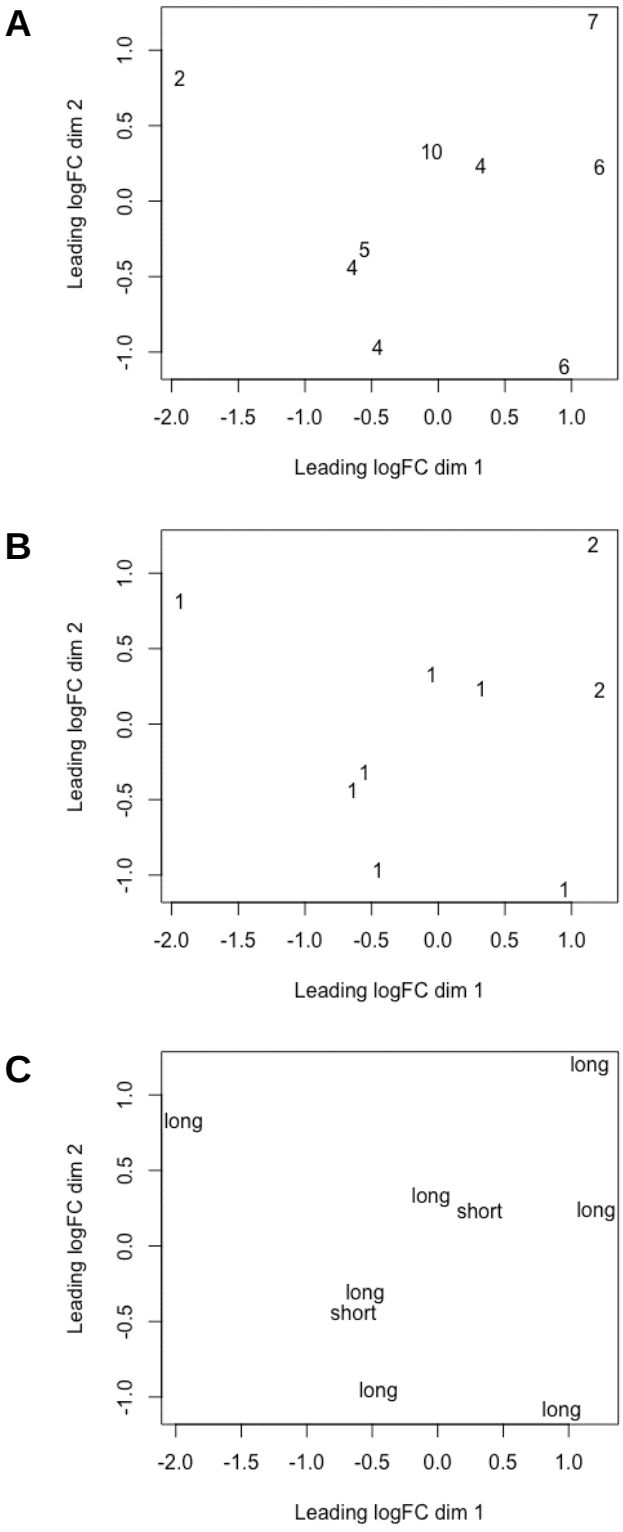


Figure 7.4 Multi-dimensional scaling (MDS) plots of potential factors influencing differential gene expression

MDS analysis of factors possibly contributing to differences in gene expression between cumulus cells from young and older women undergoing IVF with ICSI. Two-dimensional representation of the MDS results. Leading logFC dim 1: first MDS component (X axis); leading logFC dim 2: second MDS component (Y axis). A) the number of oocytes that contributed to the analysed cumulus cell population for each patient where *x* = oocyte number. B) differences based on RNA isolation batch 1 or 2. C) stimulation protocol [long or short] used for each patient prior to egg collection.

An important factor that influences the number of differentially expressed genes is the variation among the samples. The Biological Coefficient of Variation (BCV) plot is a way to visualise variances across all genes that are lowly expressed all the way to highly expressed. The common dispersion in this study was approximately 0.3 which is reasonable for this experiment (Figure 7.5). For typical, well-control experiments a value of around 0.4 for human data and 0.1 for genetically identical model organisms is expected (333).

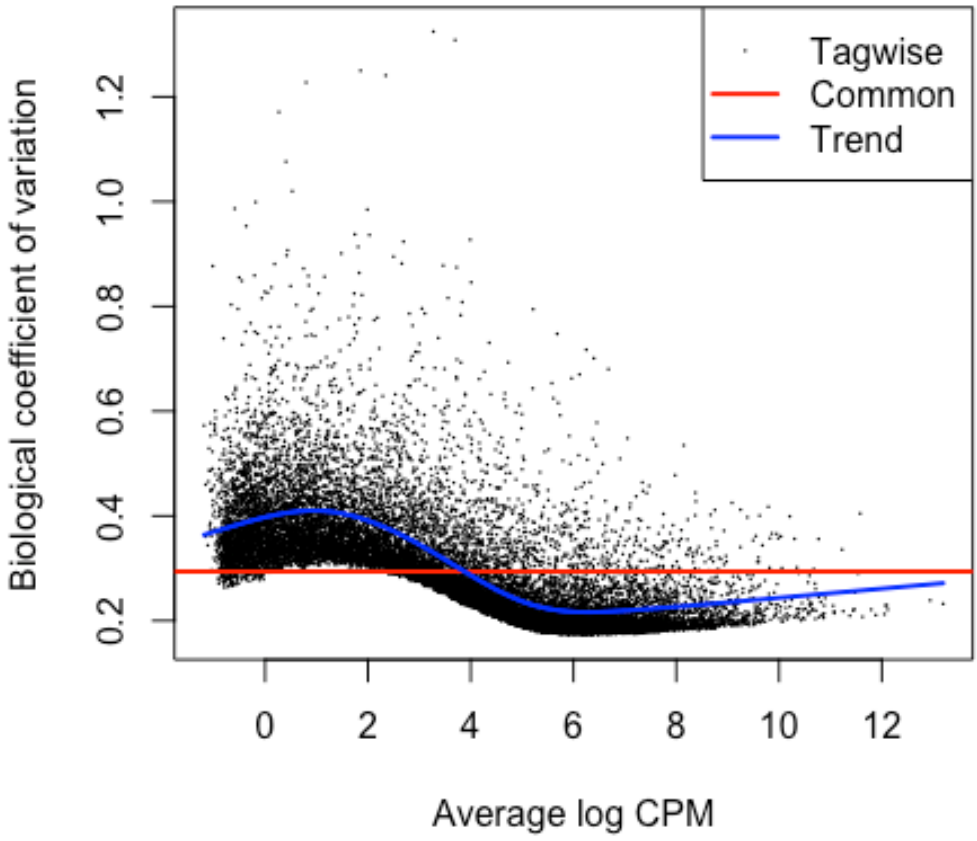


Figure 7.5 Biological coefficient of variation against gene abundance

Scatterplot of the biological coefficient of variation (BCV) against the average abundance of each gene. The plot shows the square-root estimates of the common, trended and tagwise negative binomial dispersions. The tagwise dispersion indicates that more highly expressed genes show lower dispersion, and conversely that at low expression level of genes or transcripts, the variability of gene abundance is high. CPM: counts per million.

7.3.4 Cumulus cell samples cluster based on age and show significant differences in gene expression

A total of 185 genes were found to be differentially expressed (adjusted p value<0.05) between the young and older groups and are depicted in Figure 7.6. Of these, 98 were upregulated and 83 were downregulated in the older group compared to the younger group. A heatmap of the differentially expressed genes with a false discovery rate (FDR)<0.01, associated gene names and patient ages are shown in Figure 7.7. In both Figure 7.6 and Figure 7.7 there is clear hierarchical clustering of the differentially expressed genes, indicating separation between samples on the basis of age group, young or older. The young age group were a more diverse population as seen by the more varied gene expression levels (Figure 7.6) which may be due to the wider age range within that group compared to the older group (see Section 7.3.1).

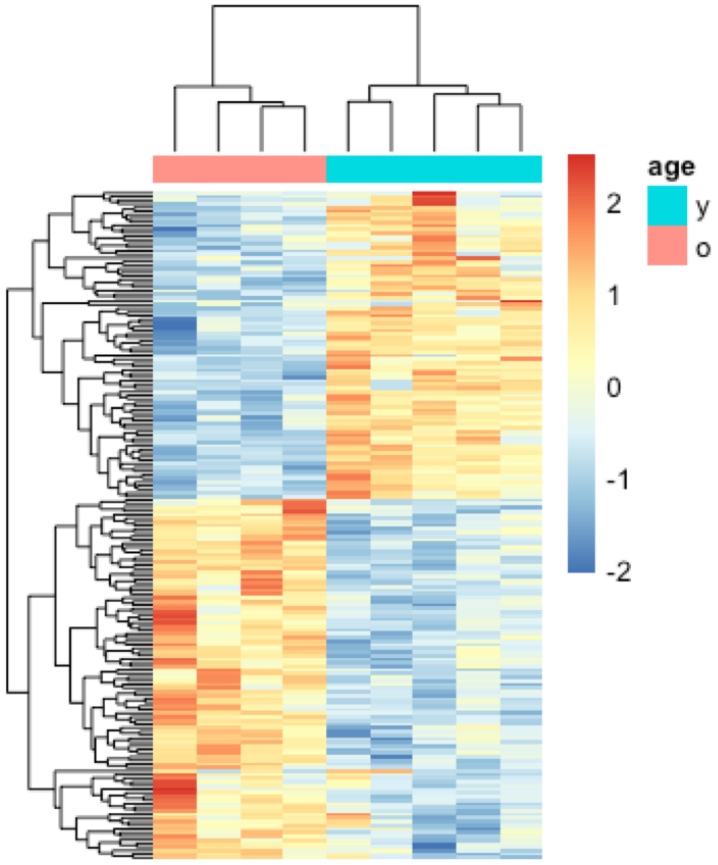


Figure 7.6 Heatmap showing all differentially expressed genes with an FDR<0.05 between cumulus cells from young and older women

A heatmap comparing counts per million (CPM) of all differentially expressed genes for each sample. The intensity of the pseudocolors reflects gene expression levels (red indicates high CPM count, navy indicates low CPM count). Hierarchical clustering of the differential expressed genes shows separation between young (y; >35 years, n=5) and older (o; ≥37 years, n=4) groups.

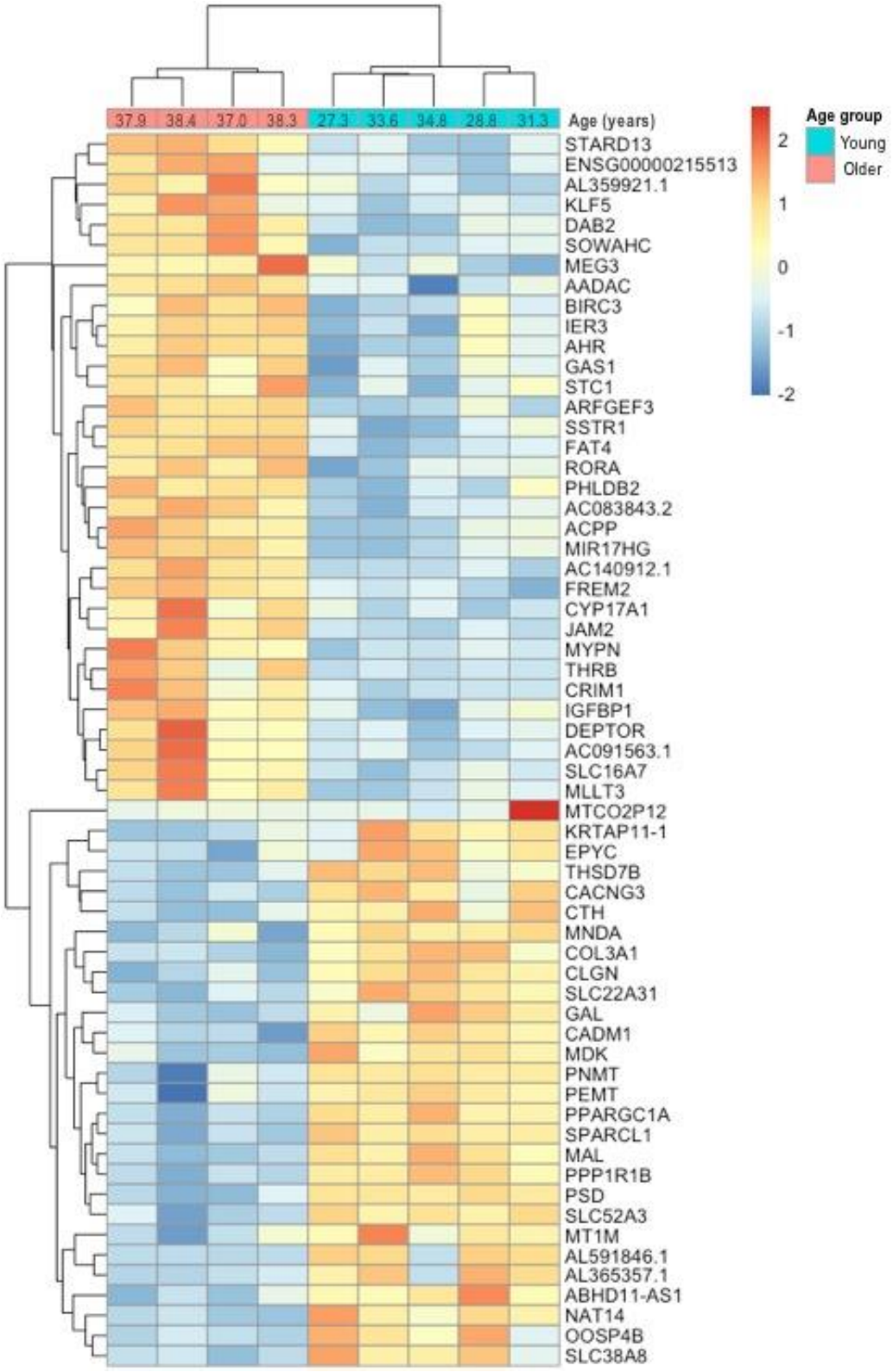


Figure 7.7 Heatmap showing differentially expressed genes with an FDR<0.01 between cumulus cells from young and older women

A heatmap comparing counts per million (CPM) of differentially expressed genes with an FDR<0.01 for each sample. The intensity of the pseudocolors reflects gene expression levels (red indicates high CPM count, navy indicates low CPM count). Gene names are listed on the right of the graph. Patient age in years is across the top of the figure.

One of the genes upregulated in the older group was CYP17A1 (Figure 7.7). This a gene largely believed to be expressed exclusively in theca cells. To investigate this further I looked at the raw read count matrix which showed CYP17A1 expression all samples, with higher transcript levels in all older patients. Reasons for this are discussed in Section 7.4.4.

7.3.5 Genes encoding enzymes and transcription regulators are differentially expressed with age

The Ensembl gene identifications of differentially expressed genes with an adjusted p value<0.05 were loaded into IPA which identified 181/185 differentially expressed genes. While most of the genes identified in the DGE analysis have protein-coding potential and associated biological functions, 13 genes were not associated with an Entrez gene name. IPA attributes a 'type' to each gene. Genes classed as 'other' accounted for 51%; those with specific classification are depicted in Figure 7.8 which shows the known genes primarily code for enzymes or transcription regulators.

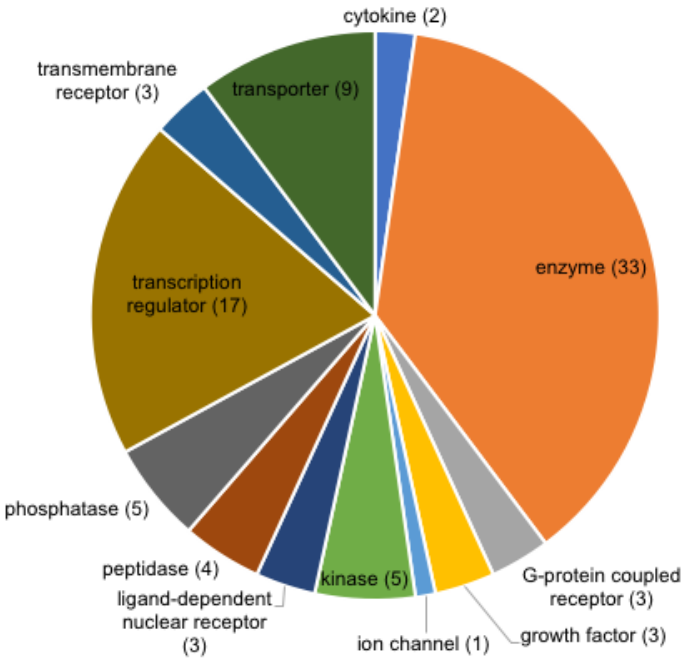


Figure 7.8 Classification of gene types of differentially expressed genes between young and older groups

Ingenuity Pathway Analysis (IPA) associated gene 'types' for the 181 IPA-recognised differentially expressed genes. Genes classified as 'other' (n=93) are not shown in this figure. Number of genes in a given category are in parenthesis.

7.3.6 Gene ontology analysis reveals enrichment of biological process terms

To gain insights into the biological implications of the differentially expressed genes, all 185 differentially expressed genes were analysed using the gene annotation programs ConsensusPathDb, over-represented GO terms were then clustered and visualised using REVIGO. A diverse set of GO terms for biological process were found to be overrepresented and were the dominant GO category (Figure 7.9) and the complete list can be found in Appendix V. Extracellular matrix organisation and structure were enriched including the genes COL11A1, LAMA4, ADAMTS14, PHLDB2, FGG, JAM2, LOX, COL2A1, MYH11, TNFRSF11B, COL3A1, and TNC. Several terms clustered under 'heart development' encompassing blood vessel morphogenesis and vasculature development (AHR, COL15A1, LOX, NGFR, DLL1, STARD13, HGF, KLF5, MIB1, SOX4, CXCR2, COL3A1, EPHB1, RORA, SEMA3C, CTH) were significantly enriched. Interestingly, there was a cluster of terms relating to apoptosis including regulation of cell death, apoptotic process, and extrinsic apoptosis signalling pathway.

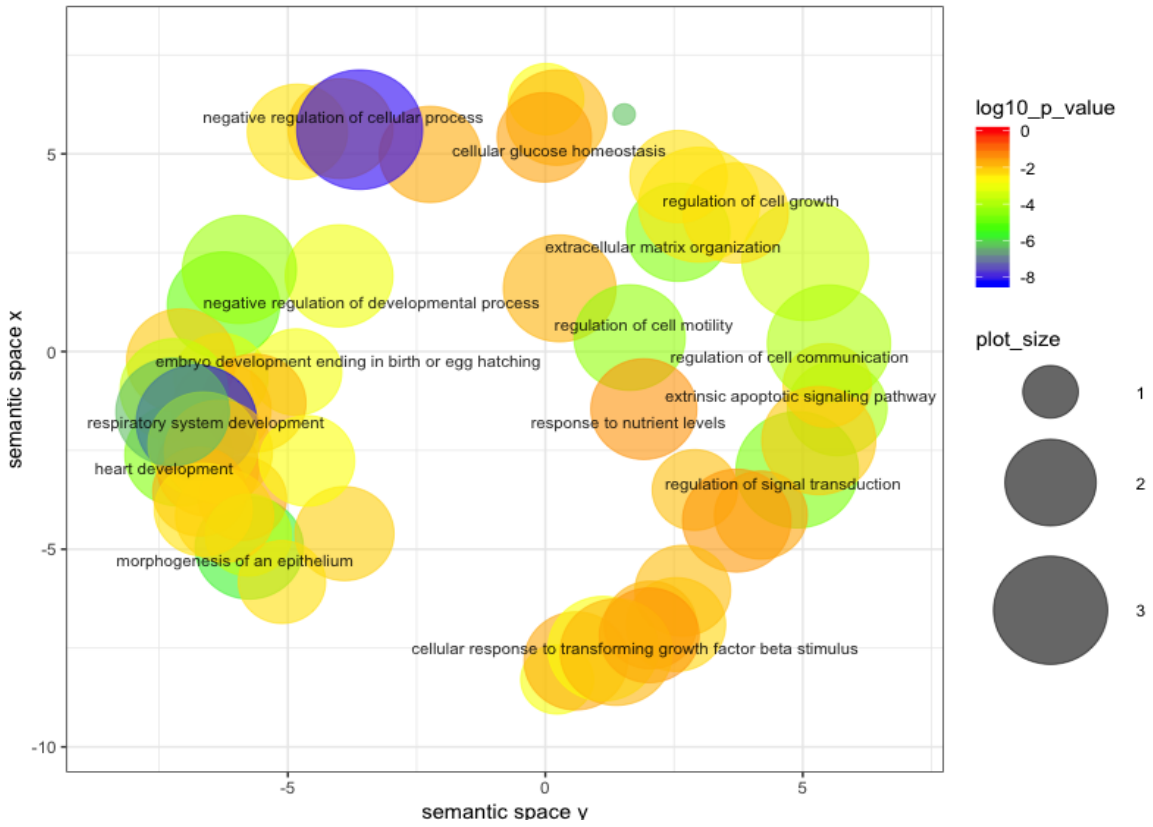


Figure 7.9 Gene ontology biological process scatterplot

Gene ontology (GO) biological process scatterplot for all genes differentially expressed with maternal age. Colours indicate the p-value of enrichment according to the legend. The size of each bubble reflects the count of each term among the enriched term list. Bubbles are annotated with GO terms of interest.

Cellular component over-representation revealed an enrichment of gene products located in or as subcomponents of the endoplasmic reticulum, plasma membrane, and extracellular exosomes (Figure 7.10). A smaller number of molecular functions were over-represented in the GO terms. The most significant molecular function enrichment was for gene products interacting with an RNA polymerase II (Figure 7.11).

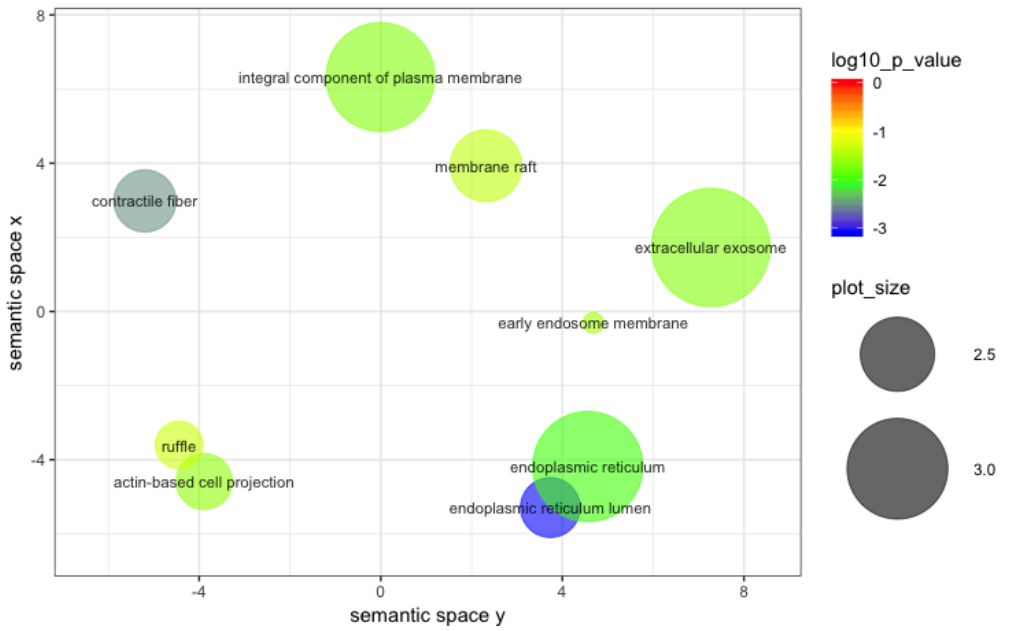


Figure 7.10 Gene ontology cellular component scatterplot

GO cellular component scatterplot for all genes differentially expressed with maternal age. Colours indicate the p-value of enrichment according to the legend. The size of each bubble reflects the count of each term among the enriched term list. Bubbles are annotated with GO terms.

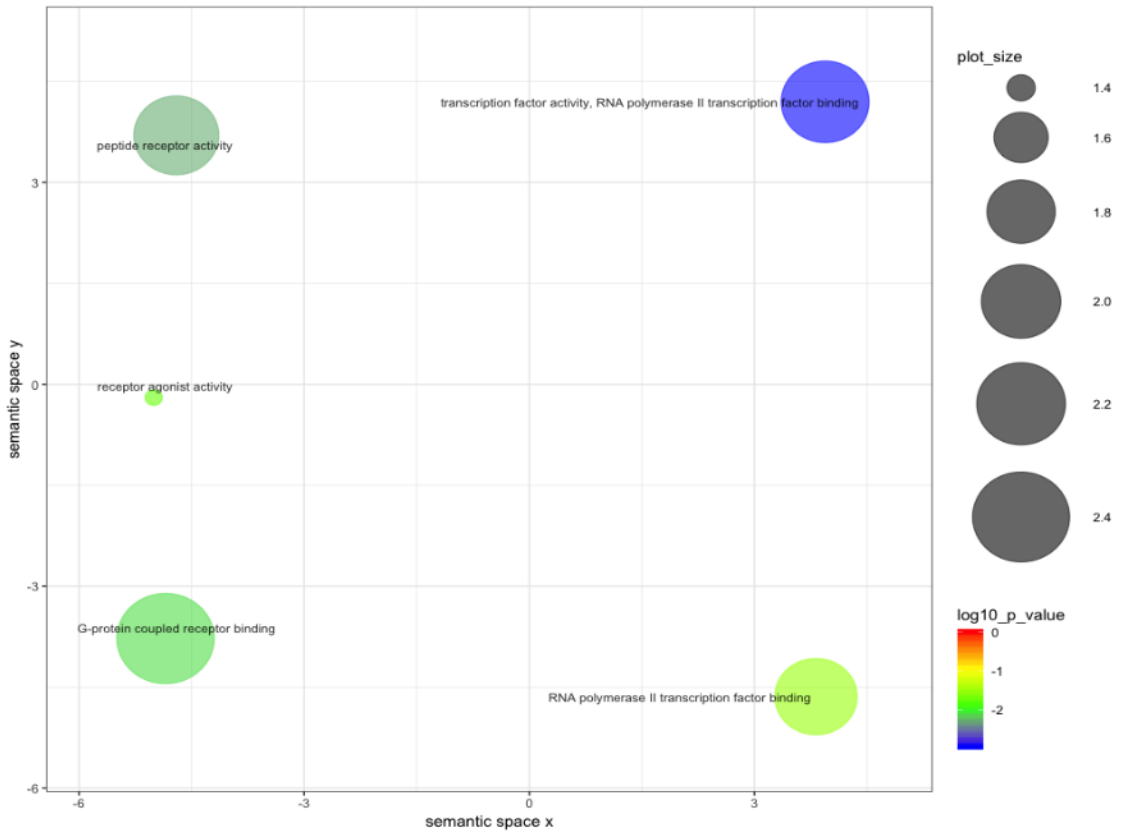


Figure 7.11 Gene ontology molecular function scatterplot

GO molecular function scatterplot for all genes differentially expressed with maternal age. Colours indicate the p-value of enrichment according to the legend. The size of each bubble reflects the count of each term among the enriched term list. Bubbles are annotated with GO terms.

7.3.7 Age-associated differentially expressed genes are associated with several putative upstream regulators

Using the top 600 differentially expressed genes (Appendix VI), an IPA analysis revealed the predicted upstream regulators and, where available, their likely activation or inhibition status. Table 7.5 shows the upstream regulators with an adjusted p value<0.01. Several regulators had positive activation scores including TNF, SMARCA4, and TREM1 which had sufficient evidence to predict an activated state. Fewer regulators had a negative activation score with EGLN and RBM5 having sufficient evidence to be predicted as inhibited with maternal age. TGFB1 is likely inhibited with maternal age which agrees with the identification of 'cellular response to transforming growth factor stimulus' biological process GO term identified above (Section 7.3.6).

Table 7.5 Upstream regulators of top 600 genes differentially expressed with maternal age

Upstream Regulator	Molecule Type	Predicted Activation State	Activation z-score	p-value of overlap	Target molecules from DGE analysis
Activation					
TNF	cytokine	Activated	3.123	2.74E-04	ADM,BHLHE40,BIRC3,BTG2,CCL20,CYBA,CYP17A1,ETS1,EXT1,FGG
SMARCA4	transcription regulator	Activated	2.982	9.09E-05	ABHD2,AHR,ARL4C,BEND5,C6orf141,CARD16,CLK1,EDNRA,FGG,HLA-J
TREM1	transmembrane receptor	Activated	2.324	3.62E-05	ABL2,ACKR3,ASPH,CCL20,INHBA,ISG15,LAMP3,LIF,MAFF,MAP3K8
TNFSF14	cytokine	-	1.958	1.53E-03	BIRC3,CCL20,INHBA,VCAM1
FOXO1	transcription regulator	-	1.954	7.69E-03	CCL20,IER3,IGF1R,IGFBP1,PPARGC1A,RICTOR,VCAM1
FOXL2	transcription regulator	-	1.782	3.17E-04	AMH,CCL20,IER3,LIF,MAFF,PPARGC1A,SOX4
PRKCD	kinase	-	1.757	6.00E-03	ARHGAP32,BIRC3,CCL20,COL1A1,KLF5,LBH,LIF,TNFRSF11B,VCAM1
PGR	ligand-dependent nuclear	-	1.666	2.06E-05	BCL6,BIRC3,EDNRA,ESR1,GAL,IER3,IGFBP1,KCNK1,KLF5,MYCN
NEDD9	other	-	1.633	3.37E-04	ADM,BHLHE40,CA9,MMP14,NRN1,STC1
	group	-	1.464	9.37E-05	CRYAB,ESR1,ETS1,IER3,MAFF,MST1R,NOX4,PMEL,PPARGC1A,SACS
PDGF BB	complex	-	1.344	8.22E-04	BHLHE40,CBX4,DAB2,FOSB,IER3,JUNB,LIF,SOCS3
TLR7/8	group	-	1.342	3.50E-03	CA2,MAP3K8,NFKBIZ,NPR1,TNFAIP6
RELA	transcription regulator	-	1.287	1.83E-03	ANKRD1,BHLHE40,BIRC3,BTG2,CCL20,COL1A1,ERAP1,FOSB,FSCN1,MST1R
PDLIM2	other	-	1.265	9.82E-05	CCL20,CITED2,CLCN4,NAP1L2,NAV1,PPP1R14A,RTN1,SLC10A4,SLC40A1,SRGAP1
PPRC1	transcription regulator	-	1.219	1.42E-04	AADAC,CCL20,CLDN1,EPHB1,GNG11,NFKBIZ,OSCAR
HIF1A	transcription regulator	-	1.211	3.99E-03	ADM,BGN,CA9,CLDN1,EGLN3,ETS1,FSCN1,LOX,MST1R,NOX4
NUPR1	transcription regulator	-	1.177	5.45E-04	ABL2,ACSS1,ADM,ASIC1,AVPI1,CITED2,COL3A1,CROT,DDIT3,DEPTOR
STAT3	transcription regulator	-	1.132	2.78E-03	ADM,BCL6,CA9,COL1A1,DDIT3,ESR1,FGG,FSCN1,IL18R1,JUNB
PRDM5	transcription regulator	-	1	1.83E-03	EDNRA,IL6R,MYD88,NCOA7,NLRC5,PPP1R12B,SIK1/SIK1B,SOCS3
MYOCD	transcription regulator	-	0.943	4.53E-04	ACTC1,COL1A1,COL3A1,MEF2C,MYH11,MYL4,SIK1/SIK1B
ITGB1	transmembrane receptor	-	0.728	7.93E-03	COL1A1,GAS1,JUNB,LRP6
GPER1	G-protein coupled	-	0.6	4.81E-03	BHLHE40,CEBPD,DDIT3,ESR1,FOSB
P38 MAPK	group	-	0.522	6.45E-03	COL3A1,ETS1,FST,IER3,INHBA,KDELR3,MAL,MYH11,PPARGC1A,VCAM1
CD40LG	cytokine	-	0.512	6.80E-03	BCL6,BIRC3,CCL20,CDK6,CHRM5,LAMP3,VCAM1
NR3C1	ligand-dependent nuclear	-	0.453	6.71E-04	ABHD2,BCL6,BHLHE40,BIRC3,C1QTNF2,CBX4,FGD4,HSPA6,IER3,IGF1R
HAND2	transcription regulator	-	0.391	2.18E-03	ACTC1,COL1A1,COL3A1,MYL4,SIK1/SIK1B
TBX5	transcription regulator	-	0.391	2.18E-03	ACTC1,COL1A1,COL3A1,MYL4,SIK1/SIK1B

Upstream Regulator	Molecule Type	Predicted Activation State	Activation z-score	p-value of overlap	Target molecules from DGE analysis
GLI1	transcription regulator	-	0.302	1.10E-04	COL1A1,GRIA3,MAPK11,MEF2C,MEST,MRPS6,MYCN,PLPP2,PSTPIP2,SYNE1
ERK	group	-	0.213	1.29E-03	COL1A1,ESR1,ETS1,FST,JUNB,LIF,MAL,MMP14,SLC4A7
EZH2	transcription regulator	-	0.156	1.58E-03	ABL2,ACKR3,BIRC3,CDK6,IGFBP1,JAM2,KCNK1,NCOA7,NGFR,PIK3IP1
ERK1/2	group	-	0.153	7.64E-04	COL3A1,CYP17A1,DDIT3,ESR1,FOSB,IGF1R,JUNB,KCNH2,MYCN,SPRY4
Unknown					
Akt	group	-	0	3.38E-06	ANKRD1,BCL6,BTG2,COL3A1,ETS1,IGF1R,MMP14,PPP1R1B,SLC4A7,SOX4
SPDEF	transcription regulator	-	0	7.04E-04	BIRC3,COL1A1,COL4A5,COL5A1,FZD8,SMAD3,TNC
PAF1	other	-	0	1.40E-03	BIRC3,CITED2,IFITM3,ISG15,NFKBIZ,OASL
SIN3A	transcription regulator	-	0	4.80E-03	BCL6,COL1A1,DDIT3,ESR1
LIF	cytokine	-	-	1.71E-05	ERAP1,HGF,HLA-G
Raf	group	-	-	1.22E-04	IER3,IGF1R,MAFF,PPARGC1A,SEMA3C,SPRY4,ST8SIA1
SP3	transcription regulator	-	-	1.56E-04	CCL20,COL1A1,COL2A1,CYP17A1,ESR1,HGF,IGF1R,MAOB,MYCN,SLC4A7
HIF1AN	enzyme	-	-	3.22E-04	ADM,CA9,EGLN3
PRKDC	kinase	-	-	5.53E-04	AHR,BIRC3,VCAM1
TMPO	other	-	-	5.53E-04	COL11A1,COL1A1,COL3A1
COLGALT1	enzyme	-	-	6.64E-04	COL1A1,COLGALT2
MYOC	other	-	-	1.53E-03	CA2,DAB2,DDIT3,FSCN1,PXDN,RAB27B,STC1
CHI3L1	enzyme	-	-	1.85E-03	ARL4C,BHLHE40,NNMT,TNC
CaMKII	complex	-	-	1.96E-03	BIRC3,COL2A1
PRKACA	kinase	-	-	1.96E-03	HSPA1A/HSPA1B,VCAM1
BMI1	transcription regulator	-	-	2.13E-03	BTG2,CADM1,CDC14A,LOX,MEG3,SMAD3
SFN	other	-	-	3.09E-03	BCL6,BTG2,DSC2,PPP1R1B
HNRNPA2B1	other	-	-	3.46E-03	CADM1,CLDN1,FSCN1,FZD8,MEIS2,MEST,PHACTR2,PPARGC1A,SLC1A1,SPAG4
NKX2-3	transcription regulator	-	-	3.85E-03	MYH11,SHOX2
TNFAIP6	other	-	-	3.85E-03	ITIH5,TNFAIP6
THBS4	other	-	-	3.85E-03	COL2A1,COL3A1
IL12B	cytokine	-	-	6.16E-03	CEBPD,INPP5D,MAP3K8
Integrin	complex	-	-	6.31E-03	AHR,ESR1
TIP60	complex	-	-	6.31E-03	COL2A1,MYCN
WWOX	enzyme	-	-	6.31E-03	COL1A1,ESR1

Upstream Regulator	Molecule Type	Predicted Activation State	Activation z-score	p-value of overlap	Target molecules from DGE analysis
ZBTB7B	transcription regulator	-	-	6.31E-03	COL1A1,COL2A1
SBDS	other	-	-	6.38E-03	CTH,DDIT3,HSPA6,MAFF,MYD88,PLAGL1,TNC
Gsk3	group	-	-	7.05E-03	DDIT3,ESR1,FOSB,IGF1R
Lh	complex	-	-	8.28E-03	ACPP,ARL4C,COL15A1,DAB2,DUSP9,MT3,PPFIA4,SNAP23,TNFRSF11B,TPM2
EPAS1	transcription regulator	-	-	8.66E-03	ADM,CA9,CLDN1,EGLN3,ITIH5,LOX,SPAG4
RNASEL	enzyme	-	-	8.87E-03	FAT4,FREM2,TIAM1
CPXM1	peptidase	-	-	9.30E-03	COL15A1,COL5A1
ITGA5	transmembrane receptor	-	-	9.30E-03	GAS1,JUNB
mir-296	microRNA	-	-	9.30E-03	CA9,COL1A1
INSR	kinase	-	-	9.30E-03	IGF1R,IGFBP1
CD99	other	-	-	9.30E-03	FOSB,NEFH
S1PR3	G-protein coupled	-	-	9.30E-03	ETS1,HGF
BHLHE41	transcription regulator	-	-	9.30E-03	CA9,MEF2C
WNT3A	cytokine	-	-	9.30E-03	AHR,LRP6
Inhibition					
EGLN	group	Inhibited	-3.079	1.70E-04	ADM,CA9,CCL28,EGLN3,FEM1C,MAP3K8,PPFIA4,SPAG4,STC1,VLDLR
RBM5	other	Inhibited	-2.186	5.31E-03	BIRC3,BTG2,GBE1,IFITM3,ISG15
CIP2A	other	-	-1.89	7.81E-04	COL15A1,CRYAB,DSC2,IER3,LUM,PRG4,SNCA
ZBED6	transcription regulator	-	-1.732	7.05E-03	ARL4C,CRIM1,LAMP3,SPTBN1
EIF2AK2	kinase	-	-1.276	7.04E-04	BHLHE40,CEBPD,DDIT3,ISG15,MT1M,NNMT,TUBA1A
PRDM1	transcription regulator	-	-1.257	6.23E-04	ERAP1,ESR1,PDCD1,PRF1
TGFB1	growth factor	-	-0.96	6.88E-04	ANKRD1,BGN,BHLHE40,C9orf3,CADM1,CITED2,COL1A1,COL2A1,COL3A1,COL5A1
Interferon	group	-	-0.796	3.48E-04	BCL6,BTG2,CTH,HLA-G,HSPA1A/HSPA1B,IL18R1,ISG15,LAMP3,LIF,MYD88
BRD4	kinase	-	-0.729	2.96E-03	ABLIM1,BHLHE40,COL1A1,COL5A1,GTF3C6,LOX,MAL,MYD88,NAV1
FSH	complex	-	-0.555	6.87E-04	ACPP,ADAMTS16,AMH,ARL4C,BTG2,COL15A1,DAB2,DUSP9,FILIP1L,MT3
HIC1	transcription regulator	-	-0.418	4.41E-03	ACKR3,CA2,FST,INHBA,LIF,SNAPC1
SMAD4	transcription regulator	-	-0.391	3.61E-03	CCL20,CITED2,CYP17A1,FSCN1,IER3,INPP5D,MST1R,SMAD3
TP73	transcription regulator	-	-0.113	1.04E-03	BHLHE40,CADM1,COL1A1,CRYAB,CTH,DDIT3,FST,HSPA1A/HSPA1B,KCNK1,MDK
SP1	transcription regulator	-	-0.026	2.20E-05	ABHD2,CCL20,CDK6,CEBPD,COL1A1,COL2A1,CTH,CYP17A1,ESR1,HGF

7.3.8 RT-PCR data agrees with RNA-seq gene expression

RT-PCR for five differentially expressed genes was performed on RNA isolated from cumulus cells from an additional 13 patients. Figure 7.12 shows the expression fold change of the genes which all showed a change in expression in the direction expected based on the RNA-seq data. Statistical significance was seen in CRIM1, and PPARGC1, with a trend towards increased expression observed in GAS1. A large variation in expression seen in the young group with respect to PPARGC1 expression as indicated by the error bars. This was observed to a smaller extent in the RNA-seq data (Figure 7.7) and similarly wide variation was also observed in GAS1. These results need to be further validated to confirm the trends observed in RNA-seq.

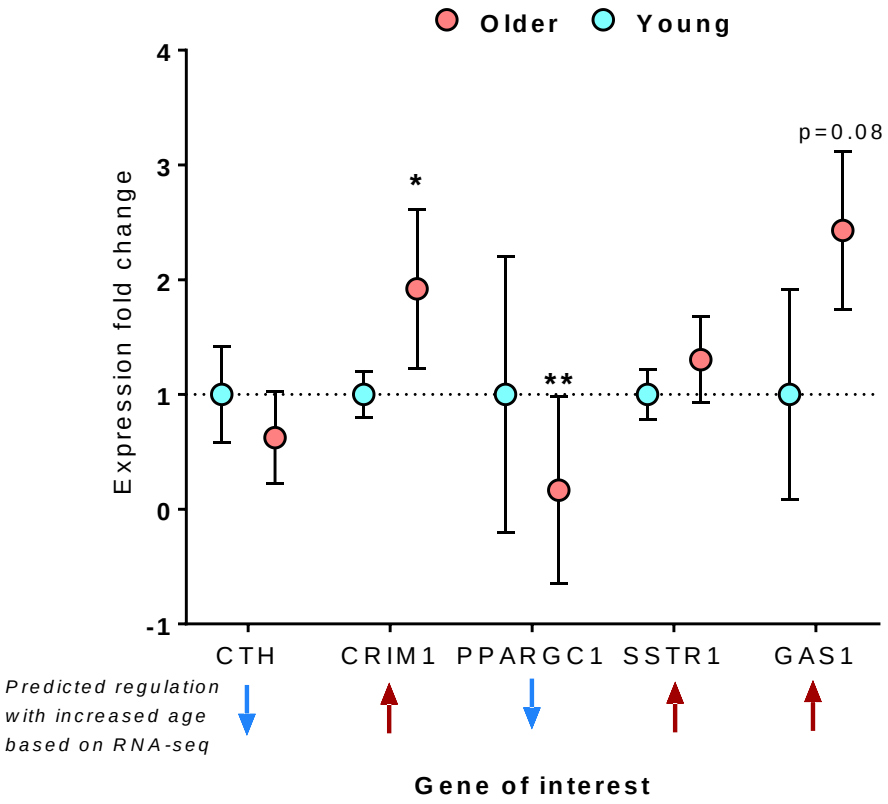


Figure 7.12 RT-PCR validation of RNA-seq results

Five candidate genes, CTH, CRIM1, PPARGC1, SSTR1, and GAS1 which all showed significant differential regulation with increased maternal age were validated using RT-PCR. The arrows underneath the figure indict the expected expression change based on the RNA-seq experiment. The dashed line at y=1 indicates no expression change, below 1 indicates decreased expression and above 1 indicates increased expression. * $p<0.05$, ** $p<0.01$.

7.3.9 Variation in differentially expressed genes between studies highlights heterogeneity of maternal age effects

Table 7.6 contains the differentially expressed genes from the present study that also appear in the previous high-throughput gene expression studies. Of the 168 genes with known functions identified in this study, 35 have been identified in other studies. The overwhelming majority of the genes identified in other studies showed the same direction of regulation with increasing maternal age (85.7%, 30/35). Interestingly, with the exception of FGD4, IER3, and VSP13A, differentially expressed genes were only identified in one other study. The results from the current study showed the highest concordance in the differentially regulated genes with that conducted by Al-Edani and colleagues using a microarray approach. Of note, they identified the highest number of differentially expressed genes of all the high-throughput studies.

Table 7.6 Comparison of differentially expressed genes identified in this study and the literature.

	Study	Current	(201)	(198)	(207)
	Technique	RNA-seq	RNA-seq	Micro-array	Micro-array
	***n* differentially expressed genes**	185	45	1874	67*
Gene		**Regulation with increased age**			
ACPP	*acid phosphatase, prostate*	Up	-	Up	-
ADAMTS14	*ADAM metallopeptidase with thrombospondin type 1 motif 14*	Down	Down	-	-
ATP11A	*ATPase phospholipid transporting 11A*	Up	-	Up	-
CBX4	*chromobox 4*	Down	-	Down	-
COL15A1	*collagen type XV alpha 1 chain*	Up	-	Up	-
CRIM1	*cysteine rich transmembrane BMP regulator 1*	Up	Up	-	-
CTH	*cystathionine gamma-lyase*	Down	-	Down	-
DAB2	*DAB2, clathrin adaptor protein*	Up	-	Down	-
EPHB1	*EPH receptor B1*	Down	-	Down	-
FGD4	*FYVE, RhoGEF and PH domain containing 4*	Up	Up	Up	-
GAS1	*growth arrest specific 1*	Up	-	Up	-
GSTM4	*glutathione S-transferase mu 4*	Down	-	Down	-
HGF	*hepatocyte growth factor*	Up	-	Up	-
HLA-G	*major histocompatibility complex, class I, G*	Up	-	Down	-
HSD17B6	*hydroxysteroid 17-beta dehydrogenase 6*	Up	-	Up	-
HSPA1-A/B	*heat shock protein family A (Hsp70) member 1A*	Up	-	Up	-
IER3	*immediate early response 3*	Up	-	Up	Up
JAM2	*junctional adhesion molecule 2*	Up	-	Up	-
KIF21A	*kinesin family member 21A*	Up	-	Up	-
KLF5	*Kruppel like factor 5*	Up	-	Up	-
LRP6	*LDL receptor related protein 6*	Up	-	Down	-
MAFF	*MAF bZIP transcription factor F*	Up	-	Up	-
MDK	*midkine*	Down	-	Down	-
MLLT3	*MLLT3, super elongation complex subunit*	Up	-	Up	-
NUDT16	*nudix hydrolase 16*	Down	-	Down	-
PPP1R12B	*protein phosphatase 1 regulatory subunit 12B*	Up	-	Down	-
RORA	*RAR related orphan receptor A*	Up	Up	-	-
SEMA3C	*semaphorin 3C*	Up	-	Up	-
SLC16A7	*solute carrier family 16 member 7*	Up	-	Up	-
SSTR1	*somatostatin receptor 1*	Up	-	Up	-
STC1	*stanniocalcin 1*	Up	-	Up	-
THRB	*thyroid hormone receptor beta*	Up	-	Down	-
TNC	*tenascin C*	Down	-	Down	-
VPS13A	*vacuolar protein sorting 13 homolog A*	Up	Up	Up	-
ZBTB7C	*zinc finger and BTB domain containing 7C*	Down	-	Down	-

** only information about upregulated genes reported, identity of 32 down-regulated genes unknown*

7.4 Discussion

To understand the overarching changes in gene expression that may occur with increasing maternal age, this study pooled cumulus cells from multiple MII oocytes from individual patients. Interestingly, distinct age group-based clustering was observed for all samples despite the difference between the mean ages being approximately seven years. Of the differentially expressed genes identified, one-fifth had been identified in one of the three prior high-throughput gene expression studies (Section 1.10.3) however the GO terms and regulators identified in this study are in agreement with those previously reported highlighting the wide ranging effect of maternal age on cumulus cell gene expression.

7.4.1 Angiogenesis and hypoxia

Age-associated hypoxia has been suggested by two groups as a mechanism of maternal oocyte aging (198, 201). Molinari and colleagues suggested this theory as an explanation for the over-representation of genes targeted by HIF-1A and upregulated of genes related to angiogenesis observed in the older maternal age group in their study (201). Key genes identified by Molinari and colleagues with respect to hypoxia were RORA and NOS2 (201). RORA was also upregulated in the older group in this study and HIF-1A was identified as a putatively activated upstream regulator, however NOS2 was not found to be differentially expressed. The EGLN (also called PHD) prolyl hydroxylase enzymes as a group are an upstream regulator that are likely inhibited with maternal age as found by the IPA analysis in this study. Cellular EGLNs function as oxygen sensors within physiological oxygen ranges and under normoxic conditions catalyse HIF prolyl hydroxylation causing their subsequent destruction (336, 337). Under hypoxic conditions EGLN function is attenuated allowing HIFs to escape degradation (336, 338), therefore putative inhibition of EGLNs with increasing maternal age is consistent with a hypoxic environment.

Both the Molinari group and the Al-Edani group found evidence that genes associated with angiogenesis were modulated with increasing maternal age (198, 201). In the microarray study by Al-Edani an upregulation of genes associated with angiogenesis (ANGPTL4, LEPR, TGFBR3, VEGFC, FGF2 and NR2F2) was found in the cumulus cells from the older maternal age group which the authors suggest this is caused by insufficient oxygen (198). Increased angiogenesis with age as a putative compensatory mechanism is also supported in the present findings with significant enrichment of biological processes clustered under heart development by GO annotation including vasculature development, blood vessel morphogenesis, and regulation of cellular component organization. Interestingly, the genes identified by Al-Edani as being associated with angiogenesis were not found to be differentially expressed in this study. Furthermore, in this study PPARGC1 was significantly downregulated with age which was further confirmed with RT-PCR. Activation of PGC-1α (PPARGC1) initiates a cellular antioxidant program that prevents reactive oxygen species accumulation, which in turn destabilizes HIF-1A. By contrast, HIF-1A impedes mitochondrial activity, either by suppressing the transcription of PGC-1α, or by promoting glycolysis, reducing mitochondrial glucose and levels of NAD+ (339). Taken together these findings suggests that in addition to increased maternal age being associated with a potentially hypoxic follicular environment, the ability of follicles to respond to hypoxia is compromised.

Increased oocyte aneuploidy is a hallmark of maternal age in human (Section 1.10.2.1). Individual oocytes with multiple segmental abnormalities are detected more often than is expected by random chance, suggesting that some gametes are predisposed to chromosome breakage, either due to intrinsic cellular defects or deficiencies of the follicular microenvironment in which they matured (340). Follicular vascularity determines the intrafollicular oxygen content and the developmental potential of the oocyte (341) and furthermore intrafollicular hypoxia has been found to have disorganised

spindles resulting in chromosomal segregation disorders and deleterious mosaicisms in the embryo (342). Hypoxia might be one of the effects of reproductive aging, which in turn may affect chromosome segregation. Further work could look to correlate oxygen tension in follicular fluid with follicular cell transcriptomes and oocyte ploidy to better understand this relationship.

7.4.2 Involvement of PI3K/AKT pathway in maternal age

Accumulating evidence points to the PI3K signalling pathway as a critical regulator of COC function modulating amongst other thing, proliferation, differentiation and stress response in granulosa cells, and meiotic maturation of oocytes (reviewed in 343). The Akt group of enzymes was identified by IPA as a likely upstream regulator although there was not sufficient evidence to determine a likely direction of activation. The serine/threonine-protein kinase family encompassing AKT1, AKT2 and AKT3 regulates many cellular processes including metabolism, proliferation, cell survival, growth and angiogenesis. AKT1 is expressed in oocytes and granulosa cells throughout human follicle development (344). Akt1 KO mice have increased apoptosis in several tissues including the ovary where there is an increase in the number of degenerating oocytes, reduced granulosa cell proliferation and a reduced number of mature follicles (345, 346). A recent study revealed that expression genes in the PI3K/AKT pathway in cumulus cells are related to oocyte competence, which interestingly identified decreased AKT1 expression with positive pregnancy outcome (347). Furthermore, there was a trend towards decreased FOXO1 expression with positive pregnancy outcome, which is predicted by IPA in this study as being an upstream regulator activated with maternal age.

7.4.3 Extracellular matrix organisation is altered with increasing maternal age

Extracellular matrix (ECM) organisation and structure were enriched in the differentially expressed genes with maternal age. The ECM within the follicle plays a critical role in numerous ovarian cell functions, including proliferation, differentiation, survival, adhesion, and migration, via mechanical and chemical signals (348-350). Among down regulated genes in the older cohort was ADAMTS14, which is a metallopeptidase with aminoprocollagen activity involved in ECM turnover (351). Junctional adhesion molecule B is encoded by JAM2 which had increased expression in the older maternal age cohort and is associated with decreased oocyte developmental competence in mice and cows (352). Improved survival of primary follicles *in vitro* with ascorbic acid treatment is caused by enhanced ECM, the upregulation of COL3A1 which was shown in this study to be downregulated with increased maternal age. Of note, type III collagen (such as COL3A1) has been identified in the theca cells rather than the granulosa cell compartment of human follicles (353), combined with the unexpected expression of CYP17A this suggests there may have been theca cells present in the analysed cell populations.

7.4.4 Likelihood of follicular cell contamination

Unexpectedly, higher expression of CYP17A was observed in the older cohort. Known to be expressed in theca cells, CYP17A1 has also been found to be upregulated in human floating granulosa cells compared with cumulus cells (52). An assessment of the raw count matrix revealed the presence of CYP17A1 transcripts at low levels in all patients, which is consistent with possible theca or granulosa cell contamination. Upregulation of FGG and COL15A1 observed in the older cohort were found to be detected only in mural granulosa rather than cumulus cells in one study which lends further support to the prospect of granulosa cell contamination (51). Altering the method of cell collection would help to prevent contamination from other follicular cell sources and is discussed below in Section 7.4.5.

The answer to why gene expression and raw read counts were notably higher in all older patient samples is less clear. The process of follicle aspiration and COC stripping does not differ based on patient age meaning there should be no procedural reason for the increase in expression. It may be that in older women follicular cells are more prone to undergo premature luteinisation. Progesterone receptors are absent in preovulatory follicles and appear in periovulatory follicles after exposure to a gonadotropin surge (354). The progesterone receptor (PGR) is a likely upstream regulator that is upregulated with maternal age (Table 7.5). A study comparing granulosa cell function in older IVF patients (>43 years) to younger patients found a significant decline in granulosa cell function that exhibited characteristics of premature luteinisation (355). Furthermore, the authors found evidence that earlier egg retrieval improved embryo numbers as well as quality and clinical pregnancy rates in the advanced maternal age cohort (355). Egg collection and hCG trigger are specifically timed, however practically in the clinic there can be appointment delays or patient error that alters this timeframe. Without having this information from the patients, it is not possible to conclude whether this may have impacted possible luteinisation.

7.4.5 Variation in findings between studies

The possibility of theca cell containment in the cumulus cell fraction has been discussed and highlights a possible explanation of some variation in gene expression between this and other studies. To allow the possibility of including cumulus cell samples from IVF laboratories in this study, cumulus cell samples were collected without specialist laboratory equipment or reagents, namely a brightfield microscope and pipettes. Stripping dishes were excluded where blood could be seen by eye or under the microscope however as the cell samples were not centrifuged and washed there is a possibility of unidentified blood contamination. Molinari and colleagues biopsied the cumulus mass of individual oocytes rather than collecting enzymatically stripped cumulus cells, this has been shown to decreases the likelihood of contamination from other cell sources (51). It has been shown

in rat COCs that there are differences in gene and protein expression between cells in proximity to the oocyte compared with peripherally located cells in the cumulus oophorus both pre- and post-ovulation (356). This method was not available in this study due to the ethics in place and the guidelines set in place by the associated IVF unit. As the transcriptome of cumulus cells from multiple MII oocytes was examined in this study, biopsy of each individual COC was not possible because of the significant increase in time and resources for the embryologists. Variation also exists in the time from egg collection to stripping in different IVF units, affecting the time the oocyte is isolated from the cumulus cells and potentially impacting gene expression.

7.4.6 Challenges with patient material

A primary limitation of this and other studies is the small number of patients included in the studies. Patient recruitment remains a challenge for studies even when remnant material such as cumulus cells are the focus. In this study patients were recruited over a period of two and a half years for the RNA-seq experiment. Of the 46 patients who consented to the study, only 18 patients aged 23 to 40 years met the inclusion and exclusion criteria.

Cumulus cells from IVF patients are subject to many effects unrelated to maternal age such as reason for treatment, hyperstimulation protocol, and maturation of collected oocytes. Variation in the use of different hyperstimulation protocols, agonist or antagonist, along with dose variations within these add a layer of complexity to the analysis as a potential confounder. A comparison of cumulus cell protein expression from oocytes obtained from the same patient after two IVF cycles with two different hyperstimulation protocols (rFSH or human menopausal gonadotrophin (hMG)) found the type of hormonal treatment influenced protein expression (357). This was supported with a following study that used microarray analyses to demonstrate that the type of controlled ovarian stimulation (rFSH,

urinary FSH, or hMG) induces specific gene expression profiles related to developmental process and anatomical structure development (358), and various metabolic pathways (359) in human cumulus cells depending on the type of gonadotropin used.

For robust evidence to be gathered about age-related changes large well-controlled cohort studies are required, with strict exclusion criteria to avoid reproductive disorders, which in an ideal world would be correlated with cycle outcome.

7.4.7 Complementary techniques and avenues for future work

The data presented here gives a snapshot of how gene expression changes across the MII cohort with increasing maternal age and future work will look at exploring that more deeply. The global gene expression pattern is a result of the collective behaviour of individual regulatory pathways, and as a result the most appropriate analytical approaches are those that focus on the network rather than individual genes (360). The IPA analysis takes into account the log fold change of the genes between the groups unlike the GO over-representation which looked exclusively at the gene list rather than direction of change. Instead of clustering by GO terms, weighted gene co-expression network analysis (WGCNA) is a method that is used to describe the correlation patterns among genes across high-throughput expression analyses (361). Rather than focusing on the annotation of the gene, WGCNA is a means of finding clusters or modules of highly correlated genes, which can then be probed further using ontological or pathway-based approaches (361).

Integrating RNA-seq data from cumulus cells with other sources of biological data such as DNA methylation, histone modification, transcription factor binding or genotyping data will allow a more complete picture of the age-related regulation of gene expression to emerge (362, 363). A few reports of these 'integrative' analyses have emerged recently in reproductive biology (364). A combined transcriptome and global DNA methylation

analysis of human primordial germ cells (PGCs) found that RNA expression over week 4 to 11 of embryo development were stable despite a striking decrease in global DNA methylation at week 10 and 11 for female and male PGCs respectively (364). Combined single-cell RNA-seq and single-cell DNA methylome sequencing of the inner cell mass (ICM) and trophectoderm (TE) cells obtained from human blastocysts was performed to explore the effects of parental-specific methylation on allele-specific gene expression (ASE) (363). The authors found very few genes with parental-specific methylation events at their promoter regions showed ASE suggesting the majority of DNA methylation differences between the parental genomes do not contribute to ASE at the blastocyst stage (363).

7.4.8 Conclusion

The results from this Chapter demonstrate that broad changes in gene expression can be detected in pooled MII oocytes from reproductively young women <35 years and reproductively older women ≥37 years. Identification of GO enrichment and upstream regulators are consistent with the growing theory that advanced maternal age may be associated with a hypoxic follicle environment. The modest overlap in specifically differentially regulated genes highlights both the variation within and between patients and highlights the need for large cohort studies to more robustly elucidate the specific mechanisms underpinning the age-related decline in fertility. Purity of the follicular cell population was also found to be a potentially important factor in the variation between studies and future work should consider more stringent methods of isolation. Integration of RNA-seq data with other sources of biological data such as epigenetic and protein data will be critical in uncovering a more complete picture of the age-related change in human follicular function.

Chapter 8

Discussion

There is a growing reliance on medical technologies to provide solutions to the age-related decline in female fertility, as a direct result of the continuing trend for later child birth in developed nations, and an increasing number of people wishing to start or complete their families later in their reproductive life. This thesis established methods of *in vitro* follicle development and identified pathways associated with female reproductive aging with the overall aim of developing a treatment for age-related infertility in women. *In vitro* culture opens a new avenue for circumventing the age-related decline in female fertility in addition to providing a critical model for understanding the molecular and functional changes that occur in follicles as maternal age increases. Through the work presented here novel findings have been made regarding i) patient variation in the health and development of follicles in cryopreserved cortical tissue before and following 6 days of *in vitro* culture; ii) the effect of LSD1 on human follicle development *in vitro*, iii) the impact of culture conditions on follicle development *in vitro*, and iv) genetic pathways differentially regulated with maternal age in human cumulus cells.

8.1 Novel findings from this thesis

8.1.1 Novel findings on *in vitro* follicle development in cryopreserved cortical tissue

In Chapter 3 I established a method of cortical strip culture to facilitate the development of follicles from the primordial stage *in vitro* for the first time in my department at the University of Oxford. Variation between patients in the health and development of follicles from cryopreserved tissue before and after *in vitro* culture had not previously been described. A recent publication in November 2018 supports these findings related to non-cultured tissue reporting a wide range in follicle survival (50-98%) across 25 patients undergoing fertility preservation (365). Furthermore, this study also demonstrates the efficacy of 3-4-hour NR incubation as a means of assessing follicle survival following cryopreservation. This thesis found that follicle health before and after culture was significantly improved with the inclusion of neutral red (NR) as a tool to identify follicles in cortical tissue. Importantly, NR could be incorporated into the existing culture protocol, permitting visualisation of follicles with an incubation of one hour.

In Chapter 6 I report the first comparison of the two most widely utilised culture medium in cortical strip culture, McCoy's 5A and αMEM, on follicle health and development in cryopreserved tissue in addition to analysing the impact of medium volume. Based on the results reported here, pieces of cryopreserved human cortical tissue should be cultured individually in a low volume of αMEM medium to give the greatest likelihood of developing heathy follicles. This is highly significant as McCoy's 5A medium is used in what is currently the most successful method of human cortical strip culture, i.e. the method that has been published as supporting follicle development from the primordial stage to the production of an MII oocyte (210).

To extend existing assisted reproductive techniques for maternal age, an increasingly plausible strategy may be to access dormant primordial follicles within cortical tissue as a possible source of extra gametes with or without cryopreservation. Those patients who donated ovarian tissue for this work had all undergone fertility preservation prior to gonadotoxic treatment. For these patients' *in vitro* follicle growth is increasingly being explored as an alternative method to circumvent some of the limitations of tissue reimplantation. In frozen-thawed transplanted ovarian tissue, follicular density is significantly lowered compared to non-transplanted tissue, with as many as 50% of the follicles in frozen-thawed transplanted tissue thought to be lost due to grafting (366). By contrast, no change in follicle density has been reported in short or long-term cortical strip culture of frozen-thawed tissue (233), suggesting that optimised *in vitro* growth systems may better retain the follicle pool, and thus fertility potential, in cryopreserved tissue. In patients for whom transplantation carries a higher risk of reintroducing malignancies, such as for ovarian or blood borne malignancies, *in vitro* culture followed by IVF circumvents transplantation entirely (250). For both patient cohorts, using a culture medium optimised for the state of the tissue, fresh or cryopreserved, is imperative.

8.1.2 Novel findings on differentially regulated gene expression pathways with age

Historically the focus on the impact of female reproductive aging has been at the end point of follicle development using IVF-derived oocytes, follicular cells or material to understand the impact of age on reproduction. In this thesis, I used RNA-seq of pooled human cumulus cells (Chapter 7) from reproductively young and older women to explore whether gene expression pathways are differentially regulated with age across a cohort of MII oocytes. What was particularly interesting was the clear difference in gene expression across a relatively short period of time. With mean ages of the two groups only seven years apart, and the mean age of the older group around 38 years old, it highlights that marked

differences in cumulus cells gene expression, and likely function, are apparent before a sharp decline in pregnancy rate is observed. Common pathways identified by other groups including angiogenesis and hypoxia response were identified as being altered with maternal age.

The relative ease of access to IVF derived material is countered by the challenge of using patients who are commonly undergoing treatment for fertility problems as a baseline for normal reproductive biology. Perhaps more importantly for the goals of this thesis, it is unlikely that an intervention at such an advanced stage of follicle development, such as during an IVF cycle, would successfully mitigate the genetic changes observed with aging. For the growing body of literature on the differences in gene or protein expression in preovulatory follicles, there is a dearth of literature about when these fertility-altering changes start to take place. Herein lies the importance of developing efficient and physiological methods of growing human follicles *in vitro* across the full span of follicle development. The patients recruited for the cortical tissue culture experiment in Chapter 3 were reproductively young, with the oldest patient only 25 years old. The variation in response to cryopreservation and culture raises interesting questions about how the variation in follicle development and oocyte competence changes with increasing maternal age. If a hypoxic follicular environment does play a role in reproductive aging as identified in Chapter 7, a similar transcriptomic analysis of follicular cells at the earlier stages of follicle development would start to answer the question of when these changes start to manifest.

8.2 Future treatments for age-related infertility

8.2.1 Cortical strip culture: economically efficient or physiologically relevant?

The duration of culture for the technique established in this study is short and follicle development comparatively rapid. It is postulated that the time taken *in vivo* for follicles to progress from the primordial to the secondary stage is around 270 days (see Section 1.5, compared to the 6 days reported here. Follicle activation in *in vitro* systems like that used in this thesis have been described as 'uncontrolled and precocious' with the rapid development thought to be the cause of the limited developmental competence *in vitro* (367). Long-term culture across weeks or months is proposed to be a more physiological environment for follicle development by occurring over a protracted time frame (216). Follicles in human cortical strips cultured for 15 days were shown to increase in follicle diameter only up to day 10 of culture (217), similarly in cortical strips cultured for up to 21 days, follicle viability declined after 11 (233) and 7 days of culture (368). Much longer term culture of cortical fragments is widely discussed in the field, most recently at the 2nd Annual UK Fertility Preservation Meeting where the importance of evaluating these two approaches was highlighted (322), but available literature is scare. Doctoral work from Professor Helen Picton's group provides evidence for the culture of ovine cortical tissue for up to 30 days with greater retention of primordial follicles and low levels of apoptosis across culture (369). A similar debate about the optimal timeframe for preantal to antral follicle development exists (210, 211, 221, 235).

From an economic perspective, short-term culture is a more attractive treatment option for clinical translation. The increased time and resources required to sustain follicles *in vitro* increases immensely when the duration of culture increases from weeks to months. Cost is a significant barrier to existing ART treatments and adding an expensive *in vitro* growth method to this is unlikely to be a feasible or attractive treatment option for patients. Furthermore, culture across several weeks, although significantly slower than the 6-9 days

employed by many groups, is still comparatively rapid when the 9-month *in vivo* development is considered. Prolonged culture also amplifies many of the concerns associated with *in vitro* technologies.

Epigenetic alterations have been a subject of concern for existing ART, with evidence that there is an increase in imprinting disorders in children conceived though IVF and ICSI (370, 371). The timing and pattern of genomic imprinting in the oocyte is crucial for normal fertilisation and embryo development, and prolonged exposure to *in vitro* conditions, is thought to increase the risk for epigenetic changes in the oocyte. In established IVF protocols, *in vivo* grown MII eggs are fertilized and sustained *in vitro* for 5-6 days of embryo development. *In vitro* maturation (IVM) extends this further by including the maturation of oocytes from small antral follicles to generate MII oocytes which are subsequently fertilized *in vitro*. Current evidence suggests that IVM induced epigenetic changes in offspring, if any, are infrequent and small in magnitude (372), although some differences in imprinting have been observed in oocytes after IVM (373).

In vitro growth requires not only oocyte maturation to occur *in vitro*, but the entire process of follicle development. After culturing oocytes within the cortex for at least a week, followed by isolated follicle culture, cumulus-oocyte complex culture, and IVM, the minimum duration of *in vitro* culture is increased by 2 to 3 weeks (210). Understanding the change to the epigenome of *in vitro* grown oocytes is clinically important for guiding efforts to develop complete *in vitro* growth methods for fertility treatment. No studies have investigated the impact of *in vitro* growth on the epigenome of oocytes or follicular cells and this is a critical area for research to move the field towards clinically viable methods. The high degree of discordance between the imprinting status of genes in humans and other species means it is imperative that these changes are investigated in humans as well as any animal models (374).

8.2.2 Adjuvant treatments during culture

Understanding the changing epigenetic landscape across follicle development is important not only to maintain normal follicle development, but to identify targets to improve follicle and oocyte quality. In Chapter 4 I demonstrated that histone methylation plays a role in human follicle development by manipulating LSD1 action using a small molecule inhibitor. This is the first report of epigenetic modification of human ovarian tissue. In principle, identifying aberrant epigenetic modifications that occur in oocytes or follicular cells with age could be rectified with the addition of epigenetic modifiers, such as that described in Chapter 4, during *in vitro* growth.

Designing and delivering adjuvant treatments in an *in vitro* setting has the advantage of avoiding unwanted off target effects and administration challenges that come with traditional drug treatments. Several compounds have been used to modulate follicle development *in vitro* with the aim of improving follicle outcomes across culture. PTEN inhibitors, resveratrol, and Activin A among others have been explored in human tissue culture with respect to follicle activation and survival. (142, 211, 292, 375). Reproductive aging is associated with mitochondrial changes (Section 1.10.2.2). A significant decline in Coenzyme Q expression was observed in the oocytes of older patients as well as aged mice. CoQ10 supplementation in an aged mouse model delayed depletion of ovarian reserve, restored oocyte mitochondrial gene expression, and improved mitochondrial activity (376). It's efficacy in improving aneuploidy in IVF patients did not reach significance but it is possible that treatment at an earlier stage of follicle development, or an alternate route of administration is required in humans (377, 378).

8.2.3 Development of 'new' oocytes

This thesis has focused on strategies to improve existing gametes and to identify intervention points to prevent deleterious changes in the future, however an emerging

approach is to generate 'new' or *in vitro* derived gametes from stem cells. The existence of oogonial or germ line stem cells has been controversial and our understanding of their properties and contribution to normal reproduction is not well understood (19-21). Putative human oogonial stem cells have been isolated and demonstrated to form follicle-like structures *in vitro* (18). These findings challenge the dogma that women are born with a finite number of eggs. Should they be capable of producing high-quality new oocytes irrespective of patient age, the therapeutic applications would be substantial. In mice, oocyte development has been accomplished starting from both induced pluripotent stem cells and primordial germ cells, which have been subsequently fertilised and yielded viable and fertile offspring (379, 380). These results certainly encourage the possibility that this could be accomplished in humans and it would greatly widen the female reproductive span by allowing women to reproduce even after the exhaustion of the primordial follicle pool. Historically, translating follicle development techniques developed in mice to large mammals has been exceptionally challenging due to the increased size and complexity of follicle development (see Section 1.11) meaning that such methods are unlikely to enter clinical practice in the foreseeable future.

8.3 Barriers to progress

8.3.1 Transparency of findings

A significant and enduring barrier to progress is a lack of standardised reporting of follicle health and staging in the field. The criteria established by Gougeon (29) is commonly cited as a basis for follicle classification however nuances in the interpretation and application of the criteria create difficultly when comparing results from different studies. Gougeon describes two single layered follicle types; primordial and primary, the difference being the morphology of the granulosa cells. Follicles pass through a stage where the granulosa cell population are neither entirely flattened nor entirely cuboidal which in this study were

termed ‘transitional’. In papers where follicles are classed as either primordial or primary, it is often unclear into which category transitional follicles have been placed (224, 233). As the flattened to cuboidal transitional is considered a hallmark of follicle activation, distinguishing between these two populations is critical in studies where follicle activation or the retention of dormant follicles is a key parameter.

A similar issue exists with the classification of primary and secondary follicles, those with one or two complete layers of cuboidal granulosa cells, respectively. Development to the secondary stage is a key milestone in preantral follicle development and marks the stage at which follicles are isolated for further follicle culture. As identified in this thesis, follicles in culture can present with a single complete layer and multiple partial granulosa cell layers. Clarity on how follicles of this type are classified is essential for findings from various studies to be compared.

8.3.2 Heterogeneity of follicle distribution

The heterogeneity of follicle distribution in the human cortex is well described in the literature and in this thesis (Section 1.3). For this work it presented challenges in downstream analyses such as immunohistochemistry because of the quantity of tissue required to process to identify a sufficient number of follicles to draw meaningful conclusions. NR was identified as a highly valuable tool in reducing the number of cortical fragments without viable follicles that were placed in culture and for identifying viable follicles appropriate for isolation after culture. Implementation of NR, or a similar non-toxic vital dye, should be incorporated into standard culture protocols to improve efficacy of culture and analysis. Heterogeneity introduces a separate challenge with respect to cortical strip culture, as the number of follicles in a given fragment of tissue can vary so dramatically. This makes it difficult to unpick what effect, if any, follicle density has on the success of *in vitro* culture and remains an interesting avenue of exploration for future work.

8.3.3 How much optimisation is feasible?

The question remains of how much optimisation can be expected with respect to the number of developmentally competent MII oocytes that can be generated from primordial follicles. A woman will generate around 300–400 mature eggs capable of fertilization during her entire reproductive life (381). In all species there is at least a 75% loss of primordial follicles by the time the individual reaches puberty, and even after puberty only a small number of follicles will ever progress to ovulation while the rest will degenerate (382). This loss represents a huge wastage of gametes which could potentially be used for *in vitro* growth, however whether these follicles are capable of development, *in vitro* or otherwise, is unknown. Work from Telfer and colleagues demonstrated that ovaries from pre-pubertal patients have abnormal follicles that are not seen in ovaries from pubertal patients (280). This provides some evidence that not all follicles in the primordial follicle pool would be capable of development and/or producing a viable pregnancy. A similar challenge is seen in IVF, where although the live birth rate per cycle has increased steadily from around 20% in 1991 to around 30% in 2016 (3), much of this is a result of optimised stimulation and laboratory techniques and it is not clear how much more room remains for improving success rates.

8.4 Final remarks

The work presented in this thesis has shed some light on methods to improve the efficacy and efficiency of human cortical strip culture as well as contributing to our understanding of the pathways underlying the age-related decline in female fertility. Many questions remain unanswered importantly with respect to when age-related changes first manifest in the ovary and this warrants future exploration. The scope for this work is immense and there will be incredibly exciting developments in this area in years to come.

References

1. Statistical bulletin: Births in England and Wales, 2013 [press release]. Online: Office for National Statistics2014.
2. Centers for Disease Control and Prevention, American Society for Reproductive Medicine, Society for Assisted Reproductive Technology. 2014 Assisted Reproductive Technology National Summary Report. https://www.cdc.gov/art/reports/2014/national-summary.html: U.S. Department of Health & Human Services National Center for Chronic Disease Prevention and Health Promotion DoRH; 2016 October 13, 2016.
3. Human Fertilisation and Embryology Authority. Fertility treatment 2014-2016 Trends and figures. www.hfea.gov.uk; 2018 April, 2018.
4. Mathews T, Hamilton BE. Mean age of mother, 1970–2000. National vital statistics reports. 2002;51(1):1-14.
5. Mathews TJ, BE H. Mean age of mothers is on the rise: United States, 2000–2014. In: Statistics NCfH, editor. Hyattsville, Maryland: Department of Health and Human Services; 2016.
6. Hamilton BE, Martin JA, Ventura SJ. National vital statistics reports. National Vital Statistics Reports. 2009;57(12).
7. European commission: Eurostat. Fertility Statistics https://ec.europa.eu/eurostat/statistics-explained/index.php?title=Fertility_statistics: European Commission; 2018 [
8. Royal College of Obstetricians and Gynaecologists. RCOG statement on later maternal age https://www.rcog.org.uk/en/legal/terms-conditions/: Royal College of Obstetricians and Gynaecologists,
; 2009 [updated 15 June 2009.
9. Daniluk JC, Koert E, Cheung A. Childless women's knowledge of fertility and assisted human reproduction: identifying the gaps. Fertility and sterility. 2012;97(2):420-6.
10. Lew R, Hammarberg K, Johnson L. Fertility facts, figures and future plans: an online survey of university students AU - Prior, Eugenie. Human Fertility. 2018:1-8.
11. Blaustein A. Anatomy and Histology of the Human Ovary. In: Blaustein A, editor. Pathology of the Female Genital Tract. New York, NY: Springer New York; 1982. p. 416-41.
12. Laronda MM, Duncan FE, Hornick JE, Xu M, Pahnke JE, Whelan KA, et al. Alginate encapsulation supports the growth and differentiation of human primordial follicles within ovarian cortical tissue. Journal of assisted reproduction and genetics. 2014;31(8):1013-28.
13. Schmidt K, Byskov A, Nyboe Andersen A, Muller J, Yding Andersen C. Density and distribution of primordial follicles in single pieces of cortex from 21 patients and in individual pieces of cortex from three entire human ovaries. Human Reproduction. 2003;18(6):1158-64.
14. Faddy M. Follicle dynamics during ovarian ageing. Molecular and cellular endocrinology. 2000;163(1-2):43-8.

15. van Wezel IL, Rodgers RJ. Morphological characterization of bovine primordial follicles and their environment in vivo. Biology of reproduction. 1996;55(5):1003-11.
16. Faddy M, Gosden R, Gougeon A, Richardson SJ, Nelson J. Accelerated disappearance of ovarian follicles in mid-life: implications for forecasting menopause. Human reproduction. 1992;7(10):1342-6.
17. Feng Y, Cui P, Lu X, Hsueh B, Möller Billig F, Zarnescu Yanez L, et al. CLARITY reveals dynamics of ovarian follicular architecture and vasculature in three-dimensions. Scientific Reports. 2017;7:44810.
18. White YAR, Woods DC, Takai Y, Ishihara O, Seki H, Tilly JL. Oocyte formation by mitotically active germ cells purified from ovaries of reproductive-age women. Nature medicine. 2012;18(3):413.
19. Zhang H, Panula S, Petropoulos S, Edsgärd D, Busayavalasa K, Liu L, et al. Adult human and mouse ovaries lack DDX4-expressing functional oogonial stem cells. Nature medicine. 2015;21(10):1116.
20. Clarkson YL, McLaughlin M, Waterfall M, Dunlop CE, Skehel PA, Anderson RA, et al. Initial characterisation of adult human ovarian cell populations isolated by DDX4 expression and aldehyde dehydrogenase activity. Scientific Reports. 2018;8(1):6953.
21. Silvestris E, Cafforio P, D'Oronzo S, Felici C, Silvestris F, Loverro G. In vitro differentiation of human oocyte-like cells from oogonial stem cells: single-cell isolation and molecular characterization. Human Reproduction. 2018;33(3):464-73.
22. Witchi E. Migration of the germ cells of human embryos from the yolk sac to the primitive gonadal folds. Contrib Embryol Carnegie Inst. 1948;32:67-80.
23. Fujimoto T, Miyayama Y, Fuyuta M. The origin, migration and fine morphology of human primordial germ cells. The Anatomical Record. 1977;188(3):315-29.
24. Baker T. A quantitative and cytological study of germ cells in human ovaries. Proc R Soc Lond B. 1963;158(972):417-33.
25. Van Wagenen G, Simpson ME. Embryology of the ovary and testis: Homo sapiens and Macaca mulatta: Yale University Press New Haven; 1965.
26. De Pol A, Vaccina F, Forabosco A, Cavazzuti E, Marzona L. Apoptosis of germ cells during human prenatal oogenesis. Human reproduction (Oxford, England). 1997;12(10):2235-41.
27. Block E. A quantitative morphological investigation of the follicular system in newborn female infants. Cells Tissues Organs. 1953;17(3):201-6.
28. Pedersen T, Peters H. Proposal for a classification of oocytes and follicles in the mouse ovary. Journal of reproduction and fertility. 1968;17(3):555-7.
29. Gougeon A. Dynamics of follicular growth in the human: a model from preliminary results. Hum Reprod. 1986;1(2):81-7.
30. Griffin J, Emery BR, Huang I, Peterson CM, Carrell DT. Comparative analysis of follicle morphology and oocyte diameter in four mammalian species (mouse, hamster, pig, and human). J Exp Clin Assist Reprod. 2006;3:2.
31. Himelstein-Braw R, Byskov AG, Peters H, Faber M. Follicular atresia in the infant human ovary. J Reprod Fertil. 1976;46(1):55-9.
32. Gougeon A. Regulation of ovarian follicular development in primates: facts and hypotheses. Endocrine reviews. 1996;17(2):121-55.
33. Ohno S, Smith J. Role of fetal follicular cells in meiosis of mammalian ooecytes. Cytogenetic and Genome Research. 1964;3(5):324-33.
34. Gougeon A, Chainy GBN. Morphometric studies of small follicles in ovaries of women at different ages. Journal of reproduction and fertility. 1987;81(2):433-42.
35. Ernst EH, Grøndahl ML, Grund S, Hardy K, Heuck A, Sunde L, et al. Dormancy and activation of human oocytes from primordial and primary follicles: molecular clues to oocyte regulation. Human Reproduction. 2017;32(8):1684-700.
36. Baca M, Zamboni L. The fine structure of human follicular oocytes. Journal of Ultrastructure Research. 1967;19(3):354-81.
37. Anderson E, Albertini DF. Gap junctions between the oocyte and companion follicle cells in the mammalian ovary. The Journal of Cell Biology. 1976;71(2):680-6.
38. El-Hayek S, Yang Q, Abbassi L, FitzHarris G, Clarke HJ. Mammalian Oocytes Locally Remodel Follicular Architecture to Provide the Foundation for Germline-Soma Communication. Current Biology. 2018;28(7):1124-31.e3.
39. Skinner MK. Regulation of primordial follicle assembly and development. Human Reproduction Update. 2005;11(5):461-71.

40. Magoffin DA, Weitsman SR. Insulin-like growth factor-I regulation of luteinizing hormone (LH) receptor messenger ribonucleic acid expression and LH-stimulated signal transduction in rat ovarian theca-interstitial cells. Biology of reproduction. 1994;51(4):766-75.
41. Strauss III JF, Wood JR, Christenson LK, McAllister JM. Strategies to elucidate the mechanism of excessive theca cell androgen production in PCOS. Molecular and cellular endocrinology. 2002;186(2):183-8.
42. Erickson GF, Li D, Shimasaki S, Ling N, Weitsman SR, Magoffin DA. Insulin-like growth factor-1 (IGF-1) stimulates the IGF binding protein system in rat theca interstitial cells. Endocrine. 1995;3(7):525-31.
43. Orisaka M, Tajima K, Mizutani T, Miyamoto K, Tsang BK, Fukuda S, et al. Granulosa cells promote differentiation of cortical stromal cells into theca cells in the bovine ovary. Biology of reproduction. 2006;75(5):734-40.
44. Honda A, Hirose M, Hara K, Matoba S, Inoue K, Miki H, et al. Isolation, characterization, and in vitro and in vivo differentiation of putative thecal stem cells. Proceedings of the National Academy of Sciences. 2007;104(30):12389-94.
45. McNatty KP, Smith DM, Makris A, Osathanondh R, Ryan KJ. The microenvironment of the human antral follicle: interrelationships among the steroid levels in antral fluid, the population of granulosa cells, and the status of the oocyte in vivo and in vitro. The Journal of Clinical Endocrinology & Metabolism. 1979;49(6):851-60.
46. Combelles CM. The antral follicle: a microenvironment for oocyte differentiation. International Journal of Developmental Biology. 2013;56(10-11-12):819-31.
47. Craig J, Orisaka M, Wang H, Orisaka S, Thompson W, Zhu C, et al. Gonadotropin and intra-ovarian signals regulating follicle development and atresia: the delicate balance between life and death. Frontiers in bioscience: a journal and virtual library. 2007;12:3628-39.
48. Oktay K, Briggs D, Gosden RG. Ontogeny of follicle-stimulating hormone receptor gene expression in isolated human ovarian follicles. The Journal of Clinical Endocrinology & Metabolism. 1997;82(11):3748-51.
49. Su Y-Q, Wigglesworth K, Pendola FL, O'brien MJ, Eppig JJ. Mitogen-activated protein kinase activity in cumulus cells is essential for gonadotropin-induced oocyte meiotic resumption and cumulus expansion in the mouse. Endocrinology. 2002;143(6):2221-32.
50. Hedin L, Rodgers RJ, Simpson ER, Richards JS. Changes in Content of Cytochrome P450 17α, Cytochrome P450scc, and 3-Hydroxy-3-Methylglutaryl CoA Reductase in Developing Rat Ovarian Fotlicles and Corpora Lutea: Correlation with Theca Cell Steroidogenesis. Biology of reproduction. 1987;37(1):211-23.
51. Grøndahl ML, Andersen CY, Bogstad J, Borgbo T, Hartvig Boujida V, Borup R. Specific genes are selectively expressed between cumulus and granulosa cells from individual human pre-ovulatory follicles. Molecular human reproduction. 2012;18(12):572-84.
52. Koks S, Velthut A, Sarapik A, Altmäe S, Reinmaa E, Schalkwyk LC, et al. The differential transcriptome and ontology profiles of floating and cumulus granulosa cells in stimulated human antral follicles. Molecular human reproduction. 2009;16(4):229-40.
53. Peluso JJ. Basic fibroblast growth factor (bFGF) regulation of the plasma membrane calcium ATPase (PMCA) as part of an anti-apoptotic mechanism of action. Biochemical Pharmacology. 2003;66(8):1363-9.
54. Jurkat-Rott K, Lehmann-Horn F. The impact of splice isoforms on voltage-gated calcium channel α1 subunits. The Journal of physiology. 2004;554(3):609-19.
55. Strickland S, Beers WH. Studies on the role of plasminogen activator in ovulation. In vitro response of granulosa cells to gonadotropins, cyclic nucleotides, and prostaglandins. Journal of Biological Chemistry. 1976;251(18):5694-702.
56. Parrott JA, Whaley PD, Skinner MK. Extrahepatic expression of fibrinogen by granulosa cells: potential role in ovulation. Endocrinology. 1993;133(4):1645-9.
57. Vanderhyden BC, Armstrong DT. Role of cumulus cells and serum on the in vitro maturation, fertilization, and subsequent development of rat oocytes. Biol Reprod. 1989;40(4):720-8.
58. Nekola M, Nalbandov A. Morphological changes of rat follicular cells as influenced by oocytes. Biology of reproduction. 1971;4(2):154-60.
59. Buccione R, Vanderhyden BC, Caron PJ, Eppig JJ. FSH-induced expansion of the mouse cumulus oophorus in vitro is dependent upon a specific factor (s) secreted by the oocyte. Developmental biology. 1990;138(1):16-25.

60. Hussein TS, Froiland DA, Amato F, Thompson JG, Gilchrist RB. Oocytes prevent cumulus cell apoptosis by maintaining a morphogenic paracrine gradient of bone morphogenetic proteins. Journal of cell science. 2005;118(22):5257-68.
61. Virant-Klun I, Bauer C, Ståhlberg A, Kubista M, Skutella T. Human oocyte maturation in vitro is improved by co-culture with cumulus cells from mature oocytes. Reproductive BioMedicine Online. 2018;36(5):508-23.
62. Richards JS, Russell DL, Robker RL, Dajee M, Alliston TN. Molecular mechanisms of ovulation and luteinization. Molecular and cellular endocrinology. 1998;145(1-2):47-54.
63. Hernandez-Gonzalez I, Gonzalez-Robayna I, Shimada M, Wayne CM, Ochsner SA, White L, et al. Gene expression profiles of cumulus cell oocyte complexes during ovulation reveal cumulus cells express neuronal and immune-related genes: does this expand their role in the ovulation process? Molecular Endocrinology. 2006;20(6):1300-21.
64. Shimada M, Hernandez-Gonzalez I, Gonzalez-Robayna I, Richards JS. Paracrine and autocrine regulation of epidermal growth factor-like factors in cumulus oocyte complexes and granulosa cells: key roles for prostaglandin synthase 2 and progesterone receptor. Molecular Endocrinology. 2006;20(6):1352-65.
65. Park JY, Su YQ, Ariga M, Law E, Jin SL, Conti M. EGF-like growth factors as mediators of LH action in the ovulatory follicle. Science. 2004;303(5658):682-4.
66. Eppig JJ. Regulation of cumulus oophorus expansion by gonadotropins in vivo and in vitro. Biology of reproduction. 1980;23(3):545-52.
67. Peng J, Wigglesworth K, Rangarajan A, Eppig JJ, Thompson TB, Matzuk MM. Amino acid 72 of mouse and human GDF9 mature domain is responsible for altered homodimer bioactivities but has subtle effects on GDF9: BMP15 heterodimer activities. Biology of reproduction. 2014;91(6):142-1.
68. Yu C, Xu Y-W, Sha Q-Q, Fan H-Y. CRL4DCAF1 is required in activated oocytes for follicle maintenance and ovulation. MHR: Basic science of reproductive medicine. 2014;21(2):195-205.
69. Chen L, Russell P, Larsen W. Functional significance of cumulus expansion in the mouse: roles for the preovulatory synthesis of hyaluronic acid within the cumulus mass. Molecular reproduction and development. 1993;34(1):87-93.
70. Salustri A, Garlanda C, Hirsch E, De Acetis M, Maccagno A, Bottazzi B, et al. PTX3 plays a key role in the organization of the cumulus oophorus extracellular matrix and in in vivo fertilization. Development. 2004;131(7):1577-86.
71. Niswender GD, Juengel JL, Silva PJ, Rollyson MK, McIntush EW. Mechanisms controlling the function and life span of the corpus luteum. Physiological reviews. 2000;80(1):1-29.
72. Gougeon A, Ecochard R, Thalabard JC. Age-Related Changes of the Population of Human Ovarian Follicles: Increase in the Disappearance Rate of Non-Growing and Early-Growing Follicles in Aging Women. Biology of Reproduction. 1994;50(3):653-63.
73. Hsueh AJ, Billig H, Tsafriri A. Ovarian follicle atresia: a hormonally controlled apoptotic process. Endocr Rev. 1994;15(6):707-24.
74. Mariño G, Niso-Santano M, Baehrecke EH, Kroemer G. Self-consumption: the interplay of autophagy and apoptosis. Nature reviews Molecular cell biology. 2014;15(2):81-94.
75. Markstrom E, Svensson E, Shao R, Svanberg B, Billig H. Survival factors regulating ovarian apoptosis -- dependence on follicle differentiation. Reproduction. 2002;123(1):23-30.
76. Rajakoski E. The ovarian follicular system in sexually mature heifers with special reference to seasonal, cyclical, and left-right variations. Acta endocrinologica. 1960;34(3 Suppl):S7-S68.
77. Teerds KJ, Dorrington JH. Immunohistochemical localization of 3-hydroxysteroid dehydrogenase in the rat ovary during follicular development and atresia. Biology of Reproduction. 1993;49(5):989-96.
78. Meng L, Jan SZ, Hamer G, van Pelt AM, van der Stelt I, Keijer J, et al. Preantral follicular atresia occurs mainly through autophagy, while antral follicles degenerate mostly through apoptosis. Biology of Reproduction. 2018;99(4):853-63.
79. Cha K-Y, Chian R-C. Maturation in vitro of immature human oocytes for clinical use. Human Reproduction Update. 1998;4(2):103-20.
80. Trounson A, Anderiesz C, Jones G. Maturation of human oocytes in vitro and their developmental competence. Reproduction. 2001;121(1):51-75.
81. Gandolfi TB, Gandolfi F. The maternal legacy to the embryo: cytoplasmic components and their effects on early development. Theriogenology. 2001;55(6):1255-76.
82. Sirard M-A, Richard F, Blondin P, Robert C. Contribution of the oocyte to embryo quality. Theriogenology. 2006;65(1):126-36.

83. Wassarman PM, Josefowicz WJ. Oocyte development in the mouse: an ultrastructural comparison of oocytes isolated at various stages of growth and meiotic competence. Journal of Morphology. 1978;156(2):209-35.
84. Picton H, Briggs D, Gosden R. The molecular basis of oocyte growth and development. Molecular and cellular endocrinology. 1998;145(1-2):27-37.
85. Baba Y, Matsuo H, Schally AV. Structure of the porcine LH-and FSH-releasing hormone. II. Confirmation of the proposed structure by conventional sequential analyses. Biochemical and biophysical research communications. 1971;44(2):459-63.
86. Schally AV, Arimura A, Kastin AJ, Matsuo H, Baba Y, Redding TW, et al. Gonadotropin-releasing hormone: one polypeptide regulates secretion of luteinizing and follicle-stimulating hormones. Science. 1971;173(4001):1036-8.
87. Belchetz PE, Plant TM, Nakai Y, Keogh EJ, Knobil E. Hypophysial responses to continuous and intermittent delivery of hypopthalamic gonadotropin-releasing hormone. Science. 1978;202(4368):631-3.
88. Green ED, Baenziger JU. Asparagine-linked oligosaccharides on lutropin, follitropin, and thyrotropin. I. Structural elucidation of the sulfated and sialylated oligosaccharides on bovine, ovine, and human pituitary glycoprotein hormones. Journal of Biological Chemistry. 1988;263(1):25-35.
89. Wildt L, Häusler A, Marshall G, Hutchison JS, Plant TM, Belchetz PE, et al. Frequency and amplitude of gonadotropin-releasing hormone stimulation and gonadotropin secretion in the rhesus monkey. Endocrinology. 1981;109(2):376-85.
90. Reame N, Sauder SE, Kelch RP, Marshall JC. Pulsatile Gonadotropin Secretion during the Human Menstrual Cycle: Evidence for Altered Frequency of Gonadotropin-Releasing Hormone Secretion*. The Journal of Clinical Endocrinology & Metabolism. 1984;59(2):328-37.
91. Soules MR, Steiner RA, Clifton DK, Cohen NL, Aksel S, Bremner WJ. Progesterone modulation of pulsatile luteinizing hormone secretion in normal women. The Journal of Clinical Endocrinology & Metabolism. 1984;58(2):378-83.
92. Knight PG, Glister C. TGF-β superfamily members and ovarian follicle development. Reproduction. 2006;132(2):191-206.
93. Welt CK, Martin KA, Taylor AE, Lambert-Messerlian GM, Crowley Jr WF, Smith JA, et al. Frequency modulation of follicle-stimulating hormone (FSH) during the luteal-follicular transition: evidence for FSH control of inhibin B in normal women. The Journal of Clinical Endocrinology & Metabolism. 1997;82(8):2645-52.
94. Stouffer RL, Woodruff TK, Dahl KD, Hess DL, Mather JP, Molskness TA. Human recombinant activin-A alters pituitary luteinizing hormone and follicle-stimulating hormone secretion, follicular development, and steroidogenesis, during the menstrual cycle in rhesus monkeys. The Journal of Clinical Endocrinology & Metabolism. 1993;77(1):241-8.
95. Shi J, Yoshino O, Osuga Y, Koga K, Hirota Y, Hirata T, et al. Bone morphogenetic protein-6 stimulates gene expression of follicle-stimulating hormone receptor, inhibin/activin β subunits, and anti-Müllerian hormone in human granulosa cells. Fertility and Sterility. 2009;92(5):1794-8.
96. Erickson GF, Magoffin DA, Dyer CA, Hofeditz C. The Ovarian Androgen Producing Cells: A Review of Structure/Function Relationships1,2. Endocrine Reviews. 1985;6(3):371-99.
97. McNatty KP, Hunter WM, McNeilly AS, Sawers RS. Changes in the concentration of pituitary and steroid hormones in the follicular fluid of human graafian follicles throughout the menstrual cycle. Journal of Endocrinology. 1975;64(3):555-71.
98. Hillier SG, Reichert Jr LE, Van Hall EV. Control of preovulatory follicular estrogen biosynthesis in the human ovary. The Journal of Clinical Endocrinology & Metabolism. 1981;52(5):847-56.
99. Billig H, Furuta I, Hsueh AJ. Estrogens inhibit and androgens enhance ovarian granulosa cell apoptosis. Endocrinology. 1993;133(5):2204-12.
100. Richards JS, Ireland JJ, Rao MC, Bernath GA, Midgley Jr AR, Reichert LE. Ovarian follicular development in the rat: hormone receptor regulation by estradiol, follicle stimulating hormone and luteinizing hormone. Endocrinology. 1976;99(6):1562-70.
101. Zhuang L-Z, Adashi EY, Hsueh AJW. Direct enhancement of gonadotropin-stimulated ovarian estrogen biosynthesis by estrogen and clomiphene citrate. Endocrinology. 1982;110(6):2219-21.
102. Kuiper GG, Carlsson B, Grandien K, Enmark E, Häggblad J, Nilsson S, et al. Comparison of the ligand binding specificity and transcript tissue distribution of estrogen receptors alpha and beta. Endocrinology. 1997;138(3):863-70.

103. Mosselman S, Polman J, Dijkema R. ERβ: identification and characterization of a novel human estrogen receptor. FEBS letters. 1996;392(1):49-53.
104. Enmark E, Pelto-Huikko M, Grandien KAJ, Lagercrantz S, Lagercrantz J, Fried G, et al. Human estrogen receptor β-gene structure, chromosomal localization, and expression pattern. The Journal of Clinical Endocrinology & Metabolism. 1997;82(12):4258-65.
105. Dupont S, Krust A, Gansmuller A, Dierich A, Chambon P, Mark M. Effect of single and compound knockouts of estrogen receptors alpha (ERalpha) and beta (ERbeta) on mouse reproductive phenotypes. Development. 2000;127(19):4277-91.
106. Krege JH, Hodgin JB, Couse JF, Enmark E, Warner M, Mahler JF, et al. Generation and reproductive phenotypes of mice lacking estrogen receptor β. Proceedings of the National Academy of Sciences. 1998;95(26):15677-82.
107. Hegele-Hartung C, Siebel P, Peters O, Kosemund D, Müller G, Hillisch A, et al. Impact of isotype-selective estrogen receptor agonists on ovarian function. Proceedings of the National Academy of Sciences. 2004;101(14):5129-34.
108. Graham JD, Clarke CL. Physiological action of progesterone in target tissues. Endocrine reviews. 1997;18(4):502-19.
109. Spelsberg TC, Steggles AW, Chytil F, O'Malley BW. Progesterone-binding Components of Chick Oviduct V. EXCHANGE OF PROGESTERONE-BINDING CAPACITY FROM TARGET TO NONTARGET TISSUE CHROMATINS. Journal of Biological Chemistry. 1972;247(5):1368-74.
110. Kastner P, Krust A, Turcotte B, Stropp U, Tora L, Gronemeyer H, et al. Two distinct estrogen-regulated promoters generate transcripts encoding the two functionally different human progesterone receptor forms A and B. The EMBO journal. 1990;9(5):1603-14.
111. Conneely OM, Mulac-Jericevic B, Demayo F, Lydon JP, O Malley BW. Reproductive functions of progesterone receptors. Recent progress in hormone research. 2002;57:339-56.
112. Conneely OM, Mulac-Jericevic B, Lydon JP. Progesterone-dependent regulation of female reproductive activity by two distinct progesterone receptor isoforms. Steroids. 2003;68(10-13):771-8.
113. Tung L, Mohamed MK, Hoeffler JP, Takimoto GS, Horwitz KB. Antagonist-occupied human progesterone B-receptors activate transcription without binding to progesterone response elements and are dominantly inhibited by A-receptors. Molecular Endocrinology. 1993;7(10):1256-65.
114. Vegeto E, Shahbaz MM, Wen DX, Goldman ME, O'Malley BW, McDonnell DP. Human progesterone receptor A form is a cell-and promoter-specific repressor of human progesterone receptor B function. Molecular Endocrinology. 1993;7(10):1244-55.
115. Mulac-Jericevic B, Mullinax RA, DeMayo FJ, Lydon JP, Conneely OM. Subgroup of reproductive functions of progesterone mediated by progesterone receptor-B isoform. Science. 2000;289(5485):1751-4.
116. Mulac-Jericevic B, Lydon JP, DeMayo FJ, Conneely OM. Defective mammary gland morphogenesis in mice lacking the progesterone receptor B isoform. Proceedings of the National Academy of Sciences. 2003;100(17):9744-9.
117. Jia X-C, Kessel B, Welsh Jr TH, Hsueh AJ. Androgen inhibition of follicle-stimulating hormone-stimulated luteinizing hormone receptor formation in cultured rat granulosa cells. Endocrinology. 1985;117(1):13-22.
118. Mora J, Thomson K, Hardy K, Fenwick M, Laird M, Franks S. Androgen Stimulates Growth of Mouse Preantral Follicles In Vitro: Interaction With Follicle-Stimulating Hormone and With Growth Factors of the TGFβ Superfamily. Endocrinology. 2017;158(4):920-35.
119. Nandedkar TD, Munshi SR. Effect of dihydrotestosterone on follicular development, ovulation and reproductive capacity of mice. Journal of reproduction and fertility. 1981;62(1):21-4.
120. Hu Y-C, Wang P-H, Yeh S, Wang R-S, Xie C, Xu Q, et al. Subfertility and defective folliculogenesis in female mice lacking androgen receptor. Proceedings of the National Academy of Sciences. 2004;101(31):11209-14.
121. Michael WP. A putative role for anti-Müllerian hormone (AMH) in optimising ovarian reserve expenditure. Journal of Endocrinology. 2017;233(1):R1-R13.
122. Munsterberg A, Lovell-Badge R. Expression of the mouse anti-mullerian hormone gene suggests a role in both male and female sexual differentiation. Development. 1991;113(2):613-24.
123. Weenen C, Laven JSE, von Bergh ARM, Cranfield M, Groome NP, Visser JA, et al. Anti-Müllerian hormone expression pattern in the human ovary: potential implications for initial and cyclic follicle recruitment. MHR: Basic science of reproductive medicine. 2004;10(2):77-83.

124. Durlinger ALL, Kramer P, Karels B, de Jong FH, Uilenbroek JTJ, Grootegoed JA, et al. Control of primordial follicle recruitment by anti-Mullerian hormone in the mouse ovary. Endocrinology. 1999;140(12):5789-96.
125. Carlsson IB, Scott JE, Visser JA, Ritvos O, Themmen APN, Hovatta O. Anti-Müllerian hormone inhibits initiation of growth of human primordial ovarian follicles in vitro. Human reproduction. 2006;21(9):2223-7.
126. Durlinger ALL, Gruijters MJG, Kramer P, Karels B, Ingraham HA, Nachtigal MW, et al. Anti-Mullerian hormone inhibits initiation of primordial follicle growth in the mouse ovary. Endocrinology. 2002;143(3):1076-84.
127. Eppig JJ, Chesnel F, Hirao Y, O'Brien MJ, Pendola FL, Watanabe S, et al. Oocyte control of granulosa cell development: how and why. Hum Reprod. 1997;12(11 Suppl):127-32.
128. Dong J, Albertini DF, Nishimori K, Kumar TR, Lu N, Matzuk MM. Growth differentiation factor-9 is required during early ovarian folliculogenesis. Nature. 1996;383(6600):531.
129. McPherron AC, Lee S-J. GDF-3 and GDF-9: two new members of the transforming growth factor-beta superfamily containing a novel pattern of cysteines. Journal of Biological Chemistry. 1993;268(5):3444-9.
130. Aaltonen J, Laitinen MP, Vuojolainen K, Jaatinen R, Horelli-Kuitunen N, Seppä L, et al. Human growth differentiation factor 9 (GDF-9) and its novel homolog GDF-9B are expressed in oocytes during early folliculogenesis. The Journal of Clinical Endocrinology & Metabolism. 1999;84(8):2744-50.
131. Hayashi M, McGee EA, Min G, Klein C, Rose UM, Duin Mv, et al. Recombinant Growth Differentiation Factor-9 (GDF-9) Enhances Growth and Differentiation of Cultured Early Ovarian Follicles*. Endocrinology. 1999;140(3):1236-44.
132. Elvin JA, Clark AT, Wang P, Wolfman NM, Matzuk MM. Paracrine actions of growth differentiation factor-9 in the mammalian ovary. Molecular endocrinology. 1999;13(6):1035-48.
133. Kaivo-Oja N, Bondestam J, Kämäräinen M, Koskimies J, Vitt U, Cranfield M, et al. Growth differentiation factor-9 induces Smad2 activation and inhibin B production in cultured human granulosa-luteal cells. The Journal of Clinical Endocrinology & Metabolism. 2003;88(2):755-62.
134. Moore RK, Otsuka F, Shimasaki S. Molecular basis of bone morphogenetic protein-15 signaling in granulosa cells. Journal of Biological Chemistry. 2003;278(1):304-10.
135. Hreinsson JG, Scott JE, Rasmussen C, Swahn ML, Hsueh AJW, Hovatta O. Growth Differentiation Factor-9 Promotes the Growth, Development, and Survival of Human Ovarian Follicles in Organ Culture. The Journal of Clinical Endocrinology & Metabolism. 2002;87(1):316-21.
136. Yan C, Wang P, DeMayo J, DeMayo FJ, Elvin JA, Carino C, et al. Synergistic Roles of Bone Morphogenetic Protein 15 and Growth Differentiation Factor 9 in Ovarian Function. Molecular Endocrinology. 2001;15(6):854-66.
137. Araújo VR, Duarte ABG, Bruno JB, Pinho Lopes CA, de Figueiredo JR. Importance of vascular endothelial growth factor (VEGF) in ovarian physiology of mammals. Zygote. 2013;21(3):295-304.
138. Hsueh AJW, Kawamura K, Cheng Y, Fauser BCJM. Intraovarian Control of Early Folliculogenesis. Endocrine Reviews. 2015;36(1):1-24.
139. Matsuda F, Inoue N, Manabe N, Ohkura S. Follicular growth and atresia in mammalian ovaries: regulation by survival and death of granulosa cells. Journal of Reproduction and Development. 2012;58(1):44-50.
140. Zhang H, Liu K. Cellular and molecular regulation of the activation of mammalian primordial follicles: somatic cells initiate follicle activation in adulthood. Human Reproduction Update. 2015;21(6):779-86.
141. John GB, Gallardo TD, Shirley LJ, Castrillon DH. Foxo3 is a PI3K-dependent molecular switch controlling the initiation of oocyte growth. Developmental Biology. 2008;321(1):197-204.
142. McLaughlin M, Kinnell HL, Anderson RA, Telfer EE. Inhibition of phosphatase and tensin homologue (PTEN) in human ovary in vitro results in increased activation of primordial follicles but compromises development of growing follicles. MHR: Basic science of reproductive medicine. 2014;20(8):736-44.
143. Grosbois J, Demeestere I. Dynamics of PI3K and Hippo signaling pathways during in vitro human follicle activation. Human Reproduction. 2018;33(9):1705-14.
144. Laitinen M, Rutanen EM, Ritvos O. Expression of c-kit ligand messenger ribonucleic acids in human ovaries and regulation of their steady state levels by gonadotropins in cultured granulosa-luteal cells. Endocrinology. 1995;136(10):4407-14.

145. Hutt KJ, McLaughlin EA, Holland MK. Kit ligand and c-Kit have diverse roles during mammalian oogenesis and folliculogenesis. MHR: Basic science of reproductive medicine. 2006;12(2):61-9.
146. Mazerbourg S, Monget P. Insulin-Like Growth Factor Binding Proteins and IGFBP Proteases: A Dynamic System Regulating the Ovarian Folliculogenesis. Frontiers in Endocrinology. 2018;9(134).
147. Bird A. DNA methylation patterns and epigenetic memory. Genes Dev. 2002;16(1):6-21.
148. Waddington CH. The epigenotype. Endeavour. 1942;1:18-20.
149. Van Holde KE, Sahasrabuddhe CG, Shaw BR. A model for particulate structure in chromatin. Nucleic Acids Res. 1974;1(11):1579-86.
150. Cooper G. Chromosomes and Chromatin. The Cell. 2 ed. Sunderland, MA: Sinauer Associates; 2000.
151. Klug W, Cummings M, Spencer C, Palladino M. Essentials of Genetics. United Kingdom: Pearson; 2009.
152. Gonzalo S. Epigenetic alterations in aging. Journal of applied physiology. 2010;109(2):586-97.
153. Bannister AJ, Kouzarides T. Regulation of chromatin by histone modifications. Cell research. 2011;21(3):381.
154. Jenuwein T, Allis CD. Translating the histone code. Science. 2001;293(5532):1074-80.
155. Ruthenburg AJ, Allis CD, Wysocka J. Methylation of lysine 4 on histone H3: intricacy of writing and reading a single epigenetic mark. Mol Cell. 2007;25(1):15-30.
156. Heijmans BT, Tobi EW, Stein AD, Putter H, Blauw GJ, Susser ES, et al. Persistent epigenetic differences associated with prenatal exposure to famine in humans. Proceedings of the National Academy of Sciences. 2008;105(44):17046-9.
157. Hannum G, Guinney J, Zhao L, Zhang L, Hughes G, Sadda S, et al. Genome-wide methylation profiles reveal quantitative views of human aging rates. Molecular cell. 2013;49(2):359-67.
158. Dang W, Steffen KK, Perry R, Dorsey JA, Johnson FB, Shilatifard A, et al. Histone H4 lysine 16 acetylation regulates cellular lifespan. Nature. 2009;459(7248):802.
159. Sen P, Shah PP, Nativio R, Berger SL. Epigenetic mechanisms of longevity and aging. Cell. 2016;166(4):822-39.
160. Arrowsmith CH, Bountra C, Fish PV, Lee K, Schapira M. Epigenetic protein families: a new frontier for drug discovery. Nature reviews Drug discovery. 2012;11(5):384-400.
161. Tarakhovsky A. Tools and landscapes of epigenetics. Nature immunology. 2010;11(7):565-8.
162. Brownell JE, Zhou J, Ranalli T, Kobayashi R, Edmondson DG, Roth SY, et al. Tetrahymena histone acetyltransferase A: a homolog to yeast Gcn5p linking histone acetylation to gene activation. Cell. 1996;84(6):843-51.
163. Bannister AJ, Zegerman P, Partridge JF, Miska EA, Thomas JO, Allshire RC, et al. Selective recognition of methylated lysine 9 on histone H3 by the HP1 chromo domain. Nature. 2001;410(6824):120-4.
164. Wang H, Huang ZQ, Xia L, Feng Q, Erdjument-Bromage H, Strahl BD, et al. Methylation of histone H4 at arginine 3 facilitating transcriptional activation by nuclear hormone receptor. Science. 2001;293(5531):853-7.
165. Paull TT, Rogakou EP, Yamazaki V, Kirchgessner CU, Gellert M, Bonner WM. A critical role for histone H2AX in recruitment of repair factors to nuclear foci after DNA damage. Current biology : CB. 2000;10(15):886-95.
166. Henry KW, Wyce A, Lo WS, Duggan LJ, Emre NC, Kao CF, et al. Transcriptional activation via sequential histone H2B ubiquitylation and deubiquitylation, mediated by SAGA-associated Ubp8. Genes Dev. 2003;17(21):2648-63.
167. Eden A, Gaudet F, Waghmare A, Jaenisch R. Chromosomal instability and tumors promoted by DNA hypomethylation. Science. 2003;300(5618):455.
168. Inge GB, Brinsden PR, Elder KT. Oocyte number per live birth in IVF: were Steptoe and Edwards less wasteful? Human Reproduction. 2005;20(3):588-92.
169. La Marca A, Minasi MG, Sighinolfi G, Greco P, Argento C, Grisendi V, et al. Female age, serum antimüllerian hormone level, and number of oocytes affect the rate and number of euploid blastocysts in in vitro fertilization/intracytoplasmic sperm injection cycles. Fertility and Sterility. 2017;108(5):777-83.e2.

170. Scheffer GJ, Broekmans FJM, Dorland M, Habbema JDF, Looman CWN, te Velde ER. Antral follicle counts by transvaginal ultrasonography are related to age in women with proven natural fertility. Fertility and Sterility. 1999;72(5):845-51.
171. Reuss ML, Kline J, Santos R, Levin B, Timor-Tritsch I. Age and the ovarian follicle pool assessed with transvaginal ultrasonography. American Journal of Obstetrics and Gynecology. 1996;174(2):624-7.
172. Hendriks DJ, Mol B-WJ, Bancsi LFJMM, te Velde ER, Broekmans FJM. Antral follicle count in the prediction of poor ovarian response and pregnancy after in vitro fertilization: A meta-analysis and comparison with basal follicle-stimulating hormone level. Fertility and Sterility. 2005;83(2):291-301.
173. Toner JP, Philput CB, Jones GS, Muasher SJ. Basal follicle-stimulating hormone level is a better predictor of in vitro fertilization performance than age. Fertility and sterility. 1991;55(4):784-91.
174. Chuang C-C, Chen C-D, Chao K-H, Chen S-U, Ho H-N, Yang Yu-S. Age is a better predictor of pregnancy potential than basal follicle-stimulating hormone levels in women undergoing in vitro fertilization. Fertility and Sterility. 2003;79(1):63-8.
175. Morin SJ, Patounakis G, Juneau CR, Neal SA, Scott JRT, Seli E. Diminished ovarian reserve and poor response to stimulation in patients <38 years old: a quantitative but not qualitative reduction in performance. Human Reproduction. 2018;33(8):1489-98.
176. Grøndahl ML, Yding Andersen C, Bogstad J, Nielsen FC, Meinertz H, Borup R. Gene expression profiles of single human mature oocytes in relation to age. Human Reproduction. 2010;25(4):957-68.
177. Steuerwald NM, Bermúdez MG, Wells D, Munné S, Cohen J. Maternal age-related differential global expression profiles observed in human oocytes. Reproductive biomedicine online. 2007;14(6):700-8.
178. Reyes JM, Silva E, Chitwood JL, Schoolcraft WB, Krisher RL, Ross PJ. Differing molecular response of young and advanced maternal age human oocytes to IVM. Human Reproduction. 2017;32(11):2199-208.
179. Navot D, Bergh RA, Williams MA, Garrisi GJ, Guzman I, Sandler B, et al. Poor oocyte quality rather than implantation failure as a cause of age-related decline in female fertility. The Lancet. 1991;337(8754):1375-7.
180. Hassold T, Hunt P. To err (meiotically) is human: the genesis of human aneuploidy. Nature Reviews Genetics. 2001;2(4):280.
181. Munné S, Alikani M, Tomkin G, Grifo J, Cohen J. Embryo morphology, developmental rates, and maternal age are correlated with chromosome abnormalities. Fertility and sterility. 1995;64(2):382-91.
182. Battaglia DE, Goodwin P, Klein NA, Soules MR. Fertilization and early embryology: Influence of maternal age on meiotic spindle assembly oocytes from naturally cycling women. Human reproduction. 1996;11(10):2217-22.
183. Fragouli E, Alfarawati S, Spath K, Jaroudi S, Sarasa J, Enciso M, et al. The origin and impact of embryonic aneuploidy. Human genetics. 2013;132(9):1001-13.
184. Franasiak JM, Forman EJ, Hong KH, Werner MD, Upham KM, Treff NR, et al. The nature of aneuploidy with increasing age of the female partner: a review of 15,169 consecutive trophectoderm biopsies evaluated with comprehensive chromosomal screening. Fertility and Sterility. 2014;101(3):656-63.e1.
185. Wallace DC. Diseases of the mitochondrial DNA. Annual review of biochemistry. 1992;61(1):1175-212.
186. Reynier P, May-Panloup P, Chretien MF, Morgan CJ, Jean M, Savagner F, et al. Mitochondrial DNA content affects the fertilizability of human oocytes. Molecular human reproduction. 2001;7(5):425-9.
187. Santos TA, El Shourbagy S, St. John JC. Mitochondrial content reflects oocyte variability and fertilization outcome. Fertility and Sterility. 2006;85(3):584-91.
188. Fragouli E, Spath K, Alfarawati S, Kaper F, Craig A, Michel C-E, et al. Altered Levels of Mitochondrial DNA Are Associated with Female Age, Aneuploidy, and Provide an Independent Measure of Embryonic Implantation Potential. PLOS Genetics. 2015;11(6):e1005241.
189. Diez-Juan A, Rubio C, Marin C, Martinez S, Al-Asmar N, Riboldi M, et al. Mitochondrial DNA content as a viability score in human euploid embryos: less is better. Fertility and Sterility. 2015;104(3):534-41.e1.

190. Victor AR, Brake AJ, Tyndall JC, Griffin DK, Zouves CG, Barnes FL, et al. Accurate quantitation of mitochondrial DNA reveals uniform levels in human blastocysts irrespective of ploidy, age, or implantation potential. Fertility and Sterility. 2017;107(1):34-42.e3.
191. Adriaenssens T, Wathlet S, Segers I, Verheyen G, De Vos A, Van der Elst J, et al. Cumulus cell gene expression is associated with oocyte developmental quality and influenced by patient and treatment characteristics. Human reproduction. 2010;25(5):1259-70.
192. Gebhardt KM, Feil DK, Dunning KR, Lane M, Russell DL. Human cumulus cell gene expression as a biomarker of pregnancy outcome after single embryo transfer. Fertility and sterility. 2011;96(1):47-52.
193. Hamel M, Dufort I, Robert C, Gravel C, Leveille MC, Leader A, et al. Identification of differentially expressed markers in human follicular cells associated with competent oocytes. Hum Reprod. 2008;23(5):1118-27.
194. Wathlet S, Adriaenssens T, Segers I, Verheyen G, Janssens R, Coucke W, et al. New candidate genes to predict pregnancy outcome in single embryo transfer cycles when using cumulus cell gene expression. Fertil Steril. 2012;98(2):432-9.e1-4.
195. Assou S, Haouzi D, Mahmoud K, Aouacheria A, Guillemin Y, Pantesco V, et al. A non-invasive test for assessing embryo potential by gene expression profiles of human cumulus cells: a proof of concept study. Mol Hum Reprod. 2008;14(12):711-9.
196. Feuerstein P, Puard V, Chevalier C, Teusan R, Cadoret V, Guerif F, et al. Genomic assessment of human cumulus cell marker genes as predictors of oocyte developmental competence: impact of various experimental factors. PLoS One. 2012;7(7):e40449.
197. Papler T, Bokal E, Lovrecic L, Kopitar A, Maver A. No specific gene expression signature in human granulosa and cumulus cells for prediction of oocyte fertilisation and embryo implantation. PLoS One. 2015;10(3).
198. Al-Edani T, Assou S, Ferrières A, Bringer Deutsch S, Gala A, Lecellier CH, et al. Female aging alters expression of human cumulus cells genes that are essential for oocyte quality. Biomed Res Int. 2014;2014:964614.
199. Ouandaogo ZG, Frydman N, Hesters L, Assou S, Haouzi D, Dechaud H, et al. Differences in transcriptomic profiles of human cumulus cells isolated from oocytes at GV, MI and MII stages after in vivo and in vitro oocyte maturation. Human Reproduction. 2012;27(8):2438-47.
200. Yerushalmi GM, Salmon-Divon M, Yung Y, Maman E, Kedem A, Ophir L, et al. Characterization of the human cumulus cell transcriptome during final follicular maturation and ovulation. MHR: Basic science of reproductive medicine. 2014;20(8):719-35.
201. Molinari E, Bar H, Pyle AM, Patrizio P. Transcriptome analysis of human cumulus cells reveals hypoxia as the main determinant of follicular senescence. Mol Hum Reprod. 2016;22(8):866-76.
202. Bouckenheimer J, Fauque P, Lecellier C-H, Bruno C, Commes T, Lemaître J-M, et al. Differential long non-coding RNA expression profiles in human oocytes and cumulus cells. Scientific Reports. 2018;8(1):2202.
203. Gleicher N, Kushnir VA, Barad DH. Preimplantation genetic screening (PGS) still in search of a clinical application: a systematic review. Reproductive Biology and Endocrinology. 2014;12(1):22.
204. Lee E, Illingworth P, Wilton L, Chambers GM. The clinical effectiveness of preimplantation genetic diagnosis for aneuploidy in all 24 chromosomes (PGD-A): systematic review. Human Reproduction. 2015;30(2):473-83.
205. Gleicher N, Orvieto R. Is the hypothesis of preimplantation genetic screening (PGS) still supportable? A review. Journal of Ovarian Research. 2017;10(1):21.
206. Rubio C, Bellver J, Rodrigo L, Castillón G, Guillén A, Vidal C, et al. In vitro fertilization with preimplantation genetic diagnosis for aneuploidies in advanced maternal age: a randomized, controlled study. Fertility and Sterility. 2017;107(5):1122-9.
207. Lee M-S, Liu C-H, Lee T-H, Wu H-M, Huang C-C, Huang L-S, et al. Association of creatin kinase B and peroxiredoxin 2 expression with age and embryo quality in cumulus cells. Journal of Assisted Reproduction and Genetics. 2010;27(11):629-39.
208. McReynolds S, Dzieciatkowska M, McCallie BR, Mitchell SD, Stevens J, Hansen K, et al. Impact of maternal aging on the molecular signature of human cumulus cells. Fertility and Sterility. 2012;98(6):1574-80.e5.
209. Eppig JJ, O'Brien MJ. Development in vitro of mouse oocytes from primordial follicles. Biology of reproduction. 1996;54(1):197-207.

210. McLaughlin M, Albertini DF, Wallace WHB, Anderson RA, Telfer EE. Metaphase II oocytes from human unilaminar follicles grown in a multi-step culture system. Mol Hum Reprod. 2018;24(3):135-42.
211. Telfer EE, McLaughlin M, Ding C, Thong KJ. A two-step serum-free culture system supports development of human oocytes from primordial follicles in the presence of activin. Hum Reprod. 2008;23(5):1151-8.
212. Hornick JE, Duncan FE, Shea LD, Woodruff TK. Isolated primate primordial follicles require a rigid physical environment to survive and grow in vitro. Human Reproduction. 2012;27(6):1801-10.
213. Hovatta O, Wright C, Krausz T, Hardy K, Winston RM. Human primordial, primary and secondary ovarian follicles in long-term culture: effect of partial isolation. Human Reproduction. 1999;14(10):2519-24.
214. Abir R, Roizman P, Fisch B, Nitke S, Okon E, Orvieto R, et al. Pilot study of isolated early human follicles cultured in collagen gels for 24 hours. Human Reproduction. 1999;14(5):1299-301.
215. Abir R, Fisch B, Nitke S, Okon E, Raz A, Rafael ZB. Morphological study of fully and partially isolated early human follicles. Fertility and sterility. 2001;75(1):141-6.
216. Picton H, Harris S, Muruvi W, Chambers E. The in vitro growth and maturation of follicles. Reproduction. 2008;136(6):703-15.
217. Wright CS, Hovatta O, Margara R, Trew G, Winston RML, Franks S, et al. Effects of follicle-stimulating hormone and serum substitution on the in-vitro growth of human ovarian follicles. Human Reproduction. 1999;14(6):1555-62.
218. Cortvrindt R, Smitz J, Van Steirteghem AC. Assessment of the need for follicle stimulating hormone in early preantral mouse follicle culture in vitro. Human Reproduction (Oxford, England). 1997;12(4):759-68.
219. Nayudu P, Osborn S. Factors influencing the rate of preantral and antral growth of mouse ovarian follicles in vitro. Journal of Reproduction and Fertility. 1992;95(2):349-62.
220. Abir R, Franks S, Mobberley MA, Moore PA, Margara RA, Winston RM. Mechanical isolation and in vitro growth of preantral and small antral human follicles. Fertility and sterility. 1997;68(4):682-8.
221. Newton H, Picton H, Gosden R. In vitro growth of oocyte–granulosa cell complexes isolated from cryopreserved ovine tissue. Journal of reproduction and fertility. 1999;115(1):141-50.
222. Roy SK, Treacy BJ. Isolation and long-term culture of human preantral follicles. Fertility and sterility. 1993;59(4):783-90.
223. Xu J, Lawson MS, Yeoman RR, Pau KY, Barrett SL, Zelinski MB, et al. Secondary follicle growth and oocyte maturation during encapsulated three-dimensional culture in rhesus monkeys: effects of gonadotrophins, oxygen and fetuin. Human Reproduction. 2011;26(5):1061-72.
224. Talevi R, Sudhakaran S, Barbato V, Merolla A, Braun S, Di Nardo M, et al. Is oxygen availability a limiting factor for in vitro folliculogenesis? PloS one. 2018;13(2):e0192501.
225. Azarbaijani BA, Sheikhi M, Oskam IC, Nurmio M, Laine T, Tinkanen H, et al. Effect of previous chemotherapy on the quality of cryopreserved human ovarian tissue in vitro. PloS one. 2015;10(7):e0133985.
226. Asadi-Azarbaijani B, Sheikhi M, Nurmio M, Tinkanen H, Juvonen V, Dunkel L, et al. Minimal residual disease of leukemia and the quality of cryopreserved human ovarian tissue in vitro. Leukemia & lymphoma. 2016;57(3):700-7.
227. Lerer-Serfaty G, Samara N, Fisch B, Shachar M, Kossover O, Seliktar D, et al. Attempted application of bioengineered/biosynthetic supporting matrices with phosphatidylinositol-trisphosphate-enhancing substances to organ culture of human primordial follicles. Journal of assisted reproduction and genetics. 2013;30(10):1279-88.
228. Kedem A, Hourvitz A, Fisch B, Shachar M, Cohen S, Ben-Haroush A, et al. Alginate scaffold for organ culture of cryopreserved-thawed human ovarian cortical follicles. Journal of assisted reproduction and genetics. 2011;28(9):761.
229. Scott JE, Carlsson IB, Bavister BD, Hovatta O. Human ovarian tissue cultures: extracellular matrix composition, coating density and tissue dimensions. Reproductive biomedicine online. 2004;9(3):287-93.
230. Huang L, Mo Y, Wang W, Li Y, Zhang Q, Yang D. Cryopreservation of human ovarian tissue by solid-surface vitrification. European Journal of Obstetrics & Gynecology and Reproductive Biology. 2008;139(2):193-8.

231. Garor R, Abir R, Erman A, Felz C, Nitke S, Fisch B. Effects of basic fibroblast growth factor on in vitro development of human ovarian primordial follicles. Fertility and sterility. 2009;91(5):1967-75.
232. Xiao Z, Wang Y, Li L-l, Li S-W. In vitro culture thawed human ovarian tissue: NIV versus slow freezing method. CryoLetters. 2013;34(5):520-6.
233. Hovatta O, Silye R, Abir R, Krausz T, Winston R. Extracellular matrix improves survival of both stored and fresh human primordial and primary ovarian follicles in long-term culture. Human reproduction (Oxford, England). 1997;12(5):1032-6.
234. Oktay K, Nugent D, Newton H, Salha O, Chatterjee P, Gosden RG. Isolation and characterization of primordial follicles from fresh and cryopreserved human ovarian tissue. Fertility and sterility. 1997;67(3):481-6.
235. Cecconi S, Barboni B, Coccia M, Mattioli M. In Vitro Development of Sheep Preantral Follicles1. Biology of Reproduction. 1999;60(3):594-601.
236. Wu J, Emery BR, Carrell DT. In Vitro Growth, Maturation, Fertilization, and Embryonic Development of Oocytes from Porcine Preantral Follicles. Biology of Reproduction. 2001;64(1):375-81.
237. Dolmans M-M, Michaux N, Camboni A, Martinez-Madrid B, Van Langendonckt A, Annarita Nottola S, et al. Evaluation of Liberase, a purified enzyme blend, for the isolation of human primordial and primary ovarian follicles. Human Reproduction. 2006;21(2):413-20.
238. Vanacker J, Camboni A, Dath C, Van Langendonckt A, Dolmans M-M, Donnez J, et al. Enzymatic isolation of human primordial and primary ovarian follicles with Liberase DH: protocol for application in a clinical setting. Fertility and Sterility. 2011;96(2):379-83.e3.
239. Telfer E. The development of methods for isolation and culture of preantral follicles from bovine and porcine ovaries. Theriogenology. 1996;45(1):101-10.
240. Xiao S, Zhang J, Romero MM, Smith KN, Shea LD, Woodruff TK. In vitro follicle growth supports human oocyte meiotic maturation. Scientific reports. 2015;5:17323.
241. Barrett SL, Shea LD, Woodruff TK. Noninvasive Index of Cryorecovery and Growth Potential for Human Follicles In Vitro1. Biology of Reproduction. 2010;82(6):1180-9.
242. Xu M, Barrett SL, West-Farrell E, Kondapalli LA, Kiesewetter SE, Shea LD, et al. In vitro grown human ovarian follicles from cancer patients support oocyte growth. Human Reproduction. 2009;24(10):2531-40.
243. Wycherley G, Downey D, Kane MT, Hynes AC. A novel follicle culture system markedly increases follicle volume, cell number and oestradiol secretion. Reproduction. 2004;127(6):669-77.
244. Revel A, Koler M, Simon A, Lewin A, Laufer N, Safran A. Oocyte collection during cryopreservation of the ovarian cortex. Fertil Steril. 2003;79(5):1237-9.
245. Gosden R. Low temperature storage and grafting of human ovarian tissue. Molecular and cellular endocrinology. 2000;163(1-2):125-9.
246. Newton H, Aubard Y, Rutherford A, Sharma V, Gosden R. Ovary and ovulation: Low temperature storage and grafting of human ovarian tissue. Human reproduction. 1996;11(7):1487-91.
247. Revel A, Laufer N, Ben Meir A, Lebovich M, Mitrani E. Micro-organ ovarian transplantation enables pregnancy: a case report. Human Reproduction. 2011;26(5):1097-103.
248. Revel A, Revel-Vilk S, Aizenman E, Porat-Katz A, Safran A, Ben-meir A, et al. At what age can human oocytes be obtained? Fertility and Sterility. 2009;92(2):458-63.
249. Wei X. DPhil Thesis. 2018.
250. Anderson RA, Wallace WHB, Telfer EE. Ovarian tissue cryopreservation for fertility preservation: clinical and research perspectives. Human Reproduction Open. 2017;2017(1):hox001-hox.
251. Picton HM, Gosden RG. In vitro growth of human primordial follicles from frozen-banked ovarian tissue. Molecular and Cellular Endocrinology. 2000;166(1):27-35.
252. Isachenko V, Mallmann P, Petrunkina AM, Rahimi G, Nawroth F, Hancke K, et al. Comparison of in vitro-and chorioallantoic membrane (CAM)-culture systems for cryopreserved medulla-contained human ovarian tissue. PLoS One. 2012;7(3):e32549.
253. Sanfilippo S, Canis M, Romero S, Sion B, Déchelotte P, Pouly J-L, et al. Quality and functionality of human ovarian tissue after cryopreservation using an original slow freezing procedure. Journal of assisted reproduction and genetics. 2013;30(1):25-34.
254. Hreinsson J, Zhang P, Swahn ML, Hultenby K, Hovatta O. Cryopreservation of follicles in human ovarian cortical tissue. Comparison of serum and human serum albumin in the cryoprotectant solutions. Hum Reprod. 2003;18(11):2420-8.

255. Allison A, Young M. Uptake of dyes and drugs by living cells in culture. Life sciences. 1964;3(12):1407-14.
256. Borenfreund E, Puerner JA. Toxicity determined in vitro by morphological alterations and neutral red absorption. Toxicology letters. 1985;24(2-3):119-24.
257. Chambers E, Gosden R, Yap C, Picton H. In situ identification of follicles in ovarian cortex as a tool for quantifying follicle density, viability and developmental potential in strategies to preserve female fertility. Human reproduction. 2010;25(10):2559-68.
258. Practice Committee of the American Society for Reproductive Medicine. Ovarian tissue cryopreservation: a committee opinion. Fertility and sterility. 2014;101(5):1237-43.
259. Donnez J, Dolmans M-M. Fertility preservation in women. New England Journal of Medicine. 2017;377(17):1657-65.
260. Yasmin E, Balachandren N, Davies MC, Jones GL, Lane S, Mathur R, et al. Fertility preservation for medical reasons in girls and women: British fertility society policy and practice guideline. Human Fertility. 2018;21(1):3-26.
261. Schneider CA, Rasband WS, Eliceiri KW. NIH Image to ImageJ: 25 years of image analysis. Nature methods. 2012;9(7):671.
262. Bates D, Mächler M, Bolker B, Walker S. Fitting linear mixed-effects models using lme4. arXiv preprint arXiv:14065823. 2014.
263. Donnez J, Martinez-Madrid B, Jadoul P, Van Langendonckt A, Demylle D, Dolmans M-M. Ovarian tissue cryopreservation and transplantation: a review. Human reproduction update. 2006;12(5):519-35.
264. Qu J, Godin PA, Nisolle M, Donnez J. Distribution and epidermal growth factor receptor expression of primordial follicles in human ovarian tissue before and after cryopreservation. Human Reproduction. 2000;15(2):302-10.
265. Hovatta O, Silye R, Krausz T, Abir R, Margara R, Trew G, et al. Cryopreservation of human ovarian tissue using dimethylsulphoxide and propanediol-sucrose as cryoprotectants. Human Reproduction. 1996;11(6):1268-72.
266. Gook DA, Edgar DH, Stern C. Effect of cooling rate and dehydration regimen on the histological appearance of human ovarian cortex following cryopreservation in 1, 2-propanediol. Hum Reprod. 1999;14(8):2061-8.
267. Siebzehnrübl E, Kohl J, Dittrich R, Wildt L. Freezing of human ovarian tissue—not the oocytes but the granulosa is the problem. Molecular and cellular endocrinology. 2000;169(1-2):109-11.
268. Maltaris T, Kaya H, Hoffmann I, Mueller A, Beckmann MW, Dittrich R. Comparison of xenografting in SCID mice and LIVE/DEAD assay as a predictor of the developmental potential of cryopreserved ovarian tissue. In Vivo. 2006;20(1):11-6.
269. Friedler S, Koc O, Gidoni Y, Raziel A, Ron-El R. Ovarian response to stimulation for fertility preservation in women with malignant disease: a systematic review and meta-analysis. Fertility and Sterility. 2012;97(1):125-33.
270. Kristensen SG, Rasmussen A, Byskov AG, Andersen CY. Isolation of pre-antral follicles from human ovarian medulla tissue. Human reproduction. 2010;26(1):157-66.
271. West ER, Shea LD, Woodruff TK, editors. Engineering the follicle microenvironment. Seminars in reproductive medicine; 2007: NIH Public Access.
272. Albertini DF, Fawcett DW, Olds PJ. Morphological variations in gap junctions of ovarian granulosa cells. Tissue and cell. 1975;7(2):389-405.
273. Albertini DF, Combelles C, Benecchi E, Carabatsos MJ. Cellular basis for paracrine regulation of ovarian follicle development. Reproduction. 2001;121(5):647-53.
274. Oktay K, Newton H, Mullan J, Gosden R. Development of human primordial follicles to antral stages in SCID/hpg mice stimulated with follicle stimulating hormone. Human reproduction (Oxford, England). 1998;13(5):1133-8.
275. Dolmans M-M, Martinez-Madrid B, Gadisseux E, Guiot Y, Yuan WY, Torre A, et al. Short-term transplantation of isolated human ovarian follicles and cortical tissue into nude mice. Reproduction. 2007;134(2):253-62.
276. Stubbs SA, Stark J, Dilworth SM, Franks S, Hardy K. Abnormal preantral folliculogenesis in polycystic ovaries is associated with increased granulosa cell division. The Journal of Clinical Endocrinology & Metabolism. 2007;92(11):4418-26.
277. Poirot C, Vacher-Lavenu M-C, Helardot P, Guibert J, Brugières L, Jouannet P. Human ovarian tissue cryopreservation: indications and feasibility. Human Reproduction. 2002;17(6):1447-52.

278. Jensen AK, Kristensen SG, Macklon KT, Jeppesen JV, Fedder J, Ernst E, et al. Outcomes of transplantations of cryopreserved ovarian tissue to 41 women in Denmark. Human Reproduction. 2015;30(12):2838-45.
279. Webber L, Stubbs S, Stark J, Trew G, Margara R, Hardy K, et al. Formation and early development of follicles in the polycystic ovary. The Lancet. 2003;362(9389):1017-21.
280. Anderson RA, McLaughlin M, Wallace WHB, Albertini DF, Telfer EE. The immature human ovary shows loss of abnormal follicles and increasing follicle developmental competence through childhood and adolescence. Human Reproduction. 2014;29(1):97-106.
281. Mosammaparast N, Kim H, Laurent B, Zhao Y, Lim HJ, Majid MC, et al. The histone demethylase LSD1/KDM1A promotes the DNA damage response. J Cell Biol. 2013;203(3):457-70.
282. Metzger E, Wissmann M, Yin N, Müller JM, Schneider R, Peters AH, et al. LSD1 demethylates repressive histone marks to promote androgen-receptor-dependent transcription. Nature. 2005;437(7057):436-9.
283. Shi Y, Lan F, Matson C, Mulligan P, Whetstine JR, Cole PA, et al. Histone demethylation mediated by the nuclear amine oxidase homolog LSD1. Cell. 2004;119(7):941-53.
284. Wang J, Hevi S, Kurash JK, Lei H, Gay F, Bajko J, et al. The lysine demethylase LSD1 (KDM1) is required for maintenance of global DNA methylation. Nat Genet. 2009;41(1):125-9.
285. Rudolph T, Yonezawa M, Lein S, Heidrich K, Kubicek S, Schäfer C, et al. Heterochromatin Formation in Drosophila Is Initiated through Active Removal of H3K4 Methylation by the LSD1 Homolog SU(VAR)3-3. Molecular Cell. 2007;26(1):103-15.
286. Katz DJ, Edwards TM, Reinke V, Kelly WG. A C. elegans LSD1 Demethylase Contributes to Germline Immortality by Reprogramming Epigenetic Memory. Cell. 2009;137(2):308-20.
287. Kim J, Singh AK, Takata Y, Lin K, Shen J, Lu Y, et al. LSD1 is essential for oocyte meiotic progression by regulating CDC25B expression in mice. Nature Communications. 2015;6:10116.
288. Duteil D, Metzger E, Willmann D, Karagianni P, Friedrichs N, Greschik H, et al. LSD1 promotes oxidative metabolism of white adipose tissue. Nat Commun. 2014;5:4093.
289. Hino S, Sakamoto A, Nagaoka K, Anan K, Wang Y, Mimasu S, et al. FAD-dependent lysine-specific demethylase-1 regulates cellular energy expenditure. Nature Communications. 2012;3:758.
290. Structural Genomics Consortium. GSK-LSD1 A chemical probe for LSD1 https://www.thesgc.org/chemical-probes/GSK-LSD1: SGC.org; 2018 [
291. Venables W, Ripley B. Random and mixed effects. Modern applied statistics with S: Springer; 2002. p. 271-300.
292. Hao J, Tuck AR, Sjödin MOD, Lindberg J, Sand A, Niklasson B, et al. Resveratrol supports and alpha-naphthoflavone disrupts growth of human ovarian follicles in an in vitro tissue culture model. Toxicology and applied pharmacology. 2018;338:73-82.
293. Bannister AJ, Kouzarides T. Reversing histone methylation. Nature. 2005;436(7054):1103.
294. Wasson JA, Simon AK, Myrick DA, Wolf G, Driscoll S, Pfaff SL, et al. Maternally provided LSD1/KDM1A enables the maternal-to-zygotic transition and prevents defects that manifest postnatally. Elife. 2016;5:e08848.
295. Serge M, Christian V, Marc-André S. Temporal expression of factors involved in chromatin remodeling and in gene regulation during early bovine in vitro embryo development. Reproduction. 2007;133(3):597-608.
296. Marcelo MS, Maren G, Bruce DM, Sarah K, Vilceu B. Developmental regulation of histone H3 methylation at lysine 4 in the porcine ovary. REPRODUCTION. 2008;135(6):829-38.
297. Oktem O, Oktay K. A novel ovarian xenografting model to characterize the impact of chemotherapy agents on human primordial follicle reserve. Cancer research. 2007;67(21):10159-62.
298. Bock C. Analysing and interpreting DNA methylation data. Nat Rev Genet. 2012;13(10):705-19.
299. Rotem A, Ram O, Shoresh N, Sperling RA, Goren A, Weitz DA, et al. Single-cell ChIP-seq reveals cell subpopulations defined by chromatin state. Nature biotechnology. 2015;33(11):1165.
300. Zuang V. The neutral red release assay: a review. ATLA-NOTTINGHAM-. 2001;29(5):575-600.
301. Hertig AT, Adams EC. Studies on the human oocyte and its follicle: I. Ultrastructural and histochemical observations on the primordial follicle stage. The Journal of cell biology. 1967;34(2):647-75.
302. Soleimani R, De Vos W, Van Oostveldt P, Lierman S, Van den Broecke R, De Sutter P, et al. Two novel techniques to detect follicles in human ovarian cortical tissue. Human Reproduction. 2006;21(7):1720-4.

303. Cortvrindt RG, Smitz JE. Fluorescent probes allow rapid and precise recording of follicle density and staging in human ovarian cortical biopsy samples. Fertility and sterility. 2001;75(3):588-93.
304. Takenaka M, Horiuchi T, Yanagimachi R. Effects of light on development of mammalian zygotes. Proceedings of the National Academy of Sciences. 2007;104(36):14289-93.
305. Hockberger PE, Skimina TA, Centonze VE, Lavin C, Chu S, Dadras S, et al. Activation of flavin-containing oxidases underlies light-induced production of H2O2 in mammalian cells. Proceedings of the National Academy of Sciences. 1999;96(11):6255-60.
306. Thermo Fisher Scientific. LIVE/DEAD™ Fixable Near-IR Dead Cell Stain Kit, for 633 or 635 nm excitation https://www.thermofisher.com/2018 [Available from: https://www.thermofisher.com/order/catalog/product/L10119.
307. Eppig JJ, O'Brien MJ. Comparison of preimplantation developmental competence after mouse oocyte growth and development in vitro and in vivo. Theriogenology. 1998;49(2):415-22.
308. O'Brien MJ, Pendola JK, Eppig JJ. A revised protocol for in vitro development of mouse oocytes from primordial follicles dramatically improves their developmental competence. Biology of reproduction. 2003;68(5):1682-6.
309. Hornick J, Duncan FE, Shea L, Woodruff TK. Multiple follicle culture supports primary follicle growth through paracrine-acting signals. Reproduction. 2013;145(1):19-32.
310. Da Silva-Buttkus P, Marcelli G, Franks S, Stark J, Hardy K. Inferring biological mechanisms from spatial analysis: Prediction of a local inhibitor in the ovary. Proceedings of the National Academy of Sciences. 2009;106(2):456.
311. Gaytan F, Morales C, Leon S, Garcia-Galiano D, Roa J, Tena-Sempere M. Crowding and follicular fate: spatial determinants of follicular reserve and activation of follicular growth in the mammalian ovary. PLoS One. 2015;10(12):e0144099.
312. Yang MY, Rajamahendran R. Morphological and Biochemical Identification of Apoptosis in Small, Medium, and Large Bovine Follicles and the Effects of Follicle-Stimulating Hormone and Insulin-Like Growth Factor-I on Spontaneous Apoptosis in Cultured Bovine Granulosa Cells1. Biology of Reproduction. 2000;62(5):1209-17.
313. Tilly JL, Tilly K. Inhibitors of oxidative stress mimic the ability of follicle-stimulating hormone to suppress apoptosis in cultured rat ovarian follicles. Endocrinology. 1995;136(1):242-52.
314. Tsai-Turton M, Luderer U. Opposing effects of glutathione depletion and follicle-stimulating hormone on reactive oxygen species and apoptosis in cultured preovulatory rat follicles. Endocrinology. 2006;147(3):1224-36.
315. Harris SE, Leese HJ, Gosden RG, Picton HM. Pyruvate and oxygen consumption throughout the growth and development of murine oocytes. Molecular Reproduction and Development: Incorporating Gamete Research. 2009;76(3):231-8.
316. Boland N, Humpherson P, Leese H, Gosden R. Pattern of lactate production and steroidogenesis during growth and maturation of mouse ovarian follicles in vitro. Biology of reproduction. 1993;48(4):798-806.
317. Dorrington J, Chuma AV, Bendell JJ. Transforming growth factor β and follicle-stimulating hormone promote rat granulosa cell proliferation. Endocrinology. 1988;123(1):353-9.
318. Hulshof SCJ, Figueiredo JR, Beckers JF, Bevers MM, van der Donk JA, van den Hurk R. Effects of fetal bovine serum, FSH and 17β-estradiol on the culture of bovine preantral follicles. Theriogenology. 1995;44(2):217-26.
319. Wandji SA, Eppig JJ, Fortune JE. FSH and growth factors affect the growth and endocrine function in vitro of granulosa cells of bovine preantral follicles. Theriogenology. 1996;45(4):817-32.
320. Telfer EE, Mclaughlin M. Strategies to support human oocyte development in vitro. International Journal of Developmental Biology. 2013;56(10-11-12):901-7.
321. Kawamura K, Cheng Y, Suzuki N, Deguchi M, Sato Y, Takae S, et al. Hippo signaling disruption and Akt stimulation of ovarian follicles for infertility treatment. Proceedings of the National Academy of Sciences. 2013;110(43):17474-9.
322. Telfer EE, editor Growing human eggs *in vitro*. 2nd UK Fertility Preservation Conference; 2018 14/09/2018; St Anne's College, Oxford, UK.
323. Faustino L, Santos R, Silva C, Pinto L, Celestino J, Campello C, et al. Goat and sheep ovarian tissue cryopreservation: effects on the morphology and development of primordial follicles and density of stromal cell. Animal reproduction science. 2010;122(1-2):90-7.

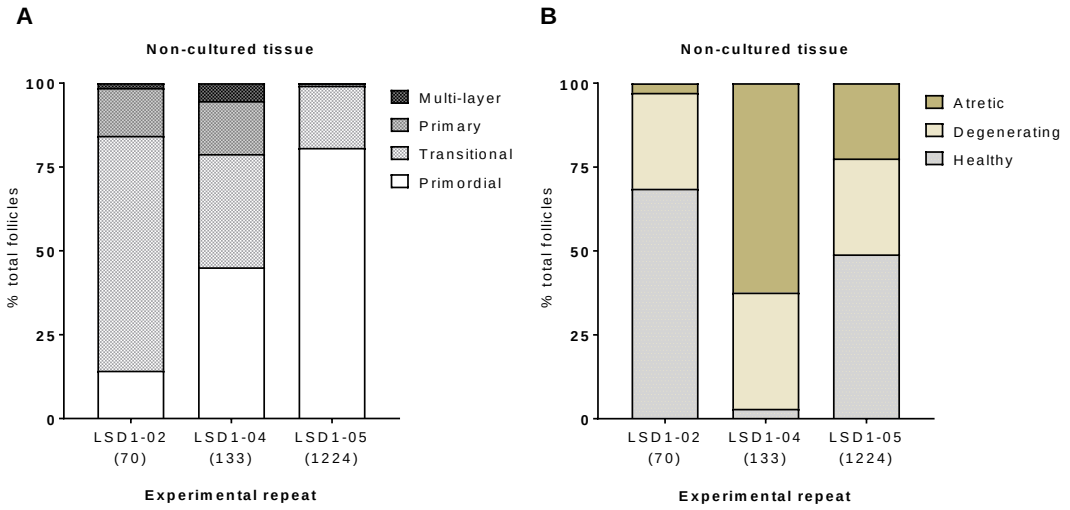
324. Oskam IC, Asadi BA, Santos RR. Histologic and ultrastructural features of cryopreserved ovine ovarian tissue: deleterious effect of 1, 2-propanediol applying different thawing protocols. Fertility and sterility. 2010;93(8):2764-6.
325. Fabbri R, Pasquinelli G, Keane D, Magnani V, Paradisi R, Venturoli S. Optimization of protocols for human ovarian tissue cryopreservation with sucrose, 1,2-propanediol and human serum. Reproductive BioMedicine Online. 2010;21(6):819-28.
326. Oskam I, Lund T, Santos R. Irreversible damage in ovine ovarian tissue after cryopreservation in propanediol: analyses after in vitro culture and xenotransplantation. Reproduction in Domestic Animals. 2011;46(5):793-9.
327. Maffei S, Hanenberg M, Pennarossa G, Silva JRV, Brevini TAL, Arav A, et al. Direct comparative analysis of conventional and directional freezing for the cryopreservation of whole ovaries. Fertility and Sterility. 2013;100(4):1122-31.
328. Lamble S, Batty E, Attar M, Buck D, Bowden R, Lunter G, et al. Improved workflows for high throughput library preparation using the transposome-based nextera system. BMC Biotechnology. 2013;13(1):104.
329. Kim D, Langmead B, Salzberg SL. HISAT: a fast spliced aligner with low memory requirements. Nat Methods. 2015;12(4):357-60.
330. Broad Institute. Picard Tools Cambridge, MA2018 [Available from: http://broadinstitute.github.io/picard.
331. Liao Y, Smyth GK, Shi W. featureCounts: an efficient general purpose program for assigning sequence reads to genomic features. Bioinformatics. 2014;30(7):923-30.
332. Gentleman RC, Carey VJ, Bates DM, Bolstad B, Dettling M, Dudoit S, et al. Bioconductor: open software development for computational biology and bioinformatics. Genome biology. 2004;5(10):R80.
333. Robinson MD, McCarthy DJ, Smyth GK. edgeR: a Bioconductor package for differential expression analysis of digital gene expression data. Bioinformatics. 2010;26(1):139-40.
334. Herwig R, Hardt C, Lienhard M, Kamburov A. Analyzing and interpreting genome data at the network level with ConsensusPathDB. Nature Protocols. 2016;11:1889.
335. Supek F, Bosnjak M, Skunca N, Smuc T. REVIGO summarizes and visualizes long lists of gene ontology terms. PLoS One. 2011;6(7):e21800.
336. Bruick RK, McKnight SL. A conserved family of prolyl-4-hydroxylases that modify HIF. Science. 2001;294(5545):1337-40.
337. Epstein ACR, Gleadle JM, McNeill LA, Hewitson KS, O'Rourke J, Mole DR, et al. C. elegans EGL-9 and mammalian homologs define a family of dioxygenases that regulate HIF by prolyl hydroxylation. Cell. 2001;107(1):43-54.
338. Ivan M, Haberberger T, Gervasi DC, Michelson KS, Günzler V, Kondo K, et al. Biochemical purification and pharmacological inhibition of a mammalian prolyl hydroxylase acting on hypoxia-inducible factor. Proceedings of the National Academy of Sciences of the United States of America. 2002;99(21):13459-64.
339. Luo C, Widlund HR, Puigserver P. PGC-1 coactivators: shepherding the mitochondrial biogenesis of tumors. Trends in cancer. 2016;2(10):619-31.
340. Babariya D, Fragouli E, Alfarawati S, Spath K, Wells D. The incidence and origin of segmental aneuploidy in human oocytes and preimplantation embryos. Human Reproduction. 2017;32(12):2549-60.
341. Chui D, Pugh N, Walker S, Gregory L, Shaw R. Follicular vascularity--the predictive value of transvaginal power Doppler ultrasonography in an in-vitro fertilization programme: a preliminary study. Human reproduction (Oxford, England). 1997;12(1):191-6.
342. Van Blerkom J, Antczak M, Schrader R. The developmental potential of the human oocyte is related to the dissolved oxygen content of follicular fluid: association with vascular endothelial growth factor levels and perifollicular blood flow characteristics. Human reproduction (Oxford, England). 1997;12(5):1047-55.
343. Makker A, Goel MM, Mahdi AA. PI3K/PTEN/Akt and TSC/mTOR signaling pathways, ovarian dysfunction and infertility: an update. Journal of molecular endocrinology. 2014:JME-14-0220.
344. Goto M, Iwase A, Ando H, Kurotsuchi S, Harata T, Kikkawa F. PTEN and Akt expression during growth of human ovarian follicles. Journal of assisted reproduction and genetics. 2007;24(11):541-6.
345. Chen WS, Xu P-Z, Gottlob K, Chen M-L, Sokol K, Shiyanova T, et al. Growth retardation and increased apoptosis in mice with homozygous disruption of the Akt1 gene. Genes & development. 2001;15(17):2203-8.

346. Brown C, LaRocca J, Pietruska J, Ota M, Anderson L, Duncan Smith S, et al. Subfertility Caused by Altered Follicular Development and Oocyte Growth in Female Mice Lacking PKBalpha/Akt11. Biology of Reproduction. 2010;82(2):246-56.
347. Artini PG, Tatone C, Sperduti S, D'Aurora M, Franchi S, Di Emidio G, et al. Cumulus cells surrounding oocytes with high developmental competence exhibit down-regulation of phosphoinositol 1,3 kinase/protein kinase B (PI3K/AKT) signalling genes involved in proliferation and survival. Human Reproduction. 2017;32(12):2474-84.
348. Rodgers RJ, Irving-Rodgers HF, Russell DL. Extracellular matrix of the developing ovarian follicle. Reproduction. 2003;126(4):415-24.
349. Kreeger PK, Deck JW, Woodruff TK, Shea LD. The in vitro regulation of ovarian follicle development using alginate-extracellular matrix gels. Biomaterials. 2006;27(5):714-23.
350. Berkholtz CB, Shea LD, Woodruff TK, editors. Extracellular matrix functions in follicle maturation. Seminars in reproductive medicine; 2006: NIH Public Access.
351. Bolz H, Ramírez A, von Brederlow B, Kubisch C. Characterization of ADAMTS14, a novel member of the ADAMTS metalloproteinase family. Biochim Biophys Acta. 2001;1522(3):221-5.
352. O'Shea LC, Mehta J, Lonergan P, Hensey C, Fair T. Developmental competence in oocytes and cumulus cells: candidate genes and networks. Systems biology in reproductive medicine. 2012;58(2):88-101.
353. Lind AK, WeijdegÅRd B, Dahm-KÄHler P, Mölne J, Sundfeldt K, BrÄNnstrÖM M. Collagens in the human ovary and their changes in the perifollicular stroma during ovulation. Acta Obstetricia et Gynecologica Scandinavica. 2010;85(12):1476-84.
354. Chandrasekher YA, Brenner R, Molskness T, Yu Q, Stouffer R. Titrating luteinizing hormone surge requirements for ovulatory changes in primate follicles. II. Progesterone receptor expression in luteinizing granulosa cells. The Journal of Clinical Endocrinology & Metabolism. 1991;73(3):584-9.
355. Yan-Guang W, David HB, Vitaly AK, Emanuela L, Qi W, David FA, et al. Aging-related premature luteinization of granulosa cells is avoided by early oocyte retrieval. Journal of Endocrinology. 2015;226(3):167-80.
356. Szołtys M, Słomczyńska M, Knapczyk-Stwora K, Durlej M, Lechowska A, Starowicz A. Immunolocalization of androgen receptor and steroidogenic enzymes in cumuli oophori of pre-and post-ovulatory rats. Acta histochemica. 2010;112(6):576-82.
357. Hamamah S, Matha V, Berthenet C, Anahory T, Loup V, Dechaud H, et al. Comparative protein expression profiling in human cumulus cells in relation to oocyte fertilization and ovarian stimulation protocol. Reproductive BioMedicine Online. 2006;13(6):807-14.
358. Cruz M, Requena A, Agudo D, García-Velasco JA. Type of gonadotropin used during controlled ovarian stimulation induces differential gene expression in human cumulus cells: A randomized study. European Journal of Obstetrics & Gynecology and Reproductive Biology. 2017;215:124-33.
359. Grøndahl ML, Borup R, Lee YB, Myrhøj V, Meinertz H, Sørensen S. Differences in gene expression of granulosa cells from women undergoing controlled ovarian hyperstimulation with either recombinant follicle-stimulating hormone or highly purified human menopausal gonadotropin. Fertility and Sterility. 2009;91(5):1820-30.
360. D'haeseleer P, Liang S, Somogyi R. Genetic network inference: from co-expression clustering to reverse engineering. Bioinformatics. 2000;16(8):707-26.
361. Zhang B, Horvath S. A general framework for weighted gene co-expression network analysis. Statistical applications in genetics and molecular biology. 2005;4(1).
362. Hawkins RD, Hon GC, Ren B. Next-generation genomics: an integrative approach. Nature Reviews Genetics. 2010;11(7):476.
363. Zhu P, Guo H, Ren Y, Hou Y, Dong J, Li R, et al. Single-cell DNA methylome sequencing of human preimplantation embryos. Nature genetics. 2018;50(1):12.
364. Guo F, Yan L, Guo H, Li L, Hu B, Zhao Y, et al. The Transcriptome and DNA Methylome Landscapes of Human Primordial Germ Cells. Cell. 2015;161(6):1437-52.
365. Kristensen SG, Liu Q, Mamsen LS, Greve T, Pors SE, Bjørn AB, et al. A simple method to quantify follicle survival in cryopreserved human ovarian tissue. Human Reproduction. 2018;33(12):2276-84.
366. Nisolle M, Casanas-Roux F, Qu J, Motta P, Donnez J. Histologic and ultrastructural evaluation of fresh and frozen-thawed human ovarian xenografts in nude mice. Fertility and sterility. 2000;74(1):122-9.

367. Bertoldo MJ, Walters KA, Ledger WL, Gilchrist RB, Mermillod P, Locatelli Y. In-vitro regulation of primordial follicle activation: challenges for fertility preservation strategies. Reproductive BioMedicine Online. 2018;36(5):491-9.
368. Louhio H, Hovatta O, Sjöberg J, Tuuri T. The effects of insulin, and insulin-like growth factors I and II on human ovarian follicles in long-term culture. MHR: Basic science of reproductive medicine. 2000;6(8):694-8.
369. Blackwell LE. In vitro growth and development of ovarian follicles for fertility preservation: University of Leeds; 2014.
370. Lazaraviciute G, Kauser M, Bhattacharya S, Haggarty P, Bhattacharya S. A systematic review and meta-analysis of DNA methylation levels and imprinting disorders in children conceived by IVF/ICSI compared with children conceived spontaneously. Human Reproduction Update. 2014;20(6):840-52.
371. DeBaun MR, Niemitz EL, Feinberg AP. Association of in vitro fertilization with Beckwith-Wiedemann syndrome and epigenetic alterations of LIT1 and H19. The American Journal of Human Genetics. 2003;72(1):156-60.
372. Pliushch G, Schneider E, Schneider T, El Hajj N, Rösner S, Strowitzki T, et al. In vitro maturation of oocytes is not associated with altered deoxyribonucleic acid methylation patterns in children from in vitro fertilization or intracytoplasmic sperm injection. Fertility and Sterility. 2015;103(3):720-7.e1.
373. Kuhtz J, Romero S, De Vos M, Smitz J, Haaf T, Anckaert E. Human in vitro oocyte maturation is not associated with increased imprinting error rates at LIT1, SNRPN, PEG3 and GTL2. Human Reproduction. 2014;29(9):1995-2005.
374. Morison IM, Ramsay JP, Spencer HG. A census of mammalian imprinting. TRENDS in Genetics. 2005;21(8):457-65.
375. Ding CC, Thong KJ, Krishna A, Telfer EE. Activin A inhibits activation of human primordial follicles in vitro. Journal of assisted reproduction and genetics. 2010;27(4):141-7.
376. Ben-Meir A, Burstein E, Borrego-Alvarez A, Chong J, Wong E, Yavorska T, et al. Coenzyme Q10 restores oocyte mitochondrial function and fertility during reproductive aging. Aging cell. 2015;14(5):887-95.
377. Bentov Y, Hannam T, Jurisicova A, Esfandiari N, Casper RF. Coenzyme Q10 supplementation and oocyte aneuploidy in women undergoing IVF-ICSI treatment. Clinical Medicine Insights: Reproductive Health. 2014;8:CMRH. S14681.
378. Taylor T, Das D, Patrick J, Katz S, Johnson L, Crain J. Embryo euploidy rates from advanced maternal age (AMA) patients with and without coenzyme Q10 (COQ10) supplemntation: a pilot study and randomized control trial. Fertility and Sterility. 2018;110(4):e406.
379. Hikabe O, Hamazaki N, Nagamatsu G, Obata Y, Hirao Y, Hamada N, et al. Reconstitution in vitro of the entire cycle of the mouse female germ line. Nature. 2016;539(7628):299.
380. Morohaku K, Tanimoto R, Sasaki K, Kawahara-Miki R, Kono T, Hayashi K, et al. Complete in vitro generation of fertile oocytes from mouse primordial germ cells. Proceedings of the National Academy of Sciences. 2016;113(32):9021-6.
381. Oktem O, Oktay K. The ovary. Annals of the New York academy of sciences. 2008;1127(1):1-9.
382. Faddy M, Gosden R. Physiology: A mathematical model of follicle dynamics in the human ovary. Human Reproduction. 1995;10(4):770-5.
383. Botling J, Edlund K, Segersten U, Tahmasebpoor S, Engström M, Sundström M, et al. Impact of Thawing on RNA Integrity and Gene Expression Analysis in Fresh Frozen Tissue. Diagnostic Molecular Pathology. 2009;18(1):44-52.

Appendix I.

Variation in follicle health and development in non-cultured tissue prior to LSD1 treatment



Supplementary Figure 1 Developmental stage and health of follicles from non-cultured human tissue cryopreserved for fertility preservation

Data is presented as percentage of total follicles with the total follicle number listed in brackets. A) The percentage of follicles at various stages of development varied between patients in non-cultured tissue. LSD1-05 had a dominant primordial population, however LSD1-02 and -04 primarily had growing follicles. B) The percentage of follicles that were healthy, degenerating, or atretic in non-cultured tissue varied between patients. Follicles in LSD1-02 and -05 were primarily healthy, however those in LSD1-04 were largely atretic. Follicle numbers in parentheses.

Appendix II.

Medium composition of McCoy's 5A and αMEM

		αMEM medium #22561021	**McCoy's 5A (modified) HEPES buffered medium** #22330021
Components	**Molecular Weight**	**Concentration (mg/L)**	**Concentration (mg/L)**
Amino Acids			
L-Alanine	89	25	13
L-Arginine	211	105	-
L-Asparagine	132	-	45
L-Asparagine-H2O	150	50	-
L-Aspartic acid	133	30	20
L-Cysteine	121	-	32
L-Cysteine hydrochloride-H2O	176	100	-
L-Cystine	313	31	-
L-Glutamic Acid	147	75	22
L-Glutamine	146	292	219
Glycine	75	50	8
L-Histidine	155	31	-
L-Histidine-HCl-H2O	210	-	21
L-Hydroxyproline	131	-	20
L-Isoleucine	131	52	39
L-Leucine	131	52	39
L-Lysine	183	73	-
L-Lysine hydrochloride	183	-	37
L-Methionine	149	15	15
L-Phenylalanine	165	32	17
L-Proline	115	40	17
L-Serine	105	25	26
L-Threonine	119	48	18
L-Tryptophan	204	10	3
L-Tyrosine	181	36	18
L-Valine	117	46	18
Vitamins			
Ascorbic Acid	176	50	0.5
Biotin	244	0.1	0.2
Choline chloride	140	1	5
D-Calcium pantothenate	477	1	0.2
Folic Acid	441	1	10

		αMEM medium #22561021	**McCoy's 5A (modified) HEPES buffered medium** #22330021
Components	**Molecular Weight**	**Concentration (mg/L)**	**Concentration (mg/L)**
i-Inositol	180	2	36
Niacinamide	122	1	0.5
Nicotinic Acid	123	-	0.5
Para-Aminobenzoic Acid	137	-	1
Pyridoxal hydrochloride	204	1	0.5
Pyridoxine hydrochloride	205	-	0.5
Riboflavin	376	0.1	0.2
Thiamine hydrochloride	337	1	0.2
Vitamin B12	1355	1.4	2
Inorganic Salts			
Calcium Chloride (CaCl2-2H2O)	147	264	132
Magnesium Sulfate (MgSO4)	120	98	-
Magnesium Sulfate (MgSO4-7H2O)	246	-	200
Potassium Chloride (KCl)	75	400	400
Sodium Bicarbonate (NaHCO3)	84	2200	2200
Sodium Chloride (NaCl)	58	6800	6460
Sodium Phosphate monobasic (NaH2PO4-2H2O)	156	158	649
Other Components			
Bacto-Peptone		-	600
D-Glucose (Dextrose)	180	1000	3000
Glutathione (reduced)	307	-	0.5
HEPES	238	-	5960
Lipoic Acid	206	0.2	-
Phenol Red	376.4	10	10
Sodium Pyruvate	110	110	-

Appendix III.

Identifying the optimal method for RNA extraction

Three isolation protocols were tested to ascertain which gave the greatest yield and highest quality RNA. Cambridge Bioscience and Qiagen technical support recommended protocols based on their in-house and customer experience given the parameters of the cells used in the study.

Materials and methods

Cumulus cell samples

Samples which were not eligible for RNA-seq analysis or qPCR validation were used in these experiments (Supplementary Table 1). Five samples were randomly allocated to each protocol.

Supplementary Table 1 Cumulus cell samples used for RNA extraction protocol assessment

	Sample number	Patient age (years)	Oocyte number	Exclusion criteria
Protocol 1: Zymo Quick-RNA Kit from pelleted cells	CC 05	28	9	GV oocytes
	CC 14	31	4	Blood clot
	CC 23	28	4	Blood clot
	CC 35	35	4	GV oocytes
	CC 53	31	4	GV oocytes
Protocol 2: Zymo Quick-RNA Kit lysed from frozen	CC 10	33	14	GV oocytes
	CC 15	35	12	GV oocytes
	CC 32	35	8	GV oocytes
	CC 42	30	6	GV oocytes
	CC 54	30	4	GV oocytes
Protocol 3: TRIzol and Qiagen RNeasy Micro Kit	CC 13	31	4	GV oocytes
	CC 22	28	5	GV oocytes
	CC 33	35	10	GV oocytes
	CC 44	30	5	GV oocytes
	CC 58	35	8	Blood clot

Protocols 1 and 2: RNA extraction using Zymo Quick-RNA Kit

Protocol 1

Frozen samples were thawed on ice and pelleted by centrifugation at 200 x g for 5 min at 4°C. Medium was discarded, the pellet resuspended in 300 µl lysis buffer and extraction continued as per the manufacturer's instructions including on column DNase digestion. RNA was eluted in 15 µl RNase-free water and stored at -80°C until QC.

Protocol 2

Frozen samples were thawed by the addition of 700 µl of lysis buffer mixed well by pipetting. The cell lysate was processed through the "Liquids/Reaction Clean-up" protocol as per the manufacturer's instructions including on column DNase digestion. RNA was eluted in 15 µl RNase-free water and stored at -80°C until QC.

RNA extraction using TRIzol and Qiagen RNeasy Micro Kit

Protocol 3

Frozen samples were thawed by the addition of 1 ml TRIzol reagent and vortexed to homogenise. Homogenate was incubated for 5 min at room temperature, chloroform (200 µl per 1 ml TRIzol) was added and shaken vigorously for 20 sec before being incubated at room temperature for a further 3 min. Samples were centrifuged at 12,000 x g for 15 min at 4°C. Centrifugation separated the mixture into a lower red phenol-chloroform, a white interphase, and a colourless upper aqueous phase. Up to 700 µl of the aqueous phase containing the RNA was transferred to a new RNase free tube. One volume of 70% ethanol was added to the aqueous phase and mixed well by pipetting. Samples were transferred to a RNeasy MinElute spin column and processed as per the manufacturer's instructions including on column DNase digestion. RNA was eluted in 15 µl RNase-free water and stored at -80°C.

Measurement of RNA quantity

RNA concentration measurements were quantified by the Qubit 2.0 fluorometer using Qubit® RNA HS Assay Kit. Briefly, 10 μL standards or diluted RNA were mixed with Qubit® Working Solution and incubated for 2 min. The two standards have 0 ng/μL and 10 ng/μL, respectively, and relative fluorescence is plotted against the two concentrations to obtain the calibration curve. Concentration values were calculated by the fluorometers built-in software.

Assessment of RNA integrity

RNA integrity was assessed using the High Sensitivity RNA ScreenTape System on the TapeStation 2200. Briefly, the High Sensitivity RNA ScreenTape device and loading tips were loaded into the 2200 TapeStation instrument. Samples were prepared by mixing 1 μL High Sensitivity RNA Sample Buffer with 2 μL RNA sample and loaded into the TapeStation instrument.

Statistics

All data analysis was performed using GraphPad Prism. A one-way ANOVA was used to test for differences between groups and $p<0.05$ was considered significant. Data is expressed as the mean ± standard deviation.

Results

Parameters of samples used for each protocol

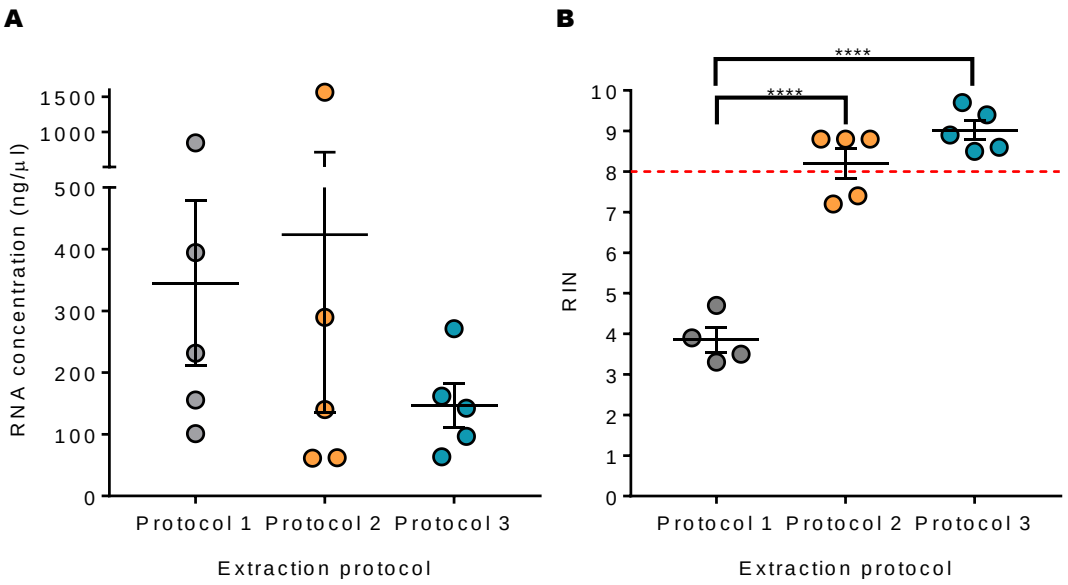
The parameters of samples randomly assigned to each protocol were not significantly different (Supplementary Table 2).

Supplementary Table 2 Characteristics of cumulus cell samples used for RNA extraction protocol assessment. Data are expressed as mean ± standard error.

	Protocol 1	Protocol 2	Protocol 3	P<0.05
Patient age	30.6 ± 1.29	32.6 ± 1.12	31.8 ± 1.39	ns
No. of oocytes/stripping dish	5.0 ± 1.0	8.8 ± 1.86	6.4 ± 1.12	ns
Time in storage (days)	555.2	536.6	533.8	ns
Time from stripping to freezing (min:sec)	30:45	27:12	22:48	ns
Volume of sample (μl)	108	84	64	ns

Effect of RNA yield and quality based on extraction protocol

There was no significant difference in the quantity of RNA isolated from each of the three protocols. A large variation in yield was observed in the two protocols using the Zymo Quick-RNA kit, while a much smaller range was observed in the TRIzol/RNeasy extracted samples (Supplementary Figure 2A). Samples lysed directly from frozen (protocols 2 and 3) had significantly higher RIN values compared those sample that were thawed and spun down before lysis (protocol 1) ($p<0.0001$ and $p<0.000$, respectively). In protocol 1 all samples had a RIN lower than 8, the recommended value for RNA-sequencing, in protocol 2 the mean RIN was above 8 however two of the 5 samples were below the recommended RIN value and in protocol 3 all samples had a RIN score above 8.

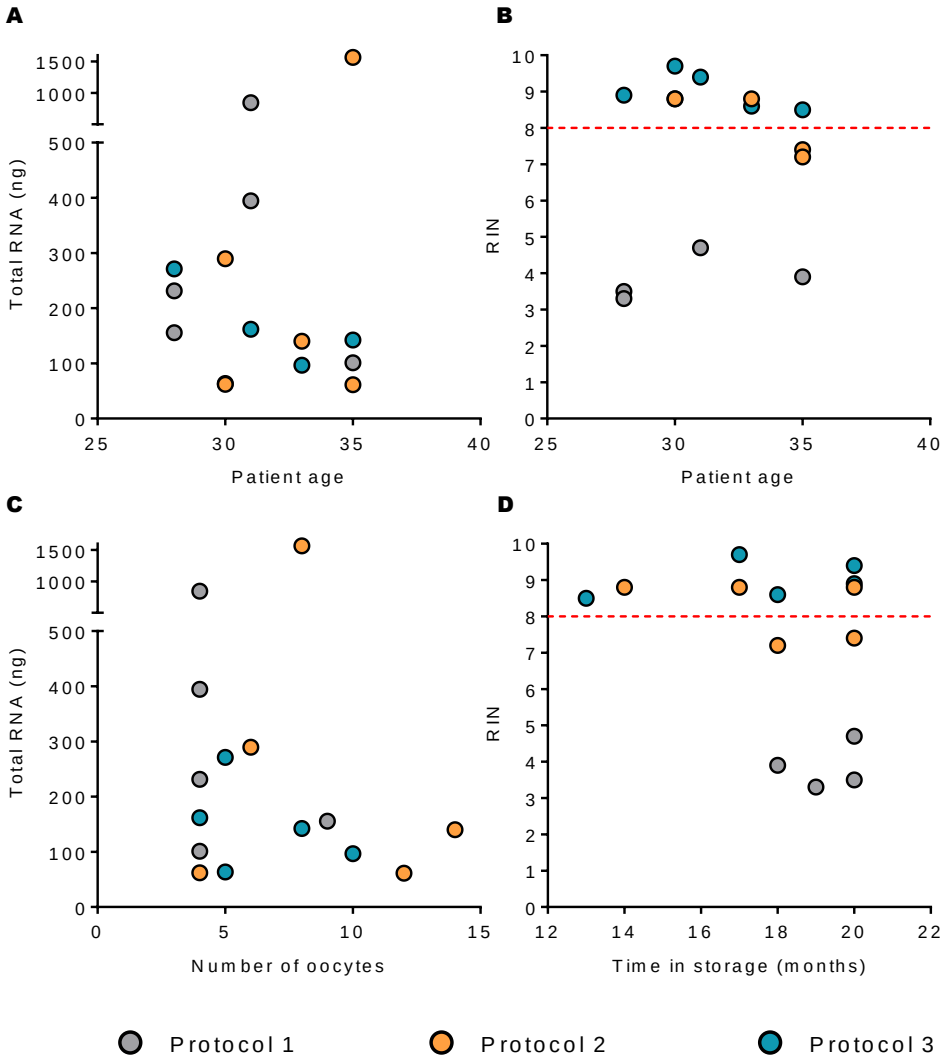


Supplementary Figure 2 RNA parameters as a function of protocol used for extraction.

A) RNA concentration was determined using Qubit and B) quality of RNA was determined using TapeStation. Protocol 1: Zymo Quick-RNA Kit using thawed and pelleted cells, Protocol 2: Zymo Quick-RNA Kit using cells lysed from frozen, Protocol 3: Qiagen RNeasy Micro Kit using TRIzol/chloroform lysed cells. Data expressed as mean ± SEM. Dashed line at Y=8 is the recommended RIN value for RNA-sequencing.

Effect of sample parameters on RNA quantity and quality

Total RNA yield was independent of patient age or the number of oocytes stripped to give a cumulus sample (Supplementary Figure 3A, C). Similarly, RIN score was independent of patient age and time the sample had been in storage at -80°C, and clustering could only be observed based on isolation protocol (Supplementary Figure 3B, D).



Supplementary Figure 3 RNA parameters as a function of sample parameters.

A) Patient age did not affect total RNA yield. B) Patient age did not affect quality of RNA. C) The number of oocytes per stripping dish did not affect total RNA yield. D) Time of sample storage did not affect quality of RNA. Protocol 1: Zymo Quick-RNA Kit using thawed and pelleted cells, Protocol 2: Zymo Quick-RNA Kit using cells lysed from frozen, Protocol 3: Qiagen RNeasy Micro Kit using TRIzol/chloroform lysed cells. Dashed line at Y=8 is the recommended RIN value for RNA-sequencing.

Discussion

Samples thawed before lysis had significantly more degraded RNA. Evidence from frozen tissue suggests that significant RNA degradation starts to occur after 30 minutes (383). A high RNase content of the cell suspensions may mean the cumulus cell samples were more

susceptible to degradation that the tonsil tissue described in the study. Furthermore, repeated freeze thaw cycles have also been demonstrated to have a detrimental effect on RNA integrity and it may be that the combination of delayed lysis and freeze-thaw between isolation and QC was more deleterious to RNA quality than either effect alone.

The protocols did not differ in the yield of RNA however there was a trend towards a lower overall yield from protocol three. This is most likely explained by technical components of this protocol whereby the aqueous phase is manually pipetted off. The white interphase contains genomic DNA and great care must be taken not to transfer this over with the aqueous RNA layer, therefore the amount of the aqueous phase isolated is limited.

Appendix IV.

RNA-seq differentially expressed gene list FDR<0.05

Ensembl ID	Gene symbol	Entrez Gene Name	Log Fold Change	FDR
ENSG00000114771	AADAC	arylacetamide deacetylase	1.354	0.00217
ENSG00000225969	ABHD11-AS1	ABHD11 antisense RNA 1 (tail to tail)	-2.591	0.00436
ENSG00000143322	ABL2	ABL proto-oncogene 2, non-receptor tyrosine kinase	1.109	0.0323
ENSG00000259820	AC0838431		1.81	0.00574
ENSG00000261227	AC1409121		2.645	0.00292
ENSG00000014257	ACPP	acid phosphatase, prostate	1.899	3.98E-05
ENSG00000154930	ACSS1	acyl-CoA synthetase short chain family member 1	-0.853	0.0264
ENSG00000138316	ADAMTS14	ADAM metallopeptidase with thrombospondin type 1 motif 14	-1.18	0.0381
ENSG00000106624	AEBP1	AE binding protein 1	-1.357	0.0377
ENSG00000106546	AHR	aryl hydrocarbon receptor	1.375	0.00371
ENSG00000165092	ALDH1A1	aldehyde dehydrogenase 1 family member A1	2.744	0.0202
ENSG00000133805	AMPD3	adenosine monophosphate deaminase 3	1.108	0.0388
ENSG00000148677	ANKRD1	ankyrin repeat domain 1	1.653	0.0119
ENSG00000165887	ANKRD2	ankyrin repeat domain 2	-2.307	0.0431
ENSG00000107282	APBA1	amyloid beta precursor protein binding family A member 1	-1.314	0.0394
ENSG00000154856	APCDD1	APC down-regulated 1	-1.738	0.0318
ENSG00000112379	ARFGEF3	ARFGEF family member 3	1.638	0.00836
ENSG00000150347	ARID5B	AT-rich interaction domain 5B	0.882	0.0371
ENSG00000188042	ARL4C	ADP ribosylation factor like GTPase 4C	1.279	0.0267
ENSG00000220517	ASS1P1	argininosuccinate synthetase 1 pseudogene 1	1.95	0.0268
ENSG00000068650	ATP11A	ATPase phospholipid transporting 11A	0.785	0.035
ENSG00000133657	ATP13A3	ATPase 13A3	0.95	0.038
ENSG00000166148	AVPR1A	arginine vasopressin receptor 1A	1.791	0.0473
ENSG00000134107	BHLHE40	basic helix-loop-helix family member e40	1.824	0.0159

Ensembl ID	Gene symbol	Entrez Gene Name	Log Fold Change	FDR
ENSG00000023445	BIRC3	baculoviral IAP repeat containing 3	1.684	0.00384
ENSG00000144857	BOC	BOC cell adhesion associated, oncogene regulated	1.554	0.0426
ENSG00000187699	C2orf88	chromosome 2 open reading frame 88	-1.133	0.0282
ENSG00000230185	C9orf147	chromosome 9 open reading frame 147	1.781	0.0111
ENSG00000006116	CACNG3	calcium voltage-gated channel auxiliary subunit gamma 3	-2.928	0.00384
ENSG00000182985	CADM1	cell adhesion molecule 1	-1.437	1.56E-05
ENSG00000141582	CBX4	chromobox 4	-0.926	0.0388
ENSG00000151882	CCL28	C-C motif chemokine ligand 28	3.244	0.01
ENSG00000105810	CDK6	cyclin dependent kinase 6	1.123	0.01
ENSG00000090539	CHRD	chordin	-1.9	0.0441
ENSG00000153132	CLGN	calmegin	-1.267	0.0016
ENSG00000164309	CMYA5	cardiomyopathy associated 5	1.047	0.0273
ENSG00000060718	COL11A1	collagen type XI alpha 1 chain	2.157	0.0152
ENSG00000204291	COL15A1	collagen type XV alpha 1 chain	1.402	0.0257
ENSG00000139219	COL2A1	collagen type II alpha 1 chain	-2.502	0.0131
ENSG00000168542	COL3A1	collagen type III alpha 1 chain	-1.384	0.00059
ENSG00000088882	CPXM1	carboxypeptidase X, M14 family member 1	-1.689	0.0431
ENSG00000150938	CRIM1	cysteine rich transmembrane BMP regulator 1	1.189	0.00253
ENSG00000164796	CSMD3	CUB and Sushi multiple domains 3	3.961	0.0222
ENSG00000116761	CTH	cystathionine gamma-lyase	-1.292	0.00791
ENSG00000180871	CXCR2	C-X-C motif chemokine receptor 2	-2.675	0.0387
ENSG00000148795	CYP17A1	cytochrome P450 family 17 subfamily A member 1	3.532	3.98E-05
ENSG00000153071	DAB2	DAB2, clathrin adaptor protein	1.497	0.00059
ENSG00000163331	DAPL1	death associated protein like 1	-1.762	0.0159
ENSG00000155792	DEPTOR	DEP domain containing MTOR interacting protein	1.768	0.00612
ENSG00000198719	DLL1	delta like canonical Notch ligand 1	-2.206	0.01
ENSG00000105877	DNAH11	dynein axonemal heavy chain 11	3.017	0.0319
ENSG00000171451	DSEL	dermatan sulphate epimerase like	0.755	0.0496
ENSG00000130829	DUSP9	dual specificity phosphatase 9	-1.312	0.0282
ENSG00000188833	ENTPD8	ectonucleoside triphosphate diphosphohydrolase 8	-1.963	0.0377
ENSG00000154928	EPHB1	EPH receptor B1	-1.496	0.01
ENSG00000083782	EPYC	epiphycan	-2.701	0.0057

Ensembl ID	Gene symbol	Entrez Gene Name	Log Fold Change	FDR
ENSG00000012232	EXTL3	exostosin like glycosyltransferase 3	-0.877	0.0468
ENSG00000135472	FAIM2	Fas apoptotic inhibitory molecule 2	-1.886	0.0387
ENSG00000196159	FAT4	FAT atypical cadherin 4	1.208	0.000107
ENSG00000139132	FGD4	FYVE, RhoGEF and PH domain containing 4	1.904	0.01
ENSG00000171557	FGG	fibrinogen gamma chain	2.417	0.0456
ENSG00000150893	FREM2	FRAS1 related extracellular matrix protein 2	1.539	0.00447
ENSG00000139926	FRMD6	FERM domain containing 6	0.887	0.0443
ENSG00000069482	GAL	galanin and GMAP prepropeptide	-2.386	2.28E-05
ENSG00000180447	GAS1	growth arrest specific 1	2.031	0.000124
ENSG00000243236	GSTA9P	glutathione S-transferase alpha 9, pseudogene	1.692	0.0453
ENSG00000168765	GSTM4	glutathione S-transferase mu 4	-0.918	0.0172
ENSG00000162882	HAAO	3-hydroxyanthranilate 3,4-dioxygenase	-1.868	0.01
ENSG00000019991	HGF	hepatocyte growth factor	1.147	0.0172
ENSG00000204632	HLA-G	major histocompatibility complex, class I, G	1.867	0.0282
ENSG00000204622	HLA-J	major histocompatibility complex, class I, J (pseudogene)	2.137	0.0412
ENSG00000025423	HSD17B6	hydroxysteroid 17-beta dehydrogenase 6	2.322	0.01
ENSG00000204388	HSPA1A/HSPA1B	heat shock protein family A (Hsp70) member 1A	1.044	0.0456
ENSG00000225217	HSPA7	heat shock protein family A (Hsp70) member 7	3.186	0.0346
ENSG00000137331	IER3	immediate early response 3	1.439	0.00224
ENSG00000184995	IFNE	interferon epsilon	1.947	0.0431
ENSG00000146678	IGFBP1	insulin like growth factor binding protein 1	3.015	0.00402
ENSG00000257704	INAFM1	InaF motif containing 1	-0.79	0.0496
ENSG00000122641	INHBA	inhibin subunit beta A	1.143	0.0192
ENSG00000123243	ITIH5	inter-alpha-trypsin inhibitor heavy chain family member 5	-1.524	0.0296
ENSG00000135916	ITM2C	integral membrane protein 2C	-0.773	0.0274
ENSG00000154721	JAM2	junctional adhesion molecule 2	1.474	0.00737
ENSG00000120049	KCNIP2	potassium voltage-gated channel interacting protein 2	-1.394	0.0371
ENSG00000135709	KIAA0513	KIAA0513	-0.841	0.0273
ENSG00000139116	KIF21A	kinesin family member 21A	0.954	0.0293
ENSG00000066735	KIF26A	kinesin family member 26A	-2.276	0.048
ENSG00000257271	KIRREL3-AS1	KIRREL3 antisense RNA 1	-1.969	0.0404
ENSG00000102554	KLF5	Kruppel like factor 5	1.437	0.0084

Ensembl ID	Gene symbol	Entrez Gene Name	Log Fold Change	FDR
ENSG00000182591	KRTAP11-1	keratin associated protein 11-1	-3.094	0.00436
ENSG00000112769	LAMA4	laminin subunit alpha 4	-0.953	0.0453
ENSG00000169783	LINGO1	leucine rich repeat and Ig domain containing 1	-1.585	0.0282
ENSG00000136153	LMO7	LIM domain 7	1.384	0.0388
ENSG00000113083	LOX	lysyl oxidase	1.474	0.0412
ENSG00000070018	LRP6	LDL receptor related protein 6	0.864	0.0387
ENSG00000185022	MAFF	MAF bZIP transcription factor F	1.03	0.0197
ENSG00000187243	MAGED4/MAGED4B	MAGE family member D4B	-3.373	0.0237
ENSG00000172005	MAL	mal, T cell differentiation protein	-3.025	5.74E-06
ENSG00000110492	MDK	midkine	-1.484	3.98E-05
ENSG00000214548	MEG3	maternally expressed 3	1.075	0.00767
ENSG00000101752	MIB1	mindbomb E3 ubiquitin protein ligase 1	0.823	0.0325
ENSG00000215417	MIR17HG	miR-17-92a-1 cluster host gene	1.959	0.00858
ENSG00000171843	MLLT3	MLLT3, super elongation complex subunit	1.462	0.00965
ENSG00000163563	MNDA	myeloid cell nuclear differentiation antigen	-2.937	0.00449
ENSG00000205364	MT1M	metallothionein 1M	-1.475	0.00253
ENSG00000229344	MTCO2P12		-4.075	0.00568
ENSG00000101825	MXRA5	matrix remodelling associated 5	-3.213	0.029
ENSG00000134323	MYCN	MYCN proto-oncogene, bHLH transcription factor	1.84	0.0293
ENSG00000133392	MYH11	myosin heavy chain 11	2.41	0.0339
ENSG00000138347	MYPN	myopalladin	2.661	0.00109
ENSG00000173559	NABP1	nucleic acid binding protein 1	0.894	0.0371
ENSG00000090971	NAT14	N-acetyltransferase 14 (putative)	-0.965	0.00818
ENSG00000064300	NGFR	nerve growth factor receptor	-2.099	0.0323
ENSG00000166741	NNMT	nicotinamide N-methyltransferase	-1.428	0.0348
ENSG00000124785	NRN1	neuritin 1	2.19	0.0267
ENSG00000122824	NUDT10	nudix hydrolase 10	-1.214	0.038
ENSG00000198585	NUDT16	nudix hydrolase 16	-1.095	0.0346
ENSG00000244479	OR2A1-AS1	OR2A1 antisense RNA 1	-1.477	0.0282
ENSG00000170909	OSCAR	osteoclast associated, immunoglobulin-like receptor	1.694	0.0431
ENSG00000179270	PCARE	photoreceptor cilium actin regulator	-2.005	0.0343
ENSG00000133027	PEMT	phosphatidylethanolamine N-methyltransferase	-1.415	0.00737

Ensembl ID	Gene symbol	Entrez Gene Name	Log Fold Change	FDR
ENSG00000142102	PGGHG	protein-glucosylgalactosylhydroxylysine glucosidase	-1.683	0.0441
ENSG00000144824	PHLDB2	pleckstrin homology like domain family B member 2	1.511	0.00116
ENSG00000100100	PIK3IP1	phosphoinositide-3-kinase interacting protein 1	2.639	0.0274
ENSG00000141744	PNMT	phenylethanolamine N-methyltransferase	-1.525	0.00222
ENSG00000109819	PPARGC1A	PPARG coactivator 1 alpha	-2.189	0.000217
ENSG00000077157	PPP1R12B	protein phosphatase 1 regulatory subunit 12B	0.958	0.0431
ENSG00000131771	PPP1R1B	protein phosphatase 1 regulatory inhibitor subunit 1B	-2.152	0.00354
ENSG00000059915	PSD	pleckstrin and Sec7 domain containing	-1.651	0.000188
ENSG00000153707	PTPRD	protein tyrosine phosphatase, receptor type D	1.297	0.0356
ENSG00000205517	RGL3	ral guanine nucleotide dissociation stimulator like 3	1.769	0.0273
ENSG00000146373	RNF217	ring finger protein 217	1.187	0.015
ENSG00000069667	RORA	RAR related orphan receptor A	1.076	0.00991
ENSG00000237846	RP11_216M211		2.142	0.0282
ENSG00000224114	RP11_343H54		-7.034	1.16E-08
ENSG00000272267	RP11_375N152		-1.492	0.0325
ENSG00000230325	RP11_385F54		3.063	0.00059
ENSG00000237916	RP11_537E181		1.783	0.0495
ENSG00000259475	RP11_654A163		1.804	0.0365
ENSG00000255393	RP11_736I101		-3.653	0.00059
ENSG00000254343	RP11_760H222		2.397	0.00818
ENSG00000261068	RP11_7K243		-1.974	0.0319
ENSG00000213058	RP4_765C72		-4.495	5.74E-06
ENSG00000215030	RPL13P12	ribosomal protein L13 pseudogene 12	-1.7	0.0172
ENSG00000139970	RTN1	reticulon 1	-1.83	0.0325
ENSG00000198832	SELENOM	selenoprotein M	-1.115	0.0118
ENSG00000075223	SEMA3C	semaphorin 3C	1.308	0.0356
ENSG00000159263	SIM2	SIM bHLH transcription factor 2	-1.675	0.0237
ENSG00000118596	SLC16A7	solute carrier family 16 member 7	1.58	0.00402
ENSG00000259803	SLC22A31	solute carrier family 22 member 31	-2.106	0.00692
ENSG00000166558	SLC38A8	solute carrier family 38 member 8	-2.489	0.0048
ENSG00000138449	SLC40A1	solute carrier family 40 member 1	1.988	0.0293
ENSG00000101276	SLC52A3	solute carrier family 52 member 3	-1.459	0.00109

Ensembl ID	Gene symbol	Entrez Gene Name	Log Fold Change	FDR
ENSG00000154760	SLFN13	schlafen family member 13	1.8	0.0443
ENSG00000184985	SORCS2	sortilin related VPS10 domain containing receptor 2	-2.251	0.0441
ENSG00000198142	SOWAHC	sosondowah ankyrin repeat domain family member C	1.394	0.00059
ENSG00000124766	SOX4	SRY-box 4	1.636	0.0415
ENSG00000152583	SPARCL1	SPARC like 1	-1.509	0.00109
ENSG00000153820	SPHKAP	SPHK1 interactor, AKAP domain containing	0.836	0.0496
ENSG00000139874	SSTR1	somatostatin receptor 1	2.087	9.28E-05
ENSG00000111728	ST8SIA1	ST8 alpha-N-acetyl-neuraminide alpha-2,8-sialyltransferase 1	-1.597	0.0499
ENSG00000138134	STAMBPL1	STAM binding protein like 1	1.584	0.0381
ENSG00000133121	STARD13	StAR related lipid transfer domain containing 13	0.999	0.00449
ENSG00000159167	STC1	stanniocalcin 1	1.698	0.00355
ENSG00000054654	SYNE2	spectrin repeat containing nuclear envelope protein 2	0.944	0.0325
ENSG00000184292	TACSTD2	tumor associated calcium signal transducer 2	2.538	0.0222
ENSG00000130775	THEMIS2	thymocyte selection associated family member 2	-1.336	0.0149
ENSG00000151090	THRB	thyroid hormone receptor beta	2.943	0.00109
ENSG00000144229	THSD7B	thrombospondin type 1 domain containing 7B	-1.799	0.00818
ENSG00000156299	TIAM1	T cell lymphoma invasion and metastasis 1	-1.461	0.0479
ENSG00000198133	TMEM229B	transmembrane protein 229B	-1.044	0.0358
ENSG00000041982	TNC	tenascin C	-1.357	0.0325
ENSG00000164761	TNFRSF11B	TNF receptor superfamily member 11b	2.571	0.0403
ENSG00000127324	TSPAN8	tetraspanin 8	2.703	0.0148
ENSG00000108312	UBTF	upstream binding transcription factor	-0.865	0.0356
ENSG00000147854	UHRF2	ubiquitin like with PHD and ring finger domains 2	0.75	0.0456
ENSG00000117597	UTP25	UTP25, small subunit processor component	0.906	0.0388
ENSG00000197969	VPS13A	vacuolar protein sorting 13 homolog A	0.773	0.0397
ENSG00000111186	WNT5B	Wnt family member 5B	-1.767	0.0286
ENSG00000257315	ZBED6	zinc finger BED-type containing 6	1.033	0.0441
ENSG00000184828	ZBTB7C	zinc finger and BTB domain containing 7C	-1.025	0.0188
ENSG00000181444	ZNF467	zinc finger protein 467	-1.808	0.0172

Appendix V.

Gene ontology analysis

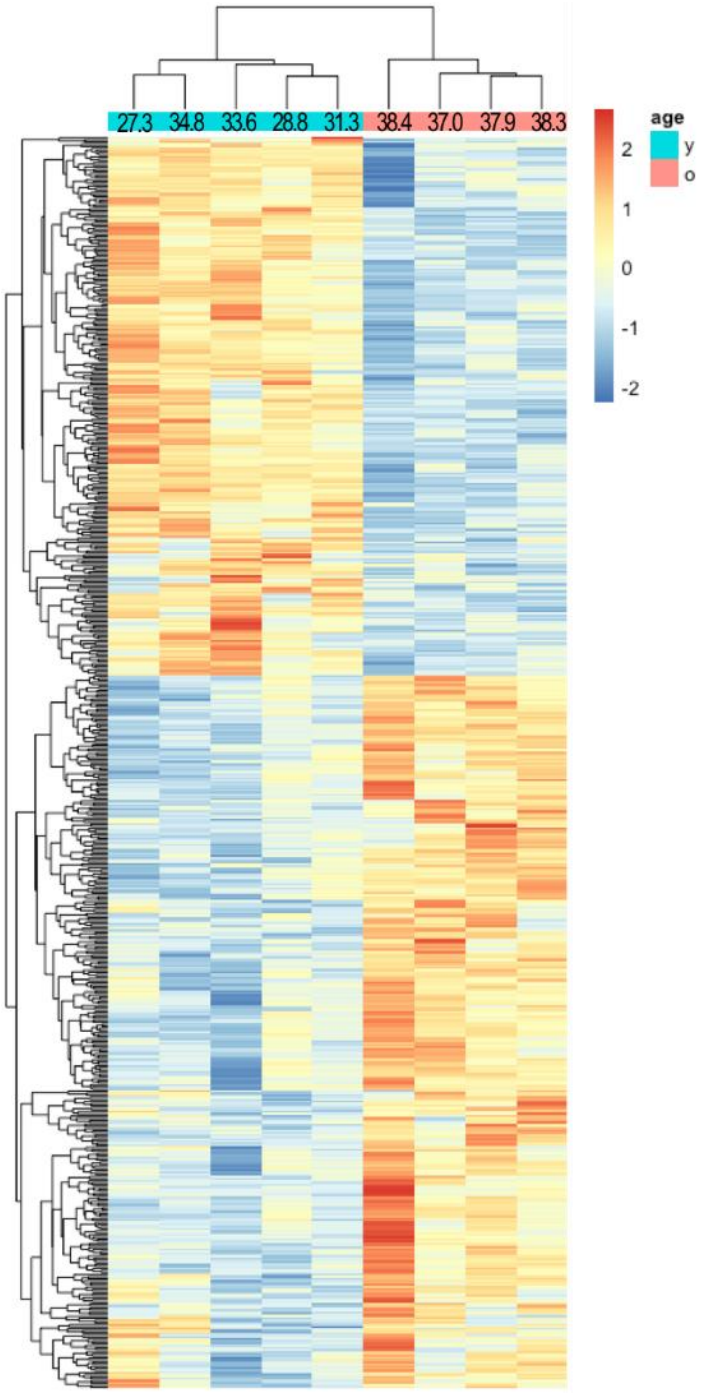
BIOLOGICAL PROCESS		**REVIGO**	**ConsensusPathDb**	
GO term	**Description**	**log10 p-value**	**p-value**	**q-value**
GO:0002009	**morphogenesis of an epithelium**	**-5.76**	1.75E-06	1.04E-04
GO:0060415	*muscle tissue morphogenesis*	*-1.57*	2.72E-02	1.03E-01
GO:0060429	*epithelium development*	*-7.55*	2.84E-08	4.50E-06
GO:0060485	*mesenchyme development*	*-1.76*	1.76E-02	8.02E-02
GO:0060537	*muscle tissue development*	*-4.25*	5.62E-05	1.14E-03
GO:0060562	*epithelial tube morphogenesis*	*-3.55*	2.81E-04	3.81E-03
GO:0002064	*epithelial cell development*	*-2.17*	6.81E-03	4.32E-02
GO:0000902	*cell morphogenesis*	*-1.44*	3.65E-02	1.24E-01
GO:0061448	*connective tissue development*	*-3.76*	1.72E-04	2.64E-03
GO:0030855	*epithelial cell differentiation*	*-2.04*	9.11E-03	5.23E-02
GO:0048754	*branching morphogenesis of an epithelial tube*	*-2.06*	8.63E-03	5.02E-02
GO:0007621	**negative regulation of female receptivity**	**-6.27**	5.41E-07	5.15E-05
GO:0060180	*female mating behaviour*	*-4.73*	1.85E-05	6.29E-04
GO:0030198	**extracellular matrix organization**	**-4.59**	2.55E-05	6.77E-04
GO:0085029	*extracellular matrix assembly*	*-2.61*	2.47E-03	2.10E-02
GO:0030199	*collagen fibril organization*	*-4.49*	3.27E-05	8.18E-04
GO:0043086	**negative regulation of catalytic activity**	**-1.81**	1.57E-02	7.62E-02
GO:2000145	**regulation of cell motility**	**-4.38**	4.17E-05	9.44E-04
GO:0051270	*regulation of cellular component movement*	*-4.36*	4.37E-05	9.47E-04
GO:0040013	*negative regulation of locomotion*	*-3.10*	7.89E-04	8.73E-03
GO:0021782	*glial cell development*	*-1.37*	4.22E-02	1.36E-01
GO:0016477	*cell migration*	*-2.61*	2.43E-03	2.10E-02
GO:0008347	*glial cell migration*	*-2.28*	5.25E-03	3.58E-02
GO:0097191	**extrinsic apoptotic signalling pathway**	**-4.08**	8.35E-05	1.53E-03
GO:0010941	*regulation of cell death*	*-5.78*	1.65E-06	1.04E-04
GO:0097192	*extrinsic apoptotic signalling pathway in absence of ligand*	*-1.69*	2.06E-02	8.98E-02
GO:0006915	*apoptotic process*	*-5.26*	5.45E-06	2.60E-04
GO:0036314	**response to sterol**	**-2.91**	1.23E-03	1.24E-02
GO:0048545	*response to steroid hormone*	*-1.80*	1.57E-02	7.62E-02
GO:0032870	*cellular response to hormone stimulus*	*-1.52*	3.04E-02	1.11E-01
GO:0010243	*response to organonitrogen compound*	*-1.65*	2.23E-02	9.32E-02
GO:0006968	**cellular defense response**	**-1.94**	1.15E-02	6.20E-02
GO:0044057	**regulation of system process**	**-3.01**	9.73E-04	1.05E-02
GO:0031667	**response to nutrient levels**	**-1.42**	3.82E-02	1.26E-01
GO:0033273	*response to vitamin*	*-1.42*	3.79E-02	1.26E-01
GO:0048522	**positive regulation of cellular process**	**-3.54**	2.88E-04	3.81E-03
GO:0009893	*positive regulation of metabolic process*	*-1.60*	2.51E-02	9.84E-02
GO:0031032	**actomyosin structure organization**	**-2.37**	4.26E-03	3.12E-02
GO:0030239	*myofibril assembly*	*-1.75*	1.77E-02	8.02E-02
GO:0001558	**regulation of cell growth**	**-2.26**	5.48E-03	3.63E-02
GO:0045926	*negative regulation of growth*	*-1.34*	4.52E-02	1.44E-01
GO:0008209	*androgen metabolic process*	*-2.82*	1.53E-03	1.42E-02

GO:0046879	*hormone secretion*	*-1.37*	4.28E-02	1.37E-01
GO:0009914	*hormone transport*	*-1.30*	4.99E-02	1.54E-01
GO:0035282	**segmentation**	**-2.95**	1.11E-03	1.15E-02
GO:0009952	*anterior/posterior pattern specification*	*-1.57*	2.71E-02	1.03E-01
GO:0045444	**fat cell differentiation**	**-2.14**	7.29E-03	4.51E-02
GO:0071229	**cellular response to acid chemical**	**-2.23**	5.91E-03	3.80E-02
GO:0051093	**negative regulation of developmental process**	**-4.95**	1.12E-05	4.43E-04
GO:2000026	*regulation of multicellular organismal development*	*-4.66*	2.21E-05	6.57E-04
GO:0022603	*regulation of anatomical structure morphogenesis*	*-2.73*	1.87E-03	1.68E-02
GO:0045595	*regulation of cell differentiation*	*-5.96*	1.09E-06	8.67E-05
GO:0051094	*positive regulation of developmental process*	*-4.45*	3.56E-05	8.48E-04
GO:0007507	**heart development**	**-4.59**	2.56E-05	6.77E-04
GO:0048514	*blood vessel morphogenesis*	*-2.67*	1.81E-02	1.43E-01
GO:0003007	*heart morphogenesis*	*-3.11*	7.71E-04	8.73E-03
GO:0072358	*cardiovascular system development*	*-3.91*	1.24E-04	2.04E-03
GO:0001944	*vasculature development*	*-3.97*	1.08E-04	1.84E-03
GO:0003208	*cardiac ventricle morphogenesis*	*-1.65*	2.22E-02	9.32E-02
GO:0035051	*cardiocyte differentiation*	*-1.66*	2.18E-02	9.32E-02
GO:0060840	*artery development*	*-1.58*	2.63E-02	1.02E-01
GO:0051128	*regulation of cellular component organization*	*-2.43*	3.67E-03	2.87E-02
GO:0009966	*regulation of signal transduction*	*-4.68*	2.07E-05	6.56E-04
GO:0023056	*positive regulation of signalling*	*-1.64*	2.32E-02	9.39E-02
GO:0023057	*negative regulation of signalling*	*-2.83*	1.49E-03	1.42E-02
GO:0048584	*positive regulation of response to stimulus*	*-1.44*	3.64E-02	1.24E-01
GO:0048585	*negative regulation of response to stimulus*	*-3.38*	4.12E-04	5.17E-03
GO:0048872	**homeostasis of number of cells**	**-1.87**	1.33E-02	6.90E-02
GO:0048878	*chemical homeostasis*	*-1.42*	3.81E-02	1.26E-01
GO:0035270	**endocrine system development**	**-3.24**	5.82E-04	6.92E-03
GO:0060541	**respiratory system development**	**-2.29**	5.10E-03	3.57E-02
GO:0009792	**embryo development ending in birth or egg hatching**	**-2.07**	8.43E-03	5.02E-02
GO:0048562	*embryonic organ morphogenesis*	*-1.50*	3.17E-02	1.14E-01
GO:0007369	*gastrulation*	*-1.78*	1.65E-02	7.77E-02
GO:0021915	*neural tube development*	*-2.02*	9.58E-03	5.43E-02
GO:0030323	*respiratory tube development*	*-1.88*	1.32E-02	6.89E-02
GO:0030324	*lung development*	*-1.92*	1.20E-02	6.41E-02
GO:0010038	**response to metal ion**	**-1.68**	2.08E-02	8.98E-02
GO:0007162	**negative regulation of cell adhesion**	**-2.41**	3.88E-03	2.98E-02
GO:0010810	*regulation of cell-substrate adhesion*	*-1.73*	1.87E-02	8.33E-02
GO:0007160	*cell-matrix adhesion*	*-2.15*	7.13E-03	4.46E-02
GO:0042060	**wound healing**	**-1.48**	3.32E-02	1.18E-01
GO:0001655	**urogenital system development**	**-1.80**	1.59E-02	7.62E-02
GO:0002683	**negative regulation of immune system process**	**-2.09**	8.05E-03	4.91E-02
GO:0001501	**skeletal system development**	**-3.66**	2.19E-04	3.22E-03
GO:0031016	**pancreas development**	**-1.61**	2.46E-02	9.76E-02
GO:0070848	**response to growth factor**	**-2.87**	1.34E-03	1.33E-02
GO:0007215	**glutamate receptor signalling pathway**	**-2.26**	5.49E-03	3.63E-02
GO:0071466	**cellular response to xenobiotic stimulus**	**-1.82**	1.51E-02	7.49E-02
GO:0001822	**kidney development**	**-1.65**	2.23E-02	9.32E-02
GO:0060993	*kidney morphogenesis*	*-1.39*	4.11E-02	1.34E-01
GO:0061326	*renal tubule development*	*-1.37*	4.22E-02	1.36E-01
GO:0072001	*renal system development*	*-1.54*	2.86E-02	1.07E-01
GO:0010646	**regulation of cell communication**	**-3.98**	1.05E-04	1.84E-03

GO:0007399	**nervous system development**	**-8.35**	4.47E-09	1.47E-06
GO:0035967	**cellular response to topologically incorrect protein**	**-1.91**	1.23E-02	6.49E-02
GO:0006986	*response to unfolded protein*	*-1.78*	1.65E-02	7.77E-02
GO:0046651	**lymphocyte proliferation**	**-1.70**	2.01E-02	8.88E-02
GO:0046649	*lymphocyte activation*	*-1.47*	3.37E-02	1.19E-01
GO:0042127	*regulation of cell proliferation*	*-4.91*	1.24E-05	4.54E-04
GO:0071560	**cellular response to transforming growth factor beta stimulus**	**-1.46**	3.46E-02	1.21E-01
GO:0007420	**brain development**	**-3.18**	6.66E-04	7.74E-03
GO:0030182	*neuron differentiation*	*-5.13*	7.35E-06	3.18E-04
GO:0048666	*neuron development*	*-2.56*	2.75E-03	2.29E-02
GO:0022008	*neurogenesis*	*-5.63*	2.36E-06	1.25E-04
GO:0007417	*central nervous system development*	*-4.10*	8.01E-05	1.52E-03
GO:0021510	*spinal cord development*	*-1.31*	4.92E-02	1.53E-01
GO:0022612	**gland morphogenesis**	**-1.77**	1.72E-02	8.02E-02
GO:0042476	*odontogenesis*	*-1.73*	1.86E-02	8.33E-02
GO:0007423	**sensory organ development**	**-1.96**	1.09E-02	5.98E-02
GO:0072359	**circulatory system development**	**-6.31**	4.93E-07	5.15E-05
GO:0035108	**limb morphogenesis**	**-2.84**	1.45E-03	1.41E-02
GO:0060173	*limb development*	*-2.48*	3.34E-03	2.74E-02
GO:0034605	**cellular response to heat**	**-1.63**	2.35E-02	9.39E-02
GO:0007167	**enzyme linked receptor protein signalling pathway**	**-2.06**	8.65E-03	5.02E-02
GO:0048523	**negative regulation of cellular process**	**-8.21**	6.17E-09	1.47E-06
GO:0009892	*negative regulation of metabolic process*	*-2.01*	9.84E-03	5.51E-02
GO:0035914	**skeletal muscle cell differentiation**	**-3.65**	2.23E-04	3.22E-03
GO:0048644	*muscle organ morphogenesis*	*-2.28*	5.27E-03	3.58E-02
GO:0007517	*muscle organ development*	*-2.97*	1.06E-03	1.12E-02
GO:0045445	*myoblast differentiation*	*-2.33*	4.64E-03	3.30E-02
GO:0042692	*muscle cell differentiation*	*-2.75*	1.78E-03	1.63E-02
GO:0045682	**regulation of epidermis development**	**-2.35**	4.44E-03	3.20E-02
GO:0001942	*hair follicle development*	*-1.45*	3.58E-02	1.24E-01
GO:0001678	**cellular glucose homeostasis**	**-1.60**	2.52E-02	9.84E-02
GO:0034097	**response to cytokine**	**-1.82**	1.50E-02	7.49E-02
GO:1901701	*cellular response to oxygen-containing compound*	*-3.44*	3.64E-04	4.68E-03
GO:0033993	*response to lipid*	*-3.37*	4.30E-04	5.25E-03
GO:0071310	*cellular response to organic substance*	*-3.85*	1.40E-04	2.23E-03
GO:0014070	*response to organic cyclic compound*	*-3.60*	2.52E-04	3.53E-03
GO:0051216	**cartilage development**	**-2.39**	4.04E-03	3.05E-02
GO:0002062	*chondrocyte differentiation*	*-1.33*	4.68E-02	1.48E-01
GO:0048705	*skeletal system morphogenesis*	*-1.54*	2.91E-02	1.08E-01
GO:0048762	**mesenchymal cell differentiation**	**-2.24**	5.77E-03	3.76E-02
GO:0051241	**negative regulation of multicellular organismal process**	**-4.24**	5.76E-05	1.14E-03
GO:0051240	*positive regulation of multicellular organismal process*	*-2.45*	3.57E-03	2.83E-02

Appendix VI.

Top 600 differentially expressed genes



Supplementary Figure 4 Heatmap showing the expression patterns of the top 600 differentially expressed genes between cumulus cells from young and older women

A heatmap comparing counts per million (CPM) of the top 600 differentially expressed genes for each sample. The intensity of the pseudocolors reflects gene expression levels (red indicates high CPM count, navy indicates low CPM count). Gene names are listed on the right of the graph. Patient age in years is across the top of the figure.